WNT and NOTCH: Joining Efforts to Maintain the Intestinal Homeostasis

Verónica Rodilla Benito

Departamento de Ciencias Fisiológicas II
Facultad de Medicina
Universitat de Barcelona

"WNT AND NOTCH: JOINING EFFORTS TO MAINTAIN THE INTESTINAL HOMEOSTASIS"

Verónica Rodilla Benito
Fundació IMIM-Hospital del Mar
2011

Co-directors: Dr. Lluis Espinosa and Dra. Anna Bigas

"*La verdadera ciencia enseña, por encima de todo, a dudar y a ser ignorante*"
Miguel de Unamuno

Departamento de Ciencias Fisiológicas II
Facultad de Medicina
Universitat de Barcelona

"WNT AND NOTCH: JOINING EFFORTS TO MAINTAIN THE INTESTINAL HOMEOSTASIS"

Memoria presentada por Verónica Rodilla Benito
para optar al título de Doctora.

Barcelona, Marzo de 2011

Este trabajo se ha realizado bajo la dirección del Dr. Lluís Espinosa Blay y la Dra. Anna Bigas Salvans, entre el Institut d'Investigacions Biomèdiques de Bellvitge (IDIBELL) y el Institut Municipal d'Investigació Mèdica (IMIM-Hospital del Mar).

Lluís Espinosa	Anna Bigas	Verónica Rodilla
Director tesis	Directora tesis	Doctoranda

Doctorado en Biomedicina de la Universitat de Barcelona

ACKNOWLEDGMENTS (Agradecimientos/Agraïments)

Agraeixo aquesta tesi a les meves quatre famílies:

A la meva **família científica**, que m'ha donat un lloc per viure durant 5 anys. Gràcies al papa i la mama: el Lluis i l'Anna, per donar-me l'oportunitat de provar-me a mi mateixa. Gràcies als meus germans grans: la Vane per ser-hi sempre; l'Àlex per escoltar-me en els moments de crisi; i la Mari, perquè has estat una santa!!! Gracias a mi hermana siamesa: Cristina, porque hemos sido el Zipi y Zape de este labo. Gràcies als meus germans petits: el Jordi, per fer veure que t'interessen els meus rotllos filosòfics sobre la ciència i compartir els teus plans de negoci; la Teresa, per ensenyar-me que és possible fer altres coses a part de treballar; el Pol, perquè tot i ser extremadament reservat, sé que et preocupes; el Ricard, pel teu entusiasme, perquè quan et veig penso que encara hi ha esperança; Erika, porque contigo han llegado los refuerzos... en todos los sentidos; Jessy, por ser así de genial, por haber encontrado tu sitio, lo suficientemente cercana para ser imprescindible y lo bastantemente alejada para estar al margen del huracán, eres sin duda la más lista del labo. Gràcies a les nou-vingudes: la Mar, per les hores de micro, per les classes bàsiques de CRC, però sobretot perquè des de que formes part de "la família", el lab és un lloc millor per viure; y Leonor, por las largas conversaciones y tu gran consejo sobre establecer "*connexions"*. Gracias a mis hermanos adoptados temporalemente: Tiago, por tu sentido del humor; MELS, por tus particularidades; Nadia, porque he econtrado una amiga; Neus, mi Fernanda, ets increïble!!!. Gràcies a tots els meus fills, aquells que he tingut al meu càrrec al llarg d'aquests anys: Teresa, mi niña de Madriz; Laura, la chica Intimissimi; Marcos, el eterno estudiante al que no le gustaba trabajar; l'Alba, la noia que va decidir ser tècnic perquè el doctorat no sempre és la millor alternativa; la Berta, perquè no sé si mai podré agrair-te com d'important ha estat que arribessis al lab just en aquest moment, ets fantàstica; Juliana, la hematóloga colombiana que se fue a Alemania por amor; la Clara, per contagiar-me una mica de la teva vitalitat. Gràcies a tots els que han passat pel Bigas' lab en algun moment o altre. Gràcies als meus veïns: els Snails, sobretot a la Rosa, la Jordina, l'Estel i la Patri; a mis compañeros de histología, Raúl y Elena, por las charlas. Gràcies als meus cosins llunyans, els que viuen a Bellvitge, sobretot a l'Antònia, l'Eder, la Violeta, l'Olguita, el Conrad i la Sònia; als que viuen al Clínic, a Raffy, por recordarme que soy más Mourinho que Guardiola.

A la meva **família suïssa**. Thanks to Freddy's lab: Marianne, Nico, Raj, Luca, Ute, Monique, Caroline, Fabian, Matteo, Craig, Olivier, Michela, Silvia and Freddy; especially to Freddy for accepting me in his lab, Michela for

EVERYTHING, Raj for the "coffee breaks", Monique for our "animal facility moments" and Luca for the Gastroenterology paper and… the rest ;-). Thanks to "Malley team": Manuel, Mame, Baris and Carla. Gracias al "Spanish group": Pablo, Paloma, Albert, Lucía y Tamara; especialmente a Tamara y Lucía por haberme hecho sentir como en casa, porque sois geniales chicas!

A la meva **família d'amics**. Gràcies a la Laure, per ser tan positiva; a la Pillu, per la teva sinceritat; al Jaume, per distreure'm amb parides vàries; al Jesús, per despenjar el telèfon i deixar-me escalfar-te l'orella durant hores; la Serra, per estar pendent sempre de com em va; a l'Esther, perquè m'ha encantat trobar-te; a la Blanca, porque sé que puedo contar contigo cuando sea. A tots vosaltres... mil gràcies.

A mi **familia**, la de verdad. Gracias a mis padres y mis hermanas por preocuparse tanto. A mi tío porque sin él no habría podido acabar la última etapa, gracias Jordi. A Rubèn, por haber tenido tanta paciencia, ha sido difícil pero sigues a mi lado.

Agraeixo a la Fundació IMIM fer-se càrrec del cost de la reprografia d'aquesta tesi.

I vull dedicar aquesta tesi a una persona molt especial, la **Júlia**.
Júlia, gràcies per haver estat allà en els bons i mals moments, per escoltar-me com cap altre, per animar-me en les crisis, per preocupar-te quan li dono més voltes del que toca a les coses, per deixar-ho tot i ajudar-me, per compartir una "mohito night" amb desconeguts de Bayer, per la teva paciència, per transmetre'm calma, per per guardar-me els secrets... en definitiva, per haver estat el pilar més important d'aquesta etapa de la meva vida.

TABLE OF CONTENTS

FIGURES AND TABLES INDEX

INTRODUCTION

I.1 Wnt signaling pathway

I.2 Notch signaling pathway

I.3 The physiology of the intestine

I.4 Colorectal cancer

MATERIAL AND METHODS

RESULTS

R.1 A common genetic program for Wnt and Notch pathways

R2. Notch is downstream of β-catenin activation

R3.The tumorigenic role of Notch activation by its ligand Jagged1 in CRC

R4. β-catenin and Notch cooperate to activate a common gene signature

R5. Notch and Wnt pathways are required to maintain stem cell compartment *in vivo*

R6.Characterization of the different roles of Jagged1 in the intestinal homeostasis and tumorigenic process

DISCUSSION AND CONCLUSIONS

ABBREVIATIONS AND ACRONYMS

ABBREVIATIONS AND ACRONYMS

βTRCP: beta-transducin repeat-containing homologue protein
APC: Adenomatous polyposis coli
APH1: Anterior pharynx defective 1
Ascl2: Achaete-scute complex homolog 2
BCL9: B-cell CLL/lymphoma 9
bHLH: basic helix-loop-helix
BSA: Bovine Serum Albumin
Ca^{+2}: Calcium
CBC: Crypt-based columnar cell
CBP: CREB binding protein
ChIP: Chromatin immunoprecipitation
CKI: Caseine kinase I
CRC: Colorectal Cancer
CRD: Cysteine-rich domain
CSC: Cancer stem cell
DAPI: 4',6-diamidino-2-phenylindole
DBZ: Dibenzazepine
DKK: Dickkopf
DMEM: Dulbecco's Modified Eagle's Medium
DNER: Delta/Notch-like EGF-related receptor
DLL: Delta-like protein
DOC: Deoxycholate
DOS: Delta-OSM11-like protein
DOXY: Doxycycline
DSL: Delta/Serrate/Lag2 motif
Dsh: Dishevelled (*Drosophila*)
Dvl: Dishevelled
DTG: Double Target Genes
ECM: Extracellular Matrix
EGF: Epidermal Growth Factor
EMT: Epithelial-to-Mesenchymal Transition
ER: Estrogen Receptor
Fabp: Fatty acid binding protein
FACS: Fluorescent Activated Cell Sorting
FAP: Familial Adenomatous Polyposis
FITC: Fluorescein isothiocyanate
FBS: Fetal Bovine Serum
FGF: Fibroblast Growth Factor
FZ: Frizzled
GFP: Green Fluorescent Protein
GOF: gain-of-function

GRG: Groucho-related protein
GSK3β: glycogen synthase kinase 3 beta
GST: Gluthathione-S-Transferase
HDAC: Hystone Deacetylase
Herp: Hes related repressor protein
Hes: Hairy and E (spl)
HGF: Hepatocyte Growth Factor
HRP: Horseradish peroxidase
HSPG: Heparan Sulfate Proteoglycans
IB: immunoblot
IGF: Insulin Growth Factor
IHC: Immunohistochemistry
IL: Interleukin
Il7r: interleukin 7 receptor
IP: Immunoprecipitation
IPTG: Isopropyl β-D-1-thiogalactopyranoside
ISC: intestinal stem cell
ISH: In Situ Hybridization
JAG: Jagged ligand
Kb: Kilobase
KO: Knockout
LEF1: Lymphoid Enhancer Factor
Lfng: Lunatic fringe
LRP: Lipo-protein receptor
LRC: Label Retaining Cell
MAb: Monoclonal Antibody
MAGP: Microfibril-associated glycoprotein
MAML: Mastermind-like
MET: Mesenchymal-to-Epithelial Transition
Mfng: Manic fringe
MIB1: Mindbomb-1
M_r: Molecular weight
MSI-1: Musashi-1
NFAT: Nuclear Factor of Activated T-Cell
NEURL: Neuralized1
NES: Nuclear Export Signal
NICD: Notch intracellular Domain
NLS: nuclear localization signal
NRR: Negative regulatory Region
O/N: Over-night
ONPG: O-nitrophenyl-β-D-galactopyranoside
PBS: Phosphate Buffered Saline
PCP: Planar Cell Polarity

PEI: Polyethylenimine, cationic polymer transfection reagent
PEST: Proline (P), Glutamic acid (E), Serine (S), Threonine (T)-rich motifs
PFA: Paraformalheyde
PI: Propidium Iodide
PLC: Phospholipase C
Poly-dI-dC: Poly-deoxyinosinic-deoxycytidylic
PYGO: Pygopus protein
RAM: $RBP_{J\kappa}$ association module
Rfng: Radical fringe
RT: Room temperature
SD: Standard Deviation
s.e.m.: Standard Error of the Mean
sFRP: Secreted Frizzled Related Protein
SMA: Smooth muscle actin
TA: Transit-amplifying
TAD: Trans-activation domain
TBS-T: Tris-Buffered Saline Tween-20
TCF: T Cell Factor
TLE: Transducin-like enhancer of split
TMD: Trans-membrane Domain
TSS: Transcription Start Site
VEGF: vascular endothelial growth factor
WB: Western Blot
WIF-1: Wnt-inhibitory factor 1
Wls: Wntless

INTRODUCTION

I1. Wnt signaling pathway

Wnt pathway regulates processes as diverse as cell polarity and cell fate specification [1]. Mutations in genes of the Wnt pathway have been associated with various oncogenic processes in tissues such as colon, breast, prostate and skin [2-4].

Three different pathways are activated upon Wnt receptor activation: the canonical Wnt/β-catenin cascade, the non-canonical planar cell polarity (PCP) pathway, and the Wnt/Ca^{2+} pathway. Of these, canonical pathway is the best characterized.

I1.1. Family members of Wnt signaling

I1.1.a Wnt ligands

Genome sequencing has revealed that mammalians have approximately 20 secreted Wnt proteins, which can be divided into 12 conserved subfamilies. Wnt proteins are a family of secreted glycoproteins, usually of 350–400 amino acids in length [**FIGURE I1**], that are found in an increasing number of organisms ranging from *C.elegans* to mammals [5]. Wnt proteins are characterized by a high number of conserved cysteine residues. Although Wnt proteins carry an N-terminal signal peptide and are secreted, they are relatively insoluble. This insolubility has been attributed to a particular protein modification, a cysteine palmitoylation, which is essential for Wnt function [6]. Hofmann and colleagues [7] reported that *porcupine,* and its worm homolog *mom-1,* encodes the enzyme that is responsible for Wnt palmitoylation [8].

Banziger and Bartscherer [9, 10] revealed in *Drosophila* another conserved gene that is essential for Wnt secretion, named *wntless (wls)* and *evenness interrupted (evi)*. The gene encodes a seven-pass transmembrane protein that is conserved from worms *(mom-3)* to humans (*hWLS*). Wntless protein resides primarily in the Golgi, where co-localizes and physically interacts with Wnts to form a multiprotein complex that is involved in intracellular trafficking, Wnt secretion and generation of Wnt gradients [11]. Thus, in the absence of *wls*/*evi*, Wnts are retained inside the producing cell and cannot be secreted.

At the functional level, Wnts act as morphogens since they generate a long-range gradient of concentration that determines their activity (reviewed in [1]). How Wnt gradients are generated is still unclear but the presence of a

palmitoyl group in the Wnt protein forces its movement away from membranes or lipid particles [12]. Alternatively, Wnts may be transported by cytonemes, which are long, thin filopodial structures [13, 14]. In addition, studies in *Drosophila* suggest that extracellular heparan sulfate proteoglycans (HSPG) could be also involved in the transport or stabilization of Wnt proteins.

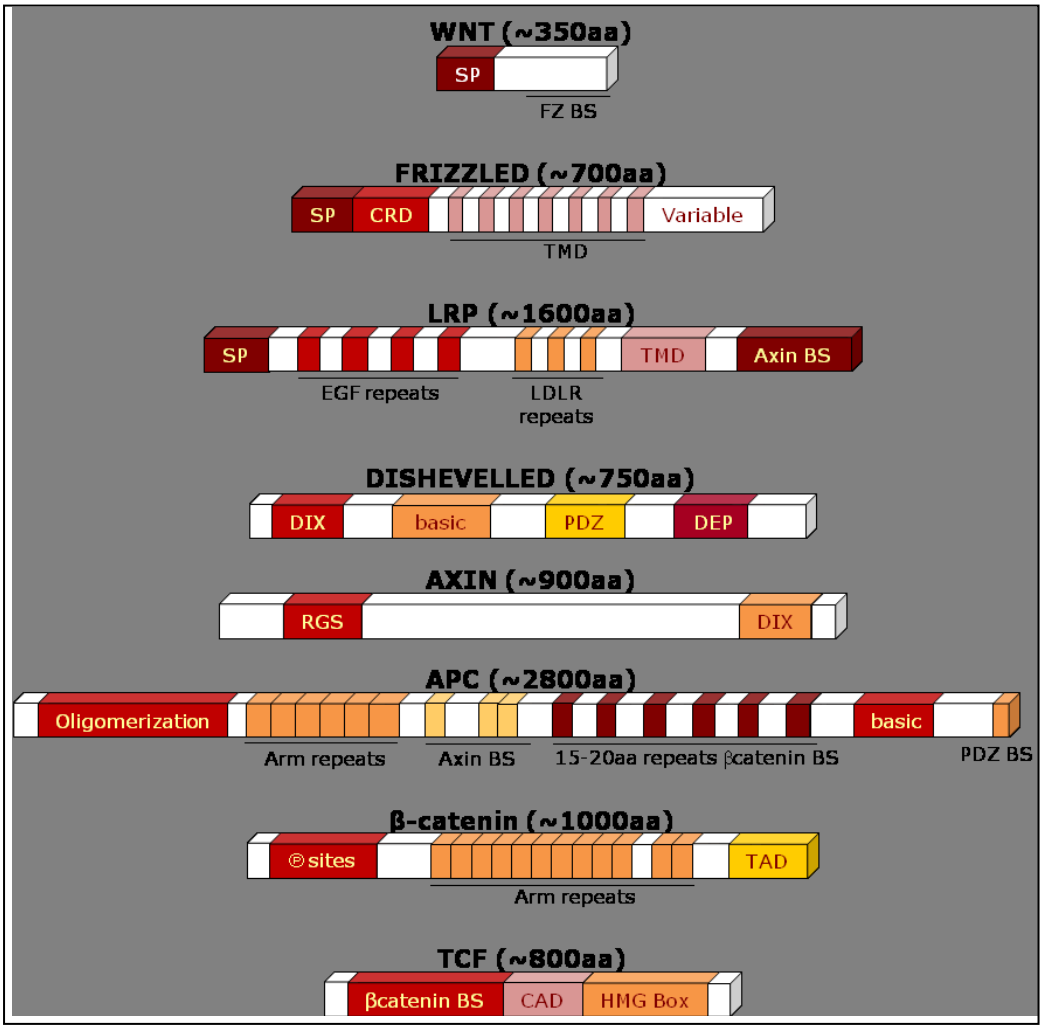

FIGURE I1. Schematic representation of intracellular Wnt signaling components. SP, signal peptide; BS, binding site; FZ, frizzled; CRD, cysteine-rich domain; TMD, transmembrane Domain; EGF, epidermal growth factor; LDLR, low-density lipoprotein receptor; LRP, LDLR-related protein; DIX; Dsh-Axin interacting domain; RGS, Regulators of G-protein Signaling domain; ARM, armadillo; ℗, phospho; TAD, transactivation Domain; CAD, context-dependent activation domain; HMG, high-mobility group; TCF, T-cell factor.

I1.1.b Wnt receptors: Frizzled and LRPs

Two distinct receptor families are critical for Wnt/β-catenin signaling [**FIGURE I1**]: the Frizzled (FZ) seven-pass transmembrane receptors [1] and the LDL receptor-related proteins 5 and 6 (LRP5 and LRP6) [15].

There are ten *Fz* genes in the mammalian genome, which show variable capacities to activate β-catenin signaling when co-expressed with Wnt and LRP5/6 [16]. Regarding LRPs, LRP6 plays a more predominant role in embryogenesis whereas LRP5 is critical for adult bone homeostasis. However, LPR5 and 6 are both required for mouse gastrulation [15]. Activation of β-catenin signaling is triggered following dimerization of FZ and one of the LRP co-receptors, and it has been proposed that Wnt is required to induce the formation of specific FZ-LRP5/6 complexes [15]. The current model [**FIGURE I2**] proposes that particular Wnt proteins activate the β-catenin or a non-canonical pathway depending on the receptor complement that is involved [17]. FZ function is essential for the activation of canonical and non-canonical pathways, but the presence of LRP5/6 co-receptor is exclusively required for the canonical/β-catenin signaling. However, some evidence suggests that LRP6 antagonizes non-canonical Wnt signaling *in vivo*, possibly via competing for Wnt ligands [18].

Other Wnt receptors exist such as RYK and ROR2, which are not required for Wnt/β-catenin signaling [17].

I1.1.c Wnt agonists

In addition to Wnt, at least two different unrelated factors can activate the FZ/LRP receptors. One of these factors is Norrin, which binds with high affinity to FZ-4 and activates the canonical signaling pathway in an LRP5/6-dependent manner [19]. The second one is R-spondin, a family of thrombospondin domain-containing proteins. In *Xenopus*, R-spondin2 acts as a Wnt agonist that synergizes with Wnts to activate the β-catenin pathway [20]. Human R-spondin1 has been found to strongly promote cell proliferation in the intestinal crypt compartment, a process involving β-catenin stabilization [21]. Indeed, studies in cultured cells demonstrate that R-spondins can physically interact with the extracellular domains of LRP6 and FZ-8 and activate Wnt reporter genes [22].

I1.1.d Wnt antagonists

Different conserved but structurally distinct families of Wnt antagonists have been identified from lower vertebrates to humans: sFRP (secreted Frizzled

Related Protein), WIF-1 (Wnt-inhibitory factor 1), Cerberus, Wise/SOST and Dickkopf (DKK).

sFRP proteins, WIF-1 and Cerberus have been shown to bind the Wnt factors and as a consequence they might inhibit multiple signaling pathways activated by these molecules [23]. Nevertheless, sFRPs and WIFs can also promote Wnt signaling by stabilizing the Wnt molecules or by facilitating Wnt secretion or transport in a context-dependent manner (reviewed in [1]). Secreted Dickkopf (DKK) proteins inhibit Wnt signaling by direct binding to LRP5/6 [24]. Through this interaction, DKK1 crosslinks LRP6 to a different class of transmembrane molecules, named Kremens [25], thus promoting the internalization and inactivation of LRP6. The secreted Wnt inhibitor, Wise, also acts by binding to LRP [26], as does the Wise family member SOST [27, 28].

I1.2. Activation cascade

I1.2.a Canonical Wnt signaling pathway

As mentioned before, generation of specific FZ/LRP co-receptor complexes by particular Wnt proteins initiate either the canonical or the alternative signaling pathways. One of the first events of canonical Wnt pathway is the recruitment of Dishevelled (DVL; or Dsh in *Drosophila*) [**FIGURE I1**], a cytoplasmic protein that functions upstream of β-catenin and the kinase GSK3β, to the FZ/LRP complex. Wnt signal induces phosphorylation of DVL (reviewed in [29]), but it is unclear whether binding of Wnt to FZ mediates DVL recruitment, how is DVL phosphorylation controlled and which is the role of phosphorylated DVL in Wnt signal transduction [**FIGURE I2**].

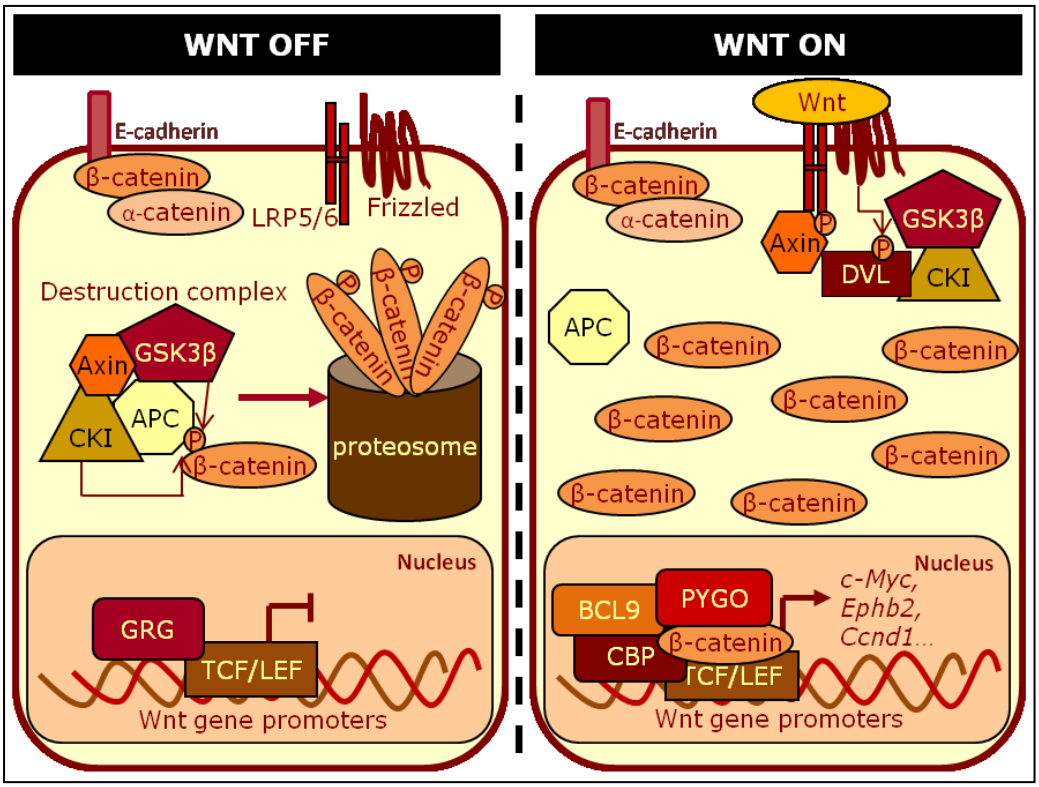

FIGURE I2. Summary of canonical Wnt signaling activation.

Interaction of AXIN with the LRP5/6 co-receptors occurs through five phosphorylated PPP(S/T)P repeats in the cytoplasmic tail of LRP [30, 31]. Phosphorylation of LRP at this region is dependent on Wnt binding and regulates AXIN recruitment. It has been demonstrated that GSK3β can phosphorylate the PPP(S/T)P motif, whereas Caseine kinase I-γ (CK1γ), the only CK1 family member that binds the membrane through palmitoylation, phosphorylates multiple motifs close to the GSK3 sites. Both kinase activities are essential for Wnt signal initiation. It remains currently under debate whether Wnt controls GSK3β-mediated phosphorylation of LRP5/6 [31] or whether CK1γ is the kinase regulated by Wnt [30].

Recruitment of DVL and AXIN to the FZ complex is required for triggering subsequent downstream events that involve classical Wnt activation, being β-catenin the principal effector of the pathway. In fact the main consequence of canonical Wnt activation is the stabilization of cytoplasmic β-catenin that under basal conditions is degraded by a *destruction complex* formed by APC, AXIN and the two kinases CK1 and GSK3β (reviewed in [32]). Degradation of β-catenin is dependent on its sequential phosphorylation by CKI and GSK3 that results in its ubiquitination-mediated degradation by the proteasome [**FIGURE I2**]. Because AXIN is a limiting and key scaffolding element of the

destruction complex, sequestration of AXIN by FZ/LRP results in its rapid disassembly [33]. Moreover, since CK1, DVL, βTrCP, and GSK3β participate in other signaling pathways; low levels of AXIN might also protect the Wnt pathway from changes in the abundance of these more promiscuous components. The APC protein contains a series of 15 and 20 amino acid repeats that are responsible for it interaction with β-catenin and three Axin-binding motifs interspersed between these β-catenin-binding motifs [**FIGURE I1**]. It has been proposed that APC is required for efficient recruitment of β-catenin to the cytoplasmic destruction complex but also for actively export nuclear β-catenin to the cytoplasm [34]. Both APC and AXIN can themselves be phosphorylated by their associated kinases, which change their affinity for specific components of the destruction complex. Crystallographic studies are starting to provide clues into the structure of this complex, being the central region of β-catenin the first component of the pathway that was crystallized. This region consists of 12 armadillo repeats of 42 amino acids each [35] [**FIGURE I1**]. Subsequently, structural interactions of AXIN, APC, E-cadherin, and TCF with β-catenin have been visualized [36]. APC, E-cadherin, and TCF bind the central part in a mutually exclusive manner, while AXIN utilizes a helix formed by the third and fourth armadillo repeats of β-catenin. For instance, AXIN binding disables the simultaneous interaction with other β-catenin partners in this region. A key function of APC is to remove phosphorylated β-catenin from the active site of the complex [37]. Armadillo is the orthologue of β-catenin in *Drosophila* and takes its name from the Armadillo repeats that regulate its association with APC, AXIN, TCF/LEF and cadherins, among others [5].

As mentioned before, Wnt activation disrupts the degradation complex thus inhibiting its intrinsic kinase activity on β-catenin. It is unclear how this occurs, but involves the Wnt-induced recruitment of AXIN to the phosphorylated tail of LRP and/or to FZ-bound DVL. As a result, stable, non-phosphorylated β-catenin accumulates and translocates into the nucleus, where it binds to the N-terminus of LEF/TCF transcription factors [38-40]. There is no a clear consensus on the mechanism by which β-catenin travels between the cytoplasm and the nucleus but it has been demonstrated that its nuclear import is independent on its Nuclear Localization Signal (NLS) and the importin machinery [41]. Two proteins, TCF and PYGO are proposed to anchor β-catenin in the nucleus, although β-catenin can still localize to the nucleus in the absence of either PYGO or TCF [42]. Once in the nucleus, β-catenin can be actively exported back to the cytoplasm by AXIN [43] or APC [34].

Association of β-catenin with the chromatin takes place through the TCF/LEF factors in specific TCF binding sites that are highly conserved from *Drosophila*

to vertebrates. Binding consensus for TCF is AGATCAAAGG [40]. There are four vertebrate TCF/LEF proteins that are highly similar at the biochemical level but dramatically differ in their embryonic or adult expression domains, thus explaining the extensive redundancy observed in some knockout models [44]. In the absence of Wnt, TCF acts as a transcriptional repressor by establishing a complex with Groucho (GRG in mouse and TLE in human) protein [45, 46] [**FIGURE I2**]. GRG is a family of repressor proteins that do not bind DNA directly, but are recruited by diverse transcription factors, including members of the HES, TCF/LEF1, and MYC families. The interaction of β-catenin with the N-terminus of TCF physically displaces GRG from TCF/LEF and facilitates the binding of co-activators such as the histone acetylase CBP/p300 [47], thus transiently converting TCF into an activator [38-40] and translating the Wnt signal into the transcription of specific TCF target genes.

Different nuclear partners of the TCF/β-catenin complex, *legless* (*Bcl9* in mouse) and *Pygopus* (*Pygo*), have been identified in genetic screens in *Drosophila* [48-50]. Mutations in these genes result in phenotypes similar to *wingless*, and over-expression of both genes promotes TCF/β-catenin activity in mammalian cells [50]. Functionally, BCL9 links PYGO to the N-terminus of β-catenin and formation of this trimeric complex has been implicated in nuclear retention of β-catenin [51] but it might also directly contribute to facilitate β-catenin-mediated transcription [52]. Although most of Wnt signaling events in *Drosophila* appear to be dependent on BCL9 and PYGO, it is unclear if this holds true during vertebrate development.

A part from its function in the Wnt pathway, β-catenin protein is a structural component of the adherent junctions by binding to the cytoplasmic tail of various cadherins, such as E-cadherin [53]. It is unclear whether the adhesive and signaling functions of β-catenin are interconnected, but it is demonstrated that newly synthesized β-catenin first saturates the pool of the adherent junction, which never becomes available for signaling. The APC complex then efficiently degrades excess of free cytoplasmic β-catenin that is the only pool capable of being regulated by Wnt signals. Interestingly, these functions are carried out by two different β-catenin homolog in *C. elegans* [54].

I1.2.b Alternative Wnt signaling pathways

A common step in the activation of all three Wnt cascades (canonical Wnt/β-catenin pathway, Planar Cell Polarity (PCP) pathway and the Calcium pathway) is the FZ-mediated recruitment of DVL (reviewed in [29]). Although, non-canonical Wnt cascades are not as well-characterized as the canonical pathway it is clearly established that both are linked for the regulation of cell

movement, including the coordinated orientation of cells within an epithelium, the orientation of stereocilia in the mammalian inner ear and the convergent extension movements that occur during gastrulation [55].

In the PCP pathway, specific Wnt-FZ interactions leads to the DVL-mediated activation of the small GTPases RhoA and Rok (Rho kinase), or of Rac and JNK, which in turn affects the dynamics of the cytoskeleton [**FIGURE I3**].

The Wnt/Ca^{2+} pathway involves G proteins, phospholipase C (PLC), phosphodiesterase (PDE) and the activation of the Ca^{2+}/calmodulin-dependent protein kinase II (CaMKII), protein kinase C (PKC), calcineurin and the nuclear factor of activated T cells (NFAT) [**FIGURE I3**].

Biochemical and genetic studies support the existence of an antagonistic crosstalk between canonical and non-canonical pathway in different contexts [56]. In this respect, it has been demonstrated that Wnt signaling can modulate microtubule organization through a mechanism involving both, binding of DVL to the microtubules and inhibition of GSK3β [57, 58].

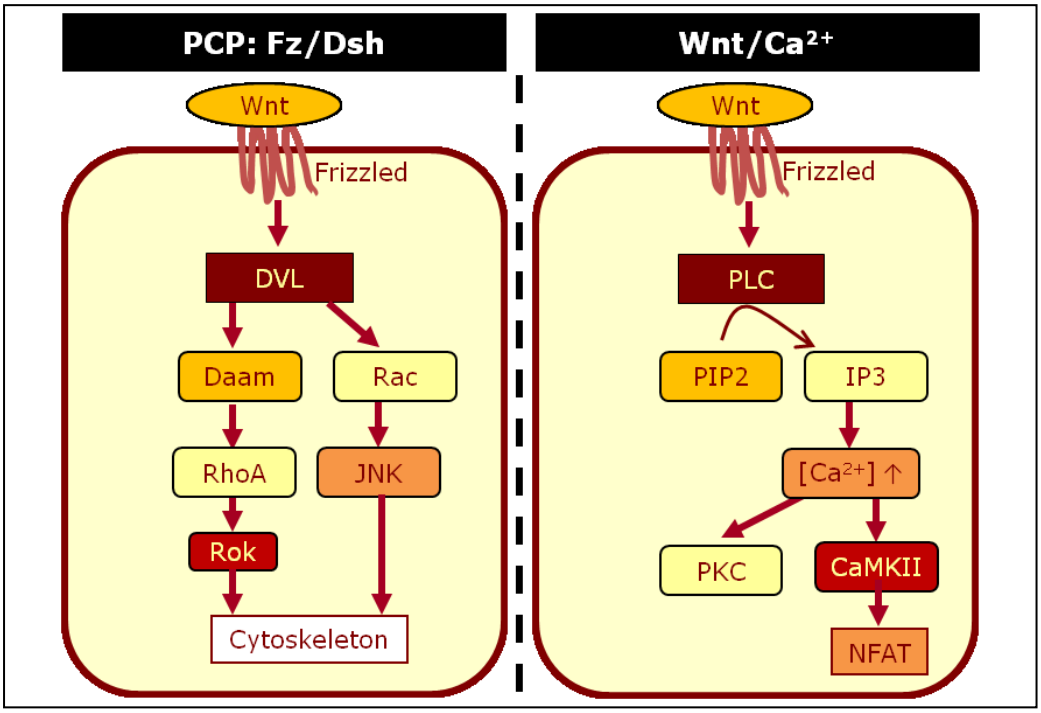

FIGURE I3. Summary of non-canonical Wnt signaling pathways.

I1.2.c Canonical Wnt target genes

Wnt signaling through the β-catenin-dependent canonical cascade induces a specific and integrated transcriptional program, which is cell type and context dependent, and control fundamental aspects of cell behavior, such as growth, differentiation or cell division. A growing number of Wnt-responsive genes have been identified in different tissues and the list is constantly increasing and updated (see *http://www.stanford.edu/group/nusselab/cgi-bin/wnt/target_genes*). *In vitro* studies led to the characterization of the optimal consensus binding site as the 5'-AAGATCAAAGG-3') sequence [59] that was confirmed in reporter assay to respond to β-catenin activation [3]. Although this has provided an important tool for Wnt research, it does not reflect the more complex behavior of endogenous TCF–β-catenin signaling [60]. Furthermore, it appears that most Wnt targets are tissue- and developmental-stage specific, and the most promising candidate for being a "general target" is *Axin2*, which expression increases in response to β-catenin activation in a large variety of tissues [61].

A recent chromatin immunoprecipitation (ChIP)-on-chip study revealed Wnt response element distribution. Wnt signaling activates gene expression through the formation of a chromatin complex formed by TCF and β-catenin. In colorectal cancer, activating Wnt pathway mutations lead the activation of a TCF7L2/TCF4 target gene program. Through a DNA array-based genome-wide analysis of TCF4 chromatin occupancy, Hatzis *et al* identified 6,868 high-confidence TCF4-binding sites. Most TCF4-binding sites were located at large distances from transcription start sites; moreover target genes are occupied by multiple binding sites. The TCF4-binding regions significantly correlate with Wnt-responsive gene expression profiles and behave as β-catenin/TCF4-dependent enhancers in transient reporter assays [62].

I1.3. Wnt mice models

Wnt signaling plays a crucial role in maintaining the balance between proliferation and differentiation throughout embryogenesis and postnatal life. Consistent with this, most of the conventional knockout mice for both canonical and non-canonical Wnt family members display early embryonic lethality, underscoring the fundamental importance of these pathways. Use of conditional or inducible mouse models allowed the study of specific Wnt functions during late development and adult life. Detailed information about available Wnt-mutant mice data is summarized in **Annex A1** and can be found on the Wnt Homepage: *http://www.stanford.edu/group/nusselab/cgi-bin/wnt/mouse*.

I2. Notch signaling pathway

Notch is an evolutionary conserved signaling pathway that is activated by cell–cell interactions and regulates multiple aspects of metazoan development [63, 64] as well as cell differentiation in several tissues. Based on its functions, it is not surprising that aberrant gain or loss of function of different Notch signaling components has been directly linked to human disorders, from developmental syndromes including Alagille, Teratology of Fallot, Syndactyly, Spondylocostal dysostosis, Familial Aortic Valve Disease [65, 66] to adult onset diseases such as CADASIL [67]. In addition, it has been found that Notch activation is responsible for T-ALL [68] and for colon cancer [69, 70], emerging as a potential therapeutic target in this specific tumors [71, 72].

I2.1. Family members of Notch signaling

Multiples proteins have been identified that participate in the regulation of Notch signaling at different levels, and are summarized in **TABLE I1**:

COMPONENT	*Drosophila*	Mammals
Receptor	Notch	Notch1-4
Ligands:		
Canonical	Delta, Serrate	Dll1, Dll3, Dll4, Jagged1-2
Non-canonical		DNER, Dlk-1, MAGP-1 and 2, F3/ Contactin1, NB-3/Contactin6
Nuclear effectors:		
DNA-binding TF	Su(H)	$RBP_{J\kappa}$/CBF-1
Transcriptional Co-activator	Mastermind	MAML 1-3
Receptor proteolysis:		
Furin convertase (S1 cleavage)	?	PC5/6, Furin
Metalloprotease (S2 cleavage)	Kuzbanian, TACE Kuzbanian-like	ADAM10/Kuzbanian, ADAM17/TACE
γ-secretase (S3/S4 cleavage)	Presenilin, Nicastrin, APH-1, PEN-2	Presenilin 1 and 2, Nicastrin, APH-1a-c, PEN-2
Glycosyltransferase modifiers:		
O-fucosyl-transferase	OFUT-1	POFUT
β1,2-GlcNAc-transferase	Fringe	Lunatic, Manic and Radical Fringe
Endosomal sorting/Membrane trafficking regulators:		
Ring Finger E3 Ubiquitin ligase (ligand endocytosis)	Mindbomb 1-2, Neuralized	Mindbomb, Skeletrophin, Neuralized 1-2
Ring Finger E3 Ubiquitin ligase (receptor endocytosis)	Deltex	Deltex 1-4

HECT Domain E3 Ubiquitin ligase (receptor endocytosis)	Nedd4, Su(Dx)	Nedd4, Itch/AIP4
Negative regulator	Numb	Numb, Numb-like, ACBD3
NICD degradation:		
F-Box Ubiquitin ligase	Archipelago	Fbw-7/SEL-10
Canonical target bHLH represor genes	E(spl)	HES, HEY

TABLE I1. Core components and modifiers of Notch pathway.

I2.1.a Notch receptors

Notch receptors are single-pass trans-membrane proteins consisting of an extracellular, a trans-membrane and an intracellular domain [**FIGURE I4**]. In the Golgi, mammalian Notch is cleaved by furin-like pro-protein convertases to generate a heterodimeric receptor that retains the N-terminal end of the protein (that will give rise to the extracellular domain of Notch) bound to the C-terminus end (that includes the trans-membrane and intracellular domains) by disulfide bridges [**FIGURE I4** and **I5**]. The extracellular domain contains multiple EGF tandem repeats that mediate interactions between Notch and its ligands. EGF repeats bind to calcium ions, and this determines the conformation and affinity of Notch for its ligands [73]. The C-terminus of the extracellular domain is characterized by the presence of a negative regulatory region (NRR) that prevents receptor activation in the absence of ligand-binding. Point mutations in this region cause ligand-independent activation of Notch that are responsible for a number of T-cell acute lymphoblastic leukemia in humans [74, 75]. The N-terminus of the trans-membrane domain (TMD) of Notch is extracellular and is constituted of a stop translocation signal and the hetero-dimerization domain. The TMD is followed by the intracellular domain, which consists of an $RBP_{J\kappa}$ association module (RAM) domain linked to seven ankyrin repeats by the nuclear localization sequence [**FIGURE I4**]. The ankyrin repeats are followed by an additional nuclear localization sequence and a transactivation domain (TAD) that differs among the four Notch paralogues. The C-terminus of the intracellular region contains the PEST domain that is the main target for the ubiquitylation that leads to degradation of NICD [76] [**FIGURE I4**].

It is still under debate whether Notch receptors have both redundant and unique functions [77].

I2.1.b Notch ligands

Canonical Notch ligands. Canonical Notch ligands are trans-membrane proteins characterized by the presence of multiple EGF repeats in tandem in

the extracellular domain, and a short and less conserved intracellular region of unknown function. There are five Notch ligands including JAG1 and JAG2, which contain a cysteine-rich domain (CRD), and DLL1, DLL3, and DLL4, which lack the CRD. The Notch binding domain comprises an N-terminal domain followed by a Delta/Serrate/Lag2 (DSL) motif and two characteristic tandem EGF repeats termed Delta-OSM11-like protein (DOS) domains [**FIGURE I4**] [78].

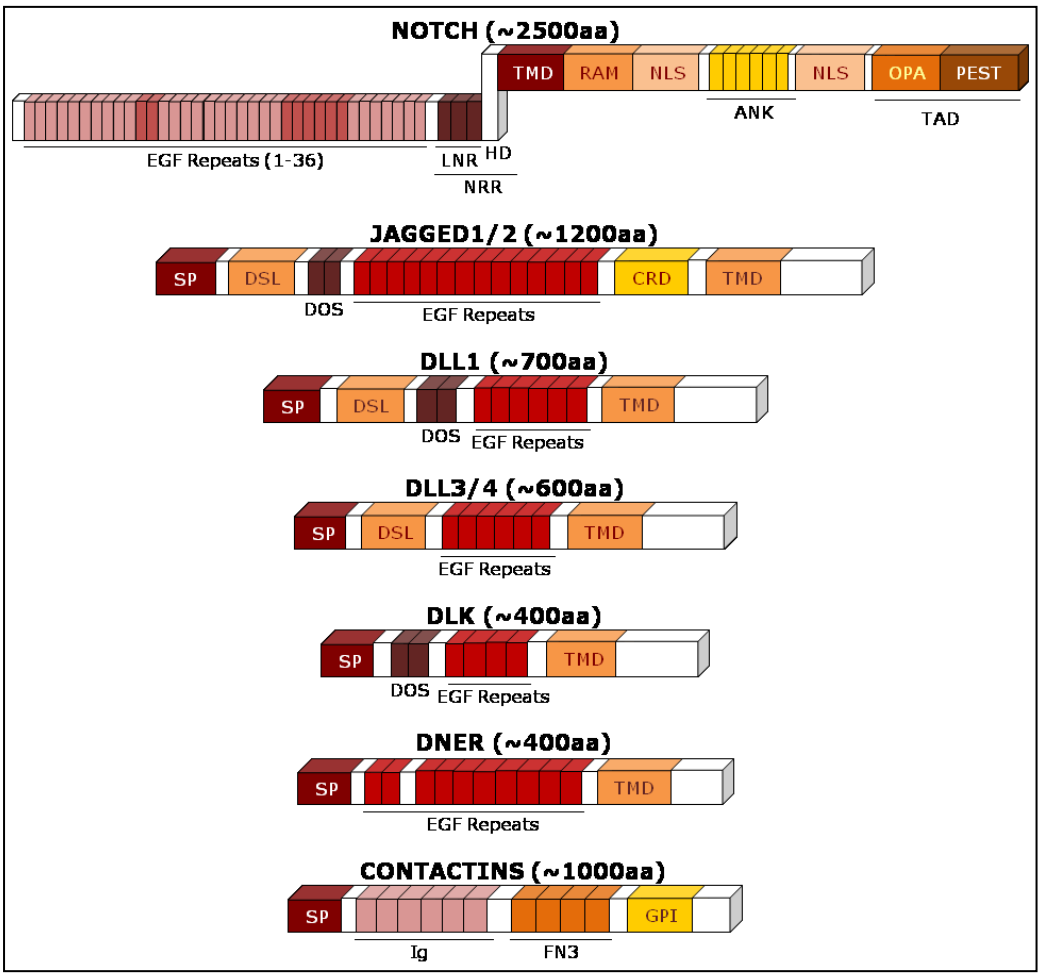

FIGURE I4. Schematic diagram of Notch signaling components. The number of EGF repeats is 36 in Notch1 and Notch2, 34 in Notch3 29 in Notch4, 6 in DLL3 and 8 in DLL4. EGF, Epidermal Growth Factor repeats; LNR, cysteine-rich Lin12-Notch repeats; HD, heterodimerization domain; NRR, Negative Regulatory Region; TMD, transmembrane domain; RAM, *RBP*$_{JK}$*–associated* module; NLS, nuclear localization signal; ANK, ankyrin; OPA, region rich in glutamine; PEST, proline (P), glutamic acid (E), serine (S), and threonine (T)-rich motifs; TAD, transactivation domain; SP, signal peptide; DSL, Delta/Serrate/Lag2 motifs; DOS, Delta and OSM11-like protein domain ; CRD, cystein-rich domain.

Non-canonical Notch ligands. Additional Notch ligands, also known as non-canonical ligands, include structurally heterogeneous trans-membrane and soluble proteins that can somehow regulate Notch signaling [79]. Delta

homologue-like 1 (DLK1), also known as Pref1, is similar to DLL ligands but lacks the DSL domain and inhibits Notch signaling by binding to Notch receptors [80, 81] [**FIGURE I4**]. A second Delta-like protein called Delta/Notch-like EGF-related receptor (DNER) contains the EGF repeats typical of the canonical ligands but lacks the DSL domain. DNER binds and activates Notch in neighboring cells through a non-canonical Deltex-dependent pathway [82] [**FIGURE I4**]. F3 and NB3, also known as contactin 1 and 6, respectively, consist of an extracellular domain formed by six repeats of the immunoglobulin-containing cell adhesion molecule domain and four repeats of the fibronectin type III domain. Both contactins activate the non-canonical Deltex-dependent pathway [83, 84] [**FIGURE I4**]. The microfibril-associated glycoprotein (MAGP) family of proteins, MAGP1 and MAGP2, are secreted ligands that can either activate or suppress Notch canonical signaling [85-87].

I2.2 Regulation of ligand-receptor interactions

Regulation of both ligand and receptor availability at the cell surface is a crucial step in the control Notch pathway activation. The simplest way of regulating availability is to restrict ligand and/or receptor expression spatially and temporally. However, post-translational modifications, such as glycosylation, and trafficking regulation of both ligands and receptor have emerged as important mechanisms for controlling productive ligand-receptor interactions and signaling [88, 89].

I2.2.a Receptor glycosylation

The specificity and intensity of the binding between Notch and its different ligands is partially regulated through glycosylation of the EGF repeats in the Notch extracellular domain. Notch glycosylation by the *O*-fucosyltransferase POFUT1 is necessary for proper receptor-ligand interactions and trafficking of Notch to the membrane [90]. POFUT1 also functions as a chaperone protein necessary for correct Notch folding, and in the absence of POFUT1, Notch signaling is blocked [91]. *O*-Fucose residues are recognized by members of the Fringe family, which are a group of β-1,3-*N*-acetyl-glucosamino-transferases that elongate the glycosaminoglycan chain by the addition of *N*-acetylglucosamines. There are three Fringe proteins in mammals, Lunatic fringe (Lfng), Manic fringe (Mfng), and Radical fringe (Rfng) [89]. Glycosylation mediated by Fringe promotes the interaction between Notch and DLL ligand and inhibits interactions between JAG and Notch [92] [**FIGURE I5**].

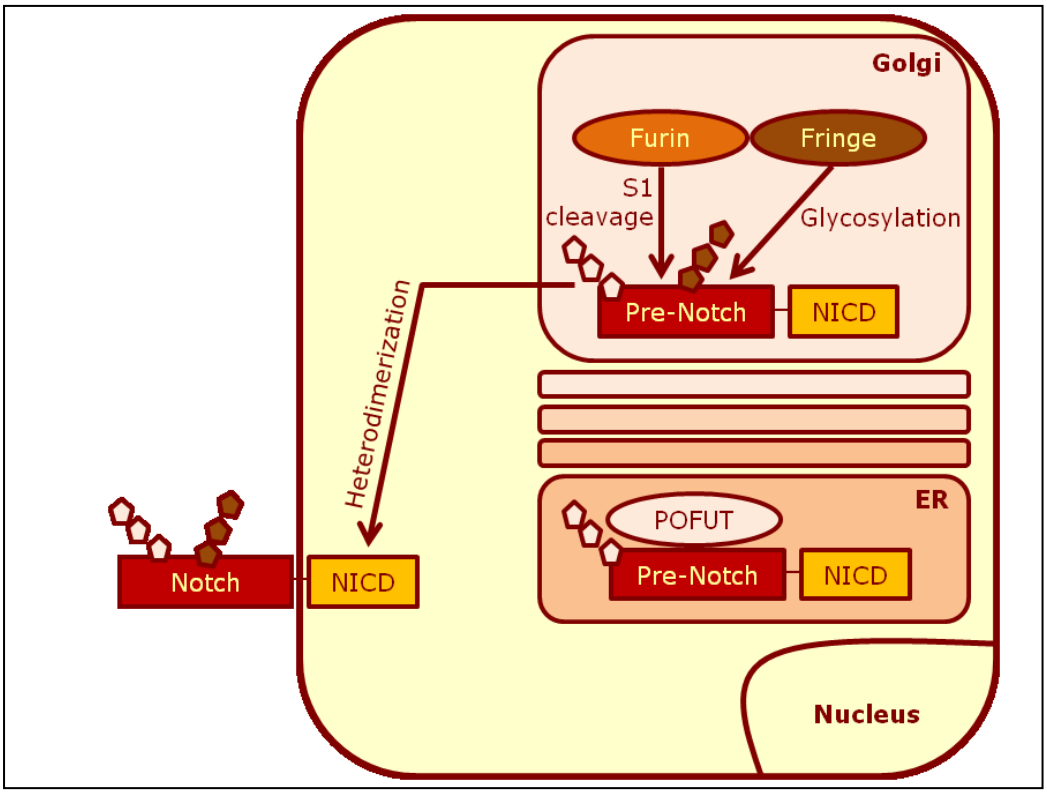

FIGURE I5. Notch receptor during the glycosylation and fucosylation processes. The intracellular and extracellular domains of the Notch receptor are synthesized as a single protein (pre-Notch). POFUT1 functions as a chaperone and is required for the transport of pre-Notch from the endoplasmic reticulum (ER) to the Golgi apparatus and for fucosylation of glycosylated serine and threonine residues of the extracellular domain within the Golgi. Glycosylation of these residues is carried out by members of the Fringe family. A Furin-like convertase cleaves pre-Notch into the extracellular and intracellular domain (S1 cleavage). This results in a heterodimeric receptor with non-covalently associated domains that is transported to the plasma membrane.

I2.2.b Ligand and receptor endocytosis and trafficking

It has been demonstrated that endocytosis and recycling of Notch ligands to the plasma membrane are required to increase the affinity of DLL and JAG ligands for the Notch receptors in order to initiate signaling; however, the mechanism involved is largely unknown [79, 93]. In mammals, ubiquitination of the intracellular domain is critical for initiating the endocytic process, and two ligand-specific ubiquitin ligases have been identified, Neuralized1 (NEURL) and Mindbomb-1 (MIB1), which ubiquitinate JAG1 and DLL1, respectively [94-97] [**FIGURE I6**].

In contrast, ubiquitination-mediated endocytosis of Notch receptors is primarily used as a mechanism to restrict its protein levels at the cell surface [98-100]. The murine E3 ubiquitin ligase ITCH, and its human homologue AIF4, promotes Notch ubiquitination thus inducing Notch1 degradation in the

lysosomes [101]. Alternatively, Notch can be re-directed to the recycling endosome to be presented again to the cell surface [102] or partially processed into its active NICD form leading to ligand-independent activation by Deltex [103] [**FIGURE I6**].

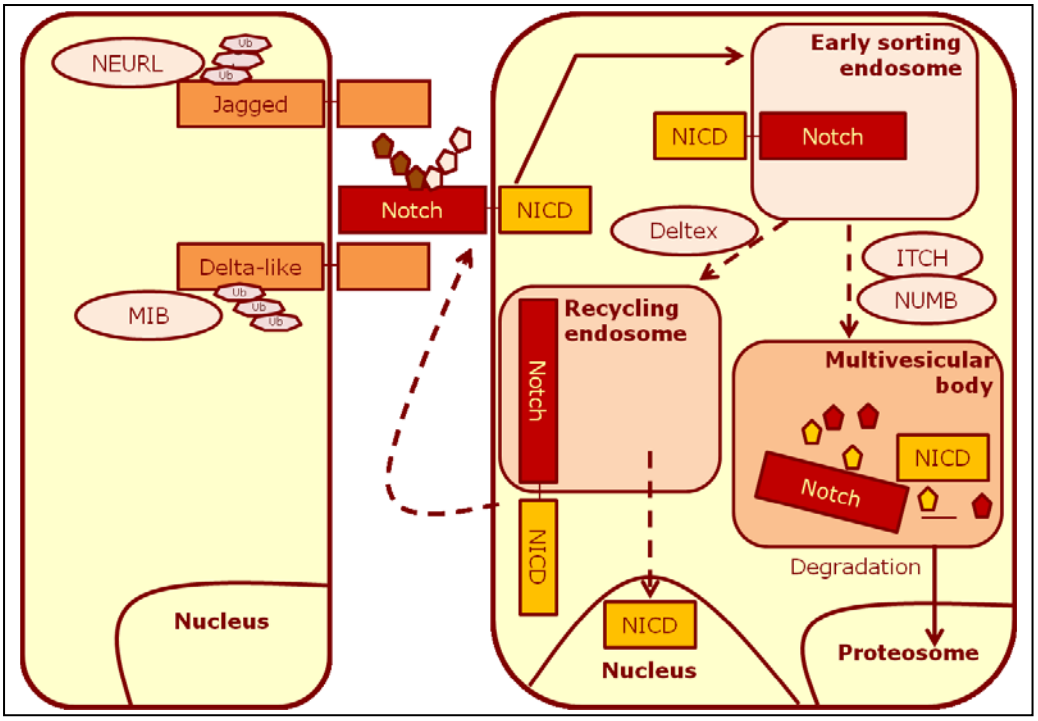

FIGURE I6. Ligand and receptor endocytosis and trafficking. The readout of receptor–ligand interaction is determined by the specific Fringe modifications that were introduced earlier in the Golgi, which affect sensitivity to the DSL (Delta (DLL)–Serrate–Lag2) ligands. Additionally, the E3 ubiquitin ligases, (MIB) and (NEURL) promote the turnover of the ligand and therefore contribute to productive ligand–receptor interactions. Numb suppresses Notch signaling by preventing nuclear localization and targeting the NICD for degradation through the E3 ligase Itch.

I2.3 Activation cascade

I2.3.a Canonical Notch signaling pathway

Notch receptor maturation and activation require several proteolytic events, and the sites for cleavage are sequentially numbered S1 to S4 [64]. The S1 site is recognized by furin-like pro-protein convertase in the Golgi network, and it is necessary for the maturation of functional Notch heterodimeric receptors [104] [**FIGURE I5**]. In mammalian cells, internalization of the ligand following Notch binding, a process known as *trans*-endocytosis, is necessary to activate Notch signaling [64, 105, 106] [**FIGURE I7**]. The current model is that the pulling force applied by ligand endocytosis on the Notch extracellular domain induces a conformational changes that exposes the hetero-

dimerization domain of Notch and allows recognition of the S2 cleavage site by a member of the disintegrin and metalloprotease domain (ADAM) family of metalloproteases [107] [**FIGURE I7**]. ADAM activity generates an unstable intermediate protein that is recognized by the γ-secretase complex and cleaved at the S3 and S4 intra-membranous sites, producing the NICD fragment, which translocates to the nucleus to regulate transcription together with RBP_{JK} [108, 109]. The γ-secretase complex is formed by the protease Presenilin and by the regulatory components Nicastrin, Presenilin Enhancer 2, and Anterior pharynx defective 1 (APH-1) [110] [**FIGURE I7**]. Mammals have two different Presenilin isoforms and at least two APH1 isoforms, and different combinations of these proteins are supposed to play different functions *in vivo* [111].

In the absence of NICD, CSL (the mammalian homologues are CBF1 in human and RBP_{JK} in mice) is bound to DNA together with nuclear co-repressor and histone deacetylases (HDAC) to suppress transcription. In the presence of NICD, this complex is displaced and a complex that includes NICD, RBP_{JK} and Mastermind-like (MAML) is then formed, converting RBP_{JK} protein from transcriptional repressor to an activator [112]. The principal and more general targets of Notch signaling are the Hairy Enhancer of Split family genes. Three domains that are conserved from nematodes to mammals compose the RBP_{JK} factor: the N-terminal domain, the β-trefoil domain and the C-terminal domain [113]. The N-terminal and the β-trefoil domains are necessary for DNA binding, and the β-trefoil domain also mediates binding to the RAM domain of the NICD. The C-terminal domain binds the ANK domain of NICD and the N-terminal domain of MAML [114]. MAML proteins are very specific Notch co-activators that share a helical structure. The N-terminal region of the helix is involved in binding to RBP_{JK} and NICD whereas the C-terminal part interacts with CBP/p300 and is necessary to promote transcriptional activation [115-117]. Duration of the Notch signal is strictly regulated, and it is mainly dependent on MAML, which promotes CDK8-mediated phosphorylation of specific residues of the PEST domain and the subsequent degradation of NICD [118].

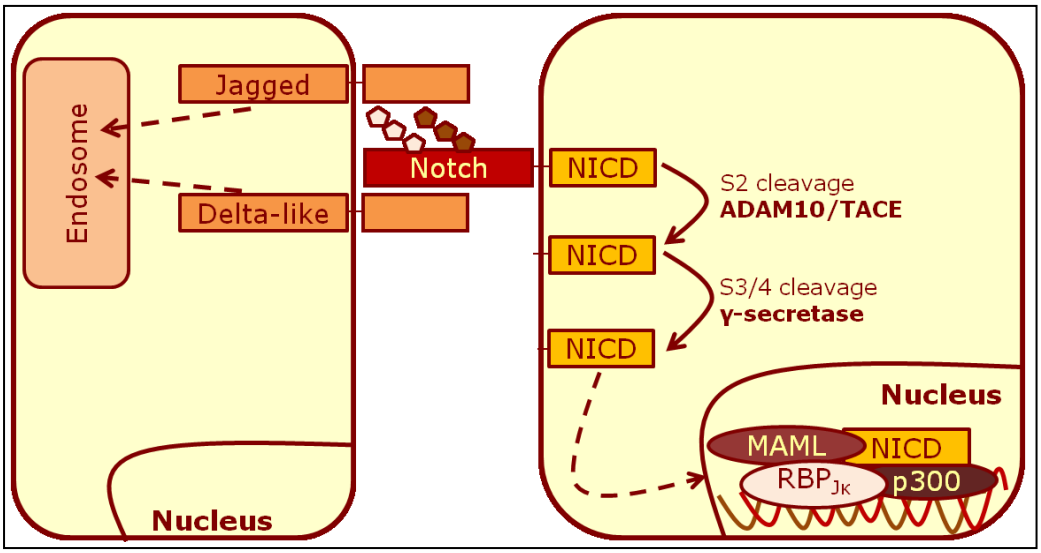

FIGURE I7. Summary of canonical Notch signaling activation. Ligand binding initiates two successive proteolytic cleavages (S2 and S3). The first is mediated by an ADAM that occurs in the extracellular domain. S2 cleavage allows access of the γ-secretase complex, which is responsible for the second proteolytic cleavage (S3), which occurs within the trans-membrane domain and liberates the NICD. The NICD translocates to the nucleus, where it interacts with RBP_{JK}, MAML and co-activators (p300).

I2.3.b Notch target genes

Primary Notch target genes include two families of evolutionarily conserved basic helix-loop-helix (bHLH) transcription factors: *Hes* (Hairy and E (spl)) and *Herp* (*Hes* related repressor protein, also known as *Hey*, *Hesr* or *Hrt*).

The HES family comprises seven members, named *Hes1* through *Hes7* and with the exception of *Hes2* and *Hes3*, all of them are established targets of Notch canonical signaling [119-121]. The HEY family includes three members, *Hey1* and *Hey2* and *HeyL*. The HES and HEY proteins have a high degree of structural similarity. Homo- and hetero-dimerization of Hes and Hey or association with other bHLH proteins occurs through the bHLH domain and the specificity of DNA binding is influenced by the composition of the dimers [122]. Generally, Hes and Hey proteins act as transcriptional repressors, a common mechanism of action that is mediated by the bHLH domain, which confers to the Hes protein the ability to recruit HDAC activities. In addition, the WRPW motif allows mammalian Hes proteins to recruit Transducin-Like Enhancer of Split factors and, as a consequence, induce the formation of a transcriptional repressor complex [120]. Different mechanisms of transcriptional regulation involve interactions with other bHLH factors and the core transcriptional machinery [122].

Although Hes and Hey are the best-known and most universal targets (and effectors) of Notch signaling, $RBP_{J\kappa}$ binding sites have been identified in a number of additional gene promoters, indicating the existence of other potential Notch targets, such as *Ccnd1* (cyclin D1) [123], *Cdkn1a* (P21) [124], *Ptcra* (pre-Tα, pre-T cell receptor alpha chain) [125], *Gata3* [126], *c-Myc* [127], *Gata2* [128] or *Il7r* [68].

I2.4. Mice models for studying Notch

Since both humans and mice, contain a single *Csl/Rbp$_{J\kappa}$* gene, inactivation of *Rbp$_{J\kappa}$* is the easiest way to study the phenotypes produced by Notch signaling lack-of-function. In this sense, conventional inactivation of *Rbp$_{J\kappa}$* in mice causes lethality during early embryogenesis due to multiple vascular abnormalities [129].

Notch1 and Notch2 share a high degree of similarity; however they do not have a redundant function during development. Thus, Notch1 deletion leads to early embryonic death. Homozygous mutant embryos die before 11.5 days of gestation; the histological analysis revealed that is not attributable to defects in placentation or vascularization, but extensive cell death [130]. In contrast, Notch2 deletion leads to embryonic and perinatal lethality due to cardiovascular and kidney defects [131]. Notch3 has a slightly different structural organization than Notch1 and Notch2, and shows a reduced trans-activation activity [132]. Notch3 expression is limited to vascular smooth muscle cells, the central nervous system, and selected populations of thymocytes and osteoclasts. Likely Notch3 deletion in mice is not lethal, although its constitutive activation is responsible for the cerebral autosomal-dominant arteriopathy with subcortical infarcts (CADASIL) syndrome in humans [133]. Notch4 plays a role in embryonic vascular morphogenesis, but it is dispensable for development since its functions overlap with those of Notch1 [134]. Specific activation of Notch4 in endothelial cells causes arterio-venous malformations in the mice brain [135].

With the exception of *Dll3*, genetic deletion of Notch ligands causes developmental defects and embryonic lethality, indicating that DSL ligands have no overlapping functions. In *Dll1*-deficient mouse embryos the segments have no cranio-caudal polarity and no epithelial somites are formed [136]. Mice with mutations in *Dll3* are viable and present a "pudgy" phenotype, characterized by vertebral and rib deformities secondary to defects in somite patterning [137]. *Dll4$^{-/-}$* embryos die before E10.5 due severe and precocious vascular defects [138]. *Jagged2* deficient mice die perinatally because of defects in craniofacial morphogenesis [139]. Mice homozygous for

the *Jagged1* die from hemorrhage early during embryogenesis, exhibiting defects in remodeling of the embryonic and yolk sac vasculature [140].

By using knockout mice models for *Hes* and *Hey* genes, it has been also possible to study the contribution of different Notch downstream effectors to the Notch LOF phenotypes. For example, it has been shown that HES1, 3, and 5 are involved in maintaining the pools of precursor cells in its undifferentiated state during development and adult life in several tissues [141-143]. Hes7 plays a critical role in somite segmentation and regulates the expression of *Lfng* during mouse development [144]. Hes6, a suppressor of HES1 activity, is expressed during neural development [145]. Hey1 and 2 and HeyL are required for normal vascular development [122]. The deletion of Hey2 or the combined deletion of Hey1 and HeyL impairs vascular development in mice, whereas the dual inactivation of Hey1 and Hey2 phenocopies the loss of Notch1 [146-149].

I3. The physiology of the intestine

I3.1. Functions of the intestinal tract

The gastrointestinal tract begins with the mouth, leads to the esophagus and extends through the stomach, small and large intestine, to end at the anus. The upper gastrointestinal tract includes the mouth cavity, esophagus and stomach. The lower gut includes the small intestine, the large intestine and the anus.

The intestine is divided in different regions [**FIGURE I8**]:

- Small intestine:
  - Duodenum, where the digestive juices from pancreas and liver are released.
  - Jejunum, in the midsection of the intestine, connecting duodenum to ileum.
  - Ileum, where most of the soluble molecules are absorbed and liberated into the blood.
- Large intestine:
  - Caecum
  - Colon (ascending, transverse, descending and sigmoid colon)
  - Rectum

Intestinal tract function is to absorb and digest nutrients from the diet and eliminate those that are not usable. The small intestine is required for absorption of most of the water and electrolytes (sodium, chloride, potassium) and essentially all organic diet molecules (including glucose, amino acids and fatty acids). In the colon takes place the terminal stage of digestion, and its main function is to form and store feces, which involves the additional recovery of water and electrolytes and the inclusion of bacteria and mucus.

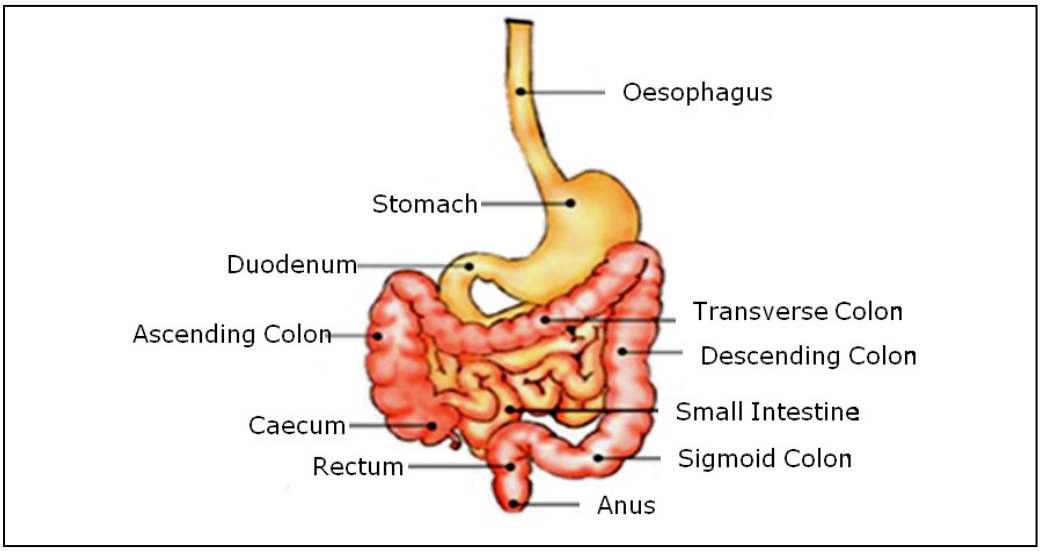

FIGURE I8. Gastrointestinal tract and all its parts.

I3.2. Layers and cell types in the gut

The gastrointestinal tract has a specific histology that reflects its functional specialization. The gastrointestinal tract can be divided into four concentric layers [**FIGURE I9**]:

- Mucosa: is the innermost layer of the gut that is surrounding the lumen, or space within the tube. This layer is in direct contact with food (or bolus), and is responsible for absorption and secretion, important processes during digestion. The mucosa can be divided into: Epithelium, *Lamina propria* and *Muscularis mucosae*. The mucosa is highly specialized and its structure reflects the varying needs of the different organs and regions of the gut. For example, in the stomach it is responsible for maintaining the low pH, for absorbing a multitude of substances in the small intestine, and for recovering water in the large intestine.

- Submucosa: consists of a dense irregular layer of connective tissue with large blood vessels, lymphatics, and nerves branching into the mucosa and muscularis externa. It contains the Meissner's plexus, and the enteric nervous plexus, situated on the inner surface of the *muscularis externa*.

- *Muscularis externa* (the external muscle layer): consists of an inner circular layer and a longitudinal outer muscular layer. The circular muscle

layer prevents food from traveling backward and the longitudinal layer shortens the tract. The coordinated contractions of these layers are called peristalsis and propel the bolus, or balled-up food, through the gastrointestinal tract. Between the two muscle layers are the myenteric or Auerbach's plexus

- Adventitia or serosa: consists of several layers of epithelia. When the adventitia is facing the mesentery or peritoneal fold, the adventitia is covered by a mesothelium supported by a thin connective tissue layer, together forming a serosa, or serous membrane.

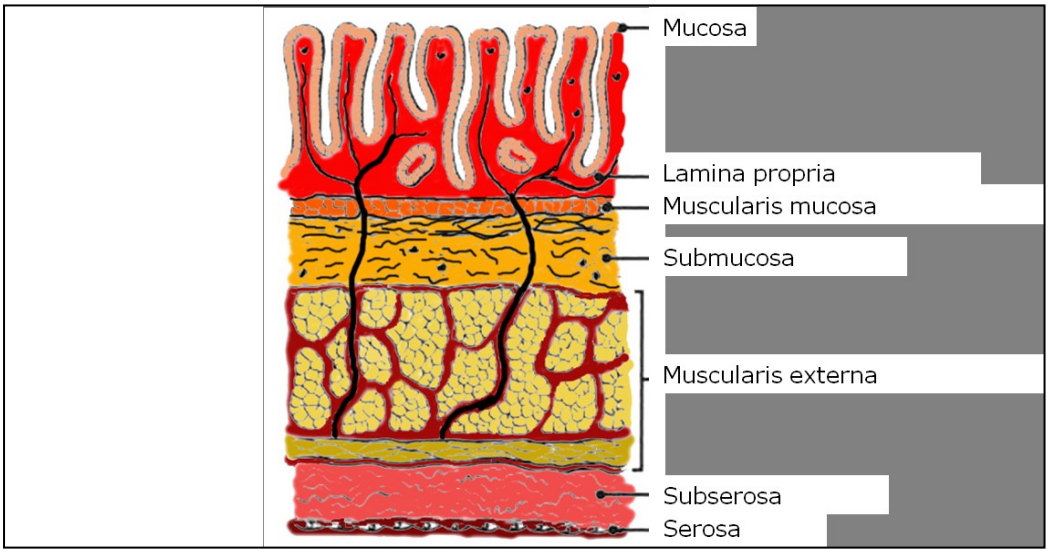

FIGURE I9. Different layers in the gut: Mucosa (epithelium, lamina propia and muscularis mucosae), submucosa, muscularis externa and serosa. Image adapted from AJCC Cancer Staging Manual, 7thEdition.

Different cell types populate the intestinal epithelium, including those involved in secretion, absorption, and hormone production:

- Absorptive cells, called enterocytes in the small intestine and colonocytes in the colon, constitute the majority of cells in the epithelial layer. They are responsible for the absorption of nutrients from the intestinal lumen and its transport across the epithelium to allow absorption through the capillaries of the underlying layer. These are polarized cells with microvilli on the apical surface facing the lumen, are also characterized by a complete range of cell-cell junctions and a complex pattern of expression of integrins along the crypt-villus axis (reviewed in [150]).

- Goblet cells are scattered among the absorptive cells. They are responsible of secreting mucus, which is necessary for the movement

and the effective dissemination of intestinal contents, and also provides protection against shear stress and chemical damage [151].

- Entero-endocrine cells are also scattered throughout the epithelial layer and include a heterogeneous population of cells responsible for releasing hormones and digestive enzymes.

- Paneth cells are mainly found in the bottom of the crypts of the small intestine and secrete a number of antimicrobial molecules when exposed to bacteria or bacterial antigens [152].

I3.3. Maintenance of gut architecture

The structure of the epithelium in the small and large intestine present many similarities, however their architecture is quite different [**FIGURE I10**]. In the small intestine, the epithelial layer covers finger-like villus structures and adjacent invaginations called crypts of Lieberkühn. This arrangement provides a large absorptive area to this epithelium. The colonic epithelium does not contain villi; instead deeper invaginations represent a compressed version of the crypt-villus architecture.

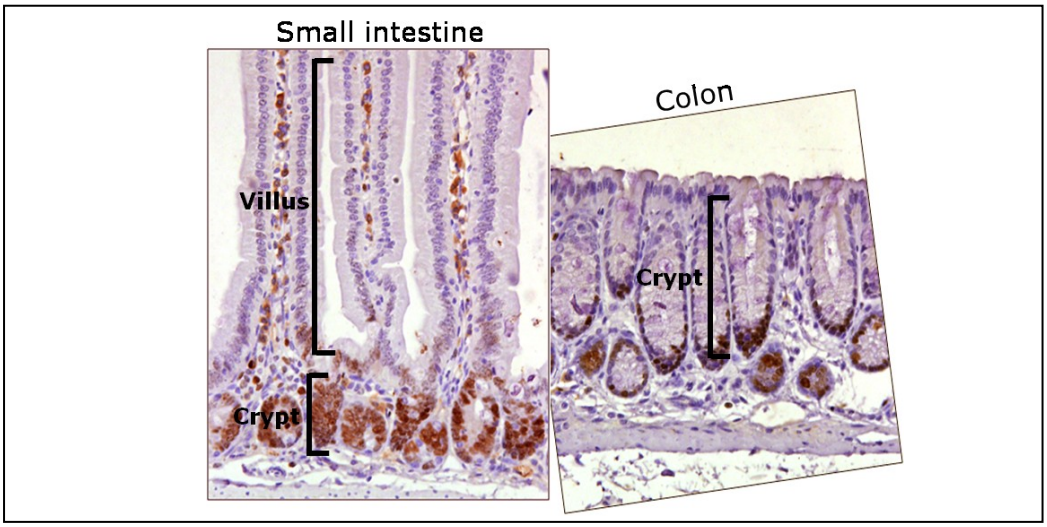

FIGURE I10. Histological differences between small and large intestine. Images of murine small and large intestine. Representative images of Ki67 staining were obtained in an Olympus IX-10 at 400X.

The intestine constitutes the most rapidly self-renewing tissue in the adult mammals. In the mouse, intestinal epithelium turns over entirely within 3–5 days [153] and the massive rate of cell production by the transit-amplifying

(TA) crypt compartment is compensated by apoptosis at the tip of the villus. The proliferating crypt precursors and differentiated villus cells form a contiguous sheet of cells that is in perpetual upward movement. Stem cells reside in the bottom of the crypt and escape of this migration. These slowly cycling stem cells produce the transit-amplifying progenitor cells that are capable of differentiating toward all epithelial lineages [154, 155] [**FIGURE I11]**. Paneth cells do not migrate upward; as a result, they accumulate at the bottom of crypts, where they remain in contact with the stem cells.

Stem cells, which reside in the intestinal tissue for the entire life of the organism, must be especially protected. The proximity of Paneth cells to stem cells confers a degree of protection through the provision of antimicrobial peptides in their surrounding area [156] and provide specific signaling that is required for stem cell differentiation [157]. Furthermore, when stem cells divide, the newly synthesized DNA is passed to the first generation of TA cells, while the original set of chromosomes stays in the mother cell during asymmetric divisions [158, 159]. This ensures that replication errors are specifically accumulated in cells whose lifetime is limited.

I3.4. Intestinal stem cells (ISC)

In 1981, Bjerknes and Cheng demonstrated the existence of a ISC compartment located at the +4 position above the Paneth cells [160] [**FIGURE I11**]. Recent studies using *in vivo* lineage tracing have shown that cells expressing *Bmi1* predominantly mark +4 position and are able to give rise to all four epithelial lineages [161]. It has been proposed that BMI^+ cells are slowly cycling stem cells. In addition, cells expressing the stem cells marker Musashi-1 (*Msi1*) are found in the same position and might represent a quiescent stem cell population [162]. Alternatively, a crypt-based columnar cell (CBCs) population that specifically express Lgr5 and is located at the bottom of the crypts, intermingled with the Paneth cells has been proposed as the proliferating ISC compartment [**FIGURE I11**] [163]. Lineage tracing has shown that $Lgr5^+$ cells behave as a long-lived and cycling multipotent stem cell population [164]. Moreover, it has been demonstrated that one single $Lgr5^+$ cell can form a long-lived, self-renewing "minigut" in culture [165]. $Lgr5^+$ stem cells are distinct from +4 LRCs in that Lgr5 stem cells do not retain DNA labels and are sensitive to CDC25 inactivation, supporting their proliferating feature [162]. Thus, the intestine contains a quiescent stem cell population at the +4 position and a cycling Lgr5 stem cell population among the Paneth cells.

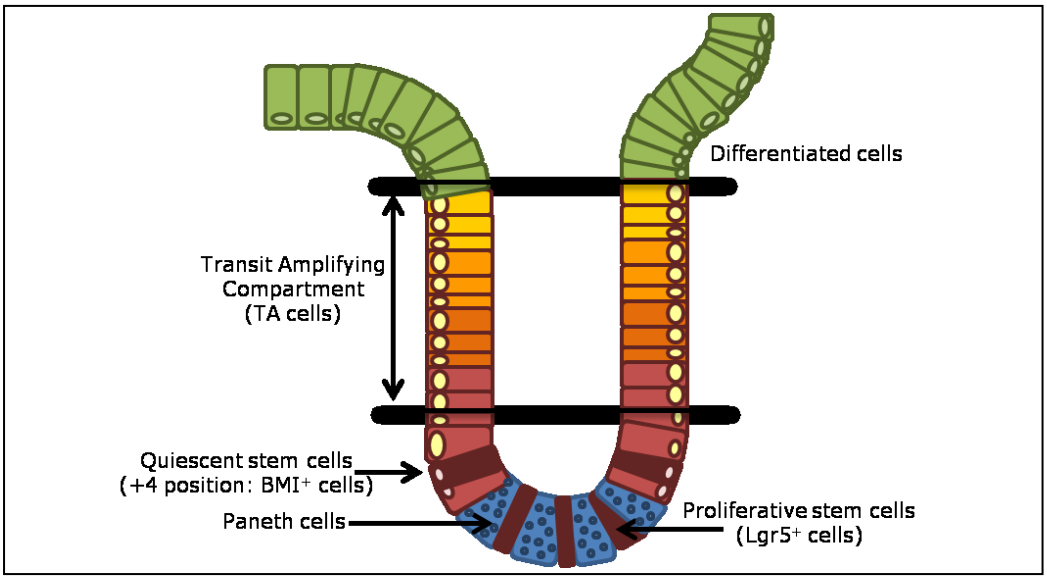

FIGURE I11. Representation of different cell types located in the intestinal crypts.

I4. Colorectal cancer

Normal intestinal epithelium is capable of continuously and perpetually renewal, while maintaining a precise balance between proliferation, differentiation, cells migration and cell death. Intestinal tumorigenesis is initiated when any of these mechanisms become altered, thus leading to increased proliferation, reduced differentiation and altered tissue homeostasis. Colorectal cancer (CRC) represents one of the principal oncologic pathologies of the intestine, affecting humans [166]. CRCs is initiated in the colon (or the rectum) as an epithelial hyperplasia that becomes increasingly dysplastic resulting in aberrant crypt foci [167]; these progress to benign tumors termed adenomas or adenomatous polyps, that can eventually develop into malignant tumor stages termed carcinomas. However, it is still unclear the cellular origin of the transformed cells that will generate the malignant tumors. Some authors propose that tumors arise from neoplastically-transformed stem cells at the base of the crypt, that progress to adenomas, which next expand by crypt fission to the surface epithelium in a 'bottom-up' fashion [168, 169] [**FIGURE I12-A**]. Alternatively, others suggest that adenomas arise from dysplastic cells located on the surface epithelium, that are next expanded by lateral migration, and grow down into the crypt through a 'top-down' mechanism [170] [**FIGURE I12-B**].

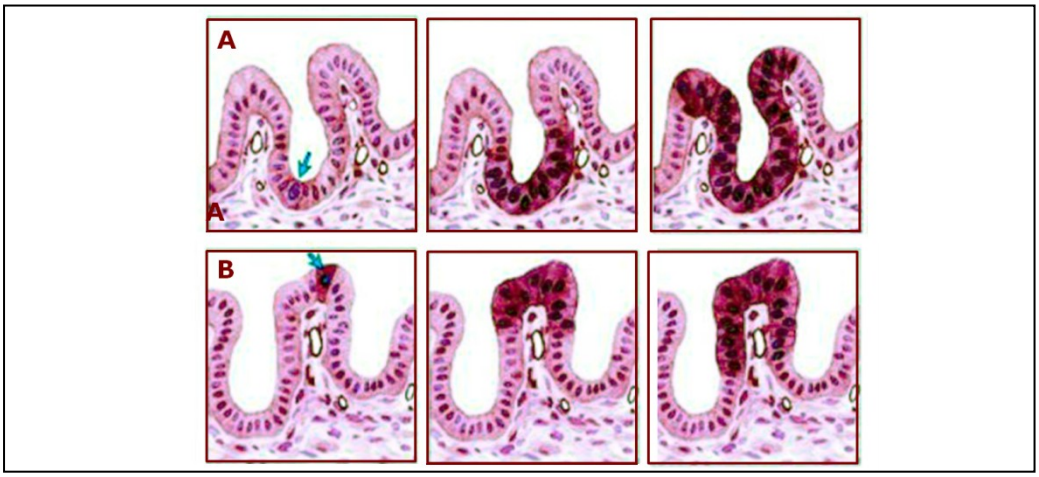

FIGURE I12. Models of morphogenesis of sporadic adenomatous polyps (adapted from Shih et al.). (A) Transformation of a single epithelial cell occurs at the base of the crypt (arrow). The transformed cell proliferates and passively migrates upward as a result of routine epithelial turnover and gradually replaces the normal epithelium from bottom-to-up. (B) Initial transformation event occurs in an epithelial cell in the inter-cryptal zone and the migration is from top-to-bottom.

CRC is one the most common causes of cancer death in Western countries (behind smoking-related cancers), and by the age of 70 years about half of the population have developed one or more intestinal adenomas. Around 15% of CRCs occur in the context of a familial predisposition, such Familial

Adenomatous Polyposis (FAP) disease, whereas the remaining (85%) arises sporadically. FAP individuals develop hundreds to thousands of adenomatous polyps in the colon and rectum at an early age, a subset of which will progress to malignant cancers if they are not surgically removed [171]. Germline mutations in the *Apc* gene, which leads to the activation of the Wnt/β-catenin pathway, were found to be the essential genetic event responsible for FAP. Subsequently, somatic mutations in the same gene have been identified in the majority (up to 85%) of sporadic CRCs and benign intestinal neoplasms. In 90% of these cases, mutation results in truncation of the APC protein [172].

The most severe and common inactivating mutations in the *APC* gene are located between codons 450 and 1578, and represent the earliest genetic alterations so far detected in the genesis of CRCs [173, 174]. Thus, mutation of the *APC* gene is linked to the initiation of intestinal tumor and likely represents a pre-requisite for entry into this process. *APC* is considered a classic tumor suppressor gene as both alleles must be inactivated for loss of tumor suppressing activity. For FAP and CRC patients, the molecular mechanisms underlying the lack of APC protein can be a second truncating mutation or, an allelic loss of the second allele (termed loss-of-heterozygosity). The second *APC* mutation represents the limiting step for tumor initiation [175-177]. Heterozygous activating mutations in the gene encoding β-catenin (*CTNNB1*) are also found in about 10% of the remaining cases of sporadic CRCs. *APC* and *CTNNB1* mutations are mutually exclusive [178], and both result in the stabilization and accumulation of β-catenin in the nucleus of a cells.

Although *APC* mutations can be considered the driving force in CRC initiation, mutations or alterations affecting oncogenes like K-Ras and tumor suppressors, like p53 are needed for tumor progression [179]. Several studies point out that tumor progression in the intestine is due by the selection of specific genetic alterations that accumulate in a strict succession. In fact, while mutation events are stochastic, the sequence in which they accumulate is non-random, supporting the argument that only certain mutations confer a selective advantage at a given stage of a tumor's natural history. Fearon and Vogelstein [180] were the first to propose such a sequential model for CRC genesis [**FIGURE I13**].

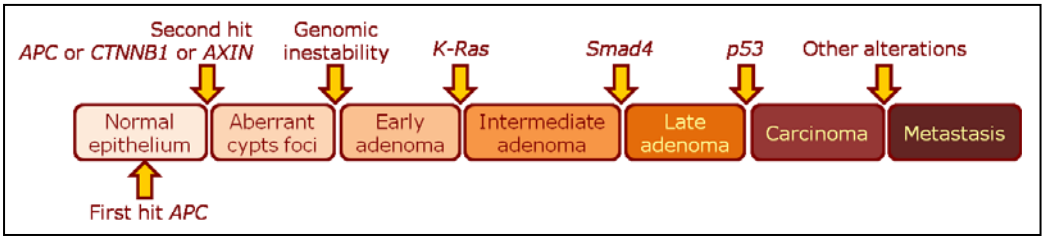

FIGURE I13. Genetic model of colorectal carcinogenesis (adapted from Fearon and Vogelstein). Mutations in *Apc*, *Ctnnb1* (β-catenin) or *Axin* genes are required for tumor initiation. Subsequent progression towards malignancy is accompanied by genomic instability and sequential mutations.

I5. Wnt and Notch in the intestinal tract

I5.1. Wnt Signaling in the normal intestine

Wnt signaling plays a crucial role during development of the gastrointestinal tract, in particular in the endoderm specification and gut tube patterning, as well as in intestinal stem cell maintenance [181, 182]. Activation of Wnt signaling is required in the posterior part of the gut tube for intestinal lineage specification, whereas in the anterior part, stomach and esophagus formation require Wnt repression [182, 183].

In the adult intestine, Wnt/β-catenin signaling has emerged as an essential signal for maintaining ISC self-renewal. Wnt-activated cells are restricted to the base of the small intestinal and colonic crypts and highest in numbers in the proximal small intestine, decreasing in frequency in a gradient toward the large intestine. Interestingly, the majority of the Wnt-receiving cells did resides in the stem cell niche of the crypt base and do not extend into the proliferative transient-amplifying cell population [184]. Accordingly, in *Tcf4*$^{-/-}$ mice the crypts of the small intestine were lost, whereas the differentiated villus epithelium remained unaffected [185]. Moreover, conditional deletion of *Ctnnb1* using Cyp450-CRE or Villin-CRE^{ERT}, and transgenic expression of *Dkk1* led to a rapid disappearance of crypts and the disruption of the intestinal epithelium in adult mice [186]. These results indicate that a TCF4-driven target gene program downstream of Wnt/β-catenin is essential to maintain intestinal crypt stem cells. This genetic program has been identified, including *c-Myc* and the intestinal stem cell marker *Lgr5* [187]. Importantly, *Lgr5* expression is highly restricted to the intestinal proliferative stem cell compartment located in the bottom of the crypts, a property that has been used by Van der Flier and co-workers to determine the intestinal stem cell transcriptome [188]. The transcription factor *Ascl2* is one of the genes of the stem cell signature and, in fact, it plays an essential role in the maintenance of LGR5^{+} intestinal stem cells. Since Wnt does not regulate *Ascl2*, these findings indicate that additional Wnt-independent signals are required for regulating intestinal stem cell identity.

I5.2. Wnt Signaling in CRC

As previously mentioned, defects in Wnt signaling can initiate intestinal cancer. The first gene of the Wnt pathway to be implicated in human cancer was APC, a gene that is silenced in 85% of human colon cancers (reviewed in [189-192]). Consequently, numerous mouse models have been generated that resembled human colon cancer, including different APC mutants, as well as mice over-expressing N-terminally truncated β-catenin [193-196]. The first

conditional mice carrying gain-of-function mutations of β-catenin in the intestinal epithelium was published by Harada *et al* [197]; These animals developed numerous polyps in the small intestine (up to 3000 per mouse at a young age) that formed contiguous sheet-like structures, as well as micro-adenomas in the colon mucosa. Other models of β-catenin GOF in the intestine activated the transgene post-natally using a CRE driven by the fatty acid binding protein gene promoter (Fabp-CRE). These mutant mice developed well-separated polyps at the crypt intervillus region (200–700 per mouse) [197]. In both models, polyps were composed uniquely of enterocytes. Interestingly, the phenotype of the GOF mutants for β-catenin is very similar to the mutants in the *Apc* gene, indicating that *Apc* mutation acts through β-catenin in adenoma formation. More recently, Clarke and collaborators genetically demonstrated that *c-Myc* is an essential downstream target gene of APC/β-catenin in the intestine. The conditional ablation of *c-Myc* using an inducible Cyp450-CRE was able to rescue APC-mutant tissue, restoring normal proliferation, inducing differentiation, and increasing crypt size [198].

Although different colorectal cancer mice models that are available represents a powerful tool for studying tumor initiation and progression, identification of the cells responsible for initiating and maintaining the tumors has remained elusive until now. Several recent studies addressed this question by conditionally ablating the *Apc* gene in different cellular compartments [199]. Specific elimination of APC in ISC, taking advantage of the Lgr5-CRE mouse line, resulted in the fast transformation of stem cells into tumor cells. These transformed cells remained located at the crypt bottom and generated multiple $LGR5^+$ adenomas in the small intestine and the colon within 3–5 weeks. In contrast, when *Apc* was deleted in short-lived transit-amplifying cells, adenoma growth was rapidly blocked. These data indicate that stem-cell-specific loss of APC results in fast and sustained tumorigenic transformation in mice. Coincident with this publication, another work in which GOF mutant of β-catenin was driven by a Prom1/CD133-CRE appeared, with comparable results [200]. *Prominin1* expression is restricted to the bottom crypts of the small intestine overlapping with $LGR5^+$ cells, although $Lgr5^+Prom1^+$ double-positive cells are not present in the colon. Accordingly, when Prom1-CRE was used to activate β-catenin expression, mice developed dysplasia in the small intestine, but not the colon [201]. Taken together, these studies demonstrated that intestinal stem cells could be transformed into CSC by aberrant Wnt/β-catenin activation. Consistent with this idea, Vermeulen et al have recently characterized the micro-environmental requirements of the colonic stem cell niche. Notably, they demonstrated that specific stromal-derived factors, such HGF, are capable of restoring the stem cell phenotype from more differentiated tumor cells.

Moreover these cancer stem cells are distinguished by the presence of high Wnt activity [202].

I5.3. Notch Signaling in the normal intestine

The Notch signaling pathway regulates intestinal epithelial cell fate and differentiation of the four specialized epithelial lineages of the gastrointestinal tract. Increased levels of Notch activity negatively regulate the transcription of the *Math1* gene through HES1, and thus the secretory lineage. Consistently, mice with targeted deletion of the *Math1* gene also fail to develop goblet, Paneth, and entero-endocrine cell compartments in the small intestine and these *Math1* negative epithelial cell progenitors exclusively form enterocytes [203]. Conversely, reduced Notch activity increases *Math1* expression causing elevated goblet cell, Paneth, and entero-endocrine differentiation in the small intestine, a phenotype that is comparable with that observed in the *Hes1* knockout mice [204, 205]. In addition to the effects of Notch signaling in inducing differentiation of gut progenitor cells toward the absorptive lineage (at expenses of the secretory lineages), Notch activation is required to maintaining the proliferative status of stem cells in the crypt [205-207].

Notch1 and Notch2 receptors act redundantly in mediating Notch signaling in the intestine as only the simultaneous inactivation or antibody-mediated inhibition of both receptors resulted in the complete conversion of the crypt progenitors into post-mitotic goblet cells [208, 209]. Recently, DLL1 and DLL4 have been identified as the physiological Notch ligands responsible for Notch activation in the murine intestinal crypts and demonstrated that they are required for the maintenance of intestinal stem cells [210].

I5.4. Notch signaling in CRC

Notch signaling plays an oncogenic role in CRC. Expression levels of Notch signaling genes including *Math1* [211], *Hes1* [212] or *Ephb2* [213] are altered in CRC tumors. Activation of Notch signaling emerges to be associated with the development of primary CRC rather than metastatic colon cancers [214]. The mechanistic contribution of Notch activation is not well understood in CRC. Moreover, mutations in Notch signaling components have not been reported.

The aberrant activation of the Notch signaling has been associated with the development of colon cancer. Knockdown of Notch1 significantly inhibited the

proliferation, colony formation, and tumor-sphere formation of SW480 and HT-29 cells, induced apoptosis and cell cycle arrest at G_0/G_1 phase, and mitigated the development and growth of implanted colon cancers *in vivo*. In contrast, Notch1 over-expression promoted the proliferation, colony formation, cell cycling, and tumor-sphere formation of colon cancer cells in vitro and the development and growth of implanted colon cancers *in vivo*, but it inhibited spontaneous apoptosis [215]. Moreover, the expression of JAG1 increased in half of human colon tumors [216]. Additionally, by *in situ* hybridization analysis, expression of Notch ligands, receptors, fringe genes and *HES1* were tested in human CRC. In a small cohort of tumors, *JAG1*, *NOTCH1*, *LFNG* and *HES1* were expressed at levels similar to, or higher than, levels observed in the crypt. However, the absolute expression levels did not correlate with patient survival [217]. Furthermore, examination of *HATH1* (human orthologue of *Math1*) expression in multiple colon tumor samples and colon cancer cell lines reveals a dramatic decrease in *HATH1* expression. *HATH1* expression in the HT29 colon cancer cell line can significantly inhibit its proliferation and anchorage-independent growth both *in vitro* and *in vivo* [218].

However, Notch activation in CRC is usually associated with the activation of other signaling pathways. For instance, K-RAS mutations are frequent in colorectal cancer (CRC) and are associated with clinical resistance to treatment with the EGFR-targeted monoclonal antibodies. DLL4 inhibition in CRC cells reduces tumor growth and stem cell frequency. Anti-DLL4 was efficacious against both wild type and mutant K-RAS colon tumors as a single agent decreasing colon cancer stem cell frequency while promoting apoptosis in tumor cells [219]. Similarly, it has been well-documented the association of matrix metalloproteinase-9 (MMP-9) and receptor Notch-1 over-expression in colon cancer. MMP-9 is also up-regulated in colitis, where it modulates tissue damage and goblet cell differentiation via proteolytic cleavage of Notch1 [220]. Likewise, it has been established the molecular link between Notch/Akt. Inhibition Notch-mediated pro-survival signaling facilitates JNK-mediated apoptosis in colon cancer cell lines [221]. As well, a remarkable synergy between Notch and Wnt signals results in inducing the formation of intestinal adenomas, particularly in the colon [222]. In the same way, the relationship between Notch signaling and KLF4 expression was investigated by Ghaleb et al in intestinal epithelial cells. KLF4 levels were increased in DBZ-treated cells. Conversely, over-expression of Notch signaling suppresses KLF4 expression in intestinal tumors and colorectal cancer cells [223]. Moreover, Wnt, Notch and TGFβ signaling pathways control tissue homeostasis and tumor development in the gut. The relationship between these pathways was investigated in a series of primary colorectal tumors and their corresponding metastases. When compared to normal mucosa, primary colorectal tumors

showed a marked increase in the levels of cytoplasmic vimentin and nuclear β-catenin, phospho-SMAD2 and HES1. Surprisingly, many regional and distant metastases have lost nuclear HES1 and pSMAD2, suggesting that the activity of the Notch and TGFβ pathways is reduced in secondary colorectal tumors [214].

I5.4.a Notch signaling in angiogenesis

Angiogenesis is an important requisite for solid tumor development and subsequent metastasis. The major driving force of angiogenesis is the angiogenic growth factors that derive from the tumor tissue itself. Among them, vascular endothelial growth factor (VEGF) is the most potent and prevalent one [224, 225]. Over-expression of VEGF has been identified in the vast majority of human solid tumors including CRC [226], and a close correlation between high levels of VEGF with angiogenesis, metastasis and poor prognosis has been demonstrated in patients with CRC [227, 228].

Different Notch signaling components such as JAG1, Notch1, Notch4 and DLL4 are highly expressed in endothelial cells [71, 229-231] and it has been shown that Notch activation affects multiple aspects of vascular development [232-234] and angiogenesis under physiological and pathological conditions. Specifically, the effects of blocking DLL4 were analyzed using the neutralizing monoclonal antibodies against DLL4 (HMD4-2). Inhibition of DLL4-Notch signaling suppressed the *in vivo* tumor growth with marked decrease of tumor vasculature [235]. On the contrary, recently it has been published that JAG1 is a potent pro-angiogenic regulator in mice that antagonizes DLL4-Notch signaling. These findings establish that the equilibrium between two Notch ligands regulates angiogenesis [71].

A recent report demonstrates the importance of Notch pathway during metastatic process. Expression of Aes, which functions as an endogenous metastasis suppressor, was decreased in liver metastases compared with primary colon tumors in both mice and humans. Aes inhibited Notch signaling by converting active $RBP_{J\kappa}$ transcription complexes into repression complexes on insoluble nuclear matrix. Genetic depletion of Aes in intestinal polyposis mice caused tumor invasion and intravasation that were suppressed by Notch signaling inhibition [70].

I5.4.b Notch signaling in CSCs

In the last few years, growing evidences indicate that tumor cells derive from cancer stem cells (CSCs). These cells are not only responsible for tumor

initiation, progression and relapse but also may well be responsible for resistance of cancers to conventional therapy. So far, CSCs have been identified in a number of human malignancies, including CRC.

Common stem cell markers such as CD133, MSI1, CD44, EpCAM and CD166 are widely expressed in colon cancer [200, 236], further confirming the putative role of CSCs in CRC development. However, whether Notch, a crucial regulator of normal stem cells, plays any role in colon CSC generation or maintenance is not yet defined. However different data support an involvement for Notch signaling in regulating colorectal CSCs: **(1)** stem cell markers are expressed in the intestinal crypts where Notch is active [157]; **(2)** stem cell markers such as *Ascl2* or *Olfm4* are Notch targets [237-239]; **(3)** the stem cell marker MSI1 is a positive regulator of Notch signaling [240, 241]; **(4)** inhibition of Notch signaling (pharmacologically or genetically) results in the elimination of the crypt compartment in mice [69, 210, 242].

Recently some publications have demonstrated the role of Notch signaling in CSC. Notch signaling is 10 to 30-fold higher in CSC compared with widely used colon cancer cell lines. Notch prevents CSC apoptosis through repression of cell cycle kinase inhibitor p27 and transcription factor MATH1 [243].

I5.4.c Notch signaling and CRC therapy

Studies in *Apc*-mutant mice have showed that Notch signaling is highly active in intestinal crypts and in the spontaneous adenomas in Apc^{Min} mice [69, 239]. Blocking Notch signaling by conditional removal of $Rbp_{J\kappa}$ in mice or treatment with γ-secretase inhibitor Dibenzazepine (DBZ) caused a complete and rapid conversion of proliferative cells in the intestinal crypts and adenomas into post-mitotic goblet cells [69]. In addition, targeting Notch in CRC, with chemical inhibitors of γ-secretase such as DBZ and Compound E significantly suppressed cell growth in human colorectal cancer cell lines HT29 and HCT116 [223, 244], and sensitize colorectal cancer cells to apoptosis induced by the chemotherapeutic agent taxane [245], or oxaliplatin- and 5-fluorouracil [246]. A different approach for targeting Notch has been developed using specific antibodies or peptides targeting Notch receptors or their ligands. For example, antibodies against DLL4 have been shown to suppress tumor angiogenesis [232, 247]. However, all these Notch-targeted based therapeutically approaches require a proper stratification of the patient populations to be effective. For example, patients with tumors carrying truncated forms of Notch or mutations in the ligase involved in NICD degradation (FBW7) may not respond to γ-secretase inhibitors. In this sense

it has been already demonstrated that T-ALL cell lines carrying *FBW7* mutations are resistant to γ-secretase inhibitors [248].

I6. Wnt and Notch interactions

Wnt signaling exhibits interactions with other signaling pathways, such as BMP, Hh and Ras [249-254]. Furthermore, association of Wnt and Notch pathways has been consistently identified in different systems [255]. For example, Wnt and Notch signaling pathways are both activated in the undifferentiated compartment of the intestine, and their activation is required for the maintenance of the stem cell compartment. In particular, it has been recently demonstrated that Paneth cells, that are in close association with the $LGR5^+$ ISC, express *Wnt3* and the Notch ligand *Dll4* being both essential signals for stem-cell maintenance [157]. In human primary melanoma, the oncogenic effect of Notch1 is mediated by β-catenin, which was up-regulated following Notch1 activation. Inhibiting β-catenin expression reversed Notch1-enhanced tumor growth and metastasis [256]. In colorectal cancer, it has been demonstrated that Notch signaling is downstream of β-catenin that induces *Jagged1* expression and Peignon *et al* have demonstrated that *Hes1* induction is mediated by β-catenin [239, 257]. Moreover, *Jagged1* has been identified as a direct transcriptional target of β-catenin in the stem cell compartment of the hair follicle [258]. In addition, it has been proposed that the Notch co-activator MAML1 could also work as a co-activator for β-catenin [259]. In *Drosophila* it has been shown that Notch can suppress the activity of Armadillo/β-catenin by promoting its degradation [260, 261].

Together, these data indicate that there are multiple interactions between Notch and Wnt pathways that are cell-type, species and context-dependent.

OBJECTIVES

OBJECTIVES

The aim of this project was to investigate the crosstalk between Wnt and Notch signaling pathways during the intestinal development and the intestinal tumorigenesis.

The specific objectives of this work were:

1. Determine whether there is a common transcriptional program for Wnt and Notch signaling pathways.
2. Study the dependence of Notch activation on Wnt/β-catenin activity or *viceversa*.
3. Investigate the contribution of Notch in the tumorigenesis in the Apc^{Min} mouse model.
4. Evaluate physical interactions between Notch and β-catenin in the intestine and study their functional relevance.
5. Characterize the differential role of Jagged1 in the intestinal homeostasis and tumoral process.

MATERIALS AND METHODS

MM1. Cell culture

All cells were grown in Dulbecco's modified Eagle's medium (DMEM) (Invitrogen) supplemented with 10% fetal bovine serum (FBS) (Biological Industries), 4.5g/l glucose (Life Technologies), 2mM de glutamine, 56U/ml penicillin and 56µg/l streptomycin. The incubator atmosphere was 5%CO_2, and the temperature was held constant at 37ºC.

The human CRC cell lines used were: HCT116, SW480 and Ls174T. As a human normal cell line used HS27, primary human fibroblast.

For the generation of Ls174T/dnTCF4/N1ICD clones, we transfected N1ICD plasmid to Ls174T/dnTCF4 cells (L8 clones [187], kindly provided by Dr. Hans Clevers, Hubrecht Institute, Utrecht, Netherlands) using PEI (See **MM2.1**). Stable transfectants were obtained after selection with 1mg/ml G418, 5µg/ml Blasticidine and 100µg/ml Zeocine and screened by western blot and immunofluorescence after doxycycline treatment. Those with higher dnTCF4 and N1ICD expression were selected.

The reagent SB216763 (Sigma) was used at 10µM/ml; Doxycycline (Sigma) was used at 1µg/ml; γ-secretase inhibitors: DAPT (Calbiochem, Cat.no-565770) and L685.458 (Sigma, L1790); PKF115–584 was a gift from Novartis.

MM2. Transfection protocols

Transfection is the process of introducing nucleic acids into cells. The term is used for non-viral methods in eukaryotic cells.

MM2.1 PEI transfection

- *Product Description:* jetPEI™ (Polyscience, Inc.) is a powerful transfection reagent that ensures effective and reproducible transfection with low toxicity. jetPEI™ is a linear polyethylenimine, synthesized and purified.
- *Chemical structure:* HO-(CH2)-2-(CH2-CH2-NH)-n-(CH2)-2-OH. JetPEI™ compacts DNA into positively charged particles capable of interacting with anionic proteoglycans at the cell surface and entering cells by endocytosis. It possesses the unique property of acting as a "proton sponge" that buffers the endosomal pH and protects DNA from degradation. Continuous proton influx also induces endosome osmotic swelling and rupture,

rupture, which provides an escape mechanism for DNA particles to the cytoplasm.

- *Protocol* for 10cm Ø plate transfection:
  - Dilute 3-5µl of PEI per 1µg of DNA into 1ml of DMEM serum free.
  - Mix gently and wait for 5min at room temperature.
  - Add x µg of DNA, mix and wait for 20-30min at room temperature.
  - Aspirate the medium of the culture and replace with 9 ml of fresh DMEM w/wo serum (depending on cell line).
  - Add the solution in the plate up to 10ml final volume.

MM2.2 siRNA transfection (Santa Cruz)

In a six well tissue culture plate, seed $2x10^5$ cells per well in 2ml antibiotic-free normal growth medium supplemented with FBS.

- *Solutions*:
  - *Solution A*: For each transfection, dilute 0.5µg of siRNA duplex into 100µl siRNA Transfection Medium (sc-36868).
  - *Solution B*: For each transfection, dilute 6µl of siRNA Transfection Reagent (sc-29528) into 100µl siRNA Transfection Medium (sc-36868).

- *Protocol* for 6-well plate transfection:
  - Add the Solution A directly to the Solution B using a pipette. Mix gently by pipetting the solution up and down and incubate the mixture 15-45min at room temperature.
  - Wash the cells once with 2ml of siRNA Transfection Medium (sc-36868). Aspirate the medium and proceed immediately to the next step.
  - For each transfection, add 0.8ml siRNA Transfection Medium to each tube containing the siRNA Transfection Reagent mixture (Solution A + Solution B). Mix gently and overlay the mixture onto the washed cells.
  - Incubate the cells O/N at 37°C in a CO_2 incubator.
  - Add 1ml of normal growth medium containing 2 times the normal serum and antibiotics concentration (2xDMEM) without removing the transfection mixture.
  - Incubate the cells for an additional 18-24h.
  - Aspirate the medium and replace with fresh 1x normal growth medium.
  - Assay the cells using the appropriate protocol 24-72h after the addition of fresh medium in the step above.

MM3. Analysis of protein expression by Western Blot

MM3.1. Analysis of endogenous proteins

- *Cell extract preparation*: wash the cells twice with PBS. Lyse cells with Lysis Buffer (10mM HEPES pH7.9, 1.5mM $MgCl_2$, 10mM KCl, 0.5mM DTT, and 1.5mM PMSF). Centrifuge the cell lysates at 13000rpm during 15min. Use 60-120µg of the supernatant for Western Blot analysis.
- *Electrophoresis and gel transfer*: separate the samples by 10-12% polyacrylamide gel electrophoresis (PAGE). After transference to a nitrocellulose membrane, analyze by Western Blot.
- *Western Blot*: before incubating with the primary antibodies, block the nitrocellulose membranes with 5% non-fat milk in TBS-T (50mM Tris, 150mM NaCl, 0.05% Tween; adjust pH to pH7.6) for 1h at room temperature. Then, incubate the membranes O/N at 4ºC with the primary antibody in blocking solution. After three washes with TBS-T, incubate the membranes for 1h with secondary antibodies (DAKO). Next, remove the excess of secondary antibody washing three times with TBS-T and then, incubate the membranes for 1min with ECL solution (Biological Industries), containing a HRP substrate. Develope the chemiluminescence signal in a radiography film.

ANTIBODY	COMPANY	SPECIE	DILUTION
β-catenin	Sigma	Rabbit	1:4000
Cleaved Notch1	Cell Signalling	Rabbit	1:1000
Tubulin	Sigma	Mouse	1:10000
Jagged1	Santa Cruz	Goat	1:5000
Myc(tag)	Handmade (Ascytes)	Mouse	1:1000
Flag(tag)	Sigma	Mouse	1:1000

TABLE MM1. Antibodies used by WB. Including company, specie and dilution data.

MM3.2. Determination of transfected proteins

- *Transfection of DNA constructs*: first, transfect the plasmids of interest together with 70ng of pGFP plasmid (as internal control for transfection efficiency) and according to PEI transfection protocol (See **MM2.1**).
- *Protein expression analysis by Western Blot*: prepare cell extracts and load equal amounts of total cellular extracts in 9% polyacrylamide-SDS-PAGE and transfer to a nitrocellulose membrane. Analyze the blots with the following primary antibodies diluted in 5%non-fat milk TBS-T: anti-myc(tag) or anti flag(tag) [**TABLE MM1**]. Use rabbit anti-mouse-HRP

(DAKO) as secondary antibody and develope blots as described before (**See MM3.1**).

MM4. RNA extraction and quantitative RT-PCR analysis

In molecular biology, quantitative real time polymerase chain reaction (qRT-PCR) is a laboratory technique based on the PCR, which is used to amplify and simultaneously quantify a targeted DNA fragment. It enables both detection and quantification (as absolute number of copies or relative amount when normalized to DNA input or additional normalizing genes) of one or more specific sequences in a DNA sample.

- *Cell culture:* seed cells in 10cm Ø plate and growth for 48h. Before achieving confluence, lyse the plates for mRNA extraction.
- *Total mRNA extraction:* extracte mRNA using the RNA extraction kit (Qiagen) according to manufacturer's instructions. Then, quantify the samples with NanoDrop spectrophotometer.
- *cDNA synthesis:* perform using RT-First Strand cDNA Synthesis kit (Amersham Pharmacia Biotech) according to manufacturer's instructions.
- *Quantitative PCR amplification of the DNA sequences:* detect the presence of gene expression in the obtained cDNA using the primers indicated in **TABLE MM2**. Perform qRT-PCR in LightCycler480 system using SYBR Green Master kit (Roche). Calculate the fold expression of the different genes relative to a *housekeeping* gene, the *β-actin* or *GAPDH* expression. The primers used for qPCR analysis are listed in Table **MM2**.

GENE	SPECIE	FORWARD PRIMER	REVERSE PRIMER
CD44	Human	AACCACACCACGGGCTTTTGAC	CCTTCTTCCTGCTTGATGACCTCG
DLL1	Human	ATCTGCCTGCCTGGATGTGATG	AGACAGCCTGGATAGCGGATACAC
DLL4	Human	TTGGATGAGCAAACCAGCACCC	TGACAGCCCGAAAGACAGATAGG
EPHB3	Human	AAAGTGGGTGGGAAGAGGTGAG	GATGTTGGGGATGCTGTTGC
HES1	Human	TACCTCTCTCCTTGGTCCTGGAAC	CAGATGCTGTCTTTGGTTTATCCG
JAGGED1	Human	CAACCGTGCCAGTGACTATTTCTGC	TGTTCCCGTGAAGCCTTTGTTACAG
JAGGED2	Human	AACGATACCACCCCGAATGAGG	GCTGCCACAGTAGTTCAGGTCTTTG
KLF5	Human	AATCCCAGAGACCGTGCGTAAC	TGTTGTGGAAGAAACTGACTTGGC
NOX1	Human	CCAGCAGAAGGTTGTGATTACCAAG	CAAGATAGAAGCAAAGGGGGTGAC
SOX9	Human	GGAGAGCGAGGAGGACAAGTTC	TTGAAGATGGCGTTGGGGG
βACTIN	Human	CGCAAGTACTCCGTGTGGA	CGGCCACATTGTGAACTTTG
RAB39B	Human	AAACGCATCAAGCTCCAGAT	TTGTGACCCACCAGAACAAA
AMOTL2	Human	AGCAGGTTAAAGGTGCTCCA	TCTGCTGTTTGTCGCTCACT
EREG	Human	CTGCCTGGGTTTCCATCTTCTAC	TGTTATTGACACTTGAGCCACACG
C-MYC	Human	CGTGGTATGTATGGGAGATGGCAG	GGACAGTAGGAAAGGAAGTGGGATG

CXCL1	Human	TTCACCCCAAGAACATCCAAAG	CAAACACATTAGGCACAATCCAGG
EPHB2	Human	CCAGACAAGCATCCAGGAGAAGTTG	AGATTGGGGAACCGACAGTGAAGG
HNRNPH1	Human	CATTTCGTCTTAGCCACGCAG	ACAAAAGCCTCGCCACTTGG
BMI	Human	CACCAGAGAGATGGACTGACAAATG	TGAGGAAACTGTGGATGAGGAGAC
CXCL2	Human	CTCAAGAATGGGCAGAAAGC	AAACACATTAGGCGCAATCC
Gapdh	Mouse	TGTTCCTACCCCCAATGTGT	TGTGAGGGAGATGCTCAGTG
Bmi1	Mouse	TGTGTCCTGTGTGGAGGGTA	TGCAACTTCTCCTCGGTCTT
Cd44	Mouse	CTCCAGACAACCACCAGGAT	ATCCGTTCTGAAACCACGTC
c-Myc	Mouse	TATCACCAGCAACAGCAGAGCGAG	AACATAGGATGGAGAGCAGAGCCC
Ephb2	Mouse	TTCTCACCTCAGTTCGCCTCTG	CAAACCCCCGTCTGTTACATACG
Hes1	Mouse	CGGCATTCCAAGCTAGAGAAGG	GGTAGGTCATGGCGTTGATCTG
Cd133	Mouse	ACGTTTGTTGTTGGTGCAAA	TCTCAAGCTGAAAAGCAGCA
Lgr5	Mouse	CGTCTTGCTGGAAATGCTTTGAC	AAGGCGTAGTCTGCTATGTGGTG
Msi1	Mouse	CTTGCCCCTGGTTACACCTA	GTGGTACCCATTGGTGAAGG
Oflm4	Mouse	ACAGAAGGAGCGCTGATGTT	GCTGGAAGTGAAGGAGATGC
Ascl2	Mouse	AGCATGGAAGCACACCTTG	AAGTGGACGTTTGCACCTTC

TABLE MM2. Primer sequences of the different genes used by expression analysis.

MM5. Chromatin Immunoprecipitation assay (ChIP)

This technique is used to analyze the association of proteins to the chromatin.

- *Cell culture*: seed cells in 10cm Ø plate and growth for 48h. Before achieving confluence, the plates with approximately $5x10^6$cells are used for the ChIP experiment.
- *Cross-linking*: the plates with 9ml of growth media. First, 1ml of Crosslink Solution (1X) is added. Treat for 10min at RT, gently shaking. After this time, stop the cross-linking by addition of 1ml of Stop Solution shaking for 5min at RT.
  - Crosslink Solution (5X): 250mM Hepes pH8, 50mM NaCl, 5mM EDTA, 2.5mM EGTA.
  - Crosslink Solution (1X): 1X Crosslink Solution, 5.55% Formaldehyde.
  - Stop Solution: 1.25M Glycine, 10mM Tris pH8.
- *Washes and lysing:* wash the plates twice with cold PBS+0.5mM EDTA. After that, spin cells 2500rpm for 5min at 4ºC. (NOTE: Pellets may be stored at -80ºC). Lyse pellets with 1ml of Lysis Buffer (10mM Tris pH8, 0.25% Triton X-100, 10mM EDTA, 500µM EGTA, 10mM Na-Butirate, 20mM β-glycerophosphate, 0.1mM Na-orthovanadate, supplemented with protease inhibitors) during 20min on ice. Centrifuge for 4min at 3000rpm. Wash the pellet in Sonication Buffer+0.1M NaCl.

- *Sonication:* resuspend the pellets in 600µl Sonication buffer (10mM Tris pH8, 0.1M NaCl, 1mM EDTA, 0.5mM EGTA, 10mM Na-Butirate, 20mM β-glycerophosphate, 0.1mM Na-Orthovanadate). Add 1%SDS before sonication. Lyse the sonicated cell at Medium power using Bioruptor Sonicator (Diagenode) during 10min to generate 800 to 1500bp DNA fragments. Spin at maximum speed for 30min at RT (a black pellet should be observed). Dilute the supernatants are (SDS from 1% to 0.1%) with Sonication Buffer. Then, concentrate the samples with VIVASPIN columns (Sartorius) at 3400 rpm RT up to final volume 0.5-0.8ml. After concentration, adjust the samples to RIPA Buffer adding 1%Triton X-100 (Pierce), 140mM NaCl, and 0.1%DOC.
- *Pre-clearing:* do 2h of pre-clearing with 50µl of protein A/G-sepharose (GE Healthcare) to remove unspecific binding of proteins to the beads, supplemented with 1%BSA, 1µg salmon DNA, and IgG antibodies (1µg/µl per IgG goat/mouse/rabbit). Performed this step at 4ºC at least twice and shake the samples all the time. NOTE: The inputs of this assay are obtained from this step (50µl).
- *Immunoprecipitation***:** remove the protein A/G sepharose used in the pre-clearing centrifuging the samples for 1min at 1200rpm. Then recover the supernatant and transfer to a new tube, where the immunoprecipitation takes place. Carry out this step O/N in RIPA Buffer (0.25M LiCl, 1% Nonidet P-40 , 1% DOC, 10mM Tris pH8, 1mM EDTA, 1mM EGTA, 10mM Na-Butirate, 0.1mM Na-ortovanadate) with 2µg of antibody (See **TABLE MM3**). NOTE: in parallel, the control samples are always immunoprecipitated with an irrelevant IgG (Sigma). The following morning, add 50µl of protein A/G-sepharose to each sample and leave in agitation for 2h at 4ºC.

ANTIBODY	COMPANY
β-catenin	BD Bioscience
Cleaved Notch1	Abcam
Notch1	Santa Cruz
IgG (non-relevant)	Sigma

TABLE MM3. Antibodies used by ChIP assay.

- *Washes:* subsequent perform washes with ice-cold buffers. First, three washes with RIPA Buffer, three washes with RIPA-Na Buffer (RIPA Buffer+1M NaCl), two washes with LiCl Buffer (1%DOC, 10mM Tris pH8, 250mM LiCl, 1M Nonidet P-40 , 1mM EDTA, 1mM EGTA, 10mM NaButirate, 20mM β-glycerophosphate, 1mM Na-orthovanadate) and finally, two washes with TE (10mM Tris pH8, 1mM EDTA).

- *Elution*: spin the samples at 1200rpm to be eluted in Elution Buffer (1%SDS, 10mM Na-Butirate, 20mM β-glycerophosphate, 30mM NaCl in TE) for 30min at RT. After that, incubate the samples at 65ºC O/N to reverse formaldehyde cross-linking.
- *DNA sequences purification:* the following morning, centrifuge the samples for 1min at maximum speed and incubate for 2h at 55ºC with 0.5µg/µl of proteinase K (Roche). Purify the eluted samples using the GFX PCR DNA and Gel Band Purification Kit (Amersham).
- *Quantitative PCR amplification of the DNA sequences:* detect the presence of promoter regions in the eluted DNA using the primers indicated in **TABLE MM4**. Calculate the protein binding to different promoters relative to the input. These values correspond to changes in input percentage over that of the control (percentage obtained with the irrelevant IgG).

PROMOTER	SENSE (5'→ 3')	ANTISENSE (5'→ 3')
SOX9	ATGAGAGACACCACCAATGCCTCC	GAGAGATAGAAGTTTGCCAATGCG
Hes1	GCCGCCAGACCTTGTGCCTG	CCGGATCCTGTGTGATCCCTAG
KLF5	CTCTGAAGTGATGAATAGGCTGTGG	GGGAGGACGGAACAATAAACTGC
NOX1	TGCTGAATCTTCCCTGTTGCC	TCTTGATGAGCCCAATAATCGG
EPHB3	CTTAGGCTTTTCGGCTCTACAATG	GCAAGACAGGCACTTAGTCCTC
Jagged1	AGAACTCAAGCCCCAAACCG	CACTCCTGGTCATAATCAAGGTCG
BMI-PRO1	TAGAGCCAACTCCACGTTCC	CGCTGGAGTGATCATAGCAA
BMI-PRO2	TGGCTTTGAAAATGTCTTTGC	TCTGCAGAAGATGCCTTTGA
BMI-PRO3	GGCATCTTCTGCAGAGTCGT	CGGTTATTTGCCCTCACACT
cMyc-PRO1	TGGATGCATTCATTTCCTGA	GTGTGGGAGCCTCTGCTAAG
cMyc-PRO2	CCTCCCATATTCTCCCGTCT	TGTGTCTGCCTGTTCCAGAG
cMyc-PRO3	GCGCCCATTAATACCCTTCT	CAGCCGAGCACTCTAGCTCT
EPHB2-PRO1	CGTTGGTGGGACTGAAAACT	GTGAGAACATGCGGTGTTTG
EPHB2-PRO2	TGAATCCTAGCCCAATTTGC	AGGGCCAGTGGTTACTTCCT
EPHB2-PRO3	AAGGCCCAGTCTCCCACT	TACCTGTCAGGGCAGGGAGT
CD44-PRO1	GCACACCAGGAAATGGTCTT	AATTCAATCAGCAGCCTTGG
CD44-PRO2	TGCGTTTGATTTCCAAACAT	CCATCTTTCCTACCCAGCAG
CD44-PRO3	ATGGTGGATGGTTGTGGTTT	CATCCTCCTGTCCATCCACT

TABLE MM4. Primer sequences of the different genes used by ChIP assay.

MM5.1. Re-Chromatin Immunoprecipitation (Re-ChIP)

After first IP, wash the samples with ice-cold buffers. Two washes with RIPA Buffer, two washes with RIPA-Na Buffer, one wash with LiCl Buffer and finally, one wash with TE. Resuspend the chromatin-protein-antibody-G/A sepharose complexes in 30µl 10mM DTT and incubate at 37ºC for 30min. Recover supernatants by centrifugation 3000rpm for 2-3 min. Dilute 25 times in RIPA buffer and incubate with second antibody O/N with rotation at 4ºC. Next morning, add 50:50 sepharose A/G and incubate for al least 2h with rotation at 4ºC. Recover the complexes of chromatin-protein-antibody-

sepharose A/G by centrifugation at 3000rpm for 2-3 min. Wash complexes twice with RIPA buffer. Elute chromatin-protein complexes as describe previously. Reverse cross-link, clean and precipitate DNA. Resuspend your DNAs in 50µl water. Keep at –20ºC.

MM6. Functional enrichment analysis

Functional annotations of genes based on Gene Ontology were extracted from Ensembl v.47 [262]. *Z* score analysis: $Z_x = X\text{-}\mu_x)/\sigma_x$ (where μ_x = mean, σ_x = standard error). Núria López-Bigas'group from Bioinformatics Department, UPF (Barcelona) displayed matrices of *Z* score values in which each cellular treated group was represented by a color-coded scale. Significance levels were corrected for multiple comparisons using false discovery rate (FDR) correction.

MM7. Soft Agar Assay

The Soft Agar Assay for Colony Formation is an anchorage independent growth test, which is used to detect malignant transformation of cells. For this assay, cells are cultured in soft agar medium for 21-28 days. After this period, the number of colonies formed per well are quantified.

- *Preparation of Base Agar*: Melt 1%Agar in a microwave and cool to 40°C in a waterbath (prepare in hood using autoclaved sterile glassware). Using falcon tubes, warm 2xDMEM+20%FBS and antibiotics to 40°C in water bath. Allow at least 30min to cool down. Mix equal volumes of the two solutions to give 0.5%Agar+1xDMEM+10%FBS. Add 1.5ml of mixture in a 35mm Ø Petri dish and set aside for 5min to allow agar to solidify.
- *Preparation of Top Agarose:* Melt 0.7%Agarose in a microwave and cool to 40°C in a waterbath. Also warm 2xDMEM/20% FBS to the same temperature. Trypsinize adherent cells to release them and count the number of cells per ml. Take care that a single cell suspension is obtained. This procedure requires 5000cells/plate. For four 35mm Ø agar plates, adjust the volume to 200000cells/ml. Add 0.1ml of cell suspension to 10ml falcon tubes, then add 3ml of 2xDMEM+20%FBS and 3ml 0.7%Agarose. Mix gently and add 1.5ml to each in duplicate plates. Only

prepare one tube at a time because the agarose does not set prematurely. Incubate plates at 37°C in humidified incubator for 10 to 30 days. Feed cells 1-2 times per week with cell culture media. Count colonies using a steroscope.

MM8. Animals

Apc$^{Min/+}$ mice (Jackson Laboratories) were from homogenous outbreed C57BL/6J background. *Jagged1* mutant mice (*Jag1*$^{+/-}$) are described in ref. [140]. *Jag1*$^{+/-}$ were backcrossed into C57BL6/J background (n>4) and crossed with *Apc*$^{Min/+}$. In our experiments, cohorts of age-matched *Apc*$^{Min/+}$*Jag1*$^{+/-}$ were compared with *Apc*$^{Min/+}$*Jag1*$^{+/+}$ and *Apc*$^{+/+}$*Jag1*$^{+/+}$. All mice were genotyped by PCR. Animals were kept under pathogen-free conditions and all procedures were approved by the Animal Care Committee.

For the ***In Vivo Tumor-Growth Assay***, twenty male *nu*/*nu* Swiss mice per experiment (Harlam) were housed in a sterile environment. Animals were injected subcutaneously with 1.5x10^6 Ls174T/dnTCF4 cells in the left flank and 1.5x10^6 Ls174T/dnTCF4/N1ICD cells in the right flank. The control group drank 1% sucrose in water and the treated group 1% sucrose, 2mg/ml doxycycline in water *ad libitum*. Tumor volumes were calculated as (length x width^2)π/6.

The intestine specific gene-targeted mice were generated by Dr. Radtke's group. They crossed floxed *Rbp*$_{J\kappa}$ mice [263] with mice carrying the villin-CRE^{ER-T2} transgene [264]. The CRE recombinase was activated by intraperitoneal injection of tamoxifen (10mg/kg body weight) into 14 day old mice for 5 consecutive days. Mice deficient for β-catenin (*Ctnnb1*^{lox}) [265] were crossed with Lox-STOP-Lox-RosaNICD-ires-GFP (N1ICD^{lox}) [143]. The active β-catenin mice, *Ctnnb1*$^{lox(ex3)}$ [197], were crossed with *Rbp*$_{J\kappa}$^{lox} villin-CRE^{ER-T2} mice. On the other hand, in our laboratory we crossed *Jag1*^{lox} mice [266] with Lox-STOP-lox-Rosa26YFP mice (YFP^{lox}) [267] and with non-inducible villin-CRE mice [264] to study the physiological role of JAG1 in the intestinal homeostasis, and finally we crossed these mice with *Apc*^{Min} mice to study the pathological role of Jagged1 during intestinal tumorigenesis.

MM9. Mucopolysaccharides Staining (Alcian blue staining)

Alcian blue stains acid mucopolysaccharides and glycosaminoglycans, for which it is one of the most used cationic dyes; the stained parts are blue to bluish-green. It binds by electrostatic forces with the negatively charged macromolecules. Gradual increases in the electrolyte concentration used to wash the bound dye selectively identify neutral, sulphated, and phosphated mucopolysaccharides.

- *Paraffin sections re-hydration:* deparaffin the sections with three subsequent washes in xylene and then rehydrate by subsequent washes (10min each) in 100% ethanol, 90% ethanol, 70% ethanol, 50% ethanol and finally, distilled water.
- Immerse in 3% of Acetic acid for 3min at RT.
- Immerse in Alcian blue (10µg/ml pH2.5) for 10min at RT.
- Wash with running water and then, wash with distillated water.
- Counterstain with Red Fast solution (Kernechtrot, Sigma) for 10min at RT.
- Wash with running water and then, wash with distillated water.
- *De-hydration and mounting:* finally de-hydrated the sections by subsequent washes (3min each) with 50% ethanol, 70% ethanol, 96% ethanol, 100% ethanol and finally, xylene. Last, cover the sections with coverslips and seal with DPX (BDH Chemicals).

MM10. Immunohistochemistry (IHC)

Immunohistochemistry or IHC refers to the process of localizing specific proteins in cells or tissue sections by using antibodies generated against antigens.

- *Paraffin sections re-hydration:* deparaffin the sections with three subsequent washes in xylene and then rehydrate by subsequent washes (10min each) in 100% ethanol, 90% ethanol, 70% ethanol, 50% ethanol and finally, distilled water.
- *Endogenous peroxidase blocking:* treat the sections with 1.5% H_2O_2 in PBS for 20min to remove the endogenous peroxidases.
- *Antigenic recovery:* do the step of antigenic recovery dependent of the primary antibody (See Retrieval in **TABLE MM5**).

- *Blocking and permeabilization:* after washing three times with PBS, the sections were treated for 1h in 1%BSA, 0.3%Triton (X-100, Pierce) in PBS at RT.
- *Primary antibody*: perform the incubation with the primary antibodies O/N at 4ºC. Dilute the following antibodies (See Dilution in **TABLE MM5**) in PBS+0.05%BSA.
- *Secondary antibody:* After washing abundantly, incubate the samples with DakoCytomation-LSAB+System-HRP Universal kit (Dako) following the manufacturer's instructions (Biotinilated secondary antibody: 30min at RT; and Streptavidine-HRP: 30min at RT).
- *Washes*: do six washes (5min each) with PBS to remove the excess of secondary antibody.
- *Development*: finally develop the sections adding DAB (Dako).
- *Hematoxylin staining*: treat the sections for 10min with hematoxylin solution (20%Mayer's hematoxylin in water). Next, wash the sections with water to remove the excess of hematoxylin.
- *De-hydration and mounting:* finally de-hydrate the sections by subsequent washes (3min each) with 50% ethanol, 70% ethanol, 96% ethanol, 100% ethanol and finally, xylene. Last, cover the sections with coverslips and seal with DPX (BDH Chemicals).

ANTIBODY	COMPANY	SPECIE	DILUTION	RETRIEVAL
β-catenin	Sigma	Rabbit	1:2000	TE 50min 100ºC
Jagged1	Santa Cruz	Goat	1:1000	TE 50min 100ºC
Myc(tag)	Handmade (Ascytes)	Mouse	1:1000	TE 50min 100ºC
Flag(tag)	Sigma	Mouse	1:2000	TE 50min 100ºC
SMA	Labvision	Mouse	1:200	TE 50MIN 100ºC
Cleaved Notch	Cell signalling	Rabbit	1:200	Citrate 20min Autoclave

TABLE MM5. Antibodies used by IHC. Including Company, Specie, Dilution and Retrieval data

MM11. Immunofluorescence

- *Seeding*: plate cells on sterile glass coverslips to achieve 70% confluence 24h later.
- *Fixation*: wash cells twice with PBS and then fix with 4%PFA for 20min at 4ºC. After that, wash abundantly.

- *Permeabilization & blocking*: incubate the sections with 0.3%Triton (X-100, Pierce), 10%FBS and 5%non-fat milk in PBS for, at least, 20min at RT.
- *Primary antibody hybridization*: dilute primary antibody in blocking solution for specific condition (See **TABLE MM6**) and incubate O/N at 4ºC.
- *Secondary antibody hybridization*: first, three washes with PBS. Detect the binding of the primary antibody with secondary antibodies (Molecular Probes, 1:2000), incubate for 90min at RT and in the dark.
- *Mounting***:** first, three washes with PBS. Mount the coverslips on slides with a drop of Vectashield Mounting Medium with DAPI (Vector Laboratories) and store at 4ºC in the dark.
- *Confocal microscopy***:** detect the fluorescence with a TCS-SP2 Leica confocal microscope.

ANTIBODY	COMPANY	SPECIE	DILUTION
β-catenin	Sigma	Rabbit	1:2000
Jagged1	Santa Cruz	Goat	1:1000
Myc(tag)	Homemade (Ascytes)	Mouse	1:1000
Flag(tag)	Sigma	Mouse	1:2000

TABLE MM6. Antibodies used by Immunofluorescence. Including company, specie and dilution data.

MM12. Tumor staining with Methylene blue

Methylene blue is a heterocyclic aromatic chemical compound with the molecular formula $C_{16}H_{18}N_3SCl$. In biology methylene blue is used as a dye for a number of different staining procedures, for example it can be used as an indicator to determine dead cells since the blue indicator turns dark in the absence of active enzymes.

- Protocol for staining intestinal tumors:
  - Fix whole intestine in 25ml of Formalin (neutral buffered formaldehyde 3.7%). Let fixation in Formalin O/N with gentle agitation.
  - Remove fixative and wash abundantly the intestines in distillated water.
  - Immerse the intestine in 0.5%Methylene blue in water for 20min at RT.
  - Wash abundantly with distillated water.

- Discolor with 70% Ethanol until the tumors were dark blue and the normal epithelium light blue.
- With stereoscope, count the number of tumors.

MM13. TUNEL assay

The DeadEnd™ Fluorometric TUNEL System (Promega) is designed for the specific detection and quantitation of apoptotic cells within a cell population. The system is non-radioactive and provides for simple, accurate and rapid detection of apoptotic cells *in situ*. The DeadEnd™ Colorimetric TUNEL System end-labels the fragmented DNA of apoptotic cells using a modified TUNEL assay. Biotinylated nucleotide is incorporated at the 3´-OH DNA ends using the Terminal Deoxynucleotidyl Transferase, Recombinant, (rTdT) enzyme. Horseradish peroxidase-labeled streptavidin (Streptavidin HRP) is then bound to these biotinylated nucleotides, which are detected using the peroxidase substrate, hydrogen peroxide, and the stable chromogen, diaminobenzidine (DAB). Using this procedure, apoptotic nuclei are stained dark brown.

- Product components:
  - Equilibration Buffer
  - Biotinylated Nucleotide Mix
  - Nucleotide Mix
  - Terminal Deoxynucleotidyl Transferase Recombinant
  - 20xSSC
  - Proteinase K
  - Streptavidin HRP (0.5mg/ml)
  - DAB 20X Chromogen
  - DAB Substrate 20X
  - Hydrogen Peroxide 20X
  - Plastic Coverslips
- Protocol for apoptosis detection in tissue:
  - *Pretreatment of Paraffin-Embedded Tissue*:
    - Wash slides twice in xylene (5min each wash).
    - Immerse in 100% ethanol for 5min.
    - Wash slides in decreasing concentrations of ethanol (100%, 95%, 85%, 70% and 50%), 3min each wash.
    - Immerse in 0.85% NaCl for 5min. Immerse in PBS for 5min.
  - *Apoptosis Detection*:

- Immerse slides in 4%Formaldehyde in PBS for 15min.
- Immerse slides twice in PBS, 5min each time.
- Add 100µl of a 20µg/ml Proteinase K solution. Incubate at RT for 15min.
- Immerse slides in PBS for 5min.
- Immerse slides in 4% Paraformaldehyde in PBS for 5min.
- Immerse slides in PBS for 5min.
- Add 100µl Equilibration Buffer. Equilibrate at RT for 5–10min.
- Add 100µl of TdT reaction mix to the tissue sections on the slides. Do not allow tissue sections to dry completely. Cover slides with plastic coverslips to ensure even distribution of the mix. Incubate slides for 60min at 37°C in a humidified chamber.
- Remove plastic coverslips. Immerse slides in 2xSSC for 15min.
- Immerse slides three times in PBS, 5min each time.
- Immerse slides in 0.3% H_2O_2 for 3–5min.
- Immerse slides three times in PBS, 5min each time.
- Add 100µl Streptavidin HRP (diluted 1:500 in PBS). Incubate slides for 30min at RT.
- Immerse slides three times in PBS, 5min each time.
- Add 100µl DAB (prepared immediately prior to use). Develop until a light brown background appears. Do not allow the background to become too dark.
- Immerse slides several times in deionized water.
- Visualize: Mount slides in an aqueous or permanent mounting medium. Observe staining with a light microscope.

MM14. Human Colorectal Samples

Samples from FAP patients were obtained from the Tumor Bank of ICO-IDIBELL. All patients gave written consent to donate the tumor specimen. The study was approved by the Ethics Committee of our institution.

MM15. Co-immunoprecipitation

When a cell is lysed under non-denaturing conditions, many protein-protein associations that exist within the intact cell are conserved. Thus we can detect and identify physiologically relevant protein-protein interactions.

- *Cell extract preparation*: wash cells twice in PBS. Scrape each plate of cells into 1ml of ice-cold CoIP lysis buffer (50mM Tris-Cl pH8.0, 120mM NaCl, 0.5% Nonidet P-40, 5µg/ml leupeptin, 10µg/ml aprotinin, 50µg/ml PMSF, 0.2mM Na-orthovanadate, 100mM NaF). Transfer each milliliter of cell suspension into a microfuge tube, and centrifuge the tubes at maximum speed for 15min at 4ºC in a microfuge. NOTE: 10% of this lysate is kept as an input.
- *Blocking and conjugation:* Add 50µl of the protein A/G-Sepharose per sample. Block the beads with 5µg of BSA in IPP Buffer (10mM Tris pH8, 500mM NaCl, 0.1%Nonidet P-40, 5mM EDTA, 50mM NaF, 0.4mM Sodium Ortovanadate, 1mM PMSF, 10µg/ml Leupeptin, 10µg/ml Aprotinin) and add 2µg of antibody. Conjugate 1h at 4ºC, shaking.
- *Immunoprecipitation*: Add the lysates obtained in the first step to the complex A/G-Sepharose-antibody. Rock the immunoprecipitate for 2h at 4ºC. NOTE: in parallel, immunoprecipitate always with an irrelevant IgG (Sigma).
- *Washes*: wash the protein A/G-sepharose in CoIP buffer. Repeat five times. Remove the liquid portion and add 60µl of 1xSDS gel-loading buffer (50mM Tris-Cl pH6.8, 14M β-mercaptoethanol, 2%SDS, 0.1%bromophenol blue, 10%glycerol) to the beads, and boil them for 4min.
- *Analysis*: elucidate the binding by WB (See **MM3.1**).

MM16. Nuclei extraction

- Harvest $0.5x10^8$ to 10^8 cells from the culture plates. Collect the cells by centrifugation at 1200rpm for 10min at RT. Rinse the cells several times with PBS.
- Resuspend the cell pellet in 3 volumes of ice-cold cell homogenization buffer (0.1%Nonidet P-40 in PBS) for 5min on ice, and then stop the reaction adding v/v of cold PBS.
- Collect the nuclei by centrifugation at 1800-2000rpm for 5min at 4ºC. Remove the supernatant (cytoplasm), and resuspend the pellet of nuclei in

the appropriated lysis buffer (depending on the experiment you need to perform).

MM17. Pull-down assay

The GST fusion protein pull-down technique uses the affinity of GST for glutathione-coupled beads to purify interacting proteins with our protein of interest. The GST fusion protein is expressed and purified from bacteria.

- *Bacteria growth*: culture bacteria (BL-21) O/N in LB/antibiotic at 37ºC shaking. Next morning, dilute the culture 1:10 in LB/antibiotic for 90min at 37ºC in agitation (exponential growth phase).
- *Induction*: induce recombinant protein production by adding IPTG 0.1mM. Culture for 3.5-5h at 37ºC in agitation. Transfer bacteria to 50ml tubes and centrifuge at 3800rpm for 20min. NOTE: Pellets could be frozen in this step at -20ºC.
- *Protein purification:* resuspend the pellet in 10mL Lysis buffer (20mM Tris-Cl pH8.0, 200mM NaCl, 1mM EDTA pH8.0, 0.1% Nonidet P-40, just before use, add protease inhibitor cocktail, 1mM DTT, 1mM PMSF, 1mg/ml Lysozyme) until completely homogenized. Sonicate three times 10sec 25% amplitude (placing at least for 10sec on ice between each sonication step). Transfer to 12mL tube. Centrifuge at 9000rpm 30min at 4ºC. Pour sonicated bacterial lysate onto previously washed glutathione sepharose beads in a 15mL tube. Incubate 2h at 4ºC shaking. Centrifuge at 1200rpm 5min at 4ºC and discard supernatant. Wash beads three times with 5mL Lysis buffer. Store at 4ºC in 1mL Lysis buffer.
- *Cell lysate*: decide comparable amounts of GST-fusion proteins to use per pull-down. Add an excess of previously washed free glutathione-sepharose beads to enable visualisation of bead pellet. Incubate the eukaryotes cells with 500µl of Eukaryotes Lysis buffer (50mM Tris-Cl pH7.5, 150mM NaCl, 1% Nonidet P-40, 5mM EGTA, 5mM EDTA, and 20mM NaF) for 20-30 min on ice. Centrifuge at 13000rpm 5min at 4ºC. NOTE: Collect 50µL of this lysate as input.
- *Blocking:* Block each GST-fusion protein with the same volume of 10mg of BSA in 500µl of Eukaryote lysis buffer. Incubate, at least 2h at 4ºC in a rotary shaker. Centrifuge at 1200rpm and discard the supernatant.
- *Pulldown*: Add the lysate to the blocked GST fusion-beads. Incubate for 45min at 4ºC shaking.

- *Washes*: Wash beads three times in 500μL Eukaryote lysis buffer mixing well and centrifuging each time at 1200rpm 2min at 4ºC.
- *Elution:* Add 60μL of 1XSDS loading buffer. Boil 10min at 95-100ºC.
- *Analysis:* the binding was elucidated by WB (See **MM3.1**).

MM18. In situ Hybridization (ISH)

ISH is a versatile and robust method for monitoring gene expression. The basic principle of ISH relies on the detection of hybridized RNA species using radiolabeled or hapten-conjugated nucleic acid probes. The ISH protocol for intestinal sections described herein is a modified version of the standard whole mount ISH protocol for embryonic specimens described by Wilkinson [268]. In brief, the method involves hybridization of formalin-fixed, paraffin-embedded intestinal sections with digoxigenin-labeled RNA probes and subsequent detection of hybrids with alkaline phosphatase coupled anti-digoxigenin antibodies.

Generation of digoxigenin RNA probes: The generation of digoxigenin RNA probes is achieved by an *in vitro* transcription reaction of linearized template DNA using T7, T3, or SP6 RNA polymerases. During the *in vitro* transcription reaction, digoxigenin-coupled UTPs are incorporated into the RNA probe. To generate anti-sense probes that will recognize sense mRNA, template DNA is cut using a restriction enzyme that creates a 5' overhang (avoid 3' overhangs) at the 5' end of the cDNA. Ensure that following the digestion the T7, T3, or SP6 promoter is at the 3' end of the template DNA. Accordingly to generate sense probes template DNA can be cut at the 3' end.

- *Digestion of plasmid DNA*: Digest 10μg of plasmid with the appropriate restriction enzyme (Ensure that template DNA is completely linearized by running an aliquot on 1% agarose gel) and purify with GE Healthcare kit.
- *In vitro transcription and digoxigenin labeling reaction*: Prepare in vitro transcription reaction in an eppendorf (20μl reaction volume) as follows: 1-2μg of linearized DNA, 1X Transcription buffer (The transcription buffer is usually supplied by manufacturer of RNA polymerases), 2μl of DTT 0.1M, 2μl Nucleotide RNA Labeling Mix 10X, 20U of RNAse inhibitor, 30U of T7 or T3 or SP6 RNA polymerase. Incubate reaction at 37°C for ≥3 hours. Clean-up cRNA products by using commercially available RNA purification columns. Typically samples are eluted from columns with 100μl DEPC-treated H_2O. Remove 1μl of purified probe to measure

concentration and 3µl for electrophoresis. To the remaining probe add an equal volume of formamide and store at -80°C. NOTE: As an alternative to using RNA purification columns researchers may follow these steps to clean up cRNA reaction: To in vitro transcription reaction add 2µl DNAse (10U/µl) for 15min and stop the reaction adding 100µl TE, add 2.5µl LiCl (4M) and 75µl ethanol. Store at -80°C for O/N. Centrifuge (13000rpm) for 15min at 4°C. Wash pellet in ice-cold 70% ethanol and resuspend in 50µl DEPC-treated H_2O.

In situ Hybridization: Prior to performing the ISH, intestinal samples must be first fixed, embedded in paraffin, cut and mounted on glass slides following standard histological practice.

- *Pre-treatment of sections prior to ISH*: Clean and bake at 200°C O/N glass jars (including covers) suitable for holding glass slides. Place slides in jar and proceed with standard dewaxing and rehydration protocol: Xylene 3 X 5 minutes, 100% ETOH - 2 X 5 minutes, 96% ETOH 1X 5min, 70% ETOH 1X 5min, 50% ETOH 1X 5min, 25% ETOH 1X 5min. Rinse twice in DEPC-treated H_2O. Treat slides with 0.2N HCl for 15 min. Wash in H_2O. Incubate sections with proteinase K in PBS buffer for 20min at 30µg/ml. Place jar with slides in a water bath if required. Rinse in 0.2%glycine/PBS solution *(Glycine should be added to PBS solution at last moment. Do not store solution for long periods of time)*. Rinse 2X in PBS. Post-Fix for 10 min with 4% PFA. Rinse 3X in PBS. Prepare acetic anhydride solution (0.25% acetic anhydride in 0.1M Triethanolamine pH8.0, add acetic anhydride solution immediately before use. Do not store). Shake vigorously and add to slides. Incubate for 5 minutes. Repeat acetic anhydride treatment once. Rinse 5X in PBS. Rinse 2X in 5xSSC (for 1 litre: 175.3g NaCl, 88.2g sodium citrate – 2 H_2O, pH4.5).
- *Pre-hybridization*: Remove excess solution from slides with tissue and place them in a covered box humidified with 5X SSC/50% Formamide. Add enough Hybridization Solution (50% Formamide, 5X SSC pH4.5, 2% Blocking powder (Roche), 0.05% CHAPS, 5mM EDTA, 50µg/ml heparin, 1µg/ml yeast RNA, heat at 65ºC for dissolving) to completely cover sections. Incubate slide box in a 65°C oven for at least 1 hour.
- *Hybridization*: Remove excess hybridization solution and replace with 500µl/slide of hybridization solution containing 500ng/ml of probe. Incubate slides in an oven at 62-70°C for 24-72 hours.
- *Post hybridization washes*: Remove excess hybridization solution and place in glass jar. Rinse in 2xSSC. Wash three times for 20 min at 65°C in 50% formamide/2xSSC pH4.5. Rinse 5X in Tris-NaCl buffer (0.1M TrisHCl pH7.5, 0.15 M NaCl, 0.1 % Tween 20).

- *Immunological Detection*: Remove excess solution from slides with tissue and place them in a covered box humidified with water. Apply Blocking Solution (1% Blocking powder (Roche) in 1X Tris-NaCl buffer. Heat at 65ºC to dissolve) over sections and incubate at RT for at least 30 minutes. Dilute sheep anti-digoxigenin antibody 1/2000 in Blocking Solution. Remove blocking solution and replace with antibody solution. Incubate O/N or longer at 4°C. Wash slides 7X in Tris-NaCl buffer. Wash slides 3X in NTM buffer (0.1M Tris pH9.5, 0.1M NaCl, 0.05M $MgCl_2$). Add NBT/BCIP solution (NTM Buffer +0.33µg/µl NBT + 0.175µg/µl BCIP) to sections in a humidified slide box. Incubate for up to 24 hours at room temperature. *(Keep slides in the dark)*. Wash slides twice in PBS. Mount the sections in 50% Glycerol in PBS.

MM19. Crypt isolation from murine small intestine

- Harvest mouse small intestine in PBS. In a 10cm Ø dish with PBS remove fat from intestine and wash. Using small scissors cut the intestine open over the full length of the organ.
- Wash in PBS.
- Open up the intestine a bit and scrape the villi using the Neubauer's coverslip leaving the crypts attached.
- Wash of the villi with PBS and cut the intestine with scissors in small 2-4mm pieces and transfer them to a 50ml tube.
- Add 10ml PBS pipet up and down for a few times with a 10ml pipette remove the supernatant and add fresh PBS. Repeat this 10-20 times until the supernatant is clear.
- Add 2mM EDTA in PBS and leave for 30 minutes on rocking tube platform in cold room.
- Remove the supernatant and add 10ml PBS/10%FBS and pipet up and down 3-5 times and collect the supernatant passing the 70µM strainer, repeat this 3 more times using new strainers (these are the different crypt elution fractions).
- Spin down the crypt fractions at 800rpm 5min to remove single cells (mostly lymphocytes). The pellets are ready for the RNA extraction.

MM20. Determination of cell cycle and cell death

MM20.1. Apoptosis and cell death

The Annexin V-FITC reagent is optimized to determine the frequency of cells that can be induced to enter the apoptotic pathway. Since most cell populations will contain a proportion of cells that are in the apoptotic and/or necrotic state, the number of cells undergoing induced apoptosis must be compared to the control untreated population.

- ❑ Wash cells twice in cold PBS; remove the PBS from the cell pellet after the second wash.
- ❑ Resuspend cells in cold 1X Binding buffer to a concentration of 10^6-10^7cells/ml.
- ❑ Put 100 µL of cells (10^5 to 10^6) to each tube (4 tubes: #1: unstained cells, #2: Annexin V-FITC only, #3: PI only, #4: Annexin V-FITC + PI).
- ❑ Add 5µL of Annexin V-FITC to tube #2 and tube #4.
- ❑ Gently vortex each tube and incubate for 15 minutes on ice, protected from light.
- ❑ Without washing, add 380 µL of cold 1X Binding buffer to each tube. Add 4µL of PI to tube #3 and tube #4.
- ❑ Analyze by flow cytometry.

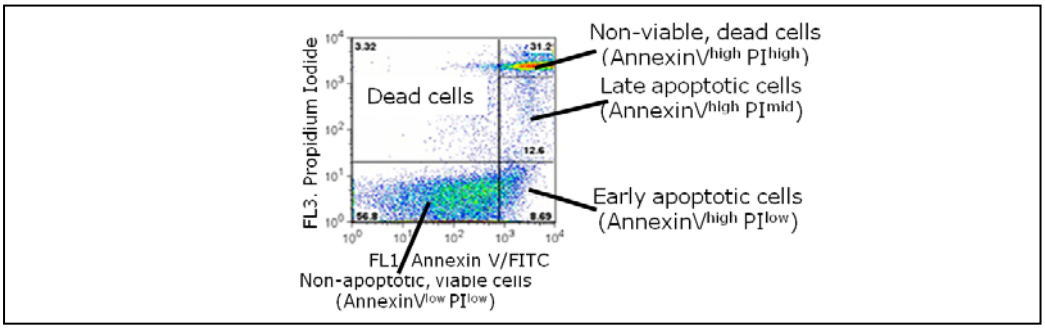

FIGURE MM1. Graph obtained from FACS analysis summarizes the different vital stages in which cells can be found according to their labeling with AnnexinV and PI.

MM20.2. Cell cycle

- × *Trypsinization*: the cells are trypsinized and counted. 1-2x10^6 cells are washed twice with ice-cold PBS. Resuspend in 500µl PBS+1%FCS.

- *Fixation*: 5ml of ice-cold 70% ethanol are prepared and the cells are added on drop-wise. At this point, cells could be stored at -20ºC (2h to 3weeks)
- *Washes*: before staining with PI, the cells are washed twice with PBS+1%FCS to remove the ethanol.
- *Staining*: after washing, the fixed cells are treated with 400µl of solution PI (1%FCS, 5µg/ml RNAse A and 50µg/ml PI, in PBS) for 30-45min at 37ºC.
- *FACS analysis:* after the staining, the cells are analyzed with a FACScan flow cytometer.

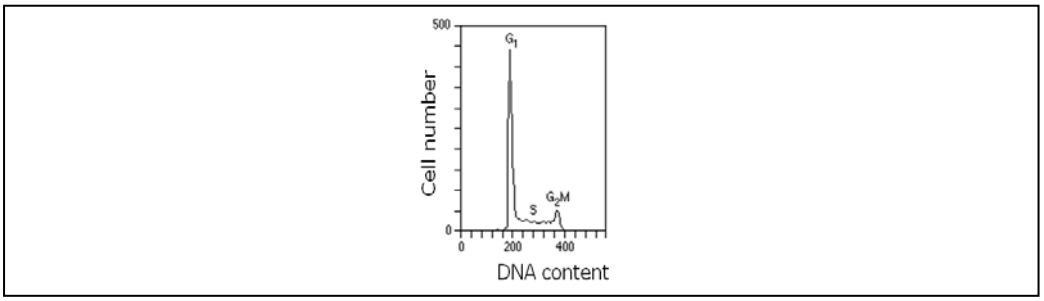

FIGURE MM2: Representation of the different cell cycle phases in which cells can be found depending on the amount of DNA they contain.

RESULTS

R1. A common genetic program for Wnt and Notch pathways

As we mentioned before, β-catenin activation is a frequent event in intestinal tumors, and the treatment with γ-secretase/Notch inhibitors promotes differentiation of the adenoma cells into goblet cells in a mice model [69], similar to the effects observed in the intestinal Notch deficient mice [209]. How Notch is activated in β-catenin-dependent tumors and what is the contribution of the Notch pathway to Wnt-dependent intestinal tumorigenesis is largely unknown.

To determine the contribution of the Notch pathway to β-catenin/TCF4-dependent tumorigenesis, we first compared the transcriptional effects of blocking Wnt, Notch or both pathways in Ls174T CRC cells that contain high levels of active Notch1 and nuclear β-catenin. To do this, we took advantage of the Ls174T/dnTCF4 cell line, carrying a doxycycline-inducible plasmid encoding a dominant negative form of TCF4 that had been generated in the laboratory of Dr. Hans Clevers. These clones require Wnt activity to maintain the undifferentiated phenotype and are capable of differentiating into goblet cells and stop proliferating in response to doxycycline treatment [187]. We blocked Notch activity by incubating with the γ-secretase and Wnt activity by inducing dnTCF4 [**FIGURE R1**].

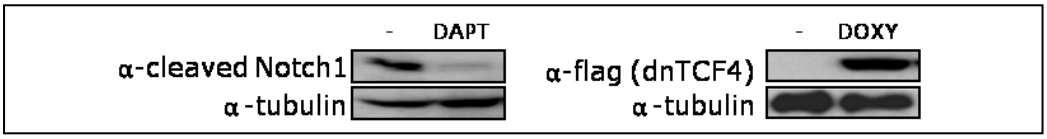

FIGURE R1. Inactivation of Notch and β-catenin (through induced expression of dn-TCF4) activities in response to DAPT and doxycycline treatments respectively. Western blot of Ls174T/dnTCF4 cells showing the blockage of Notch1 cleavage by DAPT (50μM) and the expression of dnTCF4 after 48h of doxycycline treatment.

We performed microarray analysis comparing Ls174T/dnTCF4 cells untreated, treated for 48h with doxycycline and/or with DAPT (50μM) [269], using a whole human genome oligonucleotide microarray from Agilent (G4112A). We identified 366 genes that were simultaneously down-regulated (≥1.3-fold) in response to doxycycline and DAPT treatments (See **Annex A2**) and **FIGURE R2** (left)].

This data indicated that 34% of all the Wnt/TCF4-dependent genes (down-regulated with doxycycline) were also Notch-dependent (down-regulated with DAPT). We called this group of genes: *Notch-Wnt-dependent genes*. Some of the genes in this group have been associated with cancer such as *CD44*, *EPHB3*, *HES1*, *KLF5, NOX1* or *SOX9* in different systems [213, 270-275] and a number of them had been previously identified as β-catenin/TCF targets [276-278]. In addition, blocking Notch and/or Wnt pathways, resulted in an increase

in the expression levels of several differentiation markers such as *VIL2*, *MUC20* or *TFF1* as expected [**FIGURE R2** (left)].

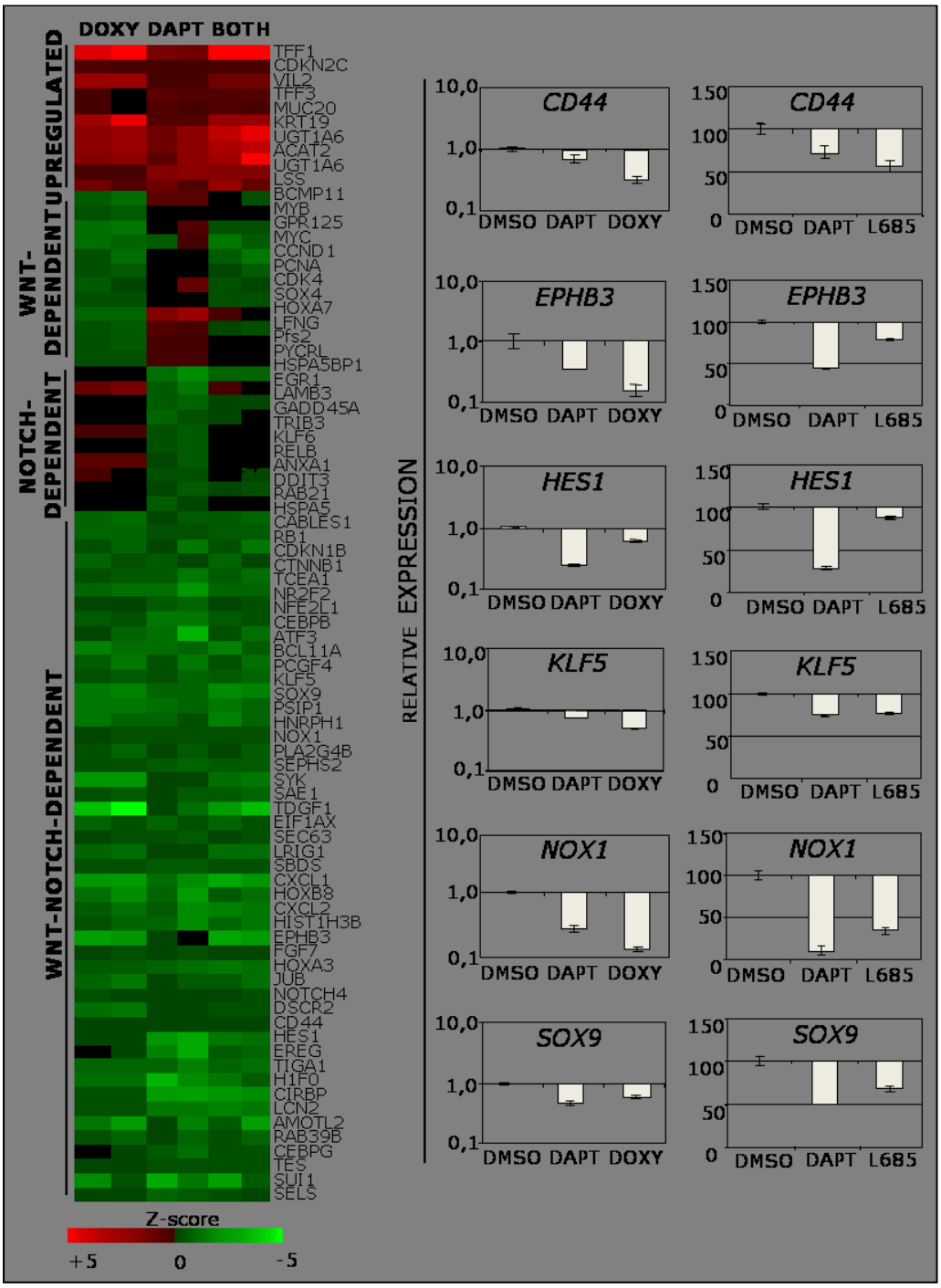

FIGURE R2. Identification of Wnt-Notch-dependent genes. Left, gene expression profile from Ls174T/dnTCF4 cells treated with Doxy, DAPT or both treatments compared with untreated cells by microarray analysis. Right, confirmation by qRT-PCR of different genes identified in the microarray.

We designed specific primers [**TABLE MM5**] for some of these Wnt-Notch-dependent genes and confirmed the microarray data by qRT-PCR [**FIGURE R2** (right)]. To determine the specificity of Notch inhibition, we used two different γ-secretase inhibitors, DAPT and L685.458, obtaining comparable results [**FIGURE R2** (right)].

Together these results indicated that there is a genetic program depending on Wnt and Notch pathways, which is expressed in human CRC cells.

R2. Notch is downstream of β-catenin activation

R2.1. Notch over-expression partially reverts the β-catenin-dependent expression pattern

The existence of a Wnt-Notch-dependent genetic program in CRC cells suggested at least two different mechanistic explanations: **(a)** Notch is downstream of β-catenin/TCF or **(b)** both, β-catenin and Notch are required to properly activate a specific gene signature in these cells [**FIGURE R3**].

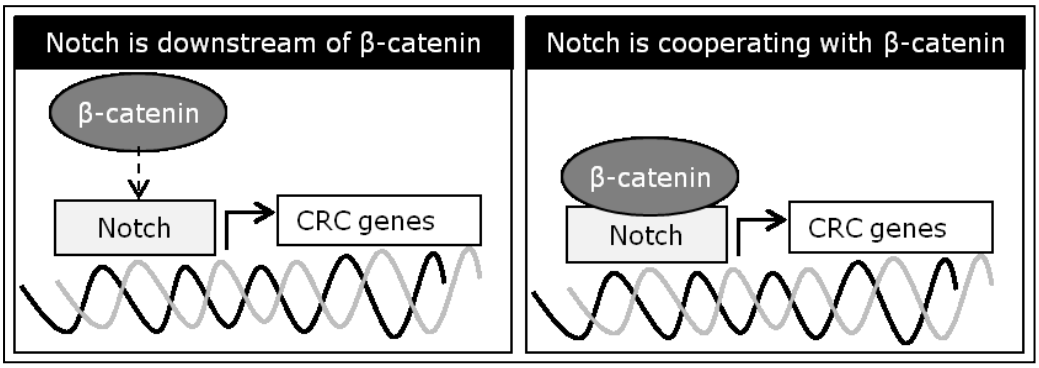

FIGURE R3. Diagram summarizing two feasible explanations to justify the microarray data.

One possible approach to test whether a protein X is downstream of a protein Y in a signaling cascade, is studying the effects of over-expressing or expressing an active form of X, when Y is inhibited. Thus, if Notch was downstream of β-catenin/TCF signaling, the ligand-independent constitutive active form of Notch1 (N1ICD) should be able to restore the transcriptional repression mediated by dnTCF4 in CRC cells.

We studied the transcriptional signature of Ls174T cell clones that expressed doxycycline-inducible dnTCF4 and N1ICD constructs (Ls174T/dnTCF4/N1ICD clones, N) compared with control clones (Ls174T/dnTCF4, C), which only expressed dnTCF4.

We performed microarray analysis from cells treated for 48h with doxycycline, using a whole human genome oligonucleotide microarray from Agilent. We found that N1ICD expression was sufficient to reactivate 31% of the genes identified as Wnt-Notch-dependent genes [**FIGURE R4** (left) and **Annex A4**)], including *EPHB3, HES1*, *KLF5*, and *NOX1*. As expected, several genes involved in intestinal differentiation, such as *FAPB1* and *FABP5*, were down-regulated in N1ICD expressing clones [**FIGURE R4** (left)] consistent with the effects of Notch in inhibiting differentiation in these cells[209].

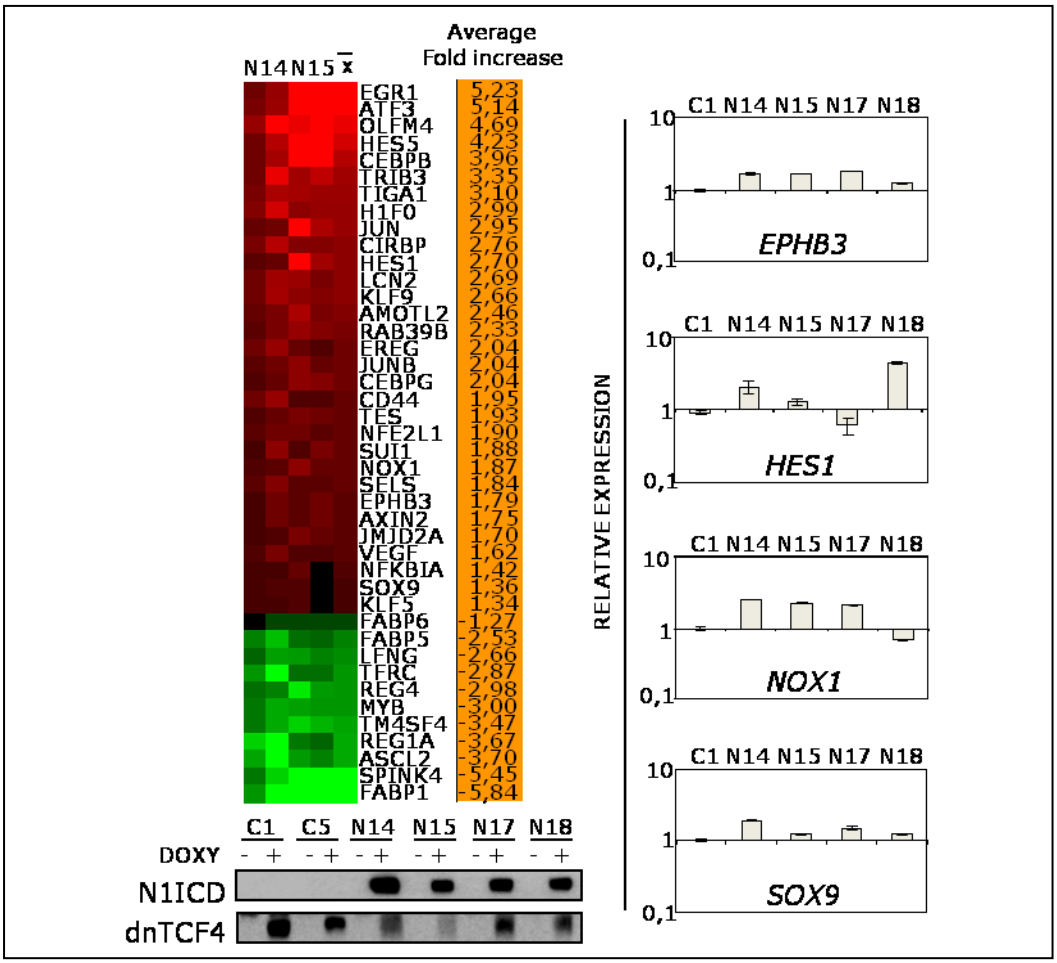

FIGURE R4. N1ICD reverts the expression of several Notch and Wnt-dependent genes. Left, by microarray analysis, we determined the changes in the expression pattern of Ls174T/dnTCF4/N1ICD clones compared to Ls174T/dnTCF4. By western blot we show the inducible expression of N1ICD and dnTCF4 in the indicated clones. Right, confirmation by qRT-PCR of different genes identified in the microarray.

Using the Genomatix Software, which includes a database with the consensus for all the transcription factors are described, we identified RBP_{Jk}-binding sites in the regulatory regions of all of the analyzed genes: *EPHB3, HES1*, *KLF5, NOX1* and *SOX9* [**FIGURE R5** and **TABLE R1**]. By ChIP assay, we found that Notch1 consistently associated to the promoters of these genes in Ls174T cells compared with the controls (non-relevant IgG and no-antibody) [**FIGURE R5**]. These results indicated that a proportion of the Wnt-Notch-dependent genes identified in our screening were in fact canonical Notch target genes, as they contain functional RBP_{Jk}-binding sites and are re-expressed in response to active Notch1. In contrast, other genes of the signature might require the participation of both Wnt and Notch pathways to be activated.

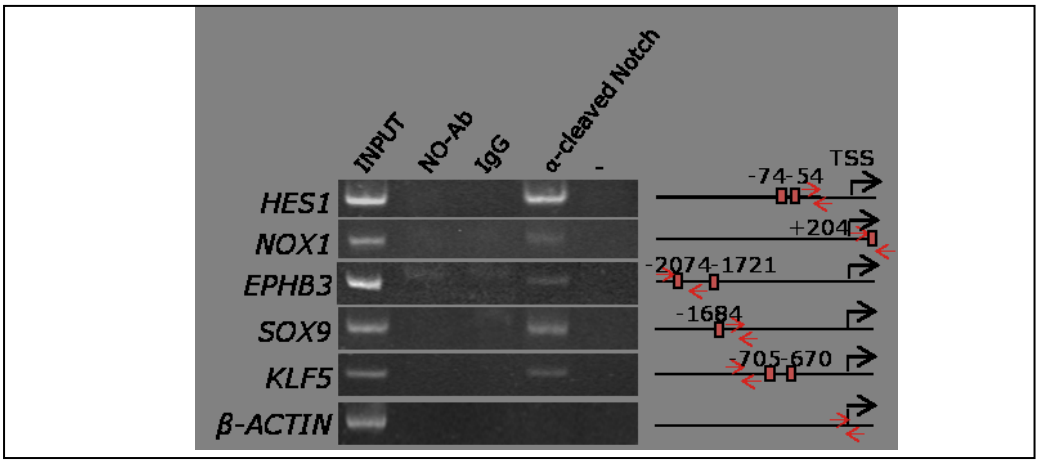

FIGURE R5. Notch is recruited to specific Notch and Wnt-dependent genes. ChIP experiment with α-cleaved Notch1 antibody and different controls in Ls174T cells and PCR of the indicated promoters. Scheme of the 2KB proximal promoter regions showing the position of the primers used around the RBP_{JK}-binding sites and the transcription start site (TSS).

GENE	RBP_{JK} CONSENSUS	POSITION FROM / TO
EPHB3	ACAATGGGAGAGTTG	-2074 / -2088
	CTAACTTCTCACTCT	-1721 / -1735
NOX1	ACAATGGGAAACTGG	204 / 218
SOX9	AGAGTTTCCCAATGC	-1684 / -1698
KLF5	TGTGTGGGAAAACGT	-705 / -719
	GGAGTGGGAAAAACC	-670 / -684
HES1	ACTGTGGGAAAGAAA	-74 / -88
	GGAAGTTTCACACGA	-54 / -68

TABLE R1. RBP_{JK}-binding sites on the Notch-dependent genes. Sequences identified with the *Genomatix* software as RBP_{JK}-binding consensus in the different promoters. The underlined sequence corresponds to the core of the motif.

We next studied (in collaboration with Andrea Grilli and Núria López-Bigas from Bioinformatics Department, UPF, Barcelona) whether the *Notch-Wnt-dependent genes* were over-represented in any specific functional category (See **MM6**). This analysis revealed that these genes were highly enriched into functional categories related with proliferation, differentiation and DNA and RNA metabolism, including transcription and replication. Interestingly, the group of genes identified as direct targets of Notch were specifically enriched in the cell cycle arrest and differentiation categories [**FIGURE R6**].

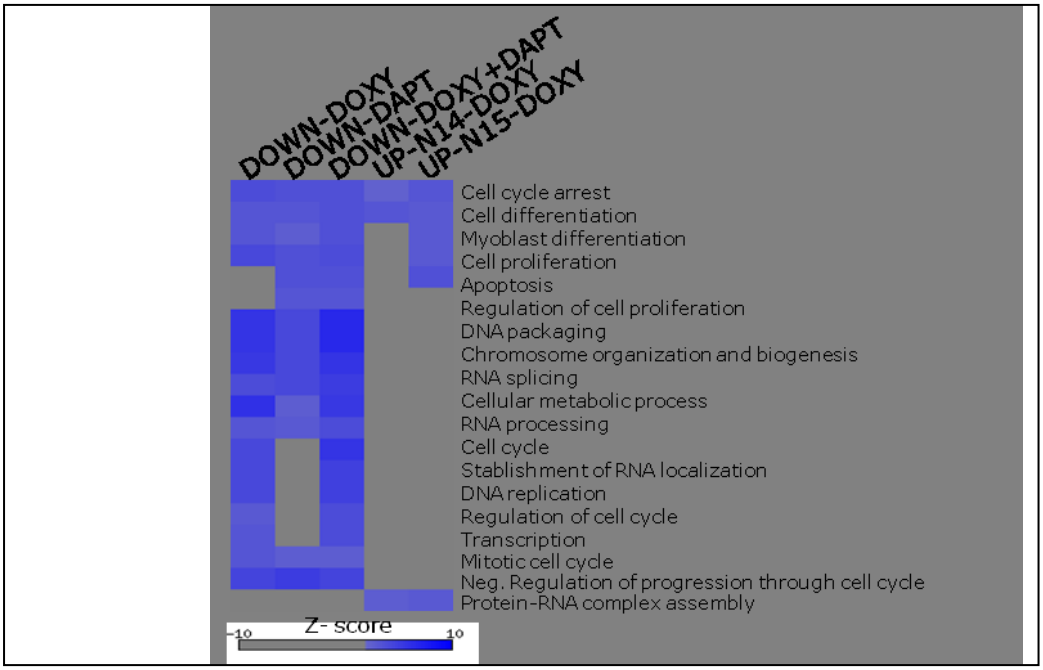

FIGURE R6. Functional annotation of genes down-regulated after inhibition of Wnt, Notch or both pathways or up-regulated in N1ICD clones (N14 and N15) based on Gene Ontology. Blue signifies over-representation of genes for the indicated groups. Grey means no significant difference from expected.

Together, these results strongly suggest that Notch is a direct regulator of specific gene transcription downstream of β-catenin/TCF; nevertheless most of the identified Wnt-Notch-dependent genes (69%) likely require the cooperative effects of Notch and β-catenin pathways.

R2.2. Notch is downstream of Wnt through transcriptional activation of Jagged1 by β-catenin/TCF

To investigate the mechanism of Notch activation downstream of β-catenin/TCF in CRC cells, we searched in the microarray data for the presence of putative Notch ligands that were regulated by Wnt/β-catenin. We found that *JAGGED1* was down-regulated 1.3-fold after doxycycline treatment in dnTCF4-expressing cells. To further analyse this possibility, by qRT-PCR, we checked the expression levels of the different Notch ligands (*DLL1, DLL4, JAG1* and *JAG2*) in these cells and found high levels of *JAGGED1* in Ls174T/dnTCF4 that consistently decreased after doxycycline treatment [**FIGURE R7** (left)]. Most important, expression of dnTCF4 resulted in a huge reduction in the protein levels of Jagged1 concomitant with a decrease in the levels of activated Notch1 [**FIGURE R7** (right)].

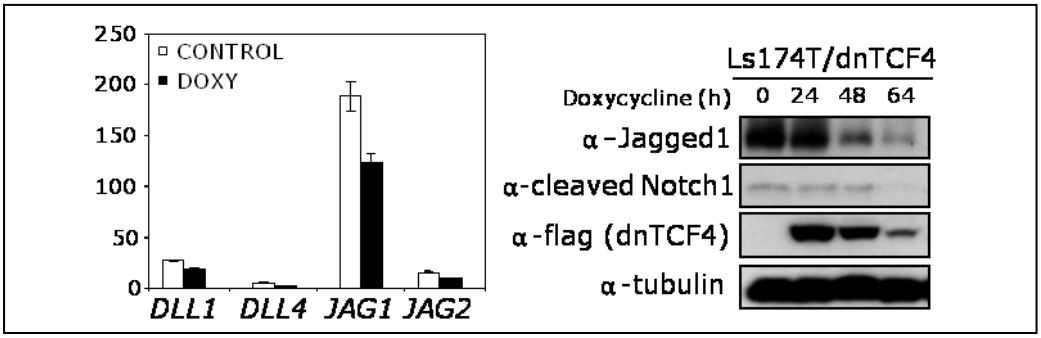

FIGURE R7. *Jagged1* is a β-catenin-dependent gene. Left, Expression levels of different Notch ligands in Ls174T/dnTCF4 cells untreated or treated for 48h with Doxycycline as determined by qRT-PCR. Right, JAGGED1 protein levels and Notch activation are reduced in the presence of dnTCF4. Western blot with α-Jagged1 and α-cleaved Notch1 antibody of Ls174T/dnTCF4 cells treated with doxycycline. α-flag staining shows the levels of dnTCF4 and tubulin is shown as a loading control.

Using the Genomatix Software, we identified two putative TCF-binding sites in the human *JAG1* promoter (-1110bp and -558bp respectively). In addition, ChIP analysis demonstrated that these sites were functional as we detected specific recruitment of β-catenin to this promoter in Ls174T [**FIGURE R8**]. As a control, we precipitated the chromatin with non-relevant IgG or with no-antibody. In order to determine whether recruitment of β-catenin to the *JAGGED1* promoter was dependent on Notch activation, we performed a ChIP assay in Ls174T cells untreated or treated with DAPT. We found that binding of β-catenin to the *JAGGED1* promoter was independent of Notch activation.

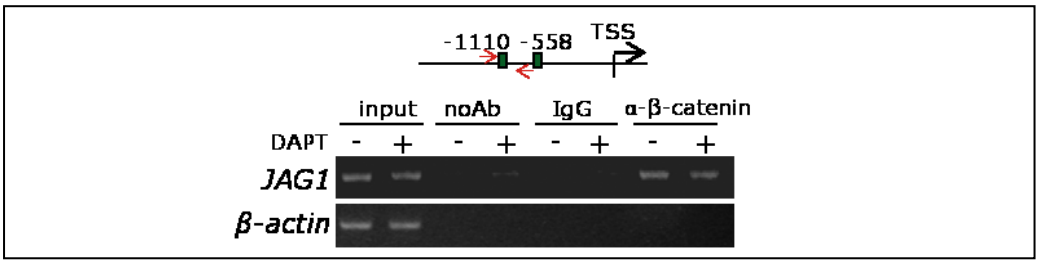

FIGURE R8. *Jagged1* is a direct β-catenin/TCF target gene. Recruitment of β-catenin to *JAGGED1* promoter in Ls174T cell line untreated or treated with DAPT. *β-actin* gene is shown as a negative control.

We next investigated whether regulation of JAGGED1 levels and Notch activation by β-catenin was a general mechanism that occurs in CRC cells. By qRT-PCR, we found that *JAGGED1* transcription was highly increased in different CRC cell lines carrying nuclear β-catenin, such as HCT116, SW480, and Ls174T, compared with the non-transformed HS27 control cells [**FIGURE R9** (upper)]. Moreover, in all these cancer cell lines β-catenin was recruited to the *JAGGED1* promoter to a different extent [**FIGURE R9** (lower)], correlating with higher JAGGED1 expression and increased levels of nuclear active Notch1 and Notch2 (cleaved Notch2 fragment of 110 KDa), as

shown by subcellular fractionation followed by western blot [**FIGURE R9** (middle)].

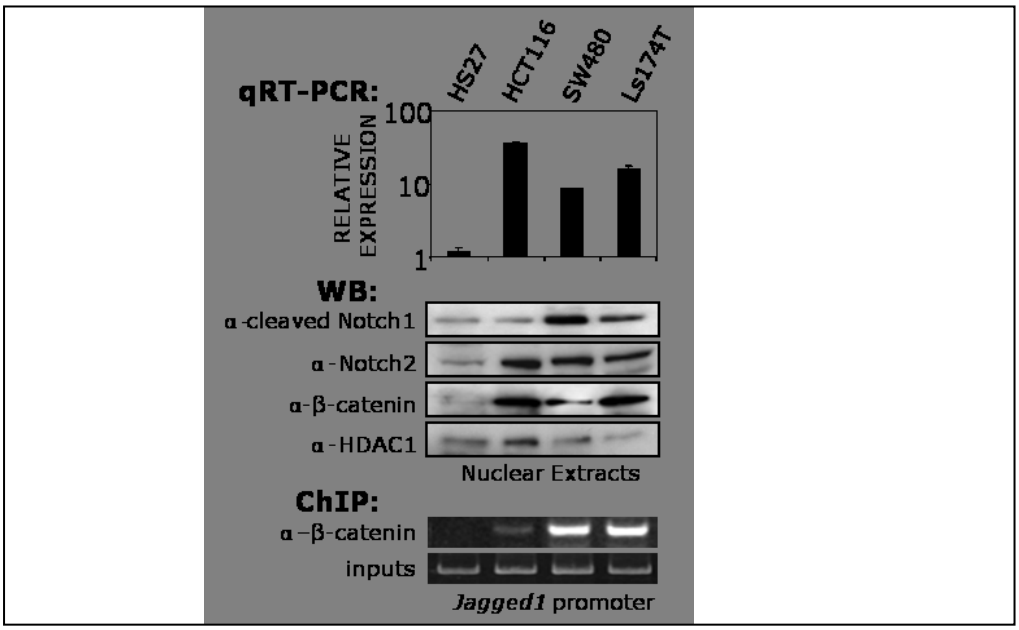

FIGURE R9. Strong correlation between the presence of β-catenin, JAGGED1 and active Notch proteins. Upper panel, qRT-PCR was used to determine the expression of *JAGGED1* in CRC cell lines compared to non-transformed HS27 cells. Middle panel, Western blot analysis of CRC nuclear extracts with α-cleaved Notch1, α-Notch2 and α-β-catenin antibodies. Lower panel, ChIP with α-β-catenin antibody in CRC cell lines compared to HS27 cells. The presence of *JAGGED1* promoter in the precipitates was determined by PCR.

To further demonstrate that JAGGED1 was the ligand responsible for activating Notch and, as a consequence, its downstream targets, we trasfected Ls174T cells with specific siRNA against *JAGGED1* and tested the expression levels of selected genes. We found that all of them were down-regulated (from 20 to 60% inhibition) compared with cells treated with scrambled siRNA [**FIGURE R10**].

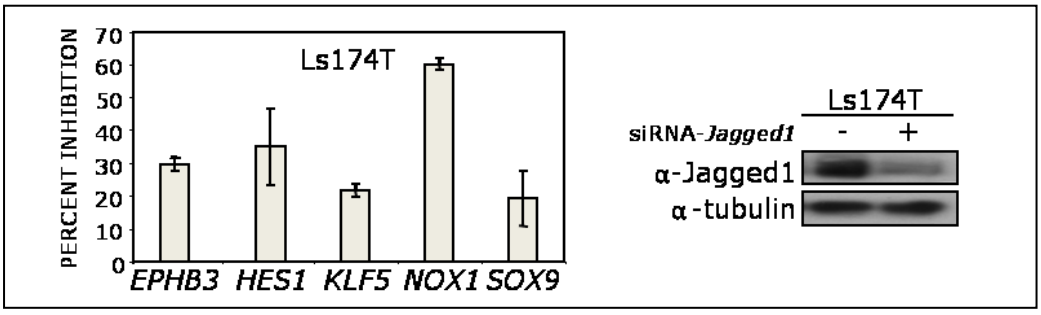

FIGURE R10. Jagged1 is responsible for the transcriptional activation of Notch target genes. Left, percent inhibition of indicated genes after siRNA-*Jagged1* transfection was determined by qRT-PCR. Right, Downregulation of *Jagged1* by siRNA was determined by western blot.

Together, these data demonstrate that *JAGGED1* is a Wnt/β-catenin target gene in CRC and it is responsible for Notch activation in this system.

R3. The tumorigenic role of Notch activation by its ligand Jagged1 in CRC

R3.1. Activated Notch1 blocks differentiation and promotes vascularization *in vivo* in the absence of β-catenin/TCF signaling

We next studied whether activated N1ICD conferred any malignant capacity to Ls174T cells in the absence of β-catenin/TCF signaling. As a first approach, we seeded the inducible Ls174T/dnTCF4 and Ls174T/dnTCF4/N1ICD cells in soft agar in the absence or presence of doxycycline and counted the number of colonies generated after 7 days. We found that doxycycline treated Ls174T/dnTCF4/N1ICD lines (in which Wnt is repressed and Notch is activated) displayed an increased clonogenic capacity in soft agar cultures compared with Ls174T/dnTCF4 clones. Two independent experiments were performed in duplicates and the average number of colonies is represented [**FIGURE R11**].

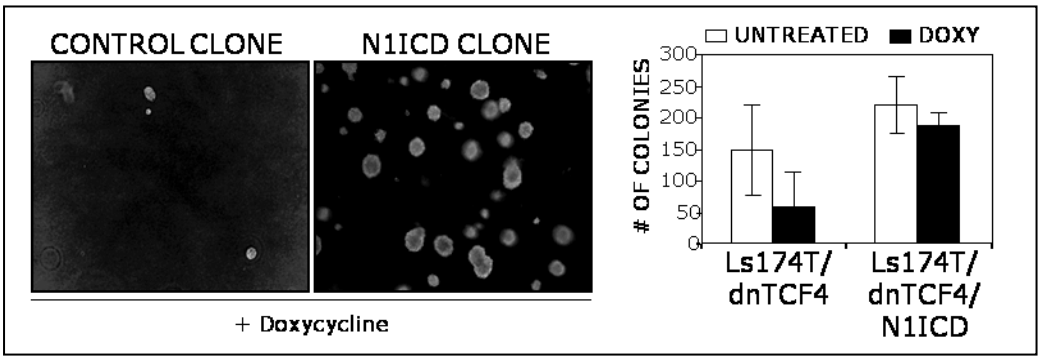

FIGURE R11. N1ICD expression promotes colony formation in soft agar in the absence of Wnt signaling. Representative images were obtained in an Olympus IX-10 at 100X. Right, quantification of the soft agar assay. Error bars represent s.e.m.

To test the tumorigenic capacity of these cells *in vivo*, in collaboration with Dr. Alberto Villanueva (ICO-IDIBELL, L'Hospitalet del Llobregat), we injected subcutaneously $1.5x10^6$ Ls174T/dnTCF4 cells in the left leg and Ls174T/dnTCF4/N1ICD cells in the right leg of nude mice. In each experiment, ten animals were left untreated and ten mice were treated with doxycycline in the drinking water for 4 weeks, and the experiment was repeated twice. We observed that the non-treated animals developed tumors in both legs, which it was expected because this CRC cell line is able to generate tumors in immunodeficient mice. Interestingly in the doxycycline-treated group, we found that Ls174T/dnTCF4/N1ICD clones generated tumors that were significantly larger compared with the ones generated by the Ls174T/dnTCF4 cells (P=0.022) [**FIGURE R12**]. These findings indicate

that Notch activation, in the absence of β-catenin activity, is capable to promote tumor growth in this system.

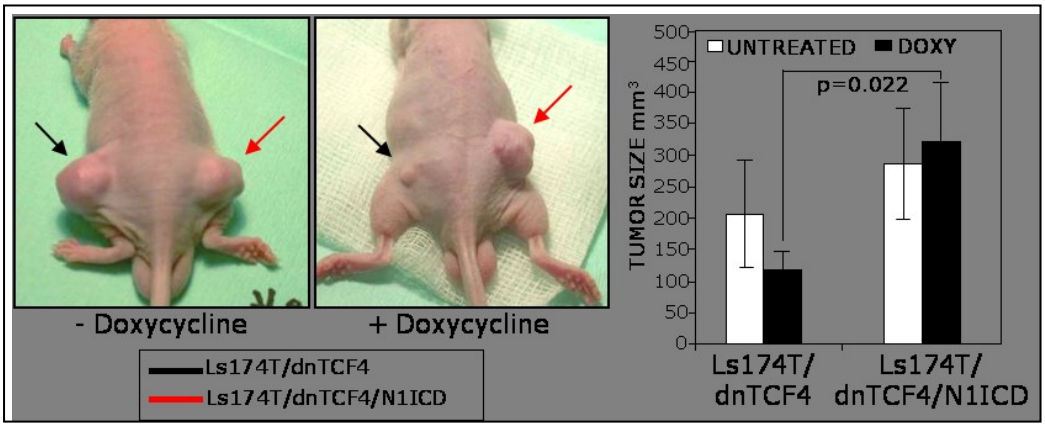

FIGURE R12. N1ICD increases tumor growth *in vivo*. Left, image of representative animals untreated or treated with doxycycline. Twenty animals were analyzed per experiment. We performed three independent experiments. Right, the graph represents the average and the s.e.m of the tumor volume (mm^3).

Moreover, a more detailed analysis of the tumors generated in these mice, demonstrated that tumors expressing N1ICD showed a strong reduction of Alcian blue staining, indicative of reduced muco-secretory differentiation, but comparable proliferation ratio (measured by Ki67 staining) [**FIGURE R13**].

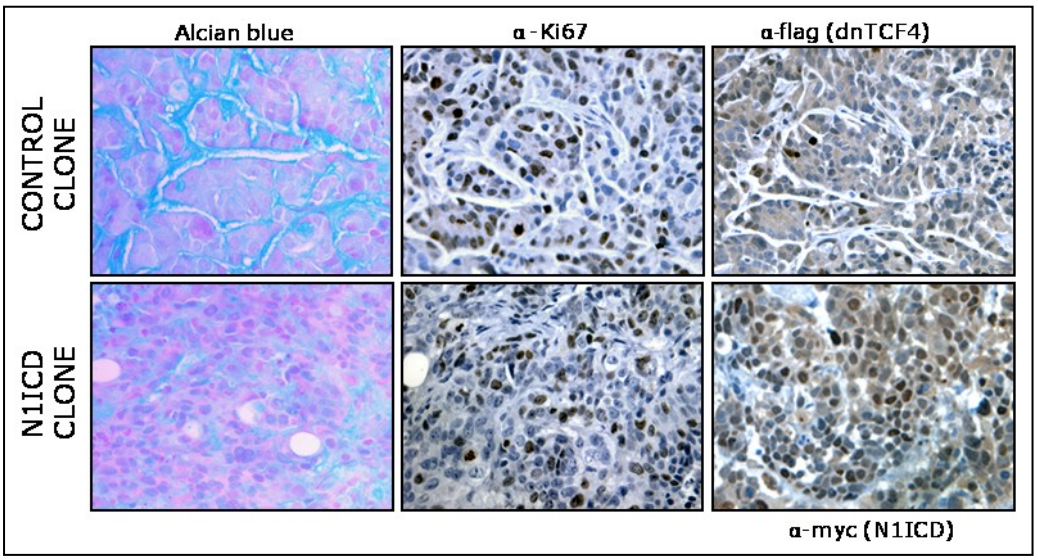

FIGURE R13. N1ICD blocks muco-secretory differentiation but does not affect proliferation. Sections of tumors generated by Ls174T/dnTCF4 and Ls174T/dnTCF4/N1ICD in Doxycycline-treated nude mice. Alcian blue staining and IHC with the α-Ki67 antibody are shown. α-flag or α-myc staining indicate expression of dnTCF4 and N1ICD in the tumors. Representative images were obtained in an Olympus IX-10 at 400X.

In addition to the effects on differentiation, we observed a strong increase in the proportion of growing areas in tumors expressing N1ICD compared with control tumors, that was concomitant with increased vascularization as detected by α-SMA staining (11 positive of 11 Ls174T/dnTCF4/N1ICD tumors analyzed, compared with 3 positive of 10 Ls174T/dnTCF4 tumors) [**FIGURE R14** (lower panels)]. Moreover, we detected high levels of endogenous Notch activity in the untreated Ls174T/dnTCF4 tumors with a specific antibody recognizing cleaved Notch1 (N1ICDv antibody) that was greatly inhibited after doxycycline treatment [**FIGURE R14** (upper panels)].

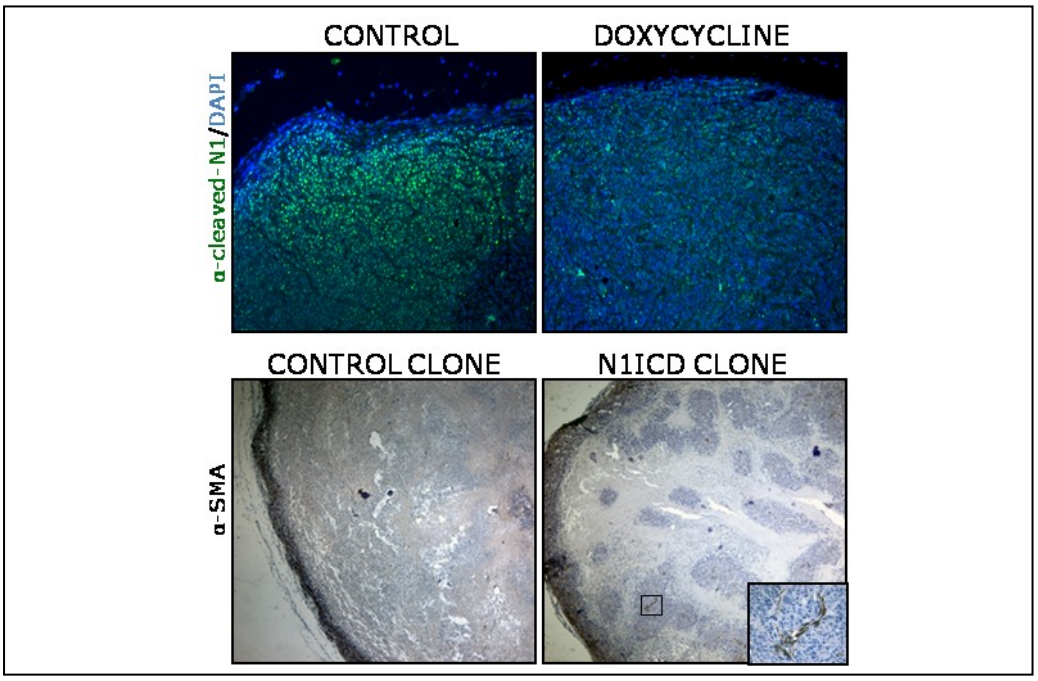

FIGURE R14. Notch promotes vascularization. Upper panel, α-cleaved Notch staining of representative Control Tumors treated or untreated with doxycycline (200x). Lower panel, α-SMA staining (40x), and detail of vascularized area (in the box, 400x).

As a control, we found that ectopic expression of the Notch ligand JAGGED1 in Ls174T/dnTCF4 was sufficient to block muco-secretory differentiation when Wnt/β-catenin signaling is switched-off (determined 48h after doxycycline treatment) [**FIGURE R15**, lower], similar to N1ICD expression [**FIGURE R15**, upper].

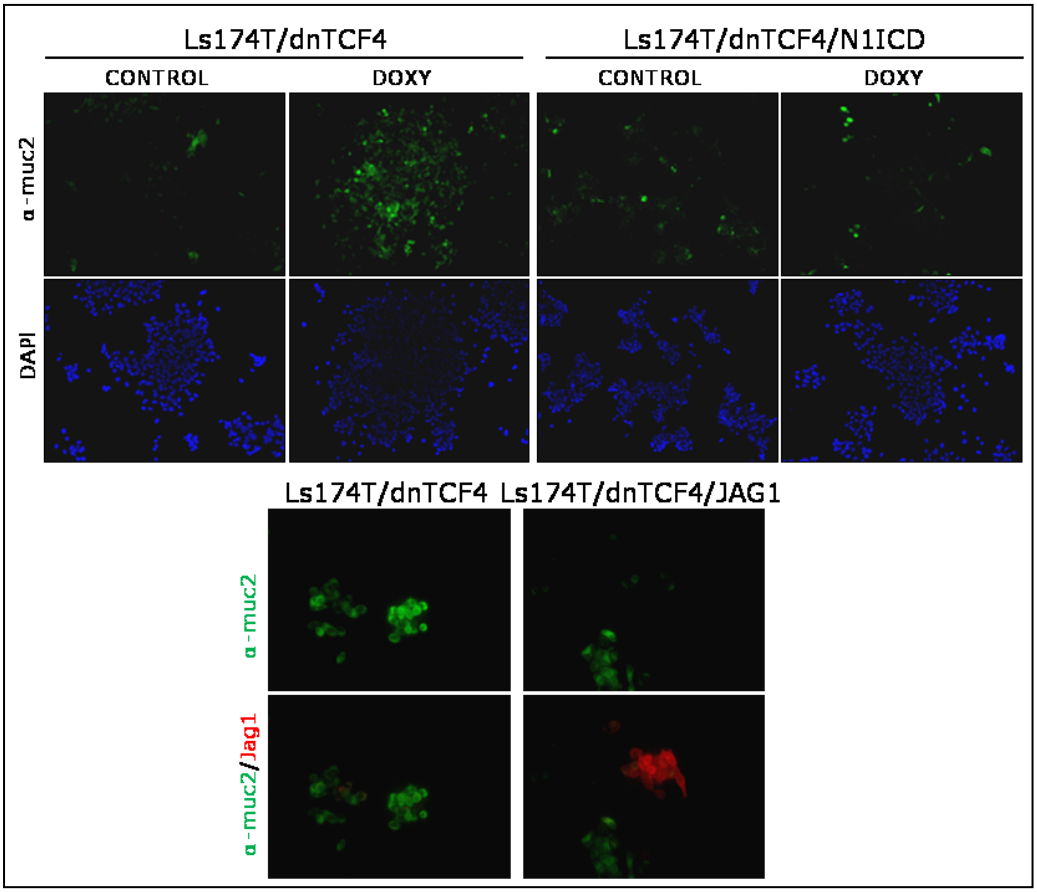

FIGURE R15. Notch signaling blocks cell differentiation in the absence of β-catenin signaling. Upper panel, immunostaining with α-muc2 antibody in the indicated clones untreated or treated with Doxy. Lower panel, Jagged1 blocks cell differentiation in the absence of β-catenin signaling. Immunostaining with α-muc2 and α-Jagged1 antibodies in Ls174T/dnTCF4 cells transfected with mock or with Jagged1 plasmids, treated with Doxy. Representative images were obtained in an Olympus IX-10 at 200 and 400X respectively.

Together, these results indicate that activated Notch1 exert a direct effect in regulating goblet cell differentiation and tumor vascularization whereas regulation of cell proliferation likely requires the contribution of β-catenin/TCF signaling pathway.

R3.2. Deletion of a single Jagged1 allele reduces tumor growth in the *Apc*$^{Min/+}$ intestine

To investigate whether Notch activation is affected by the activation of the Wnt pathway *in vivo*, we determined the levels of different Notch family members in intestinal tumors arising in the *Apc*$^{Min/+}$ mice compared with normal mucosa. By IHC, we found an over-expression of JAGGED1 in the

tumor tissue of these animals compared with the normal crypts that was concomitant with Notch1 and Notch2 activation [**FIGURE R16**].

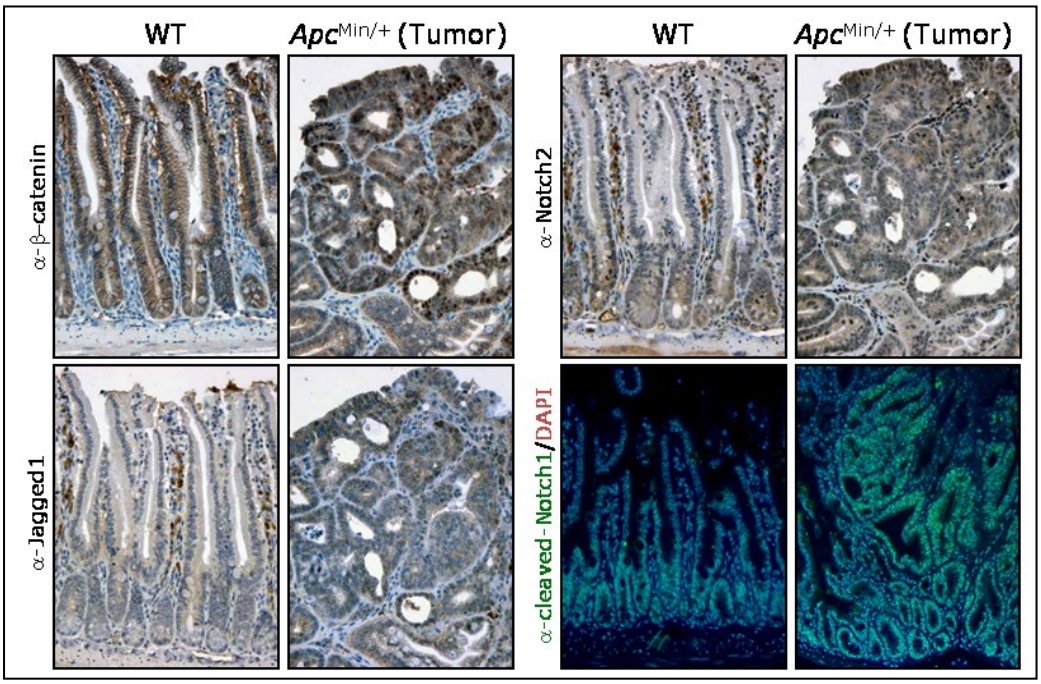

FIGURE R16. Jagged1 is over-expressed in tumors carrying nuclear β-catenin. IHC of serial section of WT intestine and *Apc*$^{Min/+}$ tumor stained with the indicated antibodies. Representative images were obtained in an Olympus IX-10 at 200X.

Then we tested the functional *in vivo* relevance of Jagged1 as an activator of Notch signaling downstream of β-catenin, by crossing the *Apc*$^{Min/+}$ mice with *JAGGED1* heterozygous (*Jag1*$^{+/-}$) animals, which are phenotypically normal (whereas *Jag1*$^{-/-}$ are lethal) [140]. A total of 23 animals of the different genotypes were sacrificed at 4 months of age and analyzed for the presence of macroscopic intestinal tumors following methylene blue staining (See **MM12**).

We found that deletion of one *Jagged1* allele was sufficient to significantly reduce the size of tumors in the *Apc* mutant background (P=0.0001) [**FIGURE R17**] concomitant with a reduction in the amount of active Notch1, whereas the nuclear levels of β-catenin in the tumors from the different genotypes were equivalent (71±8% and 66±8%, respectively) [**FIGURE R18**].

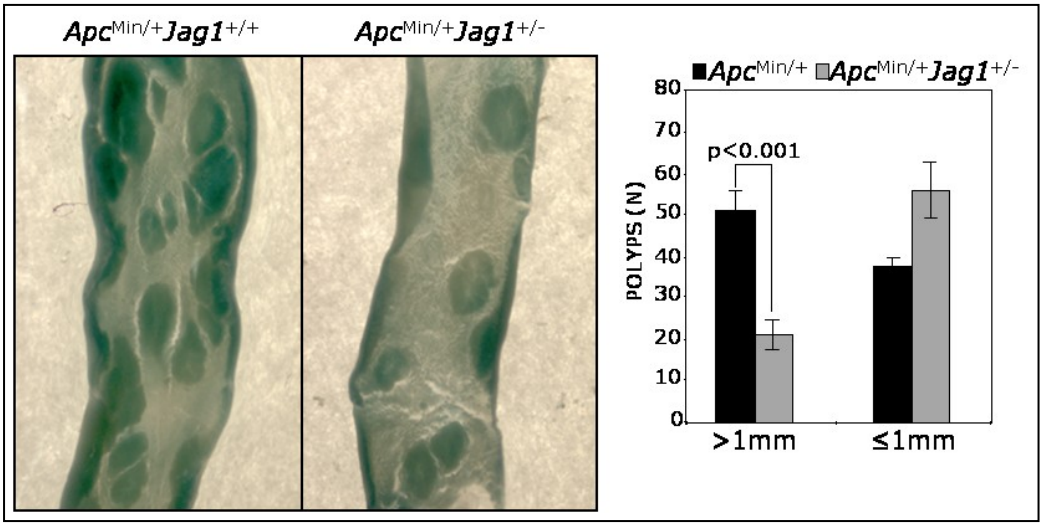

FIGURE R17. Deletion of a single *Jagged1* allele reduces tumor size in $Apc^{Min/+}$ mice. Left, images of $Apc^{Min/+}$ intestines in a $Jag1^{+/+}$ or $Jag1^{+/-}$ background. Right, the average number of visible polyps from the different genotypes at 16 weeks of age is represented. Error bars are s.e.m.

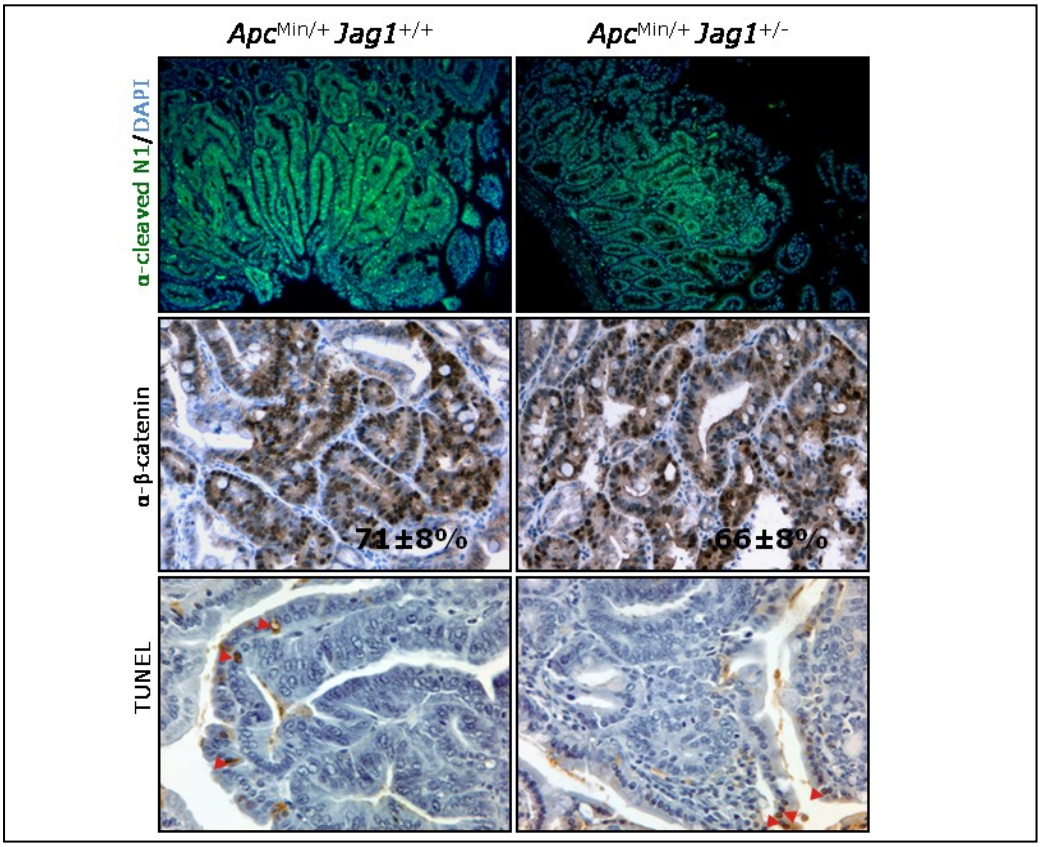

FIGURE R18. *Jagged1* reduction does not affect β-catenin levels neither apoptosis. Immunostaining with indicated antibodies of tumors from $Apc^{Min/+}$ or $Apc^{Min/+}Jag1^{+/-}$ mice. Middle, the average percentage of cells showing nuclear β-catenin is indicated. Lower, red arrows indicate apoptotic cells. Representative images were obtained in an Olympus IX-10 at 100X or 200X.

These results suggest that *Jagged1* deficiency confers a growing disadvantage to β-catenin-dependent tumors. In agreement with this, we found a reduction in the number of Ki67 positive cells in the tumors of the *Apc*$^{Min/+}$*Jag1*$^{+/-}$ double mutants compared with the ones from the *Apc*$^{Min/+}$ littermates (from 80.4±2% to 55.6±3%, *P*<0.001) [**FIGURE R19**], whereas no differences were found in the number of apoptotic cells as measured by TUNEL assay [**FIGURE R18** (lower)].

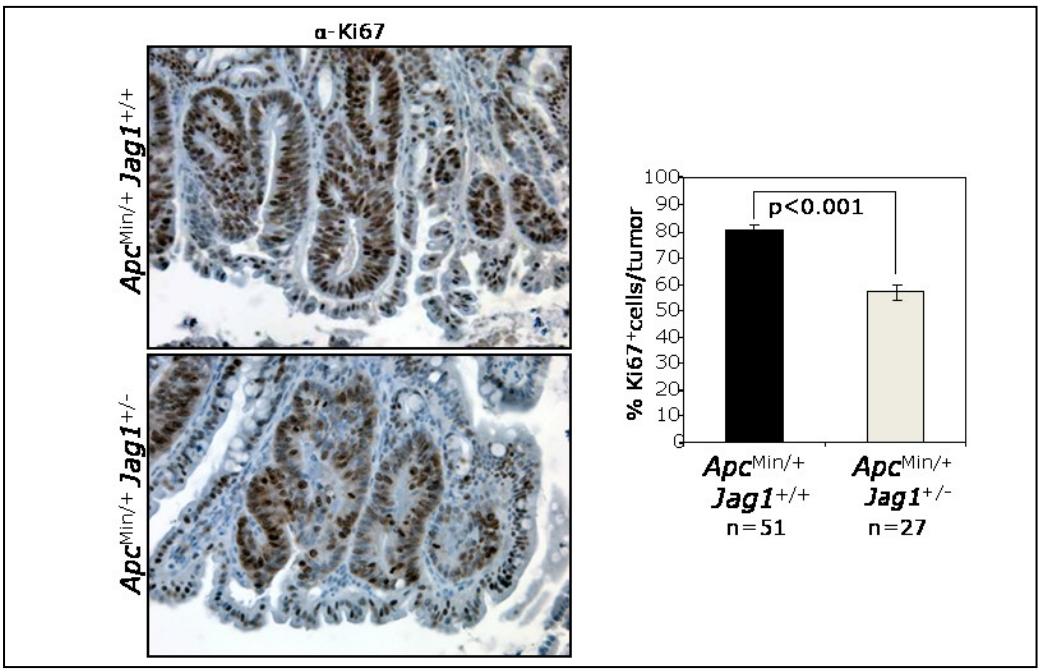

FIGURE R19. Reduction in tumor size is due by a reduction in proliferation. Representative images of α-Ki67 staining in *Apc* mutant tumors and average percentage of Ki67+ cells/tumor from 5 *Apc*$^{Min/+}$*Jag1*$^{+/+}$ and 4 *Apc*$^{Min/+}$*Jag1*$^{+/-}$. Images were obtained in an Olympus IX-10 at 200X. Error bars are s.e.m.

Moreover, the expansion of the proliferative compartment that we observed in the morphologically normal crypts of *Apc*$^{Min/+}$ mutant mice [198], was reverted in the *Apc*$^{Min/+}$*Jag1*$^{+/-}$ mice (*P*<0.001) [**FIGURE R20**]. These results demonstrate that activation of Notch by JAGGED1 confers a proliferative advantage to the tumors with *Apc* mutations.

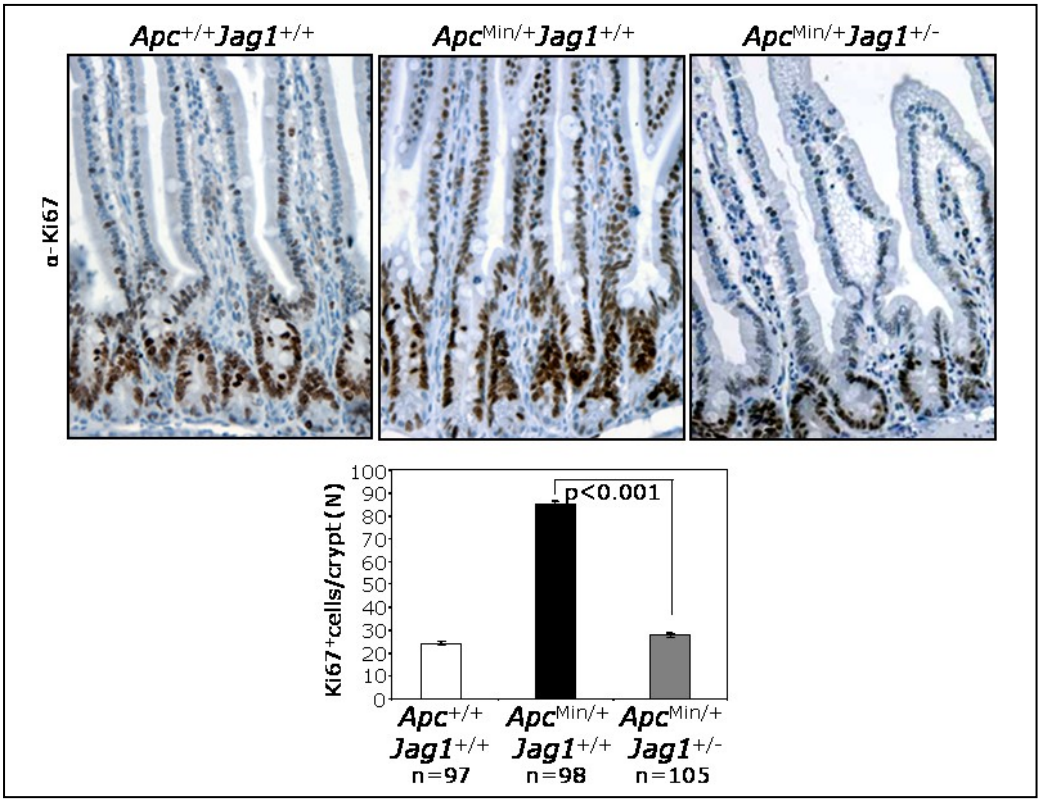

FIGURE R20. Jagged1 reduction affects not only tumors but also normal crypts. Sections of normal crypts from different genotypes stained with α-Ki67 antibody (upper) and quantification of Ki67+ cells per crypt (lower). Average number of Ki67+ cells/crypt are represented from 10 $Apc^{+/+}Jag1^{+/+}$, 5 $Apc^{Min/+}Jag1^{+/+}$ and 4 $Apc^{Min/+}Jag1^{+/-}$. Representative images were obtained in an Olympus IX-10 at 200X. Error bars are s.e.m. n, number of crypts counted.

R3.3. High levels of Jagged1 correlate with activated Notch1 and Notch2 in human colorectal tumors containing nuclear β-catenin

We next investigated whether the β-catenin-dependent Notch activation was relevant in human colorectal adenomas arising in Familial Adenomatous Polyposis (FAP) patients, which harbor *Apc* germ line mutations.

By qRT-PCR we found that *JAGGED1* mRNA levels were significantly increased in most FAP adenomas compared with normal intestinal tissue ($P<0.05$). Interestingly, some increase in *JAGGED1* expression was also detected in the normal colonic mucosa of FAP patients, compared with normal controls [**FIGURE R21**].

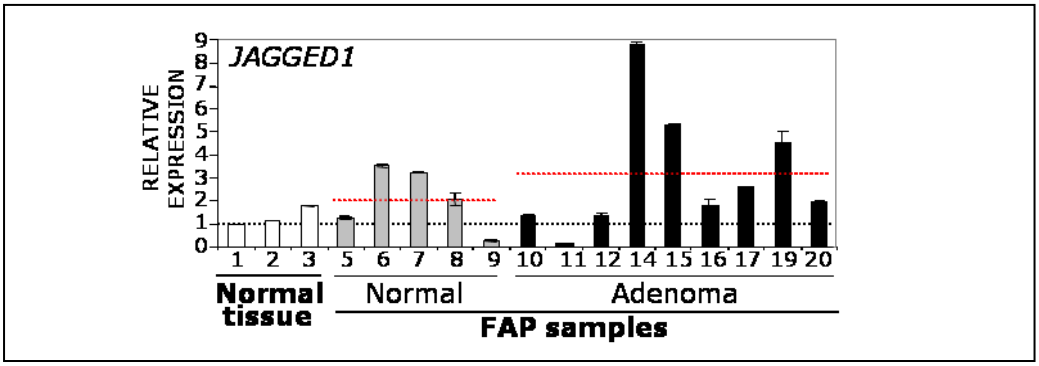

FIGURE R21. FAP samples contain increased levels of *JAGGED1* mRNA as measured by qRT-PCR. The red line indicates the average value for each group.

By IHC, we found high levels of the JAGGED1 protein confined in the tumor areas containing nuclear β-catenin staining (n=6) that were not detected in the normal adjacent tissue. This was concomitant with the presence of nuclear Notch2 [**FIGURE R22**] and active Notch1 [**FIGURE R23**].

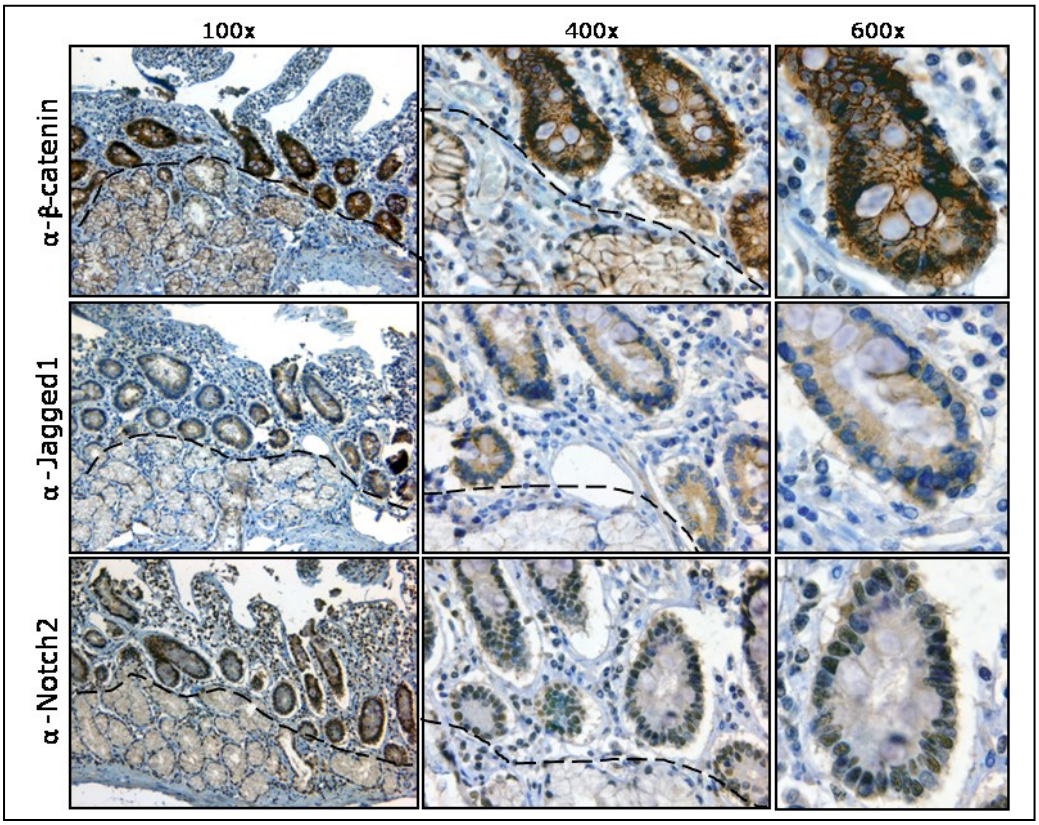

FIGURE R22. FAP samples contain increased levels of several Wnt-Notch targets. Serial sections of CRC from FAP patient were stained with the indicated antibodies. Images were obtained in an Olympus BX-60 at indicated magnifications.

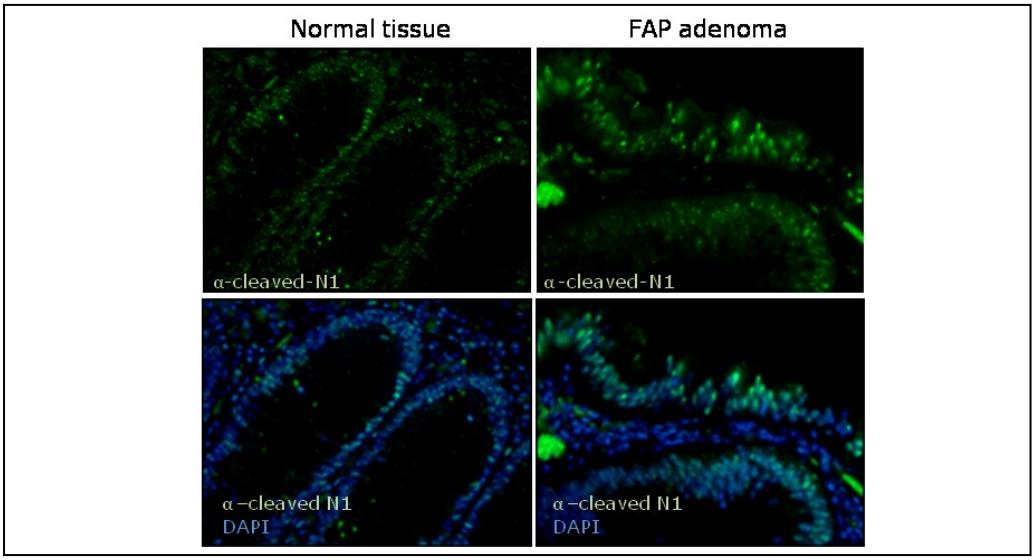

FIGURE R23. Notch1 is activated in adenomas from FAP patients. Immunoflouresence with α-cleaved Notch1 (green) from a normal tissue compared with a FAP adenoma. Nuclei were stained with DAPI (blue). Images were obtained in an Olympus BX-60 at 400X.

Further demonstrating the importance of Notch transcriptional activity in human tumors carrying active β-catenin, we found increased expression of *SOX9* (*P*=0.005), *NOX1* (*P*=0.002), *KLF5* (*P*=0.01) and *HES1* (not significant) [**FIGURE R24**], identified in our microarray screening as Notch-dependent targets [**FIGURE R4**], in the adenoma samples from FAP patients. Some of these genes were also up-regulated in the normal colonic mucosa from these patients compared with the normal controls [**FIGURE R24**] likely because of the presence of one mutated *Apc* allele [**TABLE R2**].

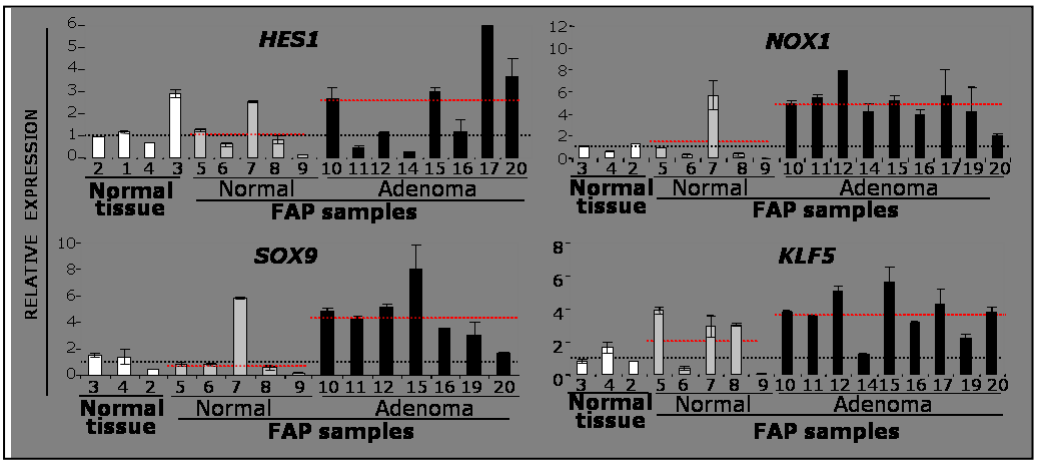

FIGURE R24. FAP samples contain increased levels of several Wnt-Notch targets. Graphs represent the mRNA levels of the indicated genes measured by qRT-PCR in normal colon tissue compared with normal adjacent and adenoma samples from FAP patients. The red line indicates the average value for each group.

FAP PATIENTS	SAMPLE NUMBERS	GERM LINE MUTATION
FAP1	5, 11, 15	c.1958 G>A; exon 14 skipping
FAP3	9, 17	c.1958+3A>G +c.1959G>A; exon 14 skipping
FAP4	8, 16, 20	c.4175C>A; p.Ser1392X
FAP6	7, 14, 19	c. 4612_4613delGA; p.Glu1538IlefsX5

TABLE R2. List of germ line mutations in the *Apc* gene of patients included in the qRT-PCR analysis.

These results indicate that Notch, downstream of Jagged1, acts as an essential mediator of β-catenin-dependent intestinal tumorigenesis and is responsible for regulating a specific transcriptional cancer signature.

R4. β-catenin and Notch cooperate to activate a common specific gene signature

R4.1. Characterization of Notch and β-catenin double target genes

Our experiments show that there is a genetic program that depends on Notch downstream of Wnt/β-catenin and find that some of these genes are over-expressed in colorectal tumors. Microarray analysis of cells lacking β-catenin signaling but expressing activated N1ICD demonstrated that 31% of genes dependent on Wnt and Notch activities were actually Notch-target genes, since they were re-expressed by active Notch in the absence of β-catenin [**FIGURE R4** and **ANNEX A3**]. However, 69% of the Wnt-Notch-dependent genes are not re-expressed with N1ICD. Thus, we investigated whether these genes, which we called *double Notch and Wnt target* genes (*dNWt* genes), require the direct participation of both transcription factors to be activated. In this case, we chose the genes that were down-regulated after DAPT treatment and dnTCF4 expression but were not rescued by activation of Notch alone and confirmed these conditions by qPCR [**FIGURE R25**].

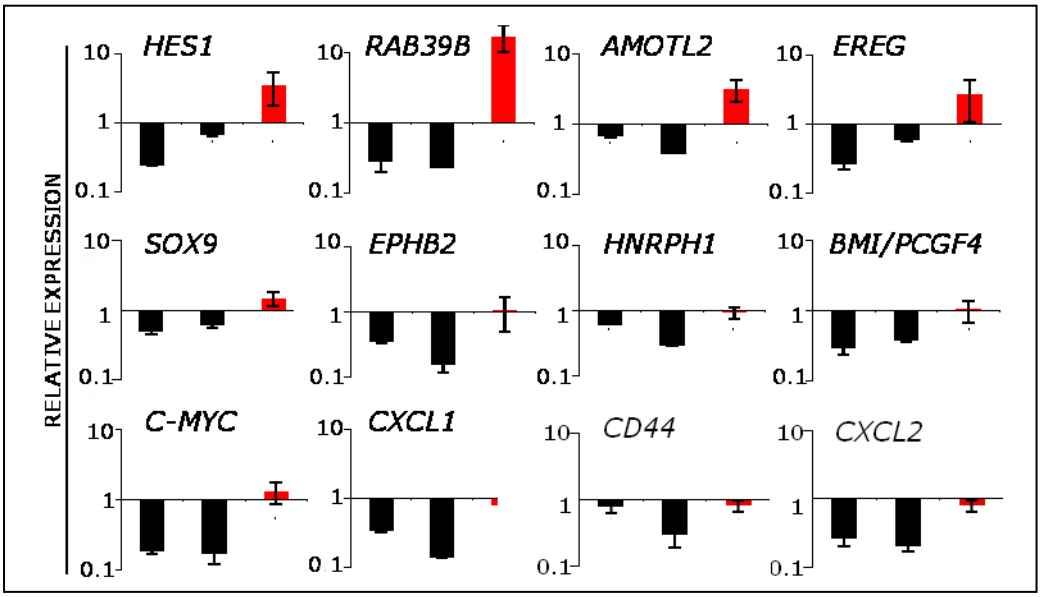

FIGURE R25. Characterization of Notch and β-catenin double-target genes. Confirmation by qPCR of different genes identified in the microarray R4. Black bars indicate inhibitory treatments (DAPT and Doxy, respectively) in Ls174T/dnTCF cells, and red bars indicate the expression after doxycycline treatment in Ls174T/dnTCF4/N1ICD. Error bars represent s.e.m.

Then, we investigated the presence of TCF and RBP_{JK} binding sequences in the promoters of our candidate genes including *EPHB2*, *BMI*, *CD44* and *c-MYC,* using the Genomatix Software. As represented in **FIGURE R26**, we found that all these genes contain both binding consensus in their regulatory

regions [**TABLE R3**]. In collaboration with Dr. Pedro Fenández Salguero (U. Extremadura, Spain), we also performed a bioinformatics analysis of the whole human genome looking for a distribution pattern of TCF and RBP_{JK} binding sites that could predict a more general cooperation between Notch and β-catenin in the chromatin. We found that both sequences are not distributed randomly but they tend to be clustered in the promoter regions close to the transcription start sites and separated by specific distances picking at 100bp [**FIGURE R26**]. Together these data suggest that Notch and β-catenin associate together in specific promoters to regulate gene transcription.

Gene	RBP_{JK} Consensus	Position	TCF Consensus	Position
EPHB2	cgagTGGGagactgg	-626bp	aaataaaCAAAgcccag	-1998bp
	tgccTGGGaaagccg	-390bp	atagaaaCAAAgcaaaa	-1859bp
			tgtgggaCAAAgggaca	-1241bp
BMI1	agacTGGGaaaattc	-1612bp	acattttCAAAgccatg	-1744bp
	aactTGAGaaaattc	-1409bp	aatttttCAAAggcatc	-1508bp
			tatctaaCAAAggttat	-84bp
CD44	CagaTGGGaaatg	-1167bp	caggcctCAAAggaaaa	-1922bp
	TgtaTGGGaagat	-1069bp	tatcattCAAAgtatga	-1407bp
C-MYC	TggcTGAGaaattgg	-925bp	ttctgatCAAAgaagag	-1257bp
	AgcgTGGGatgttag	-505bp	gagaaatCAAAggtgct	-1013bp
			tcttgatCAAAgcgcgg	-441bp

TABLE R3. Sequences identified with the *Genomatix* software as RBP_{JK} -binding consensus in the different promoters. The capital letters corresponds to the core of the motif.

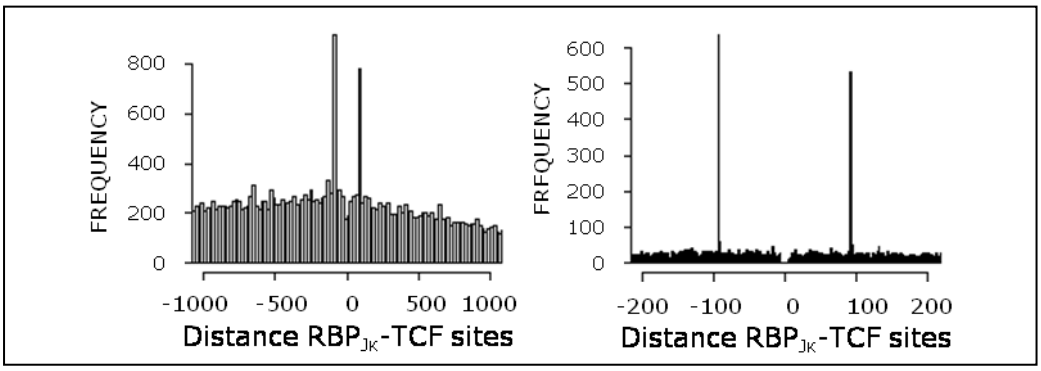

FIGURE R26. Graphs representing the number of genomic sequences containing RBP_{JK} and TCF binding sites (Y axis) separated by specific distances (X axis).

To validate this possibility, we performed ChIP assay to determine whether β-catenin and Notch are recruited to the promoters of selected Wnt-Notch-dependent genes in CRC cells. For these experiments, we used primers flanking the putative TCF and RBP_{JK}-binding sites, which are represented in **FIGURE R27,** as well as a primer pair located at -5Kb from the TSS (named PRO1) as negative control. We found that Notch and β-catenin factors were both recruited to the promoter of these genes in CRC cells [**FIGURE R28**].

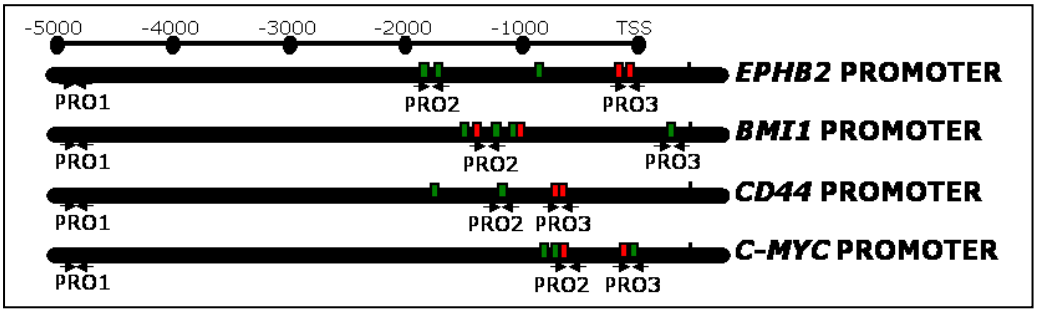

FIGURE R27. Diagram of TCF and RBP_{Jk} binding sites on the indicated promoters predicted by Genomatix Software. Red boxes symbolize RBP_{JK}-binding sites and green boxes TCF–binding sites. The arrows indicate the primers used for ChIP assays.

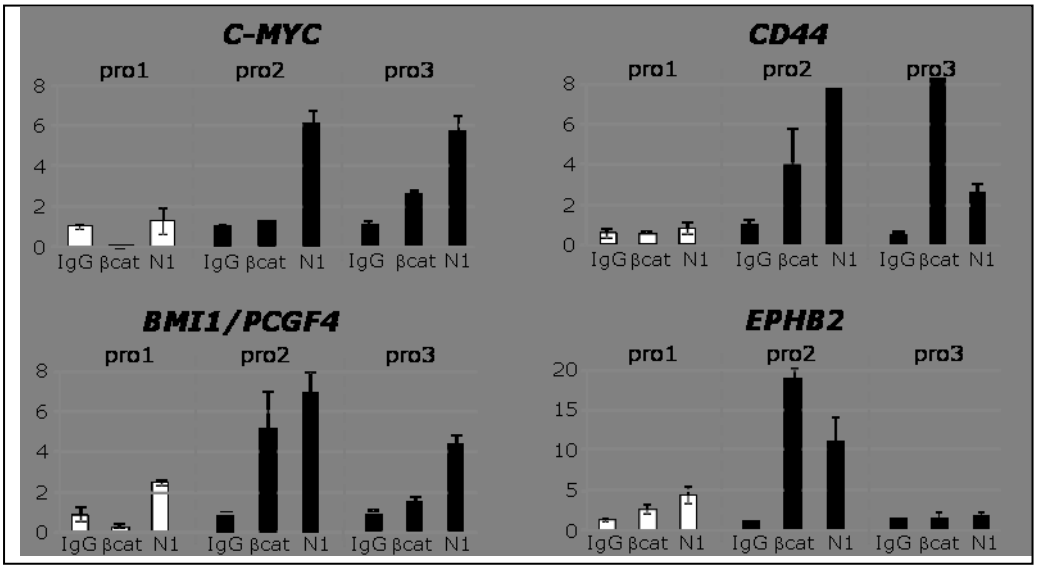

FIGURE R28. Recruitment of β-catenin and Notch1 to the *dNWt* promoters. qPCR of the indicated genes after ChIP assays with β-catenin and Notch1 antibodies, IgG was used as a control for the experiment. Error bars represent s.e.m.

Moreover, in sequential ChIP experiments we found that β-catenin and Notch bound together to the promoter region of these specific genes [**FIGURE R29**].

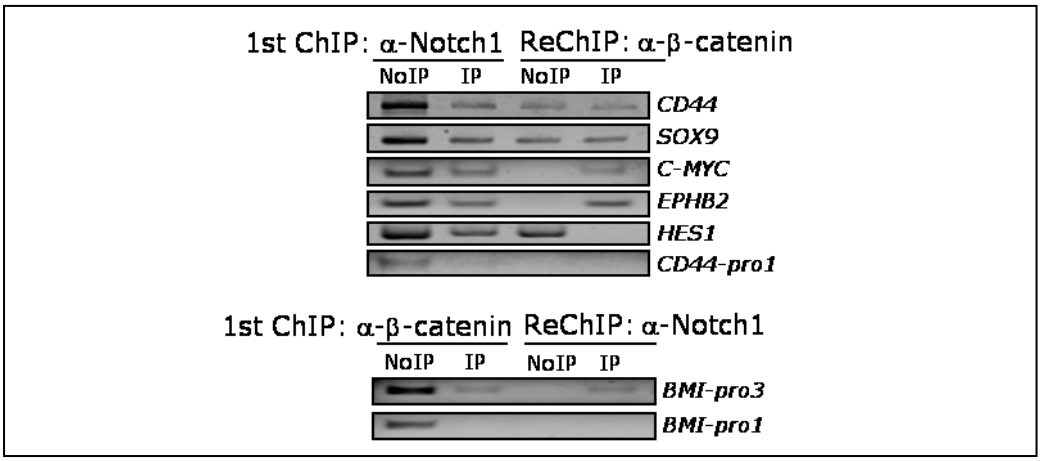

FIGURE R29. Simultaneous recruitment of β-catenin and Notch1 to the candidate gene promoters. qPCR of the indicated genes after sequential ChIP with the indicated antibodies. Primer pairs CD44-pro1 and BMI-pro1 are shown as negative controls.

R4.2. Cooperation between Notch and β-catenin in the nucleus

The finding that Notch and β-catenin were simultaneous recruitment to the promoters of specific genes suggests a physical association of these factors in the nucleus. Although interaction between Notch and β-catenin has been previously shown [279, 280], we further explored the nuclear association of both factors in CRC cells, where Notch and Wnt are aberrantly activated.

Co-precipitation experiments from CRC cells demonstrated a physical association between endogenous active Notch1 and β-catenin, which specifically occurs in cancer cells [**FIGURE R30**].

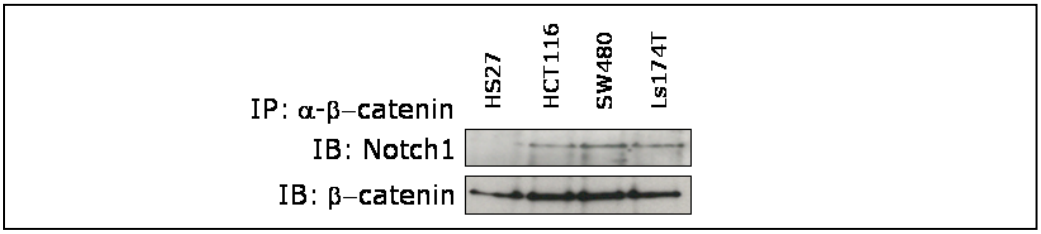

FIGURE R30. β-catenin and Notch1 interaction in CRC cells. Precipitation with β-catenin antibody and detection of Notch1 in the precipitates by WB from different CRC cell lines compared with the non-transformed cell line HS27.

In addition, this interaction took place in the nucleus and was lost following Notch inhibition by gamma-secretase inhibitor (GSI) treatment, indicating that β-catenin specifically binds active Notch [**FIGURE R31**].

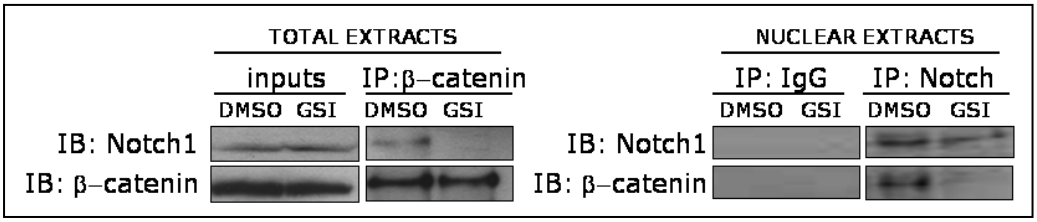

FIGURE R31. Nuclear interaction between β-catenin and Notch1 depends on Notch1 activation. Left, co-immunoprecipitation of β-catenin and Notch1 in untreated or GSI-treated CRC cells. Right, co-immunoprecipitation of β-catenin and Notch using nuclear extracts from CRC cells, in the absence or presence of GSI treatment.

We further characterized this interaction by mapping the regions of β-catenin and Notch that were involved. By pull-down experiments using different GST-β-catenin constructs (given by Dra. Duñach, UAB, Bellaterra) we identified the armadillo repeats 7-12 as the specific Notch-binding region of β-catenin [**FIGURE R32**].

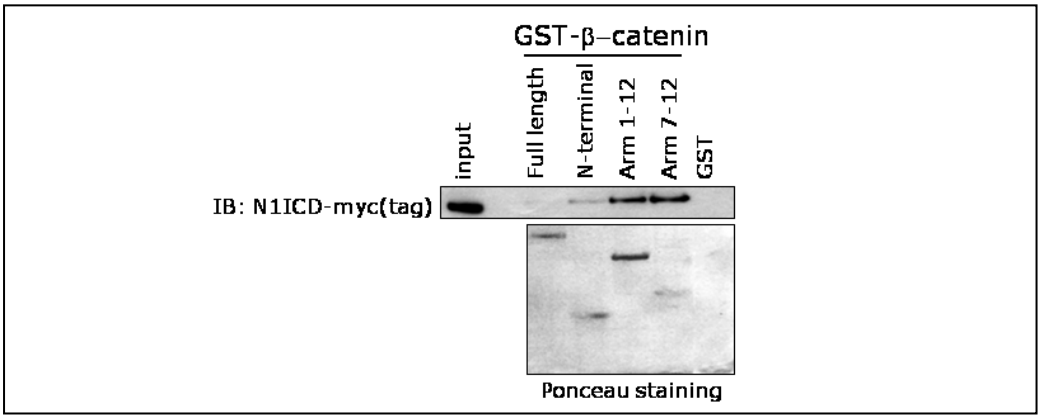

FIGURE R32. β-catenin interacts with Notch1 through Armadillo 7-12. Pull-down assay using different regions of β-catenin fused to GST and detecting Notch1 bound from a 293T lysate previously transfected with N1ICD.

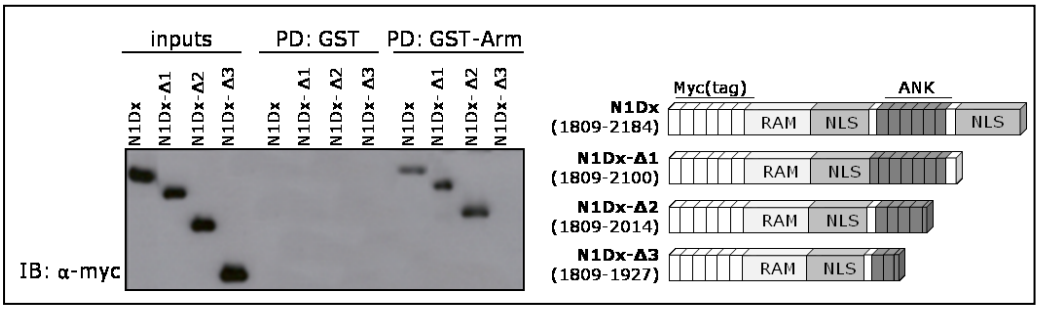

FIGURE R33. Notch1 interacts with β-catenin through residues from 1927 to 2014. Pull-down assay using GST-β-catenin(Arm) and detecting Notch1 bound from a 293T lysate previously transfected with different N1ICD constructs. Right, scheme of the Notch1 constructs.

Similarly, we determined that the region of Notch that mediates the binding to β-catenin includes residues from 1927 to 2014 and involves the domains previously found to mediate Notch dimerization (R1985) [281] [**FIGURE R33**].

R4.3. Cooperative regulation of gene transcription by Notch and Wnt pathways *in vivo*

Since Notch and β-catenin are important not only for tumor progression, but also for the maintenance of the intestinal homeostasis, we next investigated the expression pattern of some selected *dNWt* genes in the mouse small intestine. By In Situ Hybridization (ISH), we found that several of these genes were specifically expressed in the bottom of the intestinal crypts [**FIGURE R34**] where both Wnt and Notch pathways are active, and consistent with their role in the maintenance of the undifferentiated cell compartment [210, 282, 283].

To investigate the contribution of each pathway to the expression of the *dNWt* genes *in vivo*, in collaboration with Dr. Freddy Radtke (EPFL, Lausanne, Switzerland), we generated mutant mice with different combinations of gain or loss of function (GOF/LOF) mutations for Notch and Wnt pathways. Specifically, we used tamoxifen-inducible CRE recombinase driven by the villin promoter (villin-CRE$^{ER\text{-}T2}$) to conditionally delete β-catenin and/or RBP$_{J\kappa}$ in the intestine by crossing them with *Ctnnb1*^{lox} and/or *Rbp*$_{J\kappa}$^{lox} mice. In addition, these mutants were combined with mice carrying active forms of β-catenin (*Ctnnb1*$^{lox(ex3)}$ mice) and Lox-STOP-lox-Rosa26N1ICD-IRES-GFP mice (N1ICD^{lox}) under the control of this same inducible promoter.

By ISH analysis, we found that intestinal deletion of either β-catenin or RBP$_{J\kappa}$ resulted in the total loss of *Cd44* or *c-Myc* [**FIGURE R34**], and their expression was not recovered when the abrogation of one pathway was combined with the constitutive activation of the other (*Ctnnb1*$^{lox(ex3)}$ *Rbp*$_{J\kappa}$^{lox} villin-CRE$^{ER\text{-}T2}$ or N1ICD^{lox} *Ctnnb1*^{lox} villin-CRE$^{ER\text{-}T2}$).

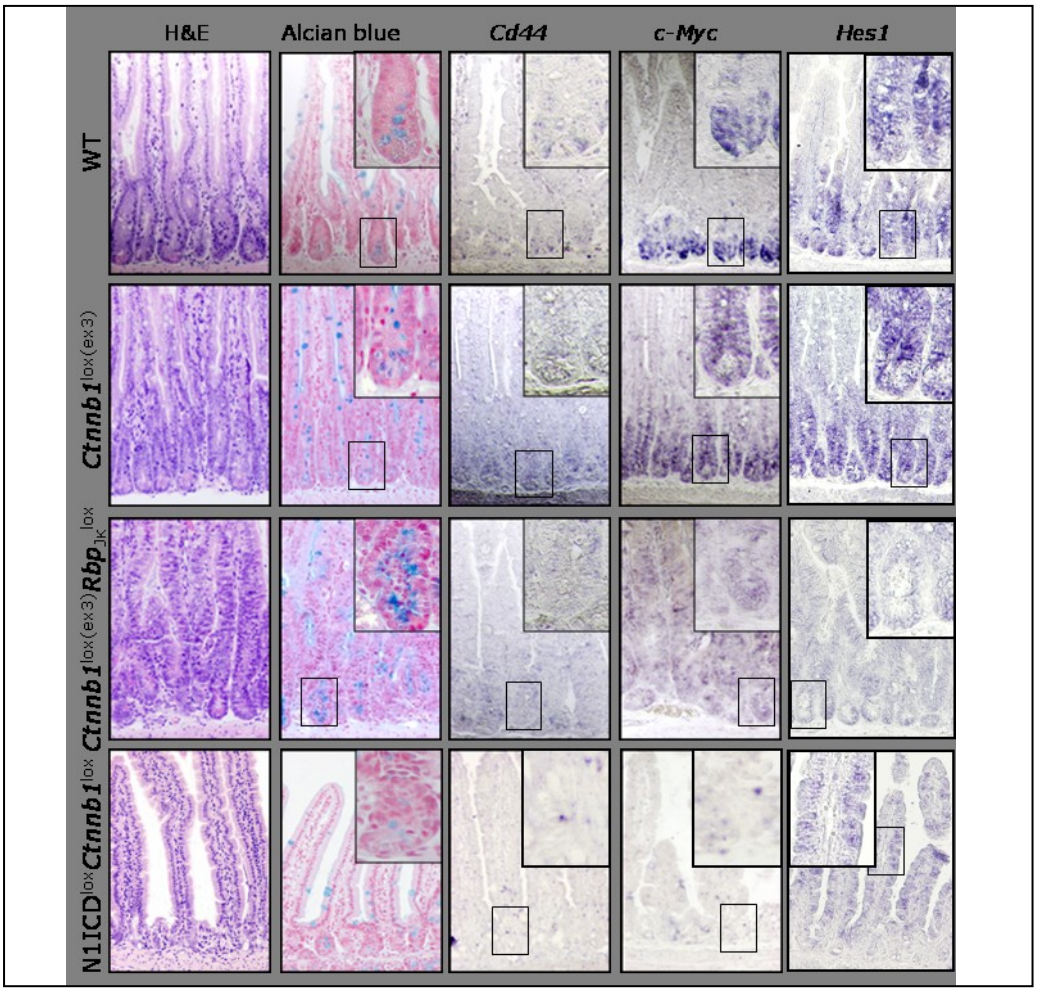

FIGURE R34. Expression pattern of *dNWt* genes in the small intestine by ISH. Hematoxilin and Alcian blue stainings show the histological differences between mutant mice.

Alcian blue staining confirmed the increase in goblet cell differentiation in the *Rbp*$_{Jk}$-deficient mice and the loss of this lineage in the N1ICD background. We also analyzed the mRNA levels of *Hes1* in the intestine of the different mutant mice. We found that *hes1* expression is misslocalized in the constitutively active β-catenin background correlating with the expansion of the crypts. A similar aberrant distribution of HES1 was observed in the combined N1ICD mice lacking β-catenin, although its expression levels were reduced, likely due to the loss of the crypt compartment in these mutants. Importantly, deletion of *Rbp*$_{Jk}$ resulted in the complete absence of HES1 [**FIGURE R34**].

Together these results confirmed our in vitro data, and demonstrated that Notch activation is sufficient to maintain *Hes1* expression, whereas other genes such as *c-Myc* or *Cd44* require the cooperative participation of Wnt

and Notch pathways. Since ISH is a non-quantitative technique, we next determined the expression levels of these genes by qRT-PCR from purified intestinal crypts of the different genotypes. Our results confirmed that simultaneous activation of Wnt and Notch pathways in the crypt compartment of the mouse intestine is required for the proper activation of specific genes identified as *dNWt*, such as *Ephb2*, c-*Myc*, *Cd44* and *Bmi1* [**FIGURE R35**].

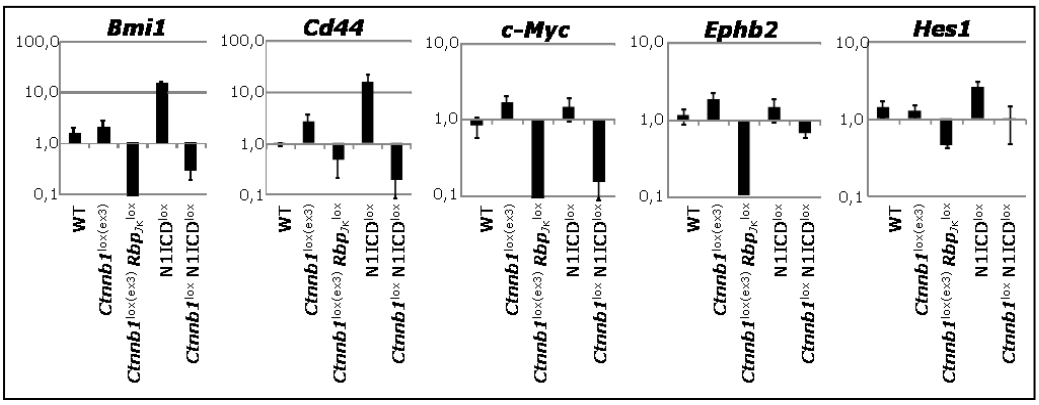

FIGURE R35. Expression levels of *dNWt* genes by qRT-PCR from crypts obtained of different mutant mice. Error bars represent s.e.m.

R5. Notch and Wnt pathways are required to maintain stem cell compartment *in vivo*

Consistent with previously published data, Hematoxilin & Eosin (H&E) staining of histological sections as well as IHC with the proliferation marker Ki67 indicated that loss of Wnt signaling led to the elimination of the stem and proliferative cell compartments of the small intestine. Moreover, comparison of *Ctnnb1*^{lox}villin-CRE$^{ER\text{-}T2}$ mice with *Ctnnb1*^{lox}/N1ICD^{lox}villin-CRE$^{ER\text{-}T2}$ demonstrated that loss of the stem cell compartment imposed by β-catenin deletion is not rescued by ectopic expression of N1ICD [**FIGURE R36**].

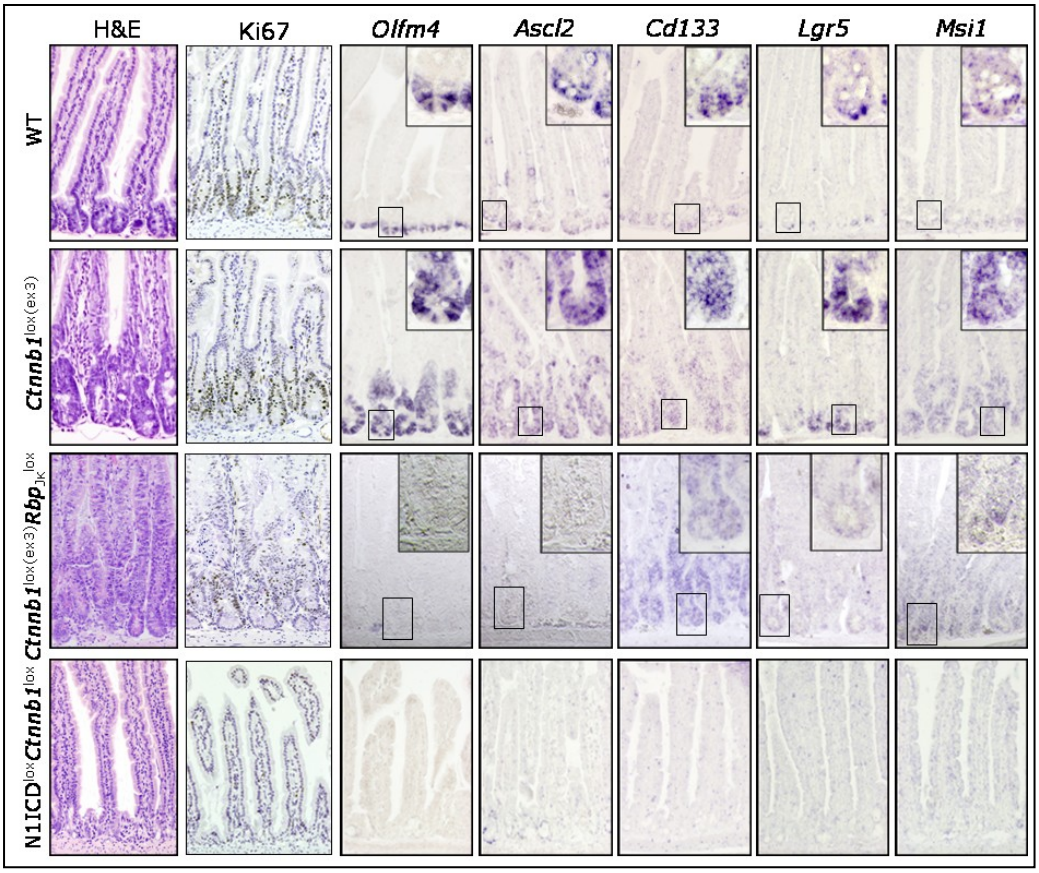

FIGURE R36. Expression pattern of stem cell markers in the small intestine by ISH. Hematoxilin and Alcian blue stainings are shown to appreciate the histological differences between mutant mice.

Similarly, loss of the stem cell compartment as a result of *Rbp*$_{Jκ}$ deletion was not reverted by the ectopic expression of active β-catenin [**FIGURE R36**, *Ctnnb1*$^{lox(ex3)}$/*Rbp*$_{Jκ}$^{lox}]. Collectively, these results suggest that simultaneous activation of Notch and Wnt pathways is a requirement for maintaining the proper homeostasis of the undifferentiated compartments of the intestine. To further investigate this possibility, we analyzed the expression pattern of

different intestinal stem cell markers (*Olfm4*, *Ascl2*, *Cd133*, *Lgr5*, *Msi1*) in the combined Notch and Wnt/β-catenin mutant phenotypes.

We found that all the analyzed genes were down-regulated in the deficient mutants on either Notch or β-catenin and this phenotype was not reverted by activation of the other pathway. These results were confirmed by qRT-PCR from isolated crypts [**FIGURE R37**]. Moreover, and consistent with previous publications, β-catenin activation resulted in a significant expansion of the stem cell compartment, as indicated the expression of the analyzed markers. This data, together with the fact that important stem cell regulators such as *Bmi1*, *c-Myc* and *Cd44* are included in the *dNWt* group of genes, demonstrates the importance of the cooperation between Notch and Wnt pathways for regulating the intestinal stem cell (ISC) compartment *in vivo*.

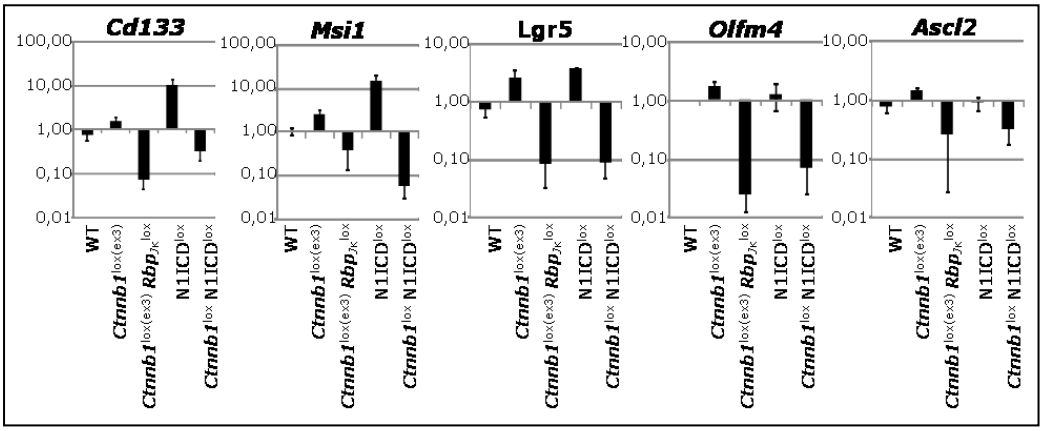

FIGURE R37. Expression levels of stem cell markers by qRT-PCR in crypts obtained from different mutant mice. Error bars represent s.e.m.

R6. Characterization of the different roles of Jagged1 in the intestinal homeostasis and tumorigenic process

R6.1. Deletion of functional Jagged1 does not disturb intestinal homeostasis but affects intestinal tumor initiation

Multiple evidences indicated that both Notch and Wnt pathway play important functions in intestinal tumorigenesis. As previously mentioned, activation of Wnt in CRC generally occurs through mutations in *Apc*, which leads to stabilization and nuclear translocation of β-catenin; moreover, we have demonstrated that Notch activation is dependent on Jagged1, downstream of β-catenin [**FIGURES R7** to **R10**].

In collaboration with Dr. Freddy Radtke's laboratory (EPFL, Switzerland), we have investigated the mechanisms responsible for Notch activation in the normal crypts of the intestine and found that DLL1 and DLL4 are the physiological Notch ligands in this compartment [210]. Based on these results together with our previous work that identified *JAGGED1* as an important β-catenin target in CRC we investigated the effect of specifically deleting *Jagged1* in the intestine and speculated that it might have a specific anti-cancer effect without affecting the normal functions of Notch in the crypts. To test this possibility, we generated a combined mice model carrying mutant *Apc* and the intestinal-specific deletion of *Jagged1* by crossing *Jagged1*$^{lox/lox}$ [266] with villin-CRE mice [284] [**FIGURE R38**] in the *Apc*$^{Min/+}$ background.

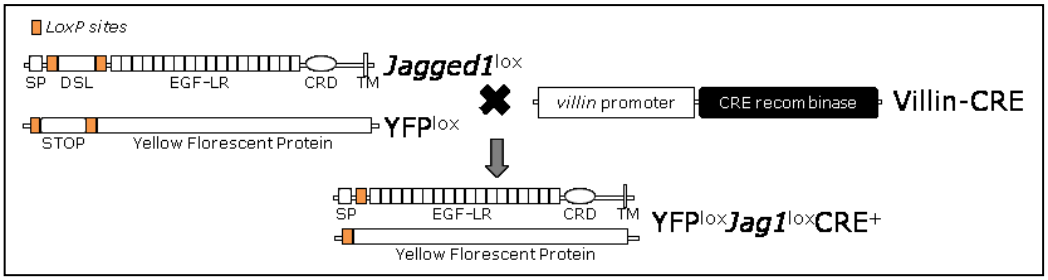

FIGURE R38. Diagram of the deletion of Jagged1 and Rosa26/YFP after crossing with villin-CRE mice.

YFP expression from the Lox-STOP-lox-ROSA26/YFP reporter mice confirmed that villin-promoter drives expression of the CRE-recombinase in all the epithelial cells of the small intestine including the Columnar Base Cells, recently identified as intestinal stem cells in the small intestine [**FIGURE R39**].

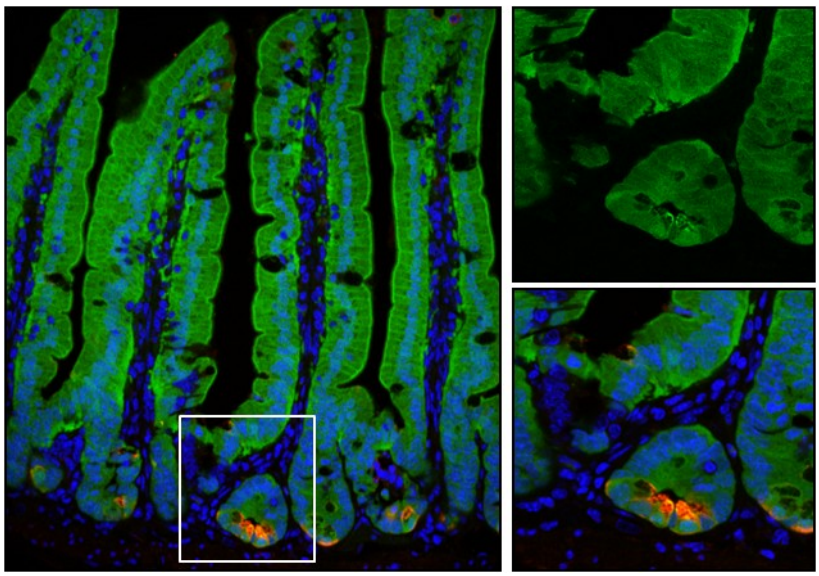

FIGURE R39. CRE expression in the small intestine. In green, the expression of YFP^+ cells; in red, Paneth cells (α-lysozyme antibody staining); in blue, nuclei staning (DAPI). Right, a magnification showing a stem cell YFP^+ between two Paneth cells (in red). Images were obtained in an Olympus BX-60 at 200X or 400x.

Additionally, by PCR we confirmed that *Jagged1* was effectively deleted in the different regions of the intestinal tract [**FIGURE R40**].

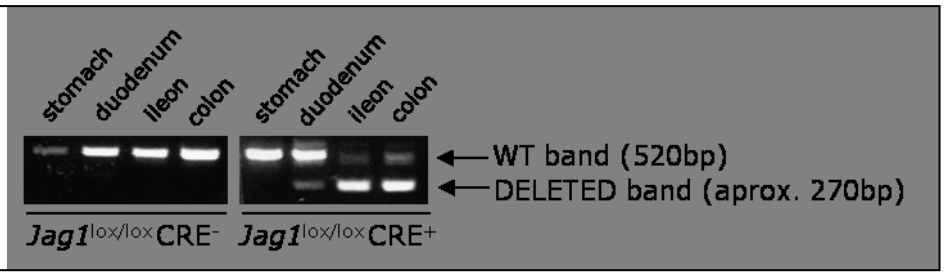

FIGURE R40. Jagged1 deletion determined by conventional PCR.

Analysis of mice carrying intestinal specific deletion of *Jagged1* demonstrated that elimination of JAG1 in this tissue, although it occurs before birth, does not lead to any apparent defect in the mutant mice. Moreover, in a six-month follow up we did not detect any growth retardation or weight loss in these mice compared with the controls [**FIGURE R41**]. Further characterization demonstrated that loss of functional JAGGED1 in the intestine does not affect its integrity nor the proportion nor distribution of the different intestinal cell lineages [**FIGURE R42**], similar to that obtained by deleting *Jagged1* in the adult intestine using an inducible villin-$CRE^{ER\text{-}T2}$ [210].

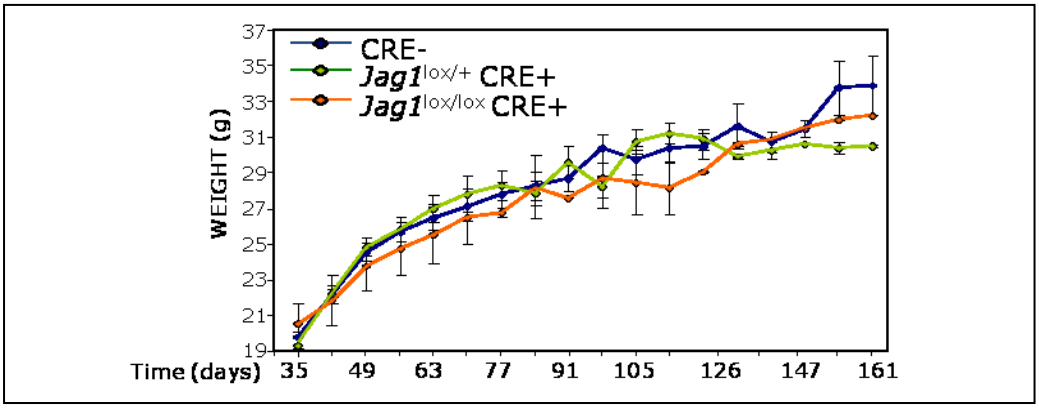

FIGURE R41. Weight chart of the different mutant mice. The weight of the animals was determined weekly during six months. Error bars are s.e.m.

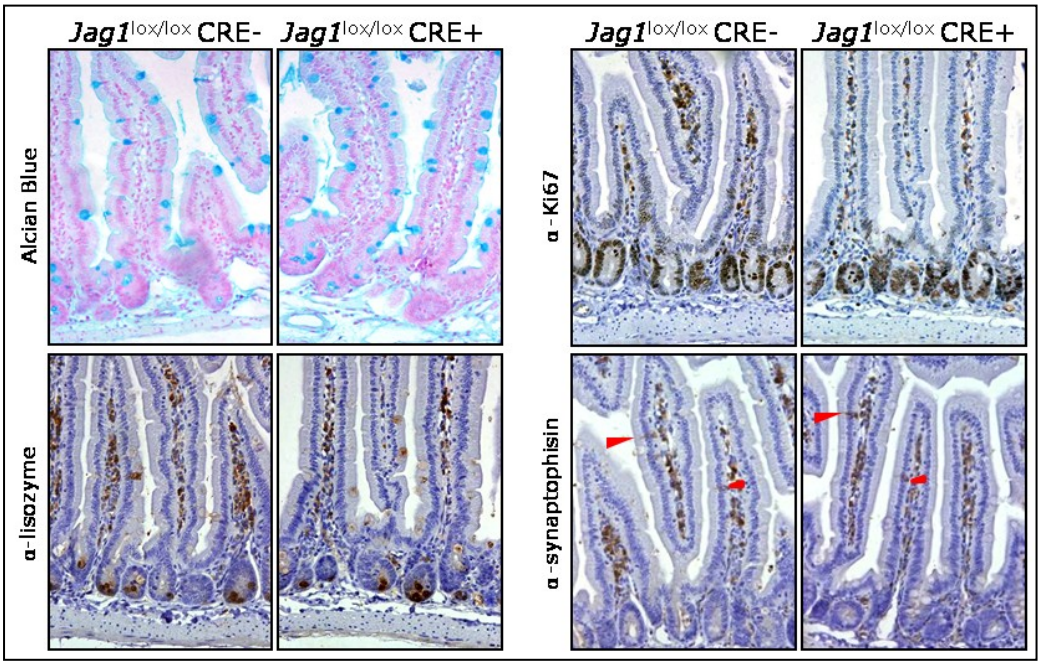

FIGURE R42. Deletion of *Jagged1* has no effect in the intestinal homeostasis. By IHC, we analyzed the cell types most representative of the small intestine. Alcian blue staining for muco-secreting cells (goblet cells); α-Ki67 staining for proliferative cells; α-lysozyme staining for Paneth cells; α-synaptophysin staining for entero-endocrine cells (Red arrows noted the positive cells). Images were obtained in an Olympus BX-60 at 200X.

R6.2. Deletion of functional Jagged1 affects intestinal tumor initiation

The functional removal of *Jagged1* does not disturb intestinal homeostasis; however, when Jaggged1 was deleted in the intestine of *Apc*^{Min} mutant mice,

we found a 70% reduction in the number of generated tumors [**FIGURE R43**].

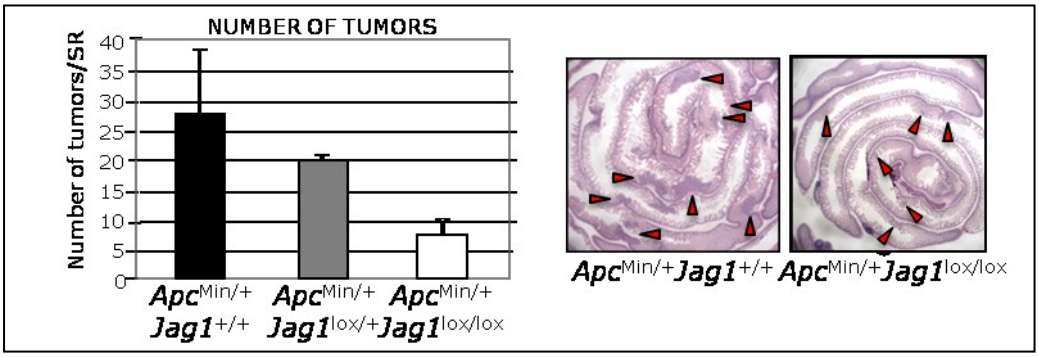

FIGURE R43. Number of tumors is reduced in the absence of Jagged1. Left, number of tumors arising in the different mutant mice. Error bars are s.e.m. Right, images from *Apc*^{Min}*Jag1*$^{+/+}$ and *Apc*^{Min}*Jag1*$^{lox/lox}$ mice obtained with stereomicroscope. Red arrows indicate the presence of intestinal tumors.

However, *Jagged1* deletion did not affect tumor stage as we found a similar percentage of dysplastic crypts, tubular adenoma or villous adenomas in the different genotypes [**FIGURE R44**, **R45**].

FIGURE R44. Tumor development in *Apc*^{Min} mice. From left to right, representative images of tumor progression from the mildest stage to the worst prognosis (within adenomas). Images were obtained in an Olympus BX-60 at the indicated magnification.

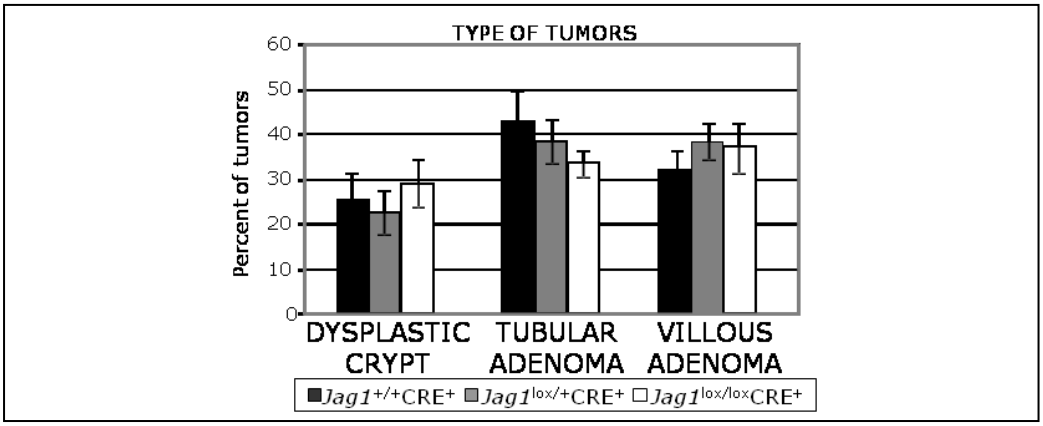

FIGURE R45. *Jagged1* deletion does not affect the tumor progression. Quantification of tumors (in percentage) according to tumor stage found in the different mutant mice. Error bars are s.e.m.

These results suggest that *Jagged1* deletion affects tumor initiation without influencing tumor progression, even though *Jagged1*-deficient tumors show increased expression of differentiation secretory cell markers [**FIGURE R46**], consistent with the role of Notch in the inhibition of the secretory linage [203, 209, 285].

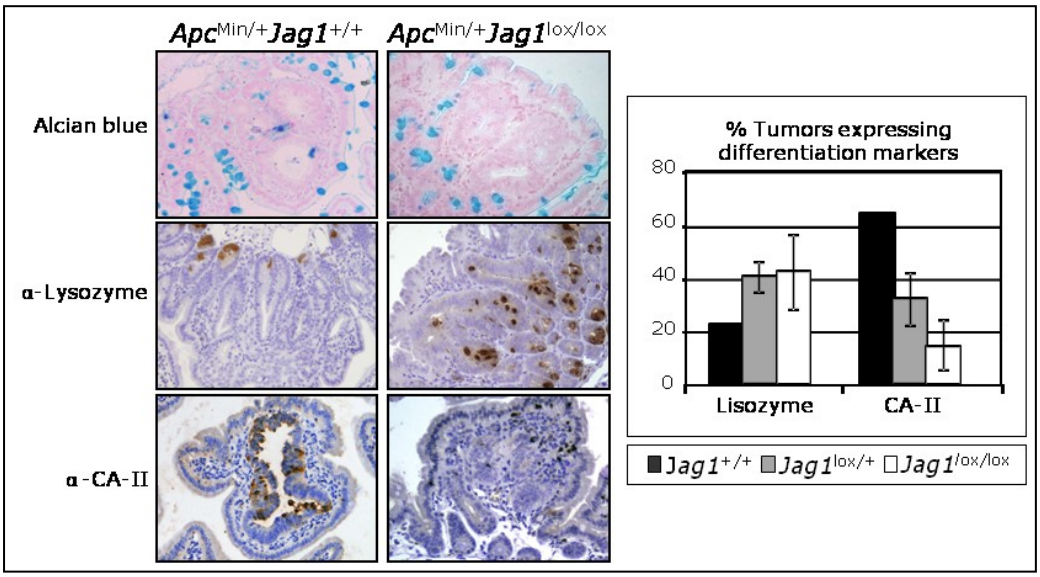

FIGURE R46. Differentiation markers are differentially expressed in $Apc^{Min/+}Jag1^{lox/lox}$CRE+ compared with $Apc^{Min/+}Jag1^{+/+}CRE^{+}$. Left, IHC of the indicated antibodies: Alcian blue staining for muco-secreting cells; α-lysozyme for Paneth cells; α-CA-II for absorptive cells. Images were obtained in an Olympus BX-60 at 200X. Right, quantification of number of tumors expressing differentiation markers. Error bars are s.e.m.

Finally, since we demonstrated that Notch activity is required to maintain the normal stem cell phenotype in the presence of active Wnt, we tested whether *Jagged1* deletion was affecting tumor stem cell compartment in the Apc^{Min}

background. As shown in **FIGURE R47**, expression levels of different stem cell markers including *Msi1* and *Lgr5,* as well as other stemness-related *dNWt* genes were reduced in the tumors generated the absence of JAGGED1 as measured by qRT-PCR.

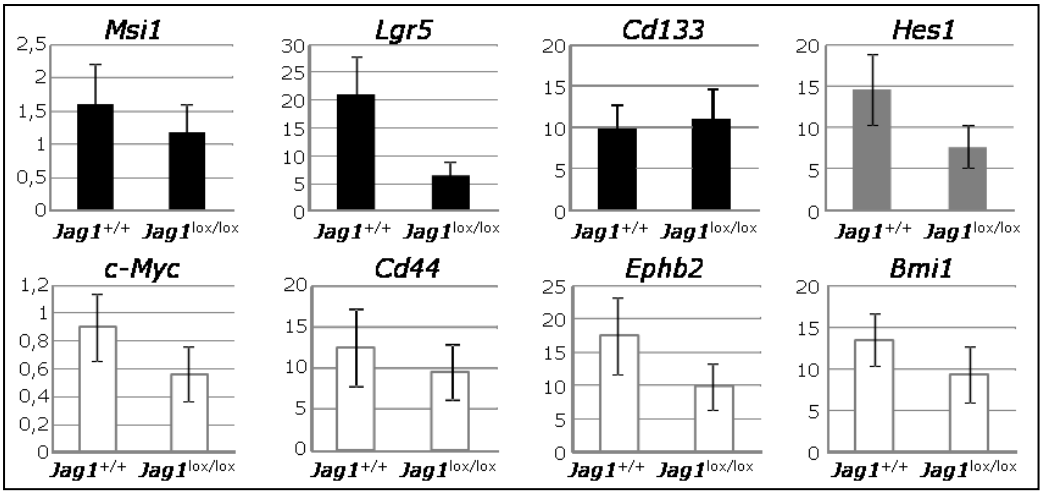

FIGURE R47. Down-regulation of stem cell markers and *dNWt* genes in *Jagged1*-deficient tumors. By qRT-PC, we compared expression levels from tumors in the presence or absence of JAGGED1. Number of animals analyzed were $Jag1^{+/+}$ (n=6) and $Jag1^{lox/lox}$ (n=8). Error bars are s.e.m.

Together our data indicate the existence of a transcriptional program regulated by Wnt and Notch that is active in the normal crypt compartment and is required to maintain intestinal homeostasis. Importantly, JAGGED1 is dispensable for normal ISC (where DLL1 and DLL4 are required for Notch activation [210]) but it is required for activating Notch cancer stem cells.

This finding opens the possibility to use a combination of Notch and β-catenin inhibitors for enhancing the anti-tumoral effects of the individual drugs. In this sense, by western blot analysis using from CRC cell lines we demonstrated that low doses of DAPT (5μM) are sufficient to completely inhibit Notch activation when combined with low doses of the Wnt inhibitor PKF115-584 (0.33μM), with a IC50=3.2μM [286] compared with the single treatments (data not shown), and we found that combination of DAPT and PKF115-584 resulted in a synergistic pro-apoptotic effect [**FIGURE R48**, left] together with an accumulation of cells in G_0/G_1 phase [**FIGURE R48**, right] indicating a potential interest of using a combination of these drugs for treating colorectal cancer.

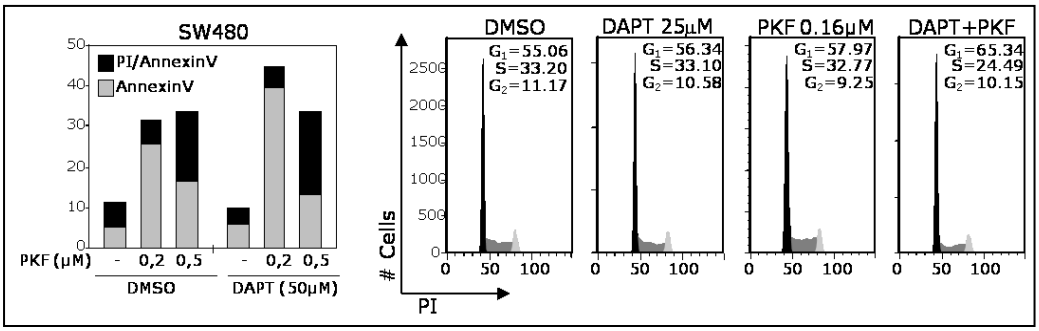

FIGURE R48. Pharmacological inhibition of Notch and Wnt pathways exert a cooperative anti-tumoral effect on CRC cells. Left, pro-apoptotic effect of DAPT and PKF in SW480 cells. Bars represent the percentage of AnnexinV$^+$ cells and AnnexinV$^+$/PI$^+$ cells measured by flow cytometry. Right, Cell cycle profiles of SW480 cells treated with the indicated concentrations of DAPT and PKF115 or a combination of both.

DISCUSSION AND CONCLUSIONS

DISCUSSION

D1. Wnt and Notch crosstalk

Previous work has shown that inactivating mutations of the Wnt/β-catenin pathway eliminate the stem/proliferative compartment of intestinal cells [185]. Similarly inactivation of the Notch pathway leads to an exhaustion of the stem cell compartment concomitant with increased goblet cell differentiation [69, 206]. Here, we have identified different mechanisms that mediate the crosstalk between Notch and Wnt pathways in CRC and determined part of its functional relevance.

D1.1. Notch is downstream of Wnt signaling

During the first part of the project, we demonstrated that activation of Notch in CRC cells is a consequence of Wnt/β-catenin activating *JAGGED1* expression. This observation is in agreement with other publications demonstrating the interaction between both pathways [256-261] and with the fact that mutations in members of the Wnt signaling but not in Notch family members are found in CRC. In addition, *JAGGED1* is a β-catenin target gene in the hair follicle where it mediates Notch activation downstream of Wnt [258]. In contrast, β-catenin levels remained unaffected in *Jagged1*-deficient tumors [**FIGURE R18**] and Notch inhibition did not modify the binding of β-catenin to its target genes [**FIGURE R8**], demonstrating that Wnt/β-catenin is not regulated by Notch in CRC cells.

In addition, we have identified a total of 366 genes that are simultaneously regulated by both Notch and Wnt in Ls174T CRC cells and 31% are reactivated by active N1ICD in the presence of dnTCF4, indicating that are directly dependent on Notch. This group of genes was sufficient to revert some of the anti-tumorigenic effects of dnTCF4 both in vitro and *in vivo*. Specifically, N1ICD expression was sufficient to inhibit cell differentiation and promoted vascularization in the absence of Wnt/β-catenin *in vivo*, in agreement with published data indicating that JAG1 is a potent pro-angiogenic effector through Notch activation [71]. In vitro, Notch activity induces the capacity of CRC cells to grow in soft agar assays, independent on Wnt activity [**FIGURE R11**]. However, N1ICD failed to promote cell proliferation in the absence of Wnt similar to that observed by Fre et al. [222], although Notch blockage by *Jagged1* deletion ($Apc^{Min/+}Jag1^{+/-}$) is sufficient to reduce proliferation in a Wnt activated background [**FIGURE R19**]. These results suggest that whereas Wnt/β-catenin activity is preferentially maintaining cell proliferation, Notch has a more prominent role inducing other oncogenic programs such as blockage of differentiation, promoting vascularization or substrate-independent growth.

As expected, one of the genes identified as direct Notch target in our arrays is *Hes1*. HES1 regulates intestinal differentiation [204] by inhibiting *Math1* thus favoring enterocytic differentiation [287] and it is over-expressed in CRC [212] and in tumors arising in *Apc* mutant mice [69]. However, and in contrast to the effects of N1ICD, we found that HES1 was not sufficient to induce tumor growth *in vivo* in the absence of β-catenin/TCF activity, indicating that other Notch targets, downstream of β-catenin, regulate specific functions in colorectal tumorigenesis. Consistently, several of the identified Notch-target genes in our screening have been involved in different aspects of intestinal differentiation or cancer including *SOX9*, *KLF5*, or *NOX1* [276-278]. Investigating the relative contribution of the different Notch-downstream targets in CRC is of crucial relevance to understand the role of Notch in Wnt-dependent tumorigenesis. Since mutations in Notch elements have not been found in CRC, it is unclear at which stage of tumor development is Notch activity required. Our results suggest that Notch is required for tumor initiation since the lack of Notch signaling in the combined $Apc^{Min}Jag1^{lox}$villin-CRE mice results in a decrease in the number of tumors without affecting tumor progression or differentiation. In fact, Fre et al. suggested that Notch must be switched off for tumors to progress from adenoma to carcinoma [222]. However, other studies suggest that Notch activity is required for tumor vascularization [71] and metastasis [70]. Our results from tumors growing in nude mice reinforce the idea that Notch activity by itself is associated with vascularization but data regarding the metastatic role of JAG1 downstream of Wnt is still lacking.

Mutations in the *Apc* gene that leads to increased Wnt activity are found in most sporadic colorectal tumors associated with higher levels of JAG1 and activated Notch. However in FAP patients, inactivation of the *Apc* allele is also found in the normal intestinal tissue. Our data indicates that JAG1 levels are increased not only in the tumors but also, in a lesser extent, in the normal tissue of FAP patients indicating that inactivation of a single *Apc* copy could activate Notch. In this sense, others and we have observed that Ki67 positive cells are aberrantly distributed throughout the intestinal glands in *Apc* mutant mice, a phenotype that is abolished in the $Apc^{Min/+}Jag1^{+/-}$ mice. This indicates that Notch but not Wnt is regulating the size of the crypt compartment or alternatively, the crypt/villus compartmentalization. Most important, in the $Apc^{Min/+}$ background tumor growth is reduced by elimination of a single *Jagged1* allele indicating that partial inhibition of Notch in an active β-catenin background may be therapeutically relevant for CRC treatment in FAP patients.

D1.2. Common Wnt and Notch dependent-genetic program

In this work we have identified a genetic program that depends on the simultaneous activity of Notch and Wnt pathways (*dNWt* genes), and is expressed in CRC cells. Importantly, this program includes several genes previously identified as important regulators of stem cell maintenance including *Bmi1*, *Cd44*, c-*Myc* or *Ephb2*, and all of them are expressed in the stem cell compartment of the intestinal crypts in mice. We demonstrated that genetically deleting Wnt or Notch pathways in this cellular compartment of the mouse intestine results in the elimination of selected *dNWt* genes, accompanied by the disruption of the stem cell compartment as indicated the absence of *Lgr5* and *Olfm4* expression. In addition, we found that some *dNWt* genes are expressed in colorectal tumors from patients as well as in mice tumors. In agreement with a role for JAG1 in regulating Notch activity in cancer, we found that intestinal epithelial deletion of *Jagged1* in Apc^{Min} mice is sufficient to prevent *Bmi1*, *Cd44*, *c-Myc* or *Ephb2* and also *Lgr5* or *Msi1* expression in intestinal tumors, and to significantly reduce tumor generation.

ChIP assays and sequential Chromatin IP demonstrated that β-catenin and Notch are recruited together to specific genes included in the *dNWt* signature. However, it remains to be determined which other elements participate in the complex that includes β-catenin and Notch factors to activate transcription. For example, we have not yet determined whether $RBP_{Jκ}$ and TCF factors participate in such complex, and whether it depends on p300 or MAML. Importantly, bioinformatics analysis of the whole genome revealed that there is a non-random distribution of TCF binding sites relative to $RBP_{Jκ}$ binding sites close to the gene promoters and at specific distances. This result suggests a more general usage of the Wnt/Notch-containing transcriptional complex for regulating gene transcription.

D2. Intestinal dual role of Jagged1: homeostasis vs. tumorigenesis

We have here shown that JAG1 is not required for the normal development of the intestine, which is in agreement with the recently published data by Radtke and collaborators [210]. Moreover, our results indicate that JAG1 is the main contributor to Notch activation downstream of the β-catenin in CRC tumors. This different ligand usage could be reflecting the fact that DLL or Jag ligands are expressed in different cell types. Thus, in normal small intestine DLL1 and DLL4 are the most prevalent ligands [283] whereas epithelial cancer cells mainly express JAG1, although we observed *Jagged1* expression in the normal epithelial cells of the crypts. Another possibility that

could explain this ligand selectivity is the modification of Notch receptor by Fringe glycosil-transferases, which are known to modulate Notch-ligand specificity [92]. In this sense Schröder, et al. characterized the expression pattern of all Notch family member in the intestine and found that Fringe are expressed in normal intestine [288]. However, further studies are necessary to define the relative contribution of these two possibilities.

Screening of genetic mutations in CRC and other tumors have shown that mutations/alteration with a comparable outcome never occur simultaneously, and for instance mutations in *Apc* and β-catenin, or Ras and BRAF are in principle exclusive. Since we demonstrated that *Apc* mutations that lead to β-catenin stabilization are sufficient to activate the Notch pathway it is not surprising that Notch mutations are not found in CRC. Moreover, the high prevalence of *Apc* mutation in CRC indicates that Wnt plays an essential role in tumorigenesis that cannot be substituted by Notch, or in other words, that both pathways are required during tumorigenesis providing different properties, which are not exchangeable.

D3. Therapeutic approaches

FAP is one of the best-studied inherited cancer syndromes. This knowledge has led to the improvement of genetic testing for establishing individual risk, improved screening and surgical management, and several clinical trials are currently focused in the prevention of polyp progression and cancer development in these patients [289, 290]. However, nowadays there is no medication that effective prevents colonic polyposis in FAP patients, and their treatment involves surgical removal of the colon (colectomy) or in some case a partial colectomy to reduce the possibility to development colon cancer. This surgery is often performed between the ages of 17 and 20 in asymptomatic members of FAP families carrying the *Apc* mutation. Non-steroidal anti-inflammatory drugs (NSAIDS such as sulindac and indomethacin) have been shown to reduce polyp size in FAP patients and different clinical trials are currently examining the possibilities for treatment.

Because we identified three different genetic signatures associated with CRC that depend on Notch, β-catenin or both pathways that are supposed to play complementary/non-overlapping functions in tumor development, we propose that using of a combination of Notch and β-catenin inhibitors will enhance the anti-tumoral effects of the individual drugs. However, this strategy needs to be tested, first in vitro and next in animal models. In agreement with our suggestion, inhibitors for Notch and β-catenin have been proposed as potential treatments for intestinal cancer [69, 286]. However, as

both pathways are also critical regulators of the homeostasis of different tissues, the use of minimal dosage for each inhibitor may determine the viability of this therapies [291]. More experiments as we proposed in **FIGURE R48** should be done to further characterize this Wnt/Notch cooperation in CRC.

An additional improvement of this type of therapies could be the use of specific inhibitors for JAG1-mediated Notch activation, for example inhibitors of glycosil-transferases that modulate Notch/Notch-ligand interaction [292] or specific blocking antibodies or peptides against JAG1 in combination with β-catenin inhibitors [293]. Actually, this strategy has been used with antibodies against Notch1 receptor or MAML-blocking peptides for T-ALL leukemias treatment [208, 294] or antibodies against DLL4 for inhibiting growth [219].

D4. Mouse models

D4.1. *Apc*^{Min} model: advantages, disadvantages and alternatives

In general, the mice models used in research do not completely phenocopy their parallel human disease despite the presence of the same identified genetic alterations. This is also the case of the *Apc*^{Min} mouse model that is the model for human FAP. Initially identified by the obvious clinical symptoms of intestinal disease, the *Apc*^{Min} mouse carries a mutation at codon 850 and develops multiple small intestinal adenomas, in addition to a smaller number of colonic polyps. The prevalence of small intestinal lesions represents one of the major differences between the human syndrome and the mouse model, the explanation for which remains unclear. The predisposition to intestinal polyposis also changes on different genetic backgrounds [295-298]. As a relatively accurate genetic model of human disease, the *Apc*^{Min} mouse has been used extensively to characterize the response to potential therapeutic strategies, and a comprehensive list of the effects of 269 chemo-preventative agents has been assembled at ***http://www.inra.fr/reseau-nacre/sci-memb/corpet/indexan.html*** [299]. The pertinent question arising from these studies is the extent to which these results relate to human disease. Although there remain immense technical difficulties in direct mouse/human comparisons, it is therefore encouraging that a meta-analysis of chemo-preventative agents used in mouse and human has shown relatively good correspondence for a number of agents, such as sulindac [300]. Furthermore microarray studies also argue in favor of the potential clinical relevance of the *Apc*^{Min} mouse studies, since transcriptional profiles derived from the mouse models successfully identified novel gene targets in human colorectal tumors [301]. Using the knockout

technology, several *Apc* mutations have been generated including *Apc*^{D716} that contains truncating mutation at codon 716 or *Apc*^{1638N} at codon 1638 [302, 303]. Like in *Apc*^{Min} mice, both knockout mutants develop polyps mainly in the small intestine. Histologically, all these *Apc* mutants form polyp adenomas indistinguishable from each other. Interestingly, however, the number of polyp is very different, even in the same C57BL/6J background. Namely, *Apc*^{D716} develops usually ~300 polyps, whereas *Apc*^{1638N} forms only ~3 polyps. Despite the numerous polyps developing in the small intestine in the *Apc*^{D716} (as well as in *Apc*^{Min}) mice, only a few polyps are formed in the colon, although the penetrance is complete. Recently, a mutant mouse strain carrying heterozygous mutations on the *Apc* gene has been generated that develop numerous polyps in the distal colon [304]. Another *Apc* gene knockout mutant was reported where both *Apc* alleles were mutated simultaneously in a tissue-specific manner using the CRE-*loxP* system [305]. Although it is quite an artificial system, it shows early changes in the intestinal cell physiology.

One of the main problems of using *Apc* mutant mice for studying cancer is that these animals do not progress into invasive or metastatic adeno-carcinomas at a significant frequency. Due to the heavy tumor load in the small intestine, most *Apc* mutant mice die young (4–5 months) because of anemia and cachexia, and some of them by intestinal intussusceptions. However, when additional mutations are introduced in these mice, the intestinal phenotypes are modified, and in some cases polyps develop into adenocarcinomas. Homozygous mutation in the *Muc2* gene that encodes the most abundant secreted gastrointestinal mucin promotes the formation of adenomas and adeno-carcinomas in the intestine [306]. Although the incidence and multiplicity are low, the adeno-carcinoma is locally invasive without distant metastasis. Loss of EphB expression strongly correlates with degree of malignancy, and reduction of EphB activity accelerates tumorigenesis in the colon and rectum of *Apc*^{Min} mice, resulting in the formation of aggressive adeno-carcinomas [213]. A selective Rac GTPase activator Tiam1 is a Wnt responsive gene expressed in the base of intestinal crypts, and up-regulated in mouse intestinal tumors and human colon adenomas. When Tiam1 deficiency was introduced into the *Apc*^{Min} mice, polyp formation and growth were significantly reduced, suggesting a Wnt signaling and gastrointestinal tumorigenesis in mouse models crosstalk between Tiam1-Rac and Wnt-signaling pathways in intestinal carcinogenesis [307].

Conditional stabilizing β-catenin mutations have also been expressed in the intestine under the control of specific promoters. For example, expression of non-degradable β-catenin from the calbindin promoter, results in the development of only a few polyps in the small intestine [308]. In contrast, activation of β-catenin by a CRE recombinase under the control of cytokeratin

19 (K19) or fatty acid binding protein (FABP) gene promoters in mice, led to the generation of 700–3000 polyps in the small intestine per mouse [197]. These results confirm the role of Wnt signaling activation in polyp formation, and indicate that polyps are initiated essentially in the rapidly multiplying cells in the proliferative zone.

D4.2. CRE expression and side effects

Another problem of conditional gene-targeting is the possible toxicity of the CRE recombinase. Although most CRE-transgenic mouse strains develop apparently normal, a study by Capecchi's group strikingly demonstrated that CRE can result in DNA damage by non-specific targeting of genomic DNA [309]. In contrast, expression of an enzymatically inactive CRE recombinase from the same transgenic construct had no effect, demonstrating that the effects on the DNA resulted from the recombinase activity of CRE. Mammalian genomes contain cryptic or pseudo *lox*P sites, which sequence can deviate considerably from the consensus *lox*P site, and which can serve as functional recognition sites for CRE [310]. A recent bioinformatics evaluation estimates that such sites are present in the mouse genome at a frequency of 1.2 per megabase [311]. The affinity of CRE for these cryptic recognition sites is much lower than for the consensus *lox*P site [310]. The toxic effects of CRE recombinase activity have been carefully investigated through retroviral infection of fibroblasts, in which the constitutive presence this protein at high levels induces growth arrest [312-315] and chromosomal abnormalities [313, 315]. Transient expression of CRE using a replication-deficient adenovirus uncovered a large range of virus concentrations sufficient for excision of a *lox*P-flanked neomycin-resistance cassette without causing noticeable DNA damage in fibroblasts [316]. This suggests that when the exposure time to the recombinase is limited, CRE can be expressed in amounts that allow efficient recombination of *lox*P-flanked target alleles with minimal toxicity. One strategy to minimize the exposure of the target cells to CRE is the use of inducible CRE expression ($CRE^{ER\text{-}T2}$) under control of the endogenous ROSA26 promoter [315]. Consistent with all this data, during the analysis of $Apc^{Min}Jag1^{lox}$villin-CRE animals, we found some pro-tumorigenic effects derived from the expression of CRE in the intestine. Specifically, we found that the number of tumors arising in our animals was significantly higher in the CRE^{+} compared with the CRE^{-} mice of the same backgrounds.

D5. Cancer stem cells

A new research field of growing interest is the study of cancer stem cells (CSC). CSCs are defined as a subpopulation of cancer cells with stem cell-like

properties, including the capacity for self-renewal, asymmetric division, and the production of daughter cells that will undergo further differentiation. Although this is still a controversial issue, what is true is that tumors include a heterogeneous population of cells and only a restricted subgroup that is characterized by the expression of specific markers is capable of re-generating a new tumor, recapitulating its original characteristics and moreover, this can be done indefinitely. What is not so clear is whether tumor stem cells are generated from mutations in normal stem cells [199] or whether differentiated tumor cells can de-differentiate in response to specific signals or by contact with a specific niche [202]. In humans, CRC is a multi-step disease, with a relatively low progression, that requires the sequential accumulation of well-established mutations in oncogens and tumor suppressors in a specific order, as described by Fearon and Vogelstein in 1990 [180]. In contrast, when APC deletion is accomplished in the stem cell compartment, such is the case of the *Apc*^{lox}/Lgr5-CRE^{ER-T2} mice model, single deletion of *Apc* is sufficient to induce tumorigenesis and promote the progression to adeno-carcinoma [199]. This result could reflect the fact that intestinal Lgr5^{+} stem cells have a higher turnover compared to other cells, which can facilitate the accumulation of mutations required for cancer progression; Moreover, it has been shown that *Apc* mutation results in the loss of asymmetric segregation of the maternal DNA in the intestinal stem cells that "protects" these cells from mutations [159].

Taking all these results together, the current knowledge about cancer origin is not sufficient to positively define whether low or high cycling stem cells, transit-amplifying cells or even more mature progenitor cells are the targets for oncogenic mutations that lead to CRC. For this reason, others and we are designing functional assays to demonstrate whether specific signaling pathways (that are involved in regulating specific cell compartment) are functionally relevant for cancer development and cancer stem cell maintenance. By ISH and RT-PCR we have already analyzed some of the stem cell markers, which are currently used to identify this population, in different Wnt and Notch mutant backgrounds (see results section). Our results strongly suggest a requirement for both Notch and Wnt pathway for maintaining CSC population. However, functional experiments are required to demonstrate this possibility. Future experiments will involve culturing crypt cells of the different mutants and culturing of isolated tumor cells obtained from *Apc*^{Min} vs. *Apc*^{Min}*Jag1*^{lox}villin-CRE. We are currently performing some of these experiments.

D6. Project summary

We have demonstrated a direct relationship between Wnt and Notch pathways that is required for maintaining the undifferentiated compartment in the normal intestine but also for providing some oncogenic capacities to the intestinal cancer cells. Moreover, we have identified two mechanisms through which Notch to β-catenin interacts to activate gene transcription: **(1)** β-catenin activates transcription of the Notch ligand *JAGGED1*, which in turns activate both Notch1 and Notch2 in tumors. This mechanism occurs in tumors carrying mutated *Apc* from mice and FAP patients [**FIGURE D1**] and **(2)** Notch and β-catenin physically interact and simultaneously bind the promoter of *dNWt* genes to activate its transcription. This group of *dNWt* target genes (characterized in this work) is expressed in the most undifferentiated compartment of the intestine (at the bottom of crypts) [**FIGURE D1**]. The lack of either Notch or β-catenin factors results in the loss of stem cell markers in both normal intestine and tumors highlighting the importance of this interaction *in vivo*.

Together our results suggest that Wnt activation is sufficient for maintaining Notch signaling in tumors and this creates a permissive scenario for the activation of three groups of genes: **(1)** genes that depend exclusively on β-catenin/TCF, which are related to proliferation and cell cycle [187]; **(2)** genes that depend exclusively on Notch that promote vascularization [**FIGURE R15**] and resistance to anoikis [**FIGURE R11**] and differentiation; **(3)** genes that require the cooperation of both β-catenin and Notch, involved in the maintenance of the stem cell features of both normal and cancer cells [**FIGURES R37, R38**].

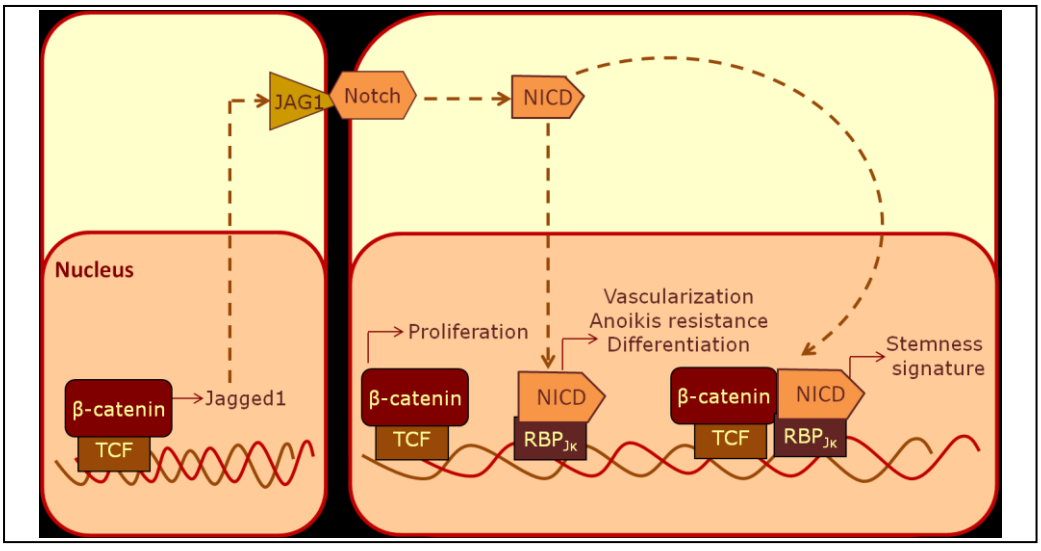

FIGURE D1. Scheme of the two mechanisms proposed for β-catenin and Notch interaction.

CONCLUSIONS

- **Inhibiting Notch or Wnt pathways results in the down-regulation of a common genetic program in Ls174T cells.** There is a genetic program depending on Wnt and Notch pathways, which is over-expressed in human CRC cells.
- **Notch over-expression partially reverts the effects of lacking Wnt/β-catenin signaling**. This demonstrates that Notch is a direct regulator of specific gene transcription downstream of β-catenin/TCF; nevertheless most of the identified Wnt-Notch-dependent genes (69%) require the cooperative effects of Notch and β-catenin pathways.
- **Notch is downstream of Wnt through transcriptional activation of Jagged1 by β-catenin/TCF.** Jagged1 is a Wnt/β-catenin target gene in CRC and its expression is responsible for Notch activation in these tumors.
- **Activated Notch1 blocks differentiation and promotes vascularization *in vivo* in the absence of β-catenin/TCF signaling.** Activated Notch1 exerts a direct effect in regulating goblet cell differentiation and tumor vascularization whereas regulation of cell proliferation requires the contribution of β-catenin/TCF signaling pathway.
- **Constitutive deletion of a single Jagged1 allele reduces tumor growth in the *Apc*$^{Min/+}$ intestine.** Jagged1 haplodeficiency confers a growing disadvantage to β-catenin-dependent tumors.
- **High levels of Jagged1 correlate with activated Notch1 and Notch2 in human colorectal tumors containing nuclear β-catenin.** Notch, downstream of Jagged1, acts as an essential mediator of β-catenin-dependent intestinal tumorigenesis (i.e., FAP) and is required to activate a specific genetic signature associated with cancer.
- **There is a genetic signature that requires both Notch and β-catenin signaling (dWNt genes).** These genes down-regulated after both DAPT treatment and dnTCF4 expression and could not be rescued by activation of Notch alone.
- **Notch and β-catenin interact in the nucleus.** By co-immunoprecipitation assays we showed that Notch and β-catenin physically associate and mapped the regions of both proteins involved in the interaction.
- **Notch and Wnt pathways are both required for maintaining stem cell compartment.** Loss of the stem cell compartment imposed by

Rbp$_{Jk}$ deletion was not reverted by the ectopic expression of active β-catenin and conversely, Wnt deficiency is not rescued by active Notch.

- **Deletion of functional Jagged1 does not disturb normal intestinal homeostasis but affects intestinal tumor generation**. Deletion of Jagged1 in the mouse intestine showed no phenotype in normal conditions but a reduction in the number of tumors was found in *Apc*^{Min}*Jag1*^{lox}villin-CRE mice**.**

BIBLIOGRAPHY

1. Logan, C.Y. and R. Nusse, *The Wnt signaling pathway in development and disease.* Annu Rev Cell Dev Biol, 2004. 20: p. 781-810.
2. Reya, T. and H. Clevers, *Wnt signalling in stem cells and cancer.* Nature, 2005. 434(7035): p. 843-50.
3. Korinek, V., et al., *Constitutive transcriptional activation by a beta-catenin-Tcf complex in APC-/- colon carcinoma.* Science, 1997. 275(5307): p. 1784-7.
4. Tsukamoto, A.S., et al., *Expression of the int-1 gene in transgenic mice is associated with mammary gland hyperplasia and adenocarcinomas in male and female mice.* Cell, 1988. 55(4): p. 619-25.
5. Cadigan, K.M. and R. Nusse, *Wnt signaling: a common theme in animal development.* Genes Dev, 1997. 11(24): p. 3286-305.
6. Willert, K., et al., *Wnt proteins are lipid-modified and can act as stem cell growth factors.* Nature, 2003. 423(6938): p. 448-52.
7. Hofmann, K., *A superfamily of membrane-bound O-acyltransferases with implications for wnt signaling.* Trends Biochem Sci, 2000. 25(3): p. 111-2.
8. Zhai, L., D. Chaturvedi, and S. Cumberledge, *Drosophila wnt-1 undergoes a hydrophobic modification and is targeted to lipid rafts, a process that requires porcupine.* J Biol Chem, 2004. 279(32): p. 33220-7.
9. Banziger, C., et al., *Wntless, a conserved membrane protein dedicated to the secretion of Wnt proteins from signaling cells.* Cell, 2006. 125(3): p. 509-22.
10. Bartscherer, K., et al., *Secretion of Wnt ligands requires Evi, a conserved transmembrane protein.* Cell, 2006. 125(3): p. 523-33.
11. Coudreuse, D.Y., et al., *Wnt gradient formation requires retromer function in Wnt-producing cells.* Science, 2006. 312(5775): p. 921-4.
12. Panakova, D., et al., *Lipoprotein particles are required for Hedgehog and Wingless signalling.* Nature, 2005. 435(7038): p. 58-65.
13. Ramirez-Weber, F.A. and T.B. Kornberg, *Cytonemes: cellular processes that project to the principal signaling center in Drosophila imaginal discs.* Cell, 1999. 97(5): p. 599-607.
14. Hsiung, F., et al., *Dependence of Drosophila wing imaginal disc cytonemes on Decapentaplegic.* Nature, 2005. 437(7058): p. 560-3.
15. He, X., et al., *LDL receptor-related proteins 5 and 6 in Wnt/beta-catenin signaling: arrows point the way.* Development, 2004. 131(8): p. 1663-77.
16. Binnerts, M.E., et al., *R-Spondin1 regulates Wnt signaling by inhibiting internalization of LRP6.* Proc Natl Acad Sci U S A, 2007. 104(37): p. 14700-5.
17. van Amerongen, R., A. Mikels, and R. Nusse, *Alternative wnt signaling is initiated by distinct receptors.* Sci Signal, 2008. 1(35): p. re9.
18. Bryja, V., et al., *The extracellular domain of Lrp5/6 inhibits noncanonical Wnt signaling in vivo.* Mol Biol Cell, 2009. 20(3): p. 924-36.
19. Xu, Q., et al., *Vascular development in the retina and inner ear: control by Norrin and Frizzled-4, a high-affinity ligand-receptor pair.* Cell, 2004. 116(6): p. 883-95.
20. Kazanskaya, O., et al., *R-Spondin2 is a secreted activator of Wnt/beta-catenin signaling and is required for Xenopus myogenesis.* Dev Cell, 2004. 7(4): p. 525-34.
21. Kim, K.A., et al., *Mitogenic influence of human R-spondin1 on the intestinal epithelium.* Science, 2005. 309(5738): p. 1256-9.
22. Nam, J.S., et al., *Mouse cristin/R-spondin family proteins are novel ligands for the Frizzled 8 and LRP6 receptors and activate beta-catenin-dependent gene expression.* J Biol Chem, 2006. 281(19): p. 13247-57.
23. Hsieh, J.C., et al., *A new secreted protein that binds to Wnt proteins and inhibits their activities.* Nature, 1999. 398(6726): p. 431-6.
24. Glinka, A., et al., *Dickkopf-1 is a member of a new family of secreted proteins and functions in head induction.* Nature, 1998. 391(6665): p. 357-62.
25. Mao, B., et al., *Kremen proteins are Dickkopf receptors that regulate Wnt/beta-catenin signalling.* Nature, 2002. 417(6889): p. 664-7.
26. Itasaki, N., et al., *Wise, a context-dependent activator and inhibitor of Wnt signalling.* Development, 2003. 130(18): p. 4295-305.
27. Semenov, M., K. Tamai, and X. He, *SOST is a ligand for LRP5/LRP6 and a Wnt signaling inhibitor.* J Biol Chem, 2005. 280(29): p. 26770-5.
28. Li, X., et al., *Sclerostin binds to LRP5/6 and antagonizes canonical Wnt signaling.* J Biol Chem, 2005. 280(20): p. 19883-7.

29. Wallingford, J.B. and R. Habas, *The developmental biology of Dishevelled: an enigmatic protein governing cell fate and cell polarity.* Development, 2005. 132(20): p. 4421-36.
30. Davidson, G., et al., *Casein kinase 1 gamma couples Wnt receptor activation to cytoplasmic signal transduction.* Nature, 2005. 438(7069): p. 867-72.
31. Zeng, X., et al., *A dual-kinase mechanism for Wnt co-receptor phosphorylation and activation.* Nature, 2005. 438(7069): p. 873-7.
32. Price, M.A., *CKI, there's more than one: casein kinase I family members in Wnt and Hedgehog signaling.* Genes Dev, 2006. 20(4): p. 399-410.
33. Lee, E., et al., *The roles of APC and Axin derived from experimental and theoretical analysis of the Wnt pathway.* PLoS Biol, 2003. 1(1): p. E10.
34. Rosin-Arbesfeld, R., F. Townsley, and M. Bienz, *The APC tumour suppressor has a nuclear export function.* Nature, 2000. 406(6799): p. 1009-12.
35. Huber, A.H., W.J. Nelson, and W.I. Weis, *Three-dimensional structure of the armadillo repeat region of beta-catenin.* Cell, 1997. 90(5): p. 871-82.
36. Choi, H.J., A.H. Huber, and W.I. Weis, *Thermodynamics of beta-catenin-ligand interactions: the roles of the N- and C-terminal tails in modulating binding affinity.* J Biol Chem, 2006. 281(2): p. 1027-38.
37. Xing, Y., et al., *Crystal structure of a beta-catenin/axin complex suggests a mechanism for the beta-catenin destruction complex.* Genes Dev, 2003. 17(22): p. 2753-64.
38. Behrens, J., et al., *Functional interaction of beta-catenin with the transcription factor LEF-1.* Nature, 1996. 382(6592): p. 638-42.
39. Molenaar, M., et al., *XTcf-3 transcription factor mediates beta-catenin-induced axis formation in Xenopus embryos.* Cell, 1996. 86(3): p. 391-9.
40. van de Wetering, M., et al., *Armadillo coactivates transcription driven by the product of the Drosophila segment polarity gene dTCF.* Cell, 1997. 88(6): p. 789-99.
41. Fagotto, F., U. Gluck, and B.M. Gumbiner, *Nuclear localization signal-independent and importin/karyopherin-independent nuclear import of beta-catenin.* Curr Biol, 1998. 8(4): p. 181-90.
42. Hoffmans, R. and K. Basler, *BCL9-2 binds Arm/beta-catenin in a Tyr142-independent manner and requires Pygopus for its function in Wg/Wnt signaling.* Mech Dev, 2007. 124(1): p. 59-67.
43. Cong, F. and H. Varmus, *Nuclear-cytoplasmic shuttling of Axin regulates subcellular localization of beta-catenin.* Proc Natl Acad Sci U S A, 2004. 101(9): p. 2882-7.
44. Galceran, J., et al., *Wnt3a-/--like phenotype and limb deficiency in Lef1(-/-)Tcf1(-/-) mice.* Genes Dev, 1999. 13(6): p. 709-17.
45. Cavallo, R.A., et al., *Drosophila Tcf and Groucho interact to repress Wingless signalling activity.* Nature, 1998. 395(6702): p. 604-8.
46. Roose, J., et al., *The Xenopus Wnt effector XTcf-3 interacts with Groucho-related transcriptional repressors.* Nature, 1998. 395(6702): p. 608-12.
47. Daniels, D.L. and W.I. Weis, *Beta-catenin directly displaces Groucho/TLE repressors from Tcf/Lef in Wnt-mediated transcription activation.* Nat Struct Mol Biol, 2005. 12(4): p. 364-71.
48. Kramps, T., et al., *Wnt/wingless signaling requires BCL9/legless-mediated recruitment of pygopus to the nuclear beta-catenin-TCF complex.* Cell, 2002. 109(1): p. 47-60.
49. Parker, D.S., J. Jemison, and K.M. Cadigan, *Pygopus, a nuclear PHD-finger protein required for Wingless signaling in Drosophila.* Development, 2002. 129(11): p. 2565-76.
50. Thompson, B., et al., *A new nuclear component of the Wnt signalling pathway.* Nat Cell Biol, 2002. 4(5): p. 367-73.
51. Townsley, F.M., A. Cliffe, and M. Bienz, *Pygopus and Legless target Armadillo/beta-catenin to the nucleus to enable its transcriptional co-activator function.* Nat Cell Biol, 2004. 6(7): p. 626-33.
52. Hoffmans, R., R. Stadeli, and K. Basler, *Pygopus and legless provide essential transcriptional coactivator functions to armadillo/beta-catenin.* Curr Biol, 2005. 15(13): p. 1207-11.
53. Peifer, M., et al., *The vertebrate adhesive junction proteins beta-catenin and plakoglobin and the Drosophila segment polarity gene armadillo form a multigene family with similar properties.* J Cell Biol, 1992. 118(3): p. 681-91.
54. Korswagen, H.C., M.A. Herman, and H.C. Clevers, *Distinct beta-catenins mediate adhesion and signalling functions in C. elegans.* Nature, 2000. 406(6795): p. 527-32.

55. Veeman, M.T., et al., *Zebrafish prickle, a modulator of noncanonical Wnt/Fz signaling, regulates gastrulation movements.* Curr Biol, 2003. 13(8): p. 680-5.
56. Kohn, A.D. and R.T. Moon, *Wnt and calcium signaling: beta-catenin-independent pathways.* Cell Calcium, 2005. 38(3-4): p. 439-46.
57. Krylova, O., M.J. Messenger, and P.C. Salinas, *Dishevelled-1 regulates microtubule stability: a new function mediated by glycogen synthase kinase-3beta.* J Cell Biol, 2000. 151(1): p. 83-94.
58. Ciani, L., et al., *A divergent canonical WNT-signaling pathway regulates microtubule dynamics: dishevelled signals locally to stabilize microtubules.* J Cell Biol, 2004. 164(2): p. 243-53.
59. van de Wetering, M., et al., *Identification and cloning of TCF-1, a T lymphocyte-specific transcription factor containing a sequence-specific HMG box.* EMBO J, 1991. 10(1): p. 123-32.
60. Barolo, S., *Transgenic Wnt/TCF pathway reporters: all you need is Lef?* Oncogene, 2006. 25(57): p. 7505-11.
61. Jho, E.H., et al., *Wnt/beta-catenin/Tcf signaling induces the transcription of Axin2, a negative regulator of the signaling pathway.* Mol Cell Biol, 2002. 22(4): p. 1172-83.
62. Hatzis, P., et al., *Genome-wide pattern of TCF7L2/TCF4 chromatin occupancy in colorectal cancer cells.* Mol Cell Biol, 2008. 28(8): p. 2732-44.
63. Artavanis-Tsakonas, S., M.D. Rand, and R.J. Lake, *Notch signaling: cell fate control and signal integration in development.* Science, 1999. 284(5415): p. 770-6.
64. Kopan, R. and M.X. Ilagan, *The canonical Notch signaling pathway: unfolding the activation mechanism.* Cell, 2009. 137(2): p. 216-33.
65. Garg, V., et al., *Mutations in NOTCH1 cause aortic valve disease.* Nature, 2005. 437(7056): p. 270-4.
66. Gridley, T., *Notch signaling and inherited disease syndromes.* Hum Mol Genet, 2003. 12 Spec No 1: p. R9-13.
67. Louvi, A., J.F. Arboleda-Velasquez, and S. Artavanis-Tsakonas, *CADASIL: a critical look at a Notch disease.* Dev Neurosci, 2006. 28(1-2): p. 5-12.
68. Weng, A.P., et al., *Growth suppression of pre-T acute lymphoblastic leukemia cells by inhibition of notch signaling.* Mol Cell Biol, 2003. 23(2): p. 655-64.
69. van Es, J.H., et al., *Notch/gamma-secretase inhibition turns proliferative cells in intestinal crypts and adenomas into goblet cells.* Nature, 2005. 435(7044): p. 959-63.
70. Sonoshita, M., et al., *Suppression of Colon Cancer Metastasis by Aes through Inhibition of Notch Signaling.* Cancer Cell, 2011. 19(1): p. 125-37.
71. Benedito, R., et al., *The notch ligands Dll4 and Jagged1 have opposing effects on angiogenesis.* Cell, 2009. 137(6): p. 1124-35.
72. Noguera-Troise, I., et al., *Blockade of Dll4 inhibits tumour growth by promoting non-productive angiogenesis.* Nature, 2006. 444(7122): p. 1032-7.
73. Cordle, J., et al., *Localization of the delta-like-1-binding site in human Notch-1 and its modulation by calcium affinity.* J Biol Chem, 2008. 283(17): p. 11785-93.
74. Malecki, M.J., et al., *Leukemia-associated mutations within the NOTCH1 heterodimerization domain fall into at least two distinct mechanistic classes.* Mol Cell Biol, 2006. 26(12): p. 4642-51.
75. Weng, A.P., et al., *Activating mutations of NOTCH1 in human T cell acute lymphoblastic leukemia.* Science, 2004. 306(5694): p. 269-71.
76. Oberg, C., et al., *The Notch intracellular domain is ubiquitinated and negatively regulated by the mammalian Sel-10 homolog.* J Biol Chem, 2001. 276(38): p. 35847-53.
77. Wu, J. and E.H. Bresnick, *Bare rudiments of notch signaling: how receptor levels are regulated.* Trends Biochem Sci, 2007. 32(10): p. 477-85.
78. Komatsu, H., et al., *OSM-11 facilitates LIN-12 Notch signaling during Caenorhabditis elegans vulval development.* PLoS Biol, 2008. 6(8): p. e196.
79. D'Souza, B., A. Miyamoto, and G. Weinmaster, *The many facets of Notch ligands.* Oncogene, 2008. 27(38): p. 5148-67.
80. Baladron, V., et al., *dlk acts as a negative regulator of Notch1 activation through interactions with specific EGF-like repeats.* Exp Cell Res, 2005. 303(2): p. 343-59.
81. Wang, Y., et al., *Pref-1, a preadipocyte secreted factor that inhibits adipogenesis.* J Nutr, 2006. 136(12): p. 2953-6.
82. Eiraku, M., et al., *DNER acts as a neuron-specific Notch ligand during Bergmann glial development.* Nat Neurosci, 2005. 8(7): p. 873-80.

83. Cui, X.Y., et al., *NB-3/Notch1 pathway via Deltex1 promotes neural progenitor cell differentiation into oligodendrocytes.* J Biol Chem, 2004. 279(24): p. 25858-65.
84. Hu, Q.D., et al., *F3/contactin acts as a functional ligand for Notch during oligodendrocyte maturation.* Cell, 2003. 115(2): p. 163-75.
85. Albig, A.R., et al., *Microfibril-associate glycoprotein-2 (MAGP-2) promotes angiogenic cell sprouting by blocking notch signaling in endothelial cells.* Microvasc Res, 2008. 76(1): p. 7-14.
86. Miyamoto, A., et al., *Microfibrillar proteins MAGP-1 and MAGP-2 induce Notch1 extracellular domain dissociation and receptor activation.* J Biol Chem, 2006. 281(15): p. 10089-97.
87. Rydziel, S., et al., *Nephroblastoma overexpressed (Nov) inhibits osteoblastogenesis and causes osteopenia.* J Biol Chem, 2007. 282(27): p. 19762-72.
88. Dale, J.K., et al., *Periodic notch inhibition by lunatic fringe underlies the chick segmentation clock.* Nature, 2003. 421(6920): p. 275-8.
89. Visan, I., et al., *Regulation of T lymphopoiesis by Notch1 and Lunatic fringe-mediated competition for intrathymic niches.* Nat Immunol, 2006. 7(6): p. 634-43.
90. Rampal, R., et al., *Highly conserved O-fucose sites have distinct effects on Notch1 function.* J Biol Chem, 2005. 280(37): p. 32133-40.
91. Stahl, M., et al., *Roles of Pofut1 and O-fucose in mammalian Notch signaling.* J Biol Chem, 2008. 283(20): p. 13638-51.
92. Stanley, P., *Regulation of Notch signaling by glycosylation.* Curr Opin Struct Biol, 2007. 17(5): p. 530-5.
93. Heuss, S.F., et al., *The intracellular region of Notch ligands Dll1 and Dll3 regulates their trafficking and signaling activity.* Proc Natl Acad Sci U S A, 2008. 105(32): p. 11212-7.
94. Jin, Y., et al., *A death-associated protein kinase (DAPK)-interacting protein, DIP-1, is an E3 ubiquitin ligase that promotes tumor necrosis factor-induced apoptosis and regulates the cellular levels of DAPK.* J Biol Chem, 2002. 277(49): p. 46980-6.
95. Koo, B.K., et al., *Mind bomb 1 is essential for generating functional Notch ligands to activate Notch.* Development, 2005. 132(15): p. 3459-70.
96. Koutelou, E., et al., *Neuralized-like 1 (Neurl1) targeted to the plasma membrane by N-myristoylation regulates the Notch ligand Jagged1.* J Biol Chem, 2008. 283(7): p. 3846-53.
97. Nakamura, H., et al., *Identification of a human homolog of the Drosophila neuralized gene within the 10q25.1 malignant astrocytoma deletion region.* Oncogene, 1998. 16(8): p. 1009-19.
98. Brou, C., *Intracellular trafficking of Notch receptors and ligands.* Exp Cell Res, 2009. 315(9): p. 1549-55.
99. Le Borgne, R., A. Bardin, and F. Schweisguth, *The roles of receptor and ligand endocytosis in regulating Notch signaling.* Development, 2005. 132(8): p. 1751-62.
100. Nichols, J.T., A. Miyamoto, and G. Weinmaster, *Notch signaling--constantly on the move.* Traffic, 2007. 8(8): p. 959-69.
101. Chastagner, P., A. Israel, and C. Brou, *AIP4/Itch regulates Notch receptor degradation in the absence of ligand.* PLoS One, 2008. 3(7): p. e2735.
102. Wilkin, M.B., et al., *Regulation of notch endosomal sorting and signaling by Drosophila Nedd4 family proteins.* Curr Biol, 2004. 14(24): p. 2237-44.
103. Mukherjee, A., et al., *Regulation of Notch signalling by non-visual beta-arrestin.* Nat Cell Biol, 2005. 7(12): p. 1191-201.
104. Blaumueller, C.M., et al., *Intracellular cleavage of Notch leads to a heterodimeric receptor on the plasma membrane.* Cell, 1997. 90(2): p. 281-91.
105. Kramer, H., *RIPping notch apart: a new role for endocytosis in signal transduction?* Sci STKE, 2000. 2000(29): p. pe1.
106. Nichols, J.T., et al., *DSL ligand endocytosis physically dissociates Notch1 heterodimers before activating proteolysis can occur.* J Cell Biol, 2007. 176(4): p. 445-58.
107. Ehebauer, M., P. Hayward, and A. Martinez-Arias, *Notch signaling pathway.* Sci STKE, 2006. 2006(364): p. cm7.
108. Schroeter, E.H., J.A. Kisslinger, and R. Kopan, *Notch-1 signalling requires ligand-induced proteolytic release of intracellular domain.* Nature, 1998. 393(6683): p. 382-6.
109. Song, W., et al., *Proteolytic release and nuclear translocation of Notch-1 are induced by presenilin-1 and impaired by pathogenic presenilin-1 mutations.* Proc Natl Acad Sci U S A, 1999. 96(12): p. 6959-63.

110. Sato, T., et al., *Active gamma-secretase complexes contain only one of each component.* J Biol Chem, 2007. 282(47): p. 33985-93.
111. Tolia, A. and B. De Strooper, *Structure and function of gamma-secretase.* Semin Cell Dev Biol, 2009. 20(2): p. 211-8.
112. Kovall, R.A., *Structures of CSL, Notch and Mastermind proteins: piecing together an active transcription complex.* Curr Opin Struct Biol, 2007. 17(1): p. 117-27.
113. Kovall, R.A. and W.A. Hendrickson, *Crystal structure of the nuclear effector of Notch signaling, CSL, bound to DNA.* EMBO J, 2004. 23(17): p. 3441-51.
114. Nam, Y., et al., *Structural basis for cooperativity in recruitment of MAML coactivators to Notch transcription complexes.* Cell, 2006. 124(5): p. 973-83.
115. Fryer, C.J., et al., *Mastermind mediates chromatin-specific transcription and turnover of the Notch enhancer complex.* Genes Dev, 2002. 16(11): p. 1397-411.
116. Nam, Y., et al., *Structural requirements for assembly of the CSL.intracellular Notch1.Mastermind-like 1 transcriptional activation complex.* J Biol Chem, 2003. 278(23): p. 21232-9.
117. Wu, L., et al., *MAML1, a human homologue of Drosophila mastermind, is a transcriptional co-activator for NOTCH receptors.* Nat Genet, 2000. 26(4): p. 484-9.
118. Fryer, C.J., J.B. White, and K.A. Jones, *Mastermind recruits CycC:CDK8 to phosphorylate the Notch ICD and coordinate activation with turnover.* Mol Cell, 2004. 16(4): p. 509-20.
119. Androutsellis-Theotokis, A., et al., *Notch signalling regulates stem cell numbers in vitro and in vivo.* Nature, 2006. 442(7104): p. 823-6.
120. Iso, T., L. Kedes, and Y. Hamamori, *HES and HERP families: multiple effectors of the Notch signaling pathway.* J Cell Physiol, 2003. 194(3): p. 237-55.
121. Katoh, M., *Identification and characterization of human HES2, HES3, and HES5 genes in silico.* Int J Oncol, 2004. 25(2): p. 529-34.
122. Fischer, A. and M. Gessler, *Delta-Notch--and then? Protein interactions and proposed modes of repression by Hes and Hey bHLH factors.* Nucleic Acids Res, 2007. 35(14): p. 4583-96.
123. Ronchini, C. and A.J. Capobianco, *Induction of cyclin D1 transcription and CDK2 activity by Notch(ic): implication for cell cycle disruption in transformation by Notch(ic).* Mol Cell Biol, 2001. 21(17): p. 5925-34.
124. Rangarajan, A., et al., *Notch signaling is a direct determinant of keratinocyte growth arrest and entry into differentiation.* EMBO J, 2001. 20(13): p. 3427-36.
125. Reizis, B. and P. Leder, *Direct induction of T lymphocyte-specific gene expression by the mammalian Notch signaling pathway.* Genes Dev, 2002. 16(3): p. 295-300.
126. Amsen, D., et al., *Direct regulation of Gata3 expression determines the T helper differentiation potential of Notch.* Immunity, 2007. 27(1): p. 89-99.
127. Weng, A.P., et al., *c-Myc is an important direct target of Notch1 in T-cell acute lymphoblastic leukemia/lymphoma.* Genes Dev, 2006. 20(15): p. 2096-109.
128. Robert-Moreno, A., et al., *RBPjkappa-dependent Notch function regulates Gata2 and is essential for the formation of intra-embryonic hematopoietic cells.* Development, 2005. 132(5): p. 1117-26.
129. Oka, C., et al., *Disruption of the mouse RBP-J kappa gene results in early embryonic death.* Development, 1995. 121(10): p. 3291-301.
130. Swiatek, P.J., et al., *Notch1 is essential for postimplantation development in mice.* Genes Dev, 1994. 8(6): p. 707-19.
131. McCright, B., J. Lozier, and T. Gridley, *Generation of new Notch2 mutant alleles.* Genesis, 2006. 44(1): p. 29-33.
132. Bellavia, D., et al., *Notch3: from subtle structural differences to functional diversity.* Oncogene, 2008. 27(38): p. 5092-8.
133. Monet, M., et al., *The archetypal R90C CADASIL-NOTCH3 mutation retains NOTCH3 function in vivo.* Hum Mol Genet, 2007. 16(8): p. 982-92.
134. Krebs, L.T., et al., *Notch signaling is essential for vascular morphogenesis in mice.* Genes Dev, 2000. 14(11): p. 1343-52.
135. Murphy, P.A., et al., *Endothelial Notch4 signaling induces hallmarks of brain arteriovenous malformations in mice.* Proc Natl Acad Sci U S A, 2008. 105(31): p. 10901-6.
136. Hrabe de Angelis, M., J. McIntyre, 2nd, and A. Gossler, *Maintenance of somite borders in mice requires the Delta homologue DII1.* Nature, 1997. 386(6626): p. 717-21.

137. Kusumi, K., et al., *The mouse pudgy mutation disrupts Delta homologue Dll3 and initiation of early somite boundaries.* Nat Genet, 1998. 19(3): p. 274-8.
138. Gale, N.W., et al., *Haploinsufficiency of delta-like 4 ligand results in embryonic lethality due to major defects in arterial and vascular development.* Proc Natl Acad Sci U S A, 2004. 101(45): p. 15949-54.
139. Jiang, R., et al., *Defects in limb, craniofacial, and thymic development in Jagged2 mutant mice.* Genes Dev, 1998. 12(7): p. 1046-57.
140. Xue, Y., et al., *Embryonic lethality and vascular defects in mice lacking the Notch ligand Jagged1.* Hum Mol Genet, 1999. 8(5): p. 723-30.
141. Hatakeyama, J., et al., *Hes genes regulate size, shape and histogenesis of the nervous system by control of the timing of neural stem cell differentiation.* Development, 2004. 131(22): p. 5539-50.
142. Kageyama, R., T. Ohtsuka, and T. Kobayashi, *The Hes gene family: repressors and oscillators that orchestrate embryogenesis.* Development, 2007. 134(7): p. 1243-51.
143. Murtaugh, L.C., et al., *Notch signaling controls multiple steps of pancreatic differentiation.* Proc Natl Acad Sci U S A, 2003. 100(25): p. 14920-5.
144. Bessho, Y., et al., *Dynamic expression and essential functions of Hes7 in somite segmentation.* Genes Dev, 2001. 15(20): p. 2642-7.
145. Bae, S., et al., *The bHLH gene Hes6, an inhibitor of Hes1, promotes neuronal differentiation.* Development, 2000. 127(13): p. 2933-43.
146. Fischer, A., et al., *Phenotypic variability in Hey2 -/- mice and absence of HEY2 mutations in patients with congenital heart defects or Alagille syndrome.* Mamm Genome, 2004. 15(9): p. 711-6.
147. Fischer, A., et al., *Combined loss of Hey1 and HeyL causes congenital heart defects because of impaired epithelial to mesenchymal transition.* Circ Res, 2007. 100(6): p. 856-63.
148. Kokubo, H., et al., *Mouse hesr1 and hesr2 genes are redundantly required to mediate Notch signaling in the developing cardiovascular system.* Dev Biol, 2005. 278(2): p. 301-9.
149. Xin, M., et al., *Essential roles of the bHLH transcription factor Hrt2 in repression of atrial gene expression and maintenance of postnatal cardiac function.* Proc Natl Acad Sci U S A, 2007. 104(19): p. 7975-80.
150. Brittan, M. and N.A. Wright, *Stem cell in gastrointestinal structure and neoplastic development.* Gut, 2004. 53(6): p. 899-910.
151. Paulus, U., et al., *The differentiation and lineage development of goblet cells in the murine small intestinal crypt: experimental and modelling studies.* J Cell Sci, 1993. 106 (Pt 2): p. 473-83.
152. Ayabe, T., et al., *Secretion of microbicidal alpha-defensins by intestinal Paneth cells in response to bacteria.* Nat Immunol, 2000. 1(2): p. 113-8.
153. Potten, C.S. and M. Loeffler, *A comprehensive model of the crypts of the small intestine of the mouse provides insight into the mechanisms of cell migration and the proliferation hierarchy.* J Theor Biol, 1987. 127(4): p. 381-91.
154. Gordon, J.I. and M.L. Hermiston, *Differentiation and self-renewal in the mouse gastrointestinal epithelium.* Curr Opin Cell Biol, 1994. 6(6): p. 795-803.
155. Potten, C.S., J.H. Hendry, and J.V. Moore, *Estimates of the number of clonogenic cells in crypts of murine small intestine.* Virchows Arch B Cell Pathol Incl Mol Pathol, 1987. 53(4): p. 227-34.
156. Bevins, C.L., E. Martin-Porter, and T. Ganz, *Defensins and innate host defence of the gastrointestinal tract.* Gut, 1999. 45(6): p. 911-5.
157. Sato, T., et al., *Paneth cells constitute the niche for Lgr5 stem cells in intestinal crypts.* Nature, 2011. 469(7330): p. 415-8.
158. Potten, C.S., G. Owen, and D. Booth, *Intestinal stem cells protect their genome by selective segregation of template DNA strands.* J Cell Sci, 2002. 115(Pt 11): p. 2381-8.
159. Quyn, A.J., et al., *Spindle orientation bias in gut epithelial stem cell compartments is lost in precancerous tissue.* Cell Stem Cell, 2010. 6(2): p. 175-81.
160. Bjerknes, M. and H. Cheng, *The stem-cell zone of the small intestinal epithelium. I. Evidence from Paneth cells in the adult mouse.* Am J Anat, 1981. 160(1): p. 51-63.
161. Sangiorgi, E. and M.R. Capecchi, *Bmi1 is expressed in vivo in intestinal stem cells.* Nat Genet, 2008. 40(7): p. 915-20.
162. Lee, G., et al., *Response of small intestinal epithelial cells to acute disruption of cell division through CDC25 deletion.* Proc Natl Acad Sci U S A, 2009. 106(12): p. 4701-6.

163. Cheng, H. and C.P. Leblond, *Origin, differentiation and renewal of the four main epithelial cell types in the mouse small intestine. V. Unitarian Theory of the origin of the four epithelial cell types.* Am J Anat, 1974. 141(4): p. 537-61.
164. Barker, N. and H. Clevers, *Tracking down the stem cells of the intestine: strategies to identify adult stem cells.* Gastroenterology, 2007. 133(6): p. 1755-60.
165. Sato, T., et al., *Single Lgr5 stem cells build crypt-villus structures in vitro without a mesenchymal niche.* Nature, 2009. 459(7244): p. 262-5.
166. Morson, B.C., *The evolution of colorectal carcinoma.* Clin Radiol, 1984. 35(6): p. 425-31.
167. Cheng, L. and M.D. Lai, *Aberrant crypt foci as microscopic precursors of colorectal cancer.* World J Gastroenterol, 2003. 9(12): p. 2642-9.
168. Preston, S.L., et al., *Bottom-up histogenesis of colorectal adenomas: origin in the monocryptal adenoma and initial expansion by crypt fission.* Cancer Res, 2003. 63(13): p. 3819-25.
169. Cortina, C., et al., *EphB-ephrin-B interactions suppress colorectal cancer progression by compartmentalizing tumor cells.* Nat Genet, 2007. 39(11): p. 1376-83.
170. Shih, I.M., et al., *Top-down morphogenesis of colorectal tumors.* Proc Natl Acad Sci U S A, 2001. 98(5): p. 2640-5.
171. Lynch, H.T. and A. de la Chapelle, *Hereditary colorectal cancer.* N Engl J Med, 2003. 348(10): p. 919-32.
172. Fodde, R. and P.M. Khan, *Genotype-phenotype correlations at the adenomatous polyposis coli (APC) gene.* Crit Rev Oncog, 1995. 6(3-6): p. 291-303.
173. Powell, S.M., et al., *APC mutations occur early during colorectal tumorigenesis.* Nature, 1992. 359(6392): p. 235-7.
174. Polakis, P., *The adenomatous polyposis coli (APC) tumor suppressor.* Biochim Biophys Acta, 1997. 1332(3): p. F127-47.
175. Ichii, S., et al., *Inactivation of both APC alleles in an early stage of colon adenomas in a patient with familial adenomatous polyposis (FAP).* Hum Mol Genet, 1992. 1(6): p. 387-90.
176. Levy, D.B., et al., *Inactivation of both APC alleles in human and mouse tumors.* Cancer Res, 1994. 54(22): p. 5953-8.
177. Rowan, A.J., et al., *APC mutations in sporadic colorectal tumors: A mutational "hotspot" and interdependence of the "two hits".* Proc Natl Acad Sci U S A, 2000. 97(7): p. 3352-7.
178. Sparks, A.B., et al., *Mutational analysis of the APC/beta-catenin/Tcf pathway in colorectal cancer.* Cancer Res, 1998. 58(6): p. 1130-4.
179. Fodde, R., R. Smits, and H. Clevers, *APC, signal transduction and genetic instability in colorectal cancer.* Nat Rev Cancer, 2001. 1(1): p. 55-67.
180. Fearon, E.R. and B. Vogelstein, *A genetic model for colorectal tumorigenesis.* Cell, 1990. 61(5): p. 759-67.
181. Lickert, H. and R. Kemler, *Functional analysis of cis-regulatory elements controlling initiation and maintenance of early Cdx1 gene expression in the mouse.* Dev Dyn, 2002. 225(2): p. 216-20.
182. Gregorieff, A., R. Grosschedl, and H. Clevers, *Hindgut defects and transformation of the gastro-intestinal tract in Tcf4(-/-)/Tcf1(-/-) embryos.* EMBO J, 2004. 23(8): p. 1825-33.
183. Okubo, T. and B.L. Hogan, *Hyperactive Wnt signaling changes the developmental potential of embryonic lung endoderm.* J Biol, 2004. 3(3): p. 11.
184. Davies, P.S., et al., *Wnt-reporter expression pattern in the mouse intestine during homeostasis.* BMC Gastroenterol, 2008. 8: p. 57.
185. Korinek, V., et al., *Depletion of epithelial stem-cell compartments in the small intestine of mice lacking Tcf-4.* Nat Genet, 1998. 19(4): p. 379-83.
186. Grigoryan, T., et al., *Deciphering the function of canonical Wnt signals in development and disease: conditional loss- and gain-of-function mutations of beta-catenin in mice.* Genes Dev, 2008. 22(17): p. 2308-41.
187. van de Wetering, M., et al., *The beta-catenin/TCF-4 complex imposes a crypt progenitor phenotype on colorectal cancer cells.* Cell, 2002. 111(2): p. 241-50.
188. van der Flier, L.G., et al., *Transcription factor achaete scute-like 2 controls intestinal stem cell fate.* Cell, 2009. 136(5): p. 903-12.
189. Kinzler, K.W. and B. Vogelstein, *Lessons from hereditary colorectal cancer.* Cell, 1996. 87(2): p. 159-70.

190. Bienz, M. and H. Clevers, *Linking colorectal cancer to Wnt signaling.* Cell, 2000. 103(2): p. 311-20.
191. Polakis, P., *Wnt signaling and cancer.* Genes Dev, 2000. 14(15): p. 1837-51.
192. Clevers, H., *Wnt/beta-catenin signaling in development and disease.* Cell, 2006. 127(3): p. 469-80.
193. Moser, A.R., H.C. Pitot, and W.F. Dove, *A dominant mutation that predisposes to multiple intestinal neoplasia in the mouse.* Science, 1990. 247(4940): p. 322-4.
194. Oshima, M., et al., *Loss of Apc heterozygosity and abnormal tissue building in nascent intestinal polyps in mice carrying a truncated Apc gene.* Proc Natl Acad Sci U S A, 1995. 92(10): p. 4482-6.
195. Wong, M.H., et al., *Forced expression of the tumor suppressor adenomatosis polyposis coli protein induces disordered cell migration in the intestinal epithelium.* Proc Natl Acad Sci U S A, 1996. 93(18): p. 9588-93.
196. Smits, R., et al., *Apc1638T: a mouse model delineating critical domains of the adenomatous polyposis coli protein involved in tumorigenesis and development.* Genes Dev, 1999. 13(10): p. 1309-21.
197. Harada, N., et al., *Intestinal polyposis in mice with a dominant stable mutation of the beta-catenin gene.* EMBO J, 1999. 18(21): p. 5931-42.
198. Sansom, O.J., et al., *Myc deletion rescues Apc deficiency in the small intestine.* Nature, 2007. 446(7136): p. 676-9.
199. Barker, N., et al., *Crypt stem cells as the cells-of-origin of intestinal cancer.* Nature, 2009. 457(7229): p. 608-11.
200. O'Brien, C.A., et al., *A human colon cancer cell capable of initiating tumour growth in immunodeficient mice.* Nature, 2007. 445(7123): p. 106-10.
201. Zhu, L., et al., *Prominin 1 marks intestinal stem cells that are susceptible to neoplastic transformation.* Nature, 2009. 457(7229): p. 603-7.
202. Vermeulen, L., et al., *Wnt activity defines colon cancer stem cells and is regulated by the microenvironment.* Nat Cell Biol, 2010. 12(5): p. 468-76.
203. Yang, Q., et al., *Requirement of Math1 for secretory cell lineage commitment in the mouse intestine.* Science, 2001. 294(5549): p. 2155-8.
204. Suzuki, K., et al., *Hes1-deficient mice show precocious differentiation of Paneth cells in the small intestine.* Biochem Biophys Res Commun, 2005. 328(1): p. 348-52.
205. Stanger, B.Z., et al., *Direct regulation of intestinal fate by Notch.* Proc Natl Acad Sci U S A, 2005. 102(35): p. 12443-8.
206. Fre, S., et al., *Notch signals control the fate of immature progenitor cells in the intestine.* Nature, 2005. 435(7044): p. 964-8.
207. Okamoto, R., et al., *Requirement of Notch activation during regeneration of the intestinal epithelia.* Am J Physiol Gastrointest Liver Physiol, 2009. 296(1): p. G23-35.
208. Wu, Y., et al., *Therapeutic antibody targeting of individual Notch receptors.* Nature, 2010. 464(7291): p. 1052-7.
209. Riccio, O., et al., *Loss of intestinal crypt progenitor cells owing to inactivation of both Notch1 and Notch2 is accompanied by derepression of CDK inhibitors p27Kip1 and p57Kip2.* EMBO Rep, 2008. 9(4): p. 377-83.
210. Pellegrinet, L., et al., *Dll1- and Dll4-mediated Notch signaling is required for homeostasis of intestinal stem cells.* Gastroenterology, 2011.
211. Aragaki, M., et al., *Proteasomal degradation of Atoh1 by aberrant Wnt signaling maintains the undifferentiated state of colon cancer.* Biochem Biophys Res Commun, 2008. 368(4): p. 923-9.
212. Fernandez-Majada, V., et al., *Nuclear IKK activity leads to dysregulated notch-dependent gene expression in colorectal cancer.* Proc Natl Acad Sci U S A, 2007. 104(1): p. 276-81.
213. Batlle, E., et al., *EphB receptor activity suppresses colorectal cancer progression.* Nature, 2005. 435(7045): p. 1126-30.
214. Veenendaal, L.M., et al., *Differential Notch and TGFbeta signaling in primary colorectal tumors and their corresponding metastases.* Cell Oncol, 2008. 30(1): p. 1-11.
215. Zhang, Y., et al., *Notch1 regulates the growth of human colon cancers.* Cancer, 2010. 116(22): p. 5207-18.
216. Guilmeau, S., et al., *Heterogeneity of Jagged1 expression in human and mouse intestinal tumors: implications for targeting Notch signaling.* Oncogene, 2010. 29(7): p. 992-1002.

217. Reedijk, M., et al., *Activation of Notch signaling in human colon adenocarcinoma.* Int J Oncol, 2008. 33(6): p. 1223-9.
218. Leow, C.C., P. Polakis, and W.Q. Gao, *A role for Hath1, a bHLH transcription factor, in colon adenocarcinoma.* Ann N Y Acad Sci, 2005. 1059: p. 174-83.
219. Fischer, M., et al., *Anti-DLL4 Inhibits Growth and Reduces Tumor Initiating Cell Frequency in Colorectal Tumors with Oncogenic KRAS Mutations.* Cancer Res, 2010.
220. Garg, P., et al., *Matrix metalloproteinase-9 functions as a tumor suppressor in colitis-associated cancer.* Cancer Res, 2010. 70(2): p. 792-801.
221. Koduru, S., et al., *Notch-1 inhibition by Withaferin-A: a therapeutic target against colon carcinogenesis.* Mol Cancer Ther, 2010. 9(1): p. 202-10.
222. Fre, S., et al., *Notch and Wnt signals cooperatively control cell proliferation and tumorigenesis in the intestine.* Proc Natl Acad Sci U S A, 2009. 106(15): p. 6309-14.
223. Ghaleb, A.M., et al., *Notch inhibits expression of the Kruppel-like factor 4 tumor suppressor in the intestinal epithelium.* Mol Cancer Res, 2008. 6(12): p. 1920-7.
224. Bergers, G. and L.E. Benjamin, *Tumorigenesis and the angiogenic switch.* Nat Rev Cancer, 2003. 3(6): p. 401-10.
225. Achen, M.G. and S.A. Stacker, *The vascular endothelial growth factor family; proteins which guide the development of the vasculature.* Int J Exp Pathol, 1998. 79(5): p. 255-65.
226. Galizia, G., et al., *Determination of molecular marker expression can predict clinical outcome in colon carcinomas.* Clin Cancer Res, 2004. 10(10): p. 3490-9.
227. Takahashi, Y., et al., *Expression of vascular endothelial growth factor and its receptor, KDR, correlates with vascularity, metastasis, and proliferation of human colon cancer.* Cancer Res, 1995. 55(18): p. 3964-8.
228. Bendardaf, R., et al., *VEGF-1 expression in colorectal cancer is associated with disease localization, stage, and long-term disease-specific survival.* Anticancer Res, 2008. 28(6B): p. 3865-70.
229. Mailhos, C., et al., *Delta4, an endothelial specific notch ligand expressed at sites of physiological and tumor angiogenesis.* Differentiation, 2001. 69(2-3): p. 135-44.
230. Alva, J.A. and M.L. Iruela-Arispe, *Notch signaling in vascular morphogenesis.* Curr Opin Hematol, 2004. 11(4): p. 278-83.
231. Dufraine, J., Y. Funahashi, and J. Kitajewski, *Notch signaling regulates tumor angiogenesis by diverse mechanisms.* Oncogene, 2008. 27(38): p. 5132-7.
232. Li, J.L., et al., *Delta-like 4 Notch ligand regulates tumor angiogenesis, improves tumor vascular function, and promotes tumor growth in vivo.* Cancer Res, 2007. 67(23): p. 11244-53.
233. Zeng, Q., et al., *Crosstalk between tumor and endothelial cells promotes tumor angiogenesis by MAPK activation of Notch signaling.* Cancer Cell, 2005. 8(1): p. 13-23.
234. Koch, U. and F. Radtke, *Notch and cancer: a double-edged sword.* Cell Mol Life Sci, 2007. 64(21): p. 2746-62.
235. Oishi, H., et al., *Blockade of delta-like ligand 4 signaling inhibits both growth and angiogenesis of pancreatic cancer.* Pancreas, 2010. 39(6): p. 897-903.
236. Ricci-Vitiani, L., et al., *Identification and expansion of human colon-cancer-initiating cells.* Nature, 2007. 445(7123): p. 111-5.
237. Moriyama, M., et al., *Multiple roles of Notch signaling in the regulation of epidermal development.* Dev Cell, 2008. 14(4): p. 594-604.
238. Fan, X., et al., *Notch pathway inhibition depletes stem-like cells and blocks engraftment in embryonal brain tumors.* Cancer Res, 2006. 66(15): p. 7445-52.
239. Rodilla, V., et al., *Jagged1 is the pathological link between Wnt and Notch pathways in colorectal cancer.* Proc Natl Acad Sci U S A, 2009. 106(15): p. 6315-20.
240. Sureban, S.M., et al., *Knockdown of RNA binding protein musashi-1 leads to tumor regression in vivo.* Gastroenterology, 2008. 134(5): p. 1448-58.
241. Kayahara, T., et al., *Candidate markers for stem and early progenitor cells, Musashi-1 and Hes1, are expressed in crypt base columnar cells of mouse small intestine.* FEBS Lett, 2003. 535(1-3): p. 131-5.
242. Wong, G.T., et al., *Chronic treatment with the gamma-secretase inhibitor LY-411,575 inhibits beta-amyloid peptide production and alters lymphopoiesis and intestinal cell differentiation.* J Biol Chem, 2004. 279(13): p. 12876-82.
243. Sikandar, S.S., et al., *NOTCH signaling is required for formation and self-renewal of tumor-initiating cells and for repression of secretory cell differentiation in colon cancer.* Cancer Res, 2010. 70(4): p. 1469-78.

244. Zheng, H., et al., *KLF4 gene expression is inhibited by the notch signaling pathway that controls goblet cell differentiation in mouse gastrointestinal tract.* Am J Physiol Gastrointest Liver Physiol, 2009. 296(3): p. G490-8.
245. Akiyoshi, T., et al., *Gamma-secretase inhibitors enhance taxane-induced mitotic arrest and apoptosis in colon cancer cells.* Gastroenterology, 2008. 134(1): p. 131-44.
246. Meng, R.D., et al., *gamma-Secretase inhibitors abrogate oxaliplatin-induced activation of the Notch-1 signaling pathway in colon cancer cells resulting in enhanced chemosensitivity.* Cancer Res, 2009. 69(2): p. 573-82.
247. Garber, K., *Notch emerges as new cancer drug target.* J Natl Cancer Inst, 2007. 99(17): p. 1284-5.
248. O'Neil, J., et al., *FBW7 mutations in leukemic cells mediate NOTCH pathway activation and resistance to gamma-secretase inhibitors.* J Exp Med, 2007. 204(8): p. 1813-24.
249. Hoppler, S. and R.T. Moon, *BMP-2/-4 and Wnt-8 cooperatively pattern the Xenopus mesoderm.* Mech Dev, 1998. 71(1-2): p. 119-29.
250. Janssen, K.P., et al., *APC and oncogenic KRAS are synergistic in enhancing Wnt signaling in intestinal tumor formation and progression.* Gastroenterology, 2006. 131(4): p. 1096-109.
251. Nusse, R., *Wnts and Hedgehogs: lipid-modified proteins and similarities in signaling mechanisms at the cell surface.* Development, 2003. 130(22): p. 5297-305.
252. Sansom, O.J., et al., *Loss of Apc allows phenotypic manifestation of the transforming properties of an endogenous K-ras oncogene in vivo.* Proc Natl Acad Sci U S A, 2006. 103(38): p. 14122-7.
253. Wilson, S.I., et al., *The status of Wnt signalling regulates neural and epidermal fates in the chick embryo.* Nature, 2001. 411(6835): p. 325-30.
254. Zorn, A.M., et al., *Regulation of Wnt signaling by Sox proteins: XSox17 alpha/beta and XSox3 physically interact with beta-catenin.* Mol Cell, 1999. 4(4): p. 487-98.
255. Hurlbut, G.D., et al., *Crossing paths with Notch in the hyper-network.* Curr Opin Cell Biol, 2007. 19(2): p. 166-75.
256. Balint, K., et al., *Activation of Notch1 signaling is required for beta-catenin-mediated human primary melanoma progression.* J Clin Invest, 2005. 115(11): p. 3166-76.
257. Peignon, G., et al., *Complex interplay between beta-catenin signalling and Notch effectors in intestinal tumorigenesis.* Gut, 2011. 60(2): p. 166-76.
258. Estrach, S., et al., *Jagged 1 is a beta-catenin target gene required for ectopic hair follicle formation in adult epidermis.* Development, 2006. 133(22): p. 4427-38.
259. Alves-Guerra, M.C., C. Ronchini, and A.J. Capobianco, *Mastermind-like 1 Is a specific coactivator of beta-catenin transcription activation and is essential for colon carcinoma cell survival.* Cancer Res, 2007. 67(18): p. 8690-8.
260. Hayward, P., et al., *Notch modulates Wnt signalling by associating with Armadillo/beta-catenin and regulating its transcriptional activity.* Development, 2005. 132(8): p. 1819-30.
261. Hayward, P., T. Balayo, and A. Martinez Arias, *Notch synergizes with axin to regulate the activity of armadillo in Drosophila.* Dev Dyn, 2006. 235(10): p. 2656-66.
262. Hubbard, T.J., et al., *Ensembl 2007.* Nucleic Acids Res, 2007. 35(Database issue): p. D610-7.
263. Han, H., et al., *Inducible gene knockout of transcription factor recombination signal binding protein-J reveals its essential role in T versus B lineage decision.* Int Immunol, 2002. 14(6): p. 637-45.
264. el Marjou, F., et al., *Tissue-specific and inducible Cre-mediated recombination in the gut epithelium.* Genesis, 2004. 39(3): p. 186-93.
265. Huelsken, J., et al., *beta-Catenin controls hair follicle morphogenesis and stem cell differentiation in the skin.* Cell, 2001. 105(4): p. 533-45.
266. Kiernan, A.E., J. Xu, and T. Gridley, *The Notch ligand JAG1 is required for sensory progenitor development in the mammalian inner ear.* PLoS Genet, 2006. 2(1): p. e4.
267. Soriano, P., *Generalized lacZ expression with the ROSA26 Cre reporter strain.* Nat Genet, 1999. 21(1): p. 70-1.
268. Wilkinson, D.G., *The psychogeriatrician's view: management of chronic disability in the community.* J Neurol Neurosurg Psychiatry, 1992. 55 Suppl: p. 41-4.
269. Leong, K.G., et al., *Jagged1-mediated Notch activation induces epithelial-to-mesenchymal transition through Slug-induced repression of E-cadherin.* J Exp Med, 2007. 204(12): p. 2935-48.

270. Dalerba, P., et al., *Phenotypic characterization of human colorectal cancer stem cells.* Proc Natl Acad Sci U S A, 2007. 104(24): p. 10158-63.
271. Laurent, E., et al., *Nox1 is over-expressed in human colon cancers and correlates with activating mutations in K-Ras.* Int J Cancer, 2008. 123(1): p. 100-7.
272. Zeilstra, J., et al., *Deletion of the WNT target and cancer stem cell marker CD44 in Apc(Min/+) mice attenuates intestinal tumorigenesis.* Cancer Res, 2008. 68(10): p. 3655-61.
273. Strom, A., et al., *The Hairy and Enhancer of Split homologue-1 (HES-1) mediates the proliferative effect of 17beta-estradiol on breast cancer cell lines.* Oncogene, 2000. 19(51): p. 5951-3.
274. Jay, P., P. Berta, and P. Blache, *Expression of the carcinoembryonic antigen gene is inhibited by SOX9 in human colon carcinoma cells.* Cancer Res, 2005. 65(6): p. 2193-8.
275. Zhang, H., et al., *Lysophosphatidic acid facilitates proliferation of colon cancer cells via induction of Kruppel-like factor 5.* J Biol Chem, 2007. 282(21): p. 15541-9.
276. Wielenga, V.J., et al., *Expression of CD44 in Apc and Tcf mutant mice implies regulation by the WNT pathway.* Am J Pathol, 1999. 154(2): p. 515-23.
277. Schwartz, D.R., et al., *Novel candidate targets of beta-catenin/T-cell factor signaling identified by gene expression profiling of ovarian endometrioid adenocarcinomas.* Cancer Res, 2003. 63(11): p. 2913-22.
278. Blache, P., et al., *SOX9 is an intestine crypt transcription factor, is regulated by the Wnt pathway, and represses the CDX2 and MUC2 genes.* J Cell Biol, 2004. 166(1): p. 37-47.
279. Shimizu, T., et al., *Stabilized beta-catenin functions through TCF/LEF proteins and the Notch/RBP-Jkappa complex to promote proliferation and suppress differentiation of neural precursor cells.* Mol Cell Biol, 2008. 28(24): p. 7427-41.
280. Jin, Y.H., et al., *Beta-catenin modulates the level and transcriptional activity of Notch1/NICD through its direct interaction.* Biochim Biophys Acta, 2009. 1793(2): p. 290-9.
281. Nam, Y., et al., *Cooperative assembly of higher-order Notch complexes functions as a switch to induce transcription.* Proc Natl Acad Sci U S A, 2007. 104(7): p. 2103-8.
282. Fevr, T., et al., *Wnt/beta-catenin is essential for intestinal homeostasis and maintenance of intestinal stem cells.* Mol Cell Biol, 2007. 27(21): p. 7551-9.
283. Sato, T., et al., *Paneth cells constitute the niche for Lgr5 stem cells in intestinal crypts.* Nature, 2010.
284. Madison, B.B., et al., *Cis elements of the villin gene control expression in restricted domains of the vertical (crypt) and horizontal (duodenum, cecum) axes of the intestine.* J Biol Chem, 2002. 277(36): p. 33275-83.
285. VanDussen, K.L. and L.C. Samuelson, *Mouse atonal homolog 1 directs intestinal progenitors to secretory cell rather than absorptive cell fate.* Dev Biol, 2010. 346(2): p. 215-23.
286. Lepourcelet, M., et al., *Small-molecule antagonists of the oncogenic Tcf/beta-catenin protein complex.* Cancer Cell, 2004. 5(1): p. 91-102.
287. Jensen, J., et al., *Control of endodermal endocrine development by Hes-1.* Nat Genet, 2000. 24(1): p. 36-44.
288. Schroder, N. and A. Gossler, *Expression of Notch pathway components in fetal and adult mouse small intestine.* Gene Expr Patterns, 2002. 2(3-4): p. 247-50.
289. Hampel, H. and P. Peltomaki, *Hereditary colorectal cancer: risk assessment and management.* Clin Genet, 2000. 58(2): p. 89-97.
290. Lal, G. and S. Gallinger, *Familial adenomatous polyposis.* Semin Surg Oncol, 2000. 18(4): p. 314-23.
291. van Es, J.H. and H. Clevers, *Notch and Wnt inhibitors as potential new drugs for intestinal neoplastic disease.* Trends Mol Med, 2005. 11(11): p. 496-502.
292. Hicks, C., et al., *Fringe differentially modulates Jagged1 and Delta1 signalling through Notch1 and Notch2.* Nat Cell Biol, 2000. 2(8): p. 515-20.
293. Zeuner, A., et al., *The Notch2-Jagged1 interaction mediates stem cell factor signaling in erythropoiesis.* Cell Death Differ, 2011. 18(2): p. 371-80.
294. Moellering, R.E., et al., *Direct inhibition of the NOTCH transcription factor complex.* Nature, 2009. 462(7270): p. 182-8.
295. Dietrich, W.F., et al., *Genetic identification of Mom-1, a major modifier locus affecting Min-induced intestinal neoplasia in the mouse.* Cell, 1993. 75(4): p. 631-9.

296. MacPhee, M., et al., *The secretory phospholipase A2 gene is a candidate for the Mom1 locus, a major modifier of ApcMin-induced intestinal neoplasia.* Cell, 1995. 81(6): p. 957-66.
297. Silverman, K.A., et al., *Identification of the modifier of Min 2 (Mom2) locus, a new mutation that influences Apc-induced intestinal neoplasia.* Genome Res, 2002. 12(1): p. 88-97.
298. Haines, J., et al., *Genetic basis of variation in adenoma multiplicity in ApcMin/+ Mom1S mice.* Proc Natl Acad Sci U S A, 2005. 102(8): p. 2868-73.
299. Corpet, D.E. and F. Pierre, *Point: From animal models to prevention of colon cancer. Systematic review of chemoprevention in min mice and choice of the model system.* Cancer Epidemiol Biomarkers Prev, 2003. 12(5): p. 391-400.
300. Corpet, D.E. and F. Pierre, *How good are rodent models of carcinogenesis in predicting efficacy in humans? A systematic review and meta-analysis of colon chemoprevention in rats, mice and men.* Eur J Cancer, 2005. 41(13): p. 1911-22.
301. Reichling, T., et al., *Transcriptional profiles of intestinal tumors in Apc(Min) mice are unique from those of embryonic intestine and identify novel gene targets dysregulated in human colorectal tumors.* Cancer Res, 2005. 65(1): p. 166-76.
302. Fodde, R., et al., *A targeted chain-termination mutation in the mouse Apc gene results in multiple intestinal tumors.* Proc Natl Acad Sci U S A, 1994. 91(19): p. 8969-73.
303. Oshima, M., et al., *Effects of docosahexaenoic acid (DHA) on intestinal polyp development in Apc delta 716 knockout mice.* Carcinogenesis, 1995. 16(11): p. 2605-7.
304. Aoki, K., et al., *Colonic polyposis caused by mTOR-mediated chromosomal instability in Apc+/Delta716 Cdx2+/- compound mutant mice.* Nat Genet, 2003. 35(4): p. 323-30.
305. Reed, K.R., et al., *PPARdelta status and Apc-mediated tumourigenesis in the mouse intestine.* Oncogene, 2004. 23(55): p. 8992-6.
306. Velcich, A., et al., *Colorectal cancer in mice genetically deficient in the mucin Muc2.* Science, 2002. 295(5560): p. 1726-9.
307. Malliri, A., et al., *The rac activator Tiam1 is a Wnt-responsive gene that modifies intestinal tumor development.* J Biol Chem, 2006. 281(1): p. 543-8.
308. Romagnolo, B., et al., *Intestinal dysplasia and adenoma in transgenic mice after overexpression of an activated beta-catenin.* Cancer Res, 1999. 59(16): p. 3875-9.
309. Schmidt, E.E., et al., *Illegitimate Cre-dependent chromosome rearrangements in transgenic mouse spermatids.* Proc Natl Acad Sci U S A, 2000. 97(25): p. 13702-7.
310. Thyagarajan, B., et al., *Mammalian genomes contain active recombinase recognition sites.* Gene, 2000. 244(1-2): p. 47-54.
311. Semprini, S., et al., *Cryptic loxP sites in mammalian genomes: genome-wide distribution and relevance for the efficiency of BAC/PAC recombineering techniques.* Nucleic Acids Res, 2007. 35(5): p. 1402-10.
312. Pfeifer, A., et al., *Delivery of the Cre recombinase by a self-deleting lentiviral vector: efficient gene targeting in vivo.* Proc Natl Acad Sci U S A, 2001. 98(20): p. 11450-5.
313. Silver, D.P. and D.M. Livingston, *Self-excising retroviral vectors encoding the Cre recombinase overcome Cre-mediated cellular toxicity.* Mol Cell, 2001. 8(1): p. 233-43.
314. de Alboran, I.M., et al., *Analysis of C-MYC function in normal cells via conditional gene-targeted mutation.* Immunity, 2001. 14(1): p. 45-55.
315. Loonstra, A., et al., *Growth inhibition and DNA damage induced by Cre recombinase in mammalian cells.* Proc Natl Acad Sci U S A, 2001. 98(16): p. 9209-14.
316. Baba, Y., et al., *Practical range of effective dose for Cre recombinase-expressing recombinant adenovirus without cell toxicity in mammalian cells.* Microbiol Immunol, 2005. 49(6): p. 559-70.

PUBLISHED PAPERS

Jagged1 is the pathological link between Wnt and Notch pathways in colorectal cancer

Verónica Rodilla[a], Alberto Villanueva[b], Antonia Obrador-Hevia[b], Àlex Robert-Moreno[a], Vanessa Fernández-Majada[a], Andrea Grilli[c], Nuria López-Bigas[c], Nicolás Bellora[c], M. Mar Albà[c], Ferran Torres[d], Mireia Duñach[e], Xavier Sanjuan[f], Sara Gonzalez[b], Thomas Gridley[g], Gabriel Capella[b], Anna Bigas[a,1,2], and Lluís Espinosa[a,1,2]

[a]Institut d'Investigació Biomèdica de Bellvitge Gran Via km 2.7, Hospitalet and Institut Municipal d'Investigacions Mèdiques-Hospital del Mar, Dr. Aiguader 88, 08003 Barcelona, Spain; [b]Institut d'Investigació Biomèdica de Bellvitge-Institut Català d'Oncologia Gran Via km 2.7, Hospitalet, 08907 Barcelona, Spain; [c]Fundació Institut Municipal de Investigació Mèdica, Universitat Pompeu Fabra, Institució Catalana de Recerca i Estudis Avançats, Barcelona, Spain; [d]Laboratory of Biostatistics and Epidemiology, Universitat Autonoma de Barcelona, Statistics and Methodology Support Unit, Institut d'Investigacions Biomèdiques August Pi i Sunyer, Hospital Clinic, 08036 Barcelona, Spain; [e]Centre d'Estudis Biofísica i Departmento Bioquímica i Biologia Molecular, Facultat de Medicina, Universitat Autònoma de Barcelona, 08193 Barcelona, Spain; [f]Servei Anatomia Patològica, Hospital Universitari de Bellvitge, Feixa Llarga, Hospitalet, 08907 Barcelona, Spain; and [g]The Jackson Laboratory, Bar Harbor, MA 04609

Edited by Mark T. Groudine, Fred Hutchinson Cancer Research Center, Seattle, WA, and approved February 23, 2009 (received for review December 27, 2008)

Notch has been linked to β-catenin-dependent tumorigenesis; however, the mechanisms leading to Notch activation and the contribution of the Notch pathway to colorectal cancer is not yet understood. By microarray analysis, we have identified a group of genes downstream of Wnt/β-catenin (down-regulated when blocking Wnt/β-catenin) that are directly regulated by Notch (repressed by γ-secretase inhibitors and up-regulated by active Notch1 in the absence of β-catenin signaling). We demonstrate that Notch is downstream of Wnt in colorectal cancer cells through β-catenin-mediated transcriptional activation of the Notch-ligand Jagged1. Consistently, expression of activated Notch1 partially reverts the effects of blocking Wnt/β-catenin pathway in tumors implanted s.c. in nude mice. Crossing *APC*$^{Min/+}$ with *Jagged1*$^{+/\Delta}$ mice is sufficient to significantly reduce the size of the polyps arising in the APC mutant background indicating that Notch is an essential modulator of tumorigenesis induced by nuclear β-catenin. We show that this mechanism is operating in human tumors from Familial Adenomatous Polyposis patients. We conclude that Notch activation, accomplished by β-catenin-mediated up-regulation of Jagged1, is required for tumorigenesis in the intestine. The Notch-specific genetic signature is sufficient to block differentiation and promote vasculogenesis in tumors whereas proliferation depends on both pathways.

beta-catenin | APC | intestine | crosstalk

The Wnt signaling pathway plays a crucial role during development of different tissues and organisms. A multiprotein complex including adenomatosis polyposis coli (APC), axin and Glycogen Synthase Kinase-3β (GSK3β) is responsible for regulating β-catenin (ctnnb1) protein levels. Activation of canonical Wnt signaling results in GSK3β inhibition, stabilization and nuclear accumulation of β-catenin and subsequent activation of lymphoid enhancer factor/T cell factor (LEF1/TCF) target genes (1).

Constitutive activation of Wnt is one of the best-characterized events in several types of cancer (2). Familial Adenomatous Polyposis (FAP), a disease characterized by the presence of hundreds of colorectal polyps, is usually associated with APC germ-line mutations. Colorectal cancer (CRC) develops upon mutational damage or loss of the wild-type allele resulting in further increased β-catenin/TCF activity (3, 4). Similarly, mice carrying germ-line mutations in APC, *APC*^{Min} (Multiple intestinal neoplasia), are predisposed to the formation of intestinal adenomas (5, 6). Canonical Wnt target genes such as c-myc, *cyclinD1*, *MMP7*, *TCF1*, and *EphB2* but also the Notch-target gene *hes1* have an increased expression in the tumors of these mice (7–9). Overexpression of *hes1* and other Notch targets has been associated with sporadic colorectal tumors (10), human medulloblastomas (11), melanomas (12), meningiomas (13), and T cell leukemias (14, 15).

Notch is a family of transmembrane receptors that plays important roles in regulating cell fate decisions. After ligand binding, Notch protein undergoes a proteolytic cleavage dependent on γ-secretase activity that releases the active intracellular domain, Notch-IC (16, 17). Once activated, Notch translocates into the nucleus to bind RBPjκ and to activate specific gene transcription (for review, see ref. 18). Different Notch receptors with specific functions have been identified but, interestingly, they all trigger the activation of the same downstream cascade. In the intestine, Notch signaling is required for the maintenance of the proliferative compartment (8, 19) and a recent report shows that both Notch1 and 2 participate in the regulation of intestinal cell differentiation (20). Different Notch ligands (Jagged1, 2 and Delta 1–4) can also confer specificity to the Notch receptors (21, 22); however, distinct functions for each ligand remain unknown on many tissues.

The cross-talk between Wnt and Notch pathways including genetic interactions in *Drosophila* (23–25), the physical binding of Notch to β-catenin (26) or their association to common cofactors (27) have been described. In mammalian cells, GSK3β directly phosphorylates the Notch protein thus modulating its transcriptional activity (28). Moreover, β-catenin activates Jagged1 transcription thus leading to Notch activation during murine hair follicle differentiation (29). Conversely, in different types of tumor cells, Notch activates the Wnt pathway stabilizing β-catenin by unknown mechanisms (12) or by transcriptional activation of slug (30).

In APC mutant mice that generate multiple intestinal tumors because of β-catenin activation, treatment with a γ-secretase/Notch inhibitor promotes differentiation of the adenoma cells into goblet cells, similar to the effect of Notch signaling deficiency in the intestine (8). How Notch is activated in β-catenin-dependent tumors and what is the contribution of the Notch pathway to Wnt-dependent intestinal tumorigenesis is largely unknown.

We have now demonstrated that β-catenin/TCF is responsible for activating Notch in CRC cells through direct regulation of Jagged1 expression. By microarray screening of colorectal cancer cells, we have identified several genes downstream of TCF/β-catenin pathway that are directly regulated by the Jagged1/Notch pathway including *hes1*, *CD44*, *KLF5*, *NOX1*, *EpHB3*, and *SOX9*.

Author contributions: A.B. and L.E. designed research; V.R., A.V., A.O.-H., A.R.-M., V.F.-M., M.D., and L.E. performed research; M.D., X.S., S.G., T.G., and G.C. contributed new reagents/analytic tools; V.R., A.G., N.L.-B., N.B., M.M.A., F.T., A.B., and L.E. analyzed data; and V.R., A.B., and L.E. wrote the paper.

The authors declare no conflict of interest.

This article is a PNAS Direct Submission.

[1]A.B. and L.E. contributed equally to this work.

[2]To whom correspondence may be addressed. E-mail: abigas@imim.es or lespinosa@imim.es.

This article contains supporting information online at www.pnas.org/cgi/content/full/0813221106/DCSupplemental.

MEDICAL SCIENCES

Consequent with a crucial role for Notch in the tumorigenesis induced by β-catenin, N1IC reverts the growth arrest imposed by dnTCF4 expression in Ls174T cells whereas deletion of a single Jagged1 allele reduces the size of tumors arising in the intestine of $APC^{Min/+}$ mice. Finally, we show correlative evidence that this mechanism operates in human adenomas of APC-associated FAP patients.

Results

Inhibiting Notch or Wnt Pathways Results in the Down-Regulation of a Common Genetic Program in Ls174T Cells. To determine the contribution of the Notch pathway to β-catenin/TCF-dependent tumorigenesis, we first compared the transcriptional effects of blocking Wnt, Notch or both pathways in the Ls174T CRC cells that contain active Notch1 (see Fig. S1*a*) and nuclear β-catenin (9). We took advantage of a published cell line carrying a doxycycline-inducible plasmid encoding a dominant negative TCF4 that does not bind β-catenin (Ls174T/dnTCF4) (9). We performed microarray analysis comparing Ls174T/dnTCF4 cells untreated, treated for 48 h with doxycycline and/or with the Notch/γ-secretase inhibitor DAPT (31), using a whole human genome oligonucleotide microarray from Agilent (G4112A). We identified 366 genes that were simultaneously down-regulated (>1.3-fold) in response to doxycycline and/or DAPT treatments (Table S1 and Fig. 1*A*) corresponding to 34% of the genes down-regulated by doxycycline. Some of the genes in this group have been associated with cancer such as *CD44*, *hes1*, *EpHB3*, *SOX9*, *NOX1*, or *KLF5* in different systems (32–40) and a number of them had been identified as β-catenin/TCF targets (9). We designed specific primers (Table S2) for some of these genes to confirm the microarray data by qRT-PCR, including the use of two different γ-secretase inhibitors, DAPT and L685,458 (Fig. S1 *b* and *c*). In addition, blocking Notch and/or Wnt pathways, resulted in an increase in the expression levels of several differentiation markers such as villin2, muc20 or TFF1 (Fig. 1*A*).

Many of the TCF4-dependent genes identified in our screening were also inhibited by the γ-secretase treatment, suggesting that at least two different mechanistical explanations: (*i*) Notch is downstream of β-catenin/TCF signaling or (*ii*) both β-catenin and Notch are required to properly activate a specific gene signature in CRC cells. To test this, we first studied the transcriptional signature of cells expressing dnTCF4 with or without the constitutively active N1IC [control (C) versus N1IC (N) clones, see Fig. S1*d*]. We found that N1IC expression is sufficient to reactivate 31% of the genes identified as common Wnt-Notch-dependent genes including *hes1*, *SOX9*, *CD44*, *KLF5*, or *NOX1* in a β-catenin/TCF-deficient background (Fig. 1*b*, Fig. S1*d*, and Table S3). Using the Genomatix software, we identified Notch/RBPjκ-binding consensus in the regulatory regions of all of the analyzed genes (*hes1*, *Nox1*, *EpHB3*, *SOX9*, *KLF5*, *CD44*) (Fig. 1*c* and Table S4). By ChIP experiments, we found that Notch1 associated to the promoters of these genes in Ls174T cells (Fig. 1*c* and Fig. S1*e*), but also in other CRC cell lines concomitant with increased transcriptional activity (Fig. S1*f*). Moreover, we found that DAPT treatment reduces the recruitment of Notch to these promoters (Fig. S1*e*). As expected, several genes involved in intestinal differentiation, such as FABP1 and FABP5, were down-regulated in N1IC-expressing clones (Fig. 1*B*) indicating the effects of Notch in inhibiting differentiation in these cells.

We next studied whether the Wnt-Notch-dependent genes were overrepresented in any specific functional category. Our analysis revealed that these genes were highly enriched into functional categories related to proliferation, differentiation and DNA and RNA metabolism, including transcription and replication. Interestingly, the putative direct targets of Notch downstream of β-catenin (those that are reexpressed in the N1IC clones) are specifically enriched for cell cycle arrest and differentiation categories (Fig. S1*g*).

Together, these results strongly suggest that Notch is a direct regulator of specific gene transcription downstream of β-catenin/TCF nevertheless most of the identified Wnt-Notch-dependent genes likely require the cooperative effects of Notch and β-catenin pathways.

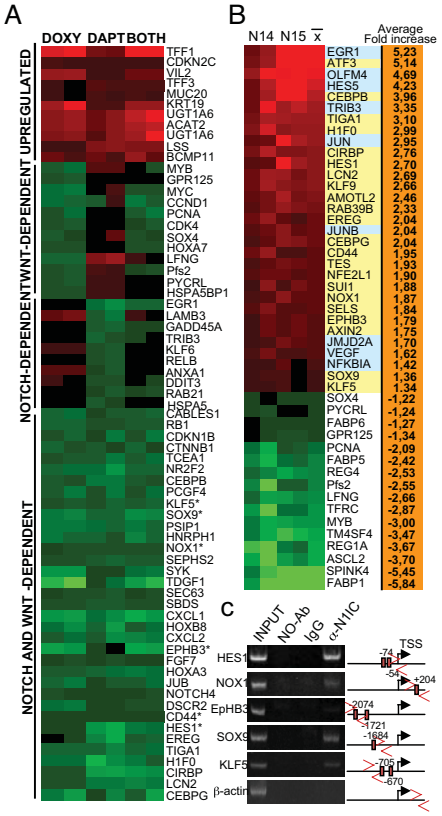

Fig. 1. Inhibition of Wnt and Notch leads to down-regulation of a common gene program. (*A*) Gene expression profile from Ls174T/dnTCF4 cells treated for 48 h with doxycyline (to inhibit Wnt signaling) or DAPT (Notch inhibitor) or both compared with untreated cells. Some top significant genes ranked by Student's *t* test are shown for each group. ⋆, genes further studied in this work. (*B*) Microarray analysis of 2 doxycycline-treated Ls174T/dnTCF4/N1IC clones (N14, N15) compared with doxycycline-treated Ls174T/dnTCF4. Color codes represent only-Notch targets (blue) and the Notch-targets downstream of Wnt (yellow). (*C*) ChIP experiment in Ls174T cells and PCR of the indicated promoters. Scheme of the 2-kb proximal promoter showing the position of the primers used, the RBP-binding sites and TSS.

Activated Notch1 Blocks Differentiation and Promotes Vasculogenesis in Vivo in the Absence of β-Catenin/TCF Signaling. We next studied whether N1IC conferred any malignant capacity to Ls174T cells in the absence of β-catenin/TCF signaling. We found that doxycycline-treated Ls174T/dnTCF4/N1IC clones displayed an increased clonogenic capacity in soft agar cultures compared with Ls174T/dnTCF4 clones (Fig. S2*a*), together with a blockage in goblet-cell differentiation (Fig. S2*b*). In contrast, N1IC expression did not revert the antiproliferative effects of dnTCF4 as indicate the cell cycle profiles (Fig. S2*c*). To test the tumorigenic capacity of these cells in vivo, we injected 1.5×10^6 cells from different control Ls174T/dnTCF4 (C1, C5) or Ls174T/dnTCF4/N1IC (N14, N15, N17, N18) s.c. in nude mice and treated or not the animals with doxycycline for 4 weeks. We found that N1IC expressing clones (Ls174T/dnTCF4/N1IC) generated tumors that were significantly

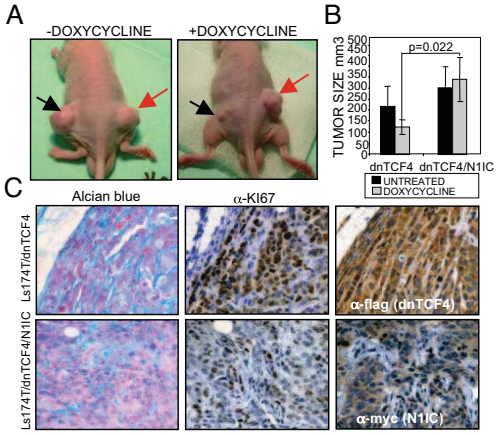

Fig. 2. Notch1 restores tumor growth in the absence of β-catenin/TCF signaling. (*A* and *B*) A total of 1.5 × 10^6 cells were implanted s.c. in nude mice [Ls174T/dnTCF4 (black arrow) and Ls174T/dnTCF4/N1IC (red arrow) clones] untreated or treated with doxycycline for 4 weeks (2 independent experiments, $n = 20$ mice each). Representative animals for each group (*A*) and average and SEM of the tumor volume (in cubic millimeters) (*B*) are shown. *P* values are based on a nonparametric ANOVA applying a rank transformation on the dependent variable. (*C*) Alcian blue staining and IHC with α-Ki67 in serial sections of representative tumors. α-flag or α-myc staining shows the expression of dnTCF4 and N1IC (400×).

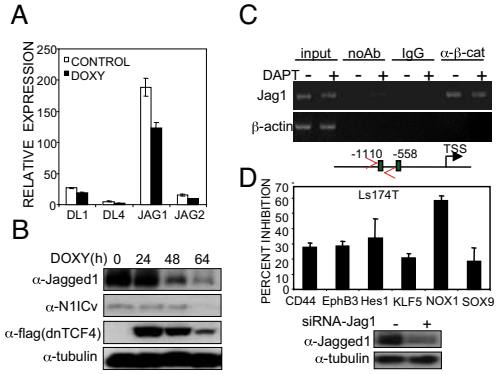

Fig. 3. Notch is downstream of Wnt/β-catenin through activation of Jagged1. (*A*) qRT-PCR of different Notch ligands in Ls174T/dnTCF4 cells untreated or treated for 48 h with doxycycline. (*B*) Western blot with the indicated antibodies of Ls174T/dnTCF4 cells treated with doxycycline for the indicated times. Tubulin is shown as loading control. (*C*) Recruitment of β-catenin to Jagged1 promoter in Ls174T cell line untreated or treated with DAPT. β-actin gene is shown as a control. (*D*) Percent transcriptional inhibition in Ls174T cells transfected with siRNA-Jag1 compared with scramble siRNA as determined by qRT-PCR. Down-regulation of Jagged1 by siRNA was determined by Western blot analysis (*Lower*).

larger compared with the doxycycline-treated control group ($P = 0.022$) (Fig. 2 *A* and *B*) although we did not detect significant differences in the proliferation ratio in the growing areas as measured by Ki67 staining (Fig. 2*C*). However, we observed that tumors expressing N1IC showed a strong reduction of Alcian blue staining indicating a blockage in mucosecreting cell differentiation (Fig. 2*C*) together with an increase in the proportion of growing areas within the tumor concomitant with the presence of vascularization as detected by α-SMA staining (11/11 in N1IC tumors versus 3/10 in control tumors). This is in contrast with the extensive necrotic areas observed in most of the control tumors (7/10) (Fig. S2*d*). Importantly, we detected high levels of endogenous Notch activity in the untreated Ls174T/dnTCF4 tumors as detected by a specific antibody recognizing cleaved Notch1 (N1ICv antibody) that was greatly inhibited after doxycycline treatment (Fig. S3*g*).

Together, these results indicate that activated Notch1 exert a direct effect in regulating goblet-cell differentiation and tumor vasculogenesis whereas regulation of cell proliferation requires the contribution of β-catenin/TCF signaling pathway.

Notch Is Downstream of Wnt Through Transcriptional Activation of Jagged1 by β-Catenin/TCF. To determine whether β-catenin/TCF is responsible for the high Notch activity that is found in CRC cells (Figs. S1*a* and S3*d*), we searched in the microarray data for the presence of Notch ligands and found that Jagged1 and Delta-like1 were down-regulated 1.3-fold after doxycycline treatment in Ls174T cells (Table S1). Using qRT-PCR, we confirmed that jagged1 is highly expressed in Ls174T/dnTCF4 and its mRNA levels decreased after doxycycline treatment (Fig. 3*A*). Most important, expression of dnTCF4 or inhibition of β-catenin with PKF115–584 (41) results in a huge reduction in the protein levels of Jagged1 concomitant with a decrease in the amount of activated Notch1 (Fig. 3*B* and Fig. S3*b*), similarly to that found in s.c. tumors (Fig. S3*g*). Of note, the disappearance of Jagged1 was delayed with respect to dnTCF4 expression likely because of the extended half-life of Jagged1 protein (24 h) (Fig. S3*a*).

By sequence analysis, we identified 2 TCF-binding consensus in the human Jagged1 promoter and showed the recruitment of β-catenin by ChIP experiments in Ls174T (Fig. 3*C* and Fig. S3*c*). We next asked whether β-catenin regulates Jagged1 and Notch activation in other CRC cell lines. We found that Jagged1 transcription was highly increased in cells carrying nuclear β-catenin, such as HCT116, SW480, and Ls174T, compared with the non-transformed HS27 control cells (Fig. S3*d*) and β-catenin was recruited to the Jagged1 promoter to a different extent, in all these cancer cell lines (Fig. S3*e*). Moreover, stabilization of β-catenin in a nontumorigenic cell line (NIH 3T3) by a 16-h treatment with the GSK3β inhibitor LiCl (30 mM) was sufficient to increase both mRNA and protein levels of Jagged1 (Fig. S3*f*). By cell fractionation followed by Western blot analysis, we detected activated Notch1 and Notch2 (cleaved Notch2 fragment of 110 kDa) in the nuclear fraction of CRC cell lines with high Jagged1 levels (Fig. S3*d*).

To demonstrate that Jagged1 was responsible for regulating Notch-targets downstream of β-catenin, we treated Ls174T cells with specific siRNA against Jagged1 and found that all of the selected genes were down-regulated (from 20 to 60% inhibition) compared with cells treated with scrambled siRNA (Fig. 3*D*). In addition, ectopic expression of Jagged1 is sufficient to block differentiation in ≈85% of the transfected Ls174T/dnTCF4 cells when Wnt/β-catenin signaling is switched off, similar to N1IC expression in these conditions (Fig. S3*h*).

Deletion of a Single Jagged1 Allele Reduces Tumor Growth in the $APC^{Min/+}$ Intestine. To investigate whether the expression of Jagged1 is altered by the activation of the Wnt pathway in vivo, we determined the levels of this protein in intestinal tumors arising in the $APC^{Min/+}$ mice compared with normal mucosa. By IHC, we found a strong overexpression of Jagged1 in the tumor tissue of these animals compared with the normal crypts that was concomitant with Notch1 and Notch2 activation (Fig. 4*A*).

To test the importance of Jagged1-dependent activation of Notch downstream of β-catenin, we crossed the $APC^{Min/+}$ mice with the Jagged1 hemizygous ($Jag1^{+/\Delta}$) mice, which are phenotypically normal (whereas $Jag1^{\Delta/\Delta}$ are lethal) (42). A total of 23 animals of the different genotypes were killed at 4 months of age and analyzed for the presence of macroscopic intestinal tumors. We found that

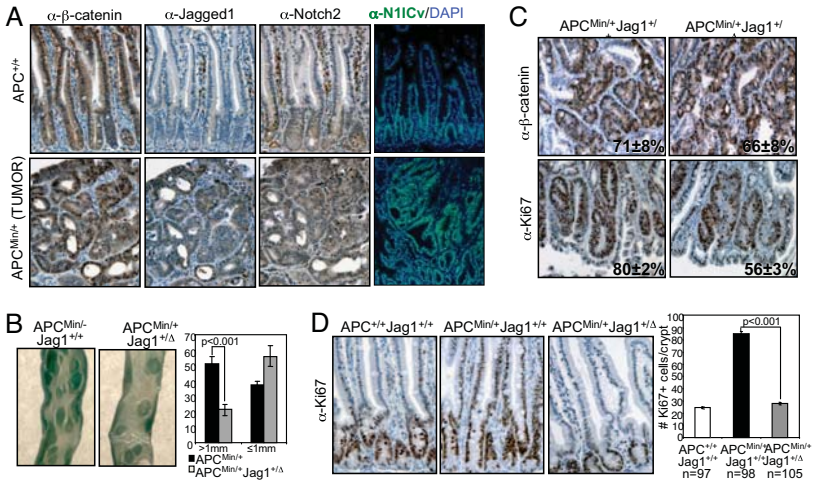

Fig. 4. Jagged1 is essential in $APC^{Min/+}$ intestinal tumorigenesis. (*A*) IHC of serial section of wild type intestine and $APC^{Min/+}$ tumor stained with the indicated antibodies (100×). (*B*) Stereoscopical image of the methylene blue staining. The average number of visible polyps in the small intestines (>1 mm or ≤1 mm) from the different genotypes at 16 weeks of age is represented. Error bars are SEM. *P* values are based on a Mann–Whitney *U* test. (*C*) (*Upper*) Immunostaining with α-β-catenin of representative tumors from different genotypes. The average percentage of cells showing nuclear β-catenin is indicated. (*Lower*) Representative images of α-Ki67 staining and average percentage and SEM of Ki67+ cells per tumor from 5 $APC^{Min/+}Jag1^{+/+}$ ($n = 51$) and 4 $APC^{Min/+}Jag1^{+/\Delta}$ ($n = 27$). (*D*) Sections of normal crypts from different genotypes stained with α-Ki67 antibody (*Left*). The average and SEM of $Ki67^+$ cells per crypt from 10 $APC^{+/+Jag1+/+}$, 5 $APC^{Min/+}Jag1^{+/+}$ and 4 $APC^{Min/+}Jag1^{+/\Delta}$ is represented (*Right*). *n*, number of crypts counted. *P* values are based on a Mann–Whitney *U* test.

deletion of one Jagged1 allele is sufficient to significantly reduce the size of tumors in the APC mutant background ($P = 0.0001$) (Fig. 4*B*) concomitant with a reduction in the amount of active Notch1 (Fig. S4), whereas the nuclear levels of β-catenin in the tumors from the different genotypes were equivalent (Fig. 4*C Upper*). This result suggests that Jagged1 deficiency confers a growing disadvantage to β-catenin-dependent tumors. In agreement with this, we found a reduction in the number of Ki67 positive cells in the tumors of the $APC^{Min/+}Jag1^{+/\Delta}$ double mutants compared with the ones from the $APC^{Min/+}$ littermates (from 80.4 ± 2% to 55.6 ± 3%, $P < 0.001$) (Fig. 4*C Lower*), whereas no differences were found in the number of apoptotic cells as measured by TUNEL assay or in the number of infiltrating lymphocytes in the tumors (Fig. S4). Moreover, the expansion of the proliferative compartment in the morphologically normal crypts of APC mutant mice described in ref. 43, is reverted in the $APC^{Min/+}Jag1^{+/\Delta}$ mice ($P < 0.001$) (Fig. 4*D*). These results demonstrate that activation of Notch by Jagged1 confers a proliferative advantage to the tumors with APC mutations.

High Levels of Jagged1 Correlate with Activated Notch1 and Notch2 in Human Colorectal Tumors Containing Nuclear β-Catenin. We next investigated whether this mechanism for Notch activation was relevant in human colorectal adenomas arising in Familial Adenomatous Polyposis (FAP) patients harboring APC germ line mutations. By qRT-PCR we found that Jagged1 mRNA levels were significantly increased in most FAP adenomas compared with normal intestinal tissue ($P = 0.05$). Interestingly, some increase in Jagged1 expression was also detected in the normal colonic mucosa of FAP patients, compared with normal controls (Fig. 5*A*). By IHC, we found high levels of the Jagged1 protein confined in the tumor areas containing nuclear β-catenin staining ($n = 6$) that were not detected in the normal adjacent tissue (Fig. 5*B* and Fig. S5*a*). This was concomitant with the presence of nuclear Notch2 (Fig. 5*B* and Fig. S5*a*) and active Notch1 (Fig. 5*C* and Fig. S5*a*). Further demonstrating the importance of Notch transcriptional activity in human tumors carrying active β-catenin, we found increased expression of *CD44* ($P = 0.0002$), *SOX9* ($P = 0.005$), *NOX1* ($P = 0.002$), *KLF5* ($P = 0.01$) and *hes1* (not significant) (Fig. 5*D*), identified in our microarray screening as Wnt-dependent Notch targets (see Fig. 1), in the adenoma samples from FAP patients. Some of these genes were also up-regulated in the normal colonic mucosa from these patients compared with the normal controls (Fig. 5*D*) likely because of the presence of 1 mutated APC allele (Fig. S5*b*). These results indicate that Notch, downstream of Jagged1, acts as an essential mediator of β-catenin-dependent intestinal tumorigenesis (i.e., FAP) and is responsible for regulating a specific transcriptional cancer signature.

Discussion

Previous work has shown that inactivating mutations of the Wnt/β-catenin pathway eliminate the stem/proliferative compartment of intestinal cells (44). Similarly inactivation of the Notch pathway leads to an exhaustion of the stem cell compartment concomitant with increased goblet cell differentiation (8, 19). Here, we define the mechanism that mediates the cross-talk between Notch and Wnt pathways in CRC and determine its functional relevance. In these tumors, the Notch ligand Jagged1 is directly regulated by β-catenin, thus leading to aberrant activation of Notch1 and 2. We identified a total of 366 genes that are simultaneously regulated by both Notch and Wnt in Ls174T CRC cells and 31% are reactivated by active N1IC in the presence of dnTCF4, indicating that are directly dependent on Notch. This group of genes was sufficient to revert some of the anti-tumorigenic effects of dnTCF4 both in vitro and in vivo, because N1IC expression inhibits differentiation and promotes vasculogenesis in the absence of Wnt/β-catenin. However, N1IC is not able to regulate proliferation in these conditions, similar to that observed by Fre et al. (52). As expected, one of the genes identified as direct Notch target in our arrays is hes1. Hes1 regulates intestinal differentiation (45) by inhibiting math1 thus favouring enterocytic differentiation (46). It is overexpressed in CRC (10) and in tumors arising in APC mutant mice (8). However, and in contrast to the effects of N1IC, we found that hes1 was not sufficient to induce tumor growth in vivo in the absence of β-catenin/TCF activity indicating that other Notch-targets down-

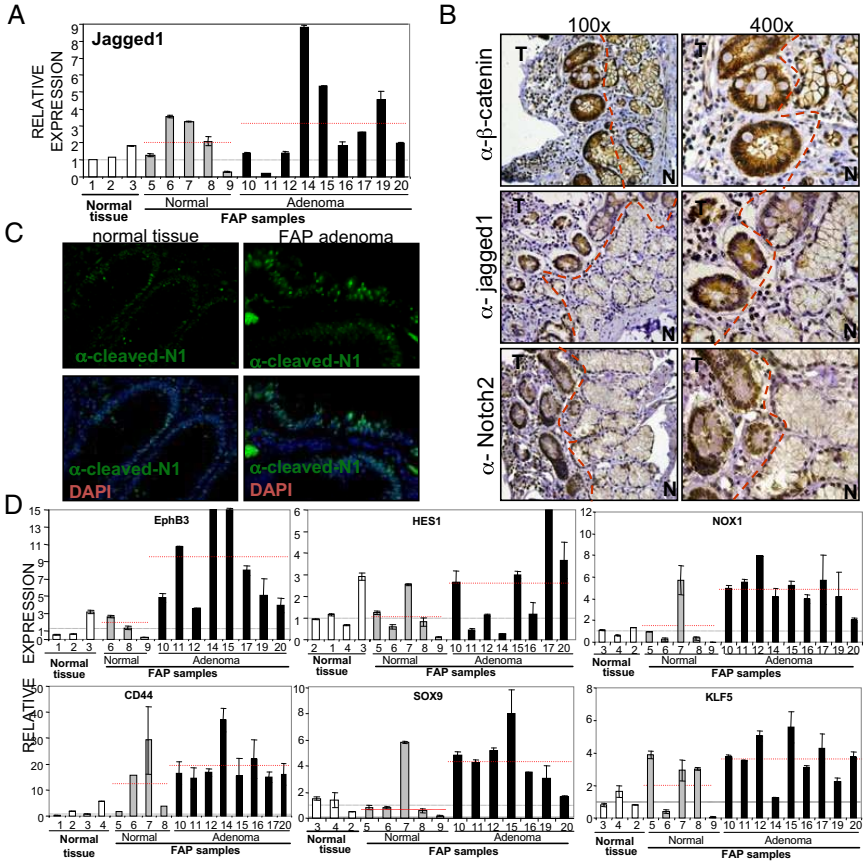

Fig. 5. Notch1 and Notch2 are activated in colorectal tumors. (*A*) Levels of Jagged1 mRNA as measured by qRT-PCR. The red line indicates the average value for each group. (*B*) Serial sections of colorectal adenoma from a FAP patient stained with the indicated antibodies. Dashed lines indicate the boundary between the normal adjacent (N) and the tumor (T) tissue. Hematoxylin (blue) was used for nuclear staining. (*C*) Immunoflouresence with α-N1ICv (green) of normal or adenoma tissue from FAP sample. Nuclei were stained with DAPI (blue) (600×). (*D*) qRT-PCR to determine the levels of the indicated genes in normal tissue compared with FAP samples. The red line indicates the average value for each group. Statistical significance of the differences between the adenoma and normal samples are calculated based on 2-sided Student's *t* test. *P* values are: *EphB3*, $P = 0.014$; *CD44*, $P = 0.0002$; *SOX9*, $P = 0.005$; NOX1, $P = 0.002$; KLF5, $P = 0.01$; and *hes1*, not significant.

stream of β-catenin participate in regulating colorectal tumorigenesis. Consistently, several of the identified Notch-target genes in our screening have been involved in different aspects of intestinal differentiation or cancer including SOX9 (38, 39) KLF5 (47), CD44 (32), or NOX1 (48).

Mutations in the APC gene have been found in most sporadic colorectal tumors and in those arising in FAP patients. We have found that Jagged1 is up-regulated in the tumors but also, in a lesser extent, in the normal adjacent tissue of FAP patients suggesting that inactivation of 1 APC allele could be sufficient to increase Notch activity. In this sense, others and we have observed that Ki67-positive cells are aberrantly distributed throughout the intestinal glands in *APC* mutant mice, a phenotype that is abolished in the $Jag1^{\Delta/+}APC^{Min/+}$ mice. This indicates that Notch is involved in the crypt/villus compartmentalization. Most important, tumor growth is reduced in $Jag1^{\Delta/+}APC^{Min/+}$ mice indicating that partial inhibition of Notch in an active β-catenin background may be therapeutically relevant for FAP patients.

Because we identified 3 different genetic signatures associated with CRC cells that depend on Notch, β-catenin or both pathways that are likely complementary for tumor development, we propose that using of a combination of Notch and β-catenin inhibitors will enhance the antitumoral effects of the individual drugs. However, this strategy needs to be tested.

In summary, our results provide an explanation for the contribution of Notch to β-catenin-dependent tumorigenesis and the mechanism for Notch activation through Jagged1. Specific inhibitors for Jagged1-mediated Notch activation [i.e., inhibitors of glycosil-transferases that modulate Notch/Notch-ligand interaction (21)] would be a new promising strategy for CRC therapy.

Materials and Methods

Animals. $APC^{Min/+}$ mice (Jackson Laboratories) were from homogenous outbred C57BL/6J background. Jagged1 mutant mice ($Jag1^{\Delta/+}$) are described in ref. 42. $Jag1^{\Delta/+}$ were backcrossed into C57BL6/J background ($n > 4$) and crossed with $APC^{Min/+}$. In our experiments, cohorts of age-matched $APC^{Min/+}Jag1^{+/\Delta}$ were compared with $APC^{Min/+}Jag^{+/+}$ and $APC^{+/+}Jag^{+/+}$. All mice were genotyped by PCR. Animals were kept under pathogen-free conditions and all procedures were approved by the Animal Care Committee.

Cell Lines and Reagents. NIH 3T3, HS27, HCT116, SW480, DLD1, and Ls174T/dnTCF4 [kindly provided by H. Clevers (Hubrecht Laboratories, Utrecht, Netherlands)]. SB216763 (Sigma) was used at 10 μM/mL. Doxycycline (Sigma) was used

at 1 μg/mL. DAPT and L685,458, γ-secretase inhibitors, were obtained from Calbiochem, PKF115–584 (41) was a gift from Novartis. Ls174T/dnTCF4 cells were transfected with Notch1IC-pCDNA3/TO using PPEI (Polysciences). Cells were selected with 1 mg/mL G418, 5 μg/mL Blasticidin, and 100 μg/mL Zeocin.

Antibodies. α-cleaved Notch1 (N1ICv) (Cell Signaling), α-Notch2 (49), α-Jagged1 (sc-6011), α-α-tubulin and α-β-catenin (C2206) from Sigma. Secondary antibodies conjugated to Horse Radish Peroxidase (HRP) were from DAKO (with AlexaFluor488 (A-11055) and 546 (A-11056) from Molecular Probes (Invitrogen) and Cy3-coupled tyramide from PerkinElmer.

Immunofluorescence. Cells were fixed in 3% paraformaldehyde, permeabilized in 0.3% Triton X-100 (Pierce). Primary antibodies were incubated overnight and secondary antibodies for 90 min. Slides were mounted in Vectashield plus DAPI (Vector) and visualized in an Olympus BX-60 or BX-61 microscope. Protocol for cleaved-Notch1 detection is described in ref. 50. For immunohistochemistry (IHC), secondary antibodies were developed with the DAB peroxidase substrate kit (Dako Cytomation).

RT-PCR. Total RNA was extracted with Qiagen kit, and RT-First Strand cDNA Synthesis kit (Amersham Pharmacia Biotech) was used. The primers used for RT-PCR analysis are listed in Table S2. qRT-PCR was performed in LightCycler480 system using SYBR Green I Master kit (Roche).

Chromatin Immunoprecipitation. ChIP assay are described in ref. 51. Briefly, Chromatin from cross-linked cells was sonicated, incubated overnight with the indicated antibodies in RIPA buffer and precipitated with protein G/A–Sepharose. Cross-linkage of the coprecipitated DNA-protein complexes was reversed, and DNA was used as a template for the PCR. α-cleaved Notch1 (ab8925; Abcam), and α-β-catenin (BD Bioscience; catalog no. 61054) antibodies were used. The primers used are listed in Table S2.

Human Colorectal Samples. Samples from FAP patients were obtained from the Tumor Bank of ICO-IDIBELL. All patients gave written consent to donate the tumor specimen. The study was approved by the Ethics Committee of our institution.

In Vivo Tumor-Growth Assay. Twenty male *nu/nu* Swiss mice per experiment (Harlam) were housed in a sterile environment. Animals were injected s.c. with 1.5×10^6 Ls174T/dnTCF4 cells in the left leg and 1.5×10^6 Ls174T/dnTCF4/N1IC cells in the right leg. The control group drank 1% sucrose and the treated group 1% sucrose, 2 mg/mL doxycycline in water ad libitum. Tumor volumes were calculated as (length $\times$ width^2)π/6.

Statistical Analysis. SAS version 9.1.3 (SAS Institute Inc.) and SPSS version 12 softwares were used.

ACKNOWLEDGMENTS. We thanks to H. Clevers, A. García de Herreros (Institut Municipal d'Investigaciones Mèdiques, Barcelona, Spain), E. Batlle (Institute for Research in Biomedicine, Barcelona, Spain), and E. Sancho (Institute for Research in Biomedicine, Barcelona, Spain) for reagents; Novartis for PKF115-584; M.E. López for technical assistance; and J. Inglés-Esteve for helpful discussions. This work was supported by an Institut d'Investigació Biomèdica de Bellvitge (V.R.) and Department d'Universitats i Recerca 2005-FI00458 (to V.F.M.) fellowships; Ministerio Educación y Ciencia Grants SAF2004-03198 and SAF2007-60080, Instituto de Salud Carlos III Grant PI041890, Fundació la Marató de TV3 Grant 051730, Fundación Mutua Madrileña; and RTICC Red Temática de Investigación Cooperativa en Cáncer Grant RD06/0020/0098. L.E. is an Investigator of the Carlos III program.

1. Willert K, Nusse R (1998) Beta-catenin: A key mediator of wnt signaling. *Curr Opin Genet Dev* :95–102.
2. Korinek V, et al. (1997) Constitutive transcriptional activation by a beta-catenin-Tcf complex in APC$^{-/-}$ colon carcinoma. *Science* 275:1784–1787.
3. Groden J, et al. (1991) Identification and characterization of the familial adenomatous polyposis coli gene. *Cell* 66:589–600.
4. Nishisho I, et al. (1991) Mutations of chromosome 5q21 genes in FAP and colorectal cancer patients. *Science* 253:665–669.
5. Moser AR, Pitot HC, Dove WF (1990) A dominant mutation that predisposes to multiple intestinal neoplasia in the mouse. *Science* 247:322–324.
6. Su LK, et al. (1992) Multiple intestinal neoplasia caused by a mutation in the murine homolog of the APC gene. *Science* 256:668–670.
7. Batlle E, et al. (2002) Beta-catenin and TCF mediate cell positioning in the intestinal epithelium by controlling the expression of EphB/ephrinB. *Cell* 111:251–263.
8. van Es JH, et al. (2005) Notch/gamma-secretase inhibition turns proliferative cells in intestinal crypts and adenomas into goblet cells. *Nature* 435:959–963.
9. van de Wetering M, et al. (2002) The beta-catenin/TCF-4 complex imposes a crypt progenitor phenotype on colorectal cancer cells. *Cell* 111:241–250.
10. Fernandez-Majada V, et al. (2007) Nuclear IKK activity leads to dysregulated notch-dependent gene expression in colorectal cancer. *Proc Natl Acad Sci USA* 104:276–281.
11. Fan X, et al. (2004) Notch1 and notch2 have opposite effects on embryonal brain tumor growth. *Cancer Res* 64:7787–7793.
12. Balint K, et al. (2005) Activation of Notch1 signaling is required for beta-catenin-mediated human primary melanoma progression. *J Clin Invest* 115:3166–3176.
13. Cuevas IC, et al. (2005) Meningioma transcript profiles reveal deregulated Notch signaling pathway. *Cancer Res* 65:5070–5075.
14. Palomero T, et al. (2006) NOTCH1 directly regulates c-MYC and activates a feed-forward-loop transcriptional network promoting leukemic cell growth. *Proc Natl Acad Sci USA* 103:18261–18266.
15. Weng AP, et al. (2006) c-Myc is an important direct target of Notch1 in T-cell acute lymphoblastic leukemia/lymphoma. *Genes Dev* 20:2096–2109.
16. Schroeter EH, Kisslinger JA, Kopan R (1998) Notch-1 signalling requires ligand-induced proteolytic release of intracellular domain. *Nature* 393:382–386.
17. Mumm JS, et al. (2000) A ligand-induced extracellular cleavage regulates gamma-secretase-like proteolytic activation of Notch1. *Mol Cell* 5:197–206.
18. Lai EC (2004) Notch signaling: Control of cell communication and cell fate. *Development* 131:965–973.
19. Fre S, et al. (2005) Notch signals control the fate of immature progenitor cells in the intestine. *Nature* 435:964–968.
20. Riccio O, et al. (2008) Loss of intestinal crypt progenitor cells owing to inactivation of both Notch1 and Notch2 is accompanied by derepression of CDK inhibitors p27(Kip1) and p57(Kip2). *EMBO Rep* 9:377–383.
21. Hicks C, et al. (2000) Fringe differentially modulates Jagged1 and Delta1 signalling through Notch1 and Notch2. *Nat Cell Biol* 2:515–520.
22. Lindsell CE, Boulter J, diSibio G, Gossler A, Weinmaster G (1996) Expression patterns of Jagged, Delta1, Notch1, Notch2, and Notch3 genes identify ligand-receptor pairs that may function in neural development. *MolCell Neurosci* 8:14–27.
23. Couso JP, Martinez Arias A (1994) Notch is required for wingless signaling in the epidermis of Drosophila. *Cell* 79:259–272.
24. Giraldez AJ, Cohen SM (2003) Wingless and Notch signaling provide cell survival cues and control cell proliferation during wing development. *Development* 130:6533–6543.
25. Axelrod JD, Matsuno K, Artavanis-Tsakonas S, Perrimon N (1996) Interaction between Wingless and Notch signaling pathways mediated by dishevelled. *Science* 271:1826–1832.
26. Hayward P, Balayo T, Martinez Arias A (2006) Notch synergizes with axin to regulate the activity of armadillo in Drosophila. *Dev Dyn* 235:2656–2666.
27. Alves-Guerra MC, Ronchini C, Capobianco AJ (2007) Mastermind-like 1 Is a specific coactivator of beta-catenin transcription activation and is essential for colon carcinoma cell survival. *Cancer Res* 67:8690–8698.
28. Espinosa L, Ingles-Esteve J, Aguilera C, Bigas A (2003) Phosphorylation by glycogen synthase kinase-3 beta down-regulates Notch activity, a link for Notch and Wnt pathways. *J Biol Chem* 278:32227–32235.
29. Estrach S, Ambler CA, Lo Celso C, Hozumi K, Watt FM (2006) Jagged 1 is a beta-catenin target gene required for ectopic hair follicle formation in adult epidermis. *Development* 133:4427–4438.
30. Leong KG, et al. (2007) Jagged1-mediated Notch activation induces epithelial-to-mesenchymal transition through Slug-induced repression of E-cadherin. *J Exp Med* 204:2935–2948.
31. Weinmaster G, Kopan R (2006) A garden of Notch-ly delights. *Development* 133:3277–3282.
32. Dalerba P, et al. (2007) Phenotypic characterization of human colorectal cancer stem cells. *Proc Natl Acad Sci USA* 104:10158–10163.
33. Baba I, et al. (2000) Involvement of deregulated epiregulin expression in tumorigenesis in vivo through activated Ki-Ras signaling pathway in human colon cancer cells. *Cancer Res* 60:6886–6889.
34. Kim JH, et al. (2004) The Bmi-1 oncoprotein is overexpressed in human colorectal cancer and correlates with the reduced p16INK4a/p14ARF proteins. *Cancer Lett* 203:217–224.
35. Pardal R, Molofsky AV, He S, Morrison SJ (2005) Stem cell self-renewal and cancer cell proliferation are regulated by common networks that balance the activation of proto-oncogenes and tumor suppressors. *Cold Spring Harb Symp Quant Biol* 70:177–185.
36. Blache P, et al. (2004) SOX9 is an intestine crypt transcription factor, is regulated by the Wnt pathway, and represses the CDX2 and MUC2 genes. *J Cell Biol* 166:37–47.
37. Batlle E, et al. (2005) EphB receptor activity suppresses colorectal cancer progression. *Nature* 435:1126–1130.
38. Bastide P, et al. (2007) Sox9 regulates cell proliferation and is required for Paneth cell differentiation in the intestinal epithelium. *J Cell Biol* 178:635–648.
39. Mori-Akiyama Y, et al. (2007) SOX9 is required for the differentiation of paneth cells in the intestinal epithelium. *Gastroenterology* 133:539–546.
40. Laurent E, et al. (2008) Nox1 is over-expressed in human colon cancers and correlates with activating mutations in K-Ras. *Int J Cancer* 123:100–107.
41. Lepourcelet M, et al. (2004) Small-molecule antagonists of the oncogenic Tcf/beta-catenin protein complex. *Cancer Cell* 5:91–102.
42. Xue Y, et al. (1999) Embryonic lethality and vascular defects in mice lacking the Notch ligand Jagged1. *Hum Mol Genet* 8:723–730.
43. Sansom OJ, et al. (2007) Myc deletion rescues Apc deficiency in the small intestine. *Nature* 446:676–679.
44. Korinek V, et al. (1998) Depletion of epithelial stem-cell compartments in the small intestine of mice lacking Tcf-4. *Nat Genet* 19:379–383.
45. Suzuki K, et al. (2005) Hes1-deficient mice show precocious differentiation of Paneth cells in the small intestine. *Biochem Biophys Res Commun* 328:348–352.
46. Jensen J, et al. (2000) Control of endodermal endocrine development by Hes-1. *Nat Genet* 24:36–44.
47. Nandan MO, et al. (2008) Kruppel-like factor 5 mediates cellular transformation during oncogenic KRAS-induced intestinal tumorigenesis. *Gastroenterology* 134:120–130.
48. Szanto I, et al. (2005) Expression of NOX1, a superoxide-generating NADPH oxidase, in colon cancer and inflammatory bowel disease. *J Pathol* 207:164–176.
49. Zagouras P, Stifani S, Blaumueller CM, Carcangiu ML, Artavanis Tsakonas S (1995) Alterations in Notch signaling in neoplastic lesions of the human cervix. *Proc Natl Acad Sci USA* 92:6414–6418.
50. Robert-Moreno A, et al. (2008) Impaired embryonic haematopoiesis yet normal arterial development in the absence of the Notch ligand Jagged1. *EMBO J* 27:1886–1895.
51. Aguilera C, Hoya-Arias R, Haegeman G, Espinosa L, Bigas A (2004) Recruitment of IkappaBalpha to the hes1 promoter is associated with transcriptional repression. *Proc Natl Acad Sci USA* 101:16537–16542.
52. Fre S, et al. (February 27, 2009) Notch and Wnt signals cooperatively control cell proliferation and tumorigenesis in the intestine. *Proc Natl Acad Sci USA*, 10.1073/pnas.0900427106.

Supporting Information

Rodilla et al. 10.1073/pnas.0813221106

SI Methods

Colony Formation in Soft Agar. For anchorage-independent growth, 10^4 cells were resuspended in 1.5 mL of growth medium containing 0.4% agarose and plated on 6-cm plates on a solidified bottom layer made of 0.6% agarose in medium. 50 μL of growth medium was added daily. Colonies were counted after 20 days and imaged at 100x magnification. Each experiment was performed in duplicates.

Cell Fractionation. Nuclei were isolated in 0.1% Nonidet P-40/PBS for 5min on ice, followed by centrifugation at 720*g*, washed twice with PBS and lysed for 30min in 50 mM Tris·HCl (pH7.5), 150 mM NaCl, 1% Nonidet P-40, 5 mM EGTA, 5 mM EDTA, 20 mM NaF, and complete protease inhibitor mixture (Roche). The supernatant was the cytoplasmic fraction.

Microarrays. Total RNA was isolated from Ls174T/dnTCF4 cells with different treatments: DMSO, DAPT, doxycycline, DAPT plus doxycycline, using RNA extraction kit (Qiagen). Samples were labeled with Cy3 and Cy5 by cDNA synthesis with Agilent low RNA input fluorescent linear amplification kits. Samples were hybridized on Whole Human Genome Oligo Microarrays (G4122A). Raw data were processed using a web implementation of Limma (1) and normalized by robust correction using the global lowess algorithm with scaling (2). For determining significant hits, the Significance Analysis of Microarray (SAM) statistic was performed with the normalized log2 ratios of the 2 replicate microarray hybridizations, using one class and 2 class unpaired tests for the standard *t* test, running on the R based implementation of SAM (samr) (3) on a web based implementation (SAMi) (Lozano et al., unpublished data).

Functional Enrichment Analysis. Functional annotation of genes based on Gene Ontology (4) were extracted from Ensembl v.47 (5). *Z* score analysis: $Z_x = X - \mu_x)/\sigma_{\bar{x}}$ (where μ_x = mean, $\sigma_{\bar{x}}$ = standard error). We display matrices of *Z* score values in which each cell is represented by a color-coded scale. Significance levels were corrected for multiple comparisons using false discovery rate (FDR) correction.

1. Smyth GK, Michaud J, Scott HS (2005) Use of within-array replicate spots for assessing differential expression in microarray experiments. *Bioinformatics* 21:2067–2075.
2. Smyth GK, Speed T (2003) Normalization of cDNA microarray data. *Methods* 31:265–273.
3. Tusher VG, Tibshirani R, Chu G (2001) Significance analysis of microarrays applied to the ionizing radiation response. *Proc Natl Acad Sci USA* 98:5116–5121.
4. Consortium GO (2006) The Gene Ontology (GO) project in 2006. *Nucleic Acids Res* 34:D322–D326.
5. Hubbard TJ, et al. (2007) Ensembl 2007. *Nucleic Acids Res* 35:D610–D617.

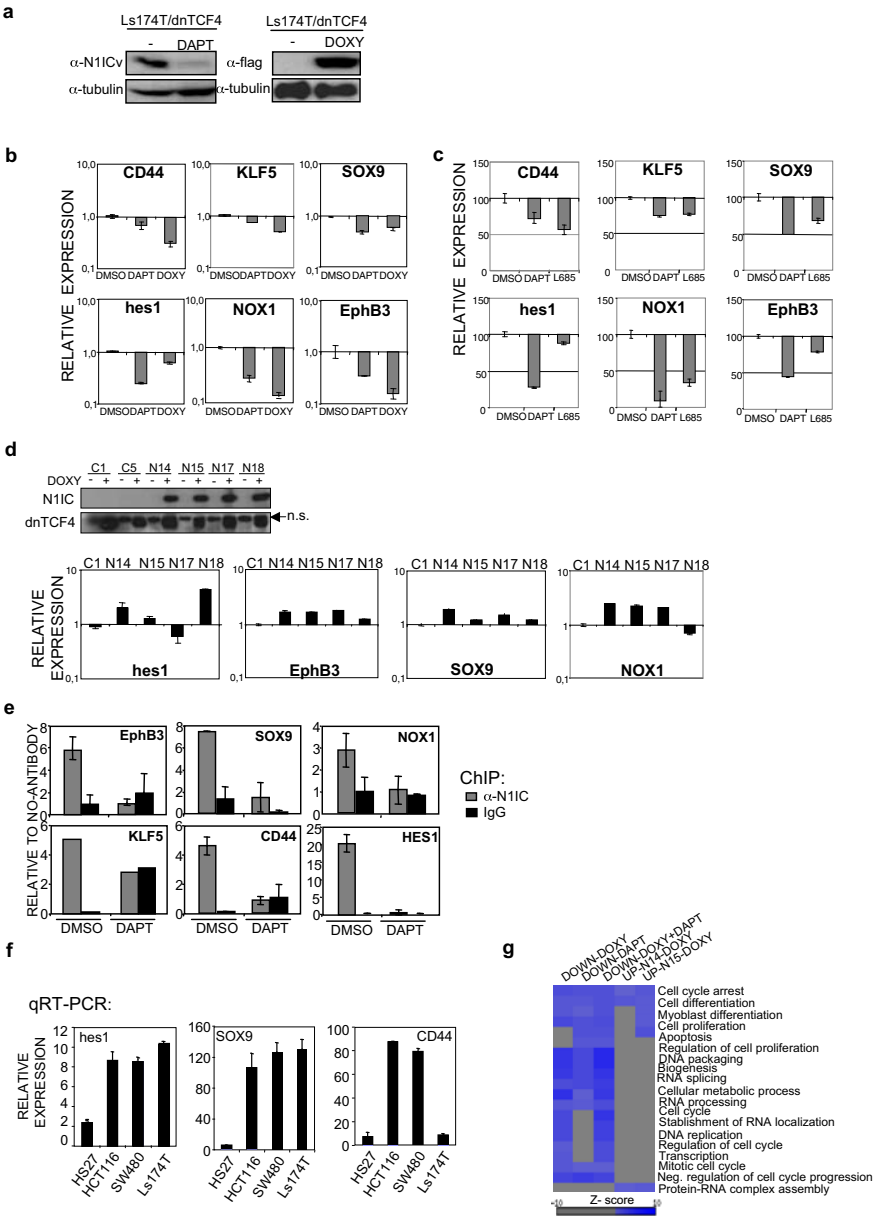

Fig. S1. (*a*) Down-regulation of Notch and β-catenin activities in response to DAPT and doxycycline treatments respectively. Western blot of Ls174T/dnTCF4 cells showing the blockage of Notch1 activation by DAPT (50 μM) and the expression levels of inducible dnTCF4 after doxycycline treatment in the conditions used for the microarray experiments in Fig. 1*a*. (*b*) Confirmation by qRT-PCR of different genes identified in the microarray screening from Fig. 1*a*. (*c*) Inhibition of different genes identified in the microarray screening with 2 different Notch inhibitors (DAPT and L685,458). (*d*) Confirmation by qRT-PCR of different genes identified in the microarray screening from Fig. 1*b*. (*Upper*) The inducible expression of N1IC and dnTCF4 by Western blot. (*e*) ChIP with anti-cleaved Notch antibody and qPCR analysis on the indicated promoters in Ls174T cells untreated or treated with DAPT. (*f*) (*Upper*) ChIP with the α-Notch1 antibody and qPCR analysis of the indicated promoters in different CRC cell lines. (*Lower*) Expression levels of these genes determined by qRT-PCR. (*g*) Functional annotation of genes down-regulated after inhibition of Wnt, Notch or both pathways or up-regulated in 2 N1IC-expressing clones (N14 and N15) based on Gene Ontology. Blue signifies over-representation of genes for the indicated groups. Gray means no significant difference from expected.

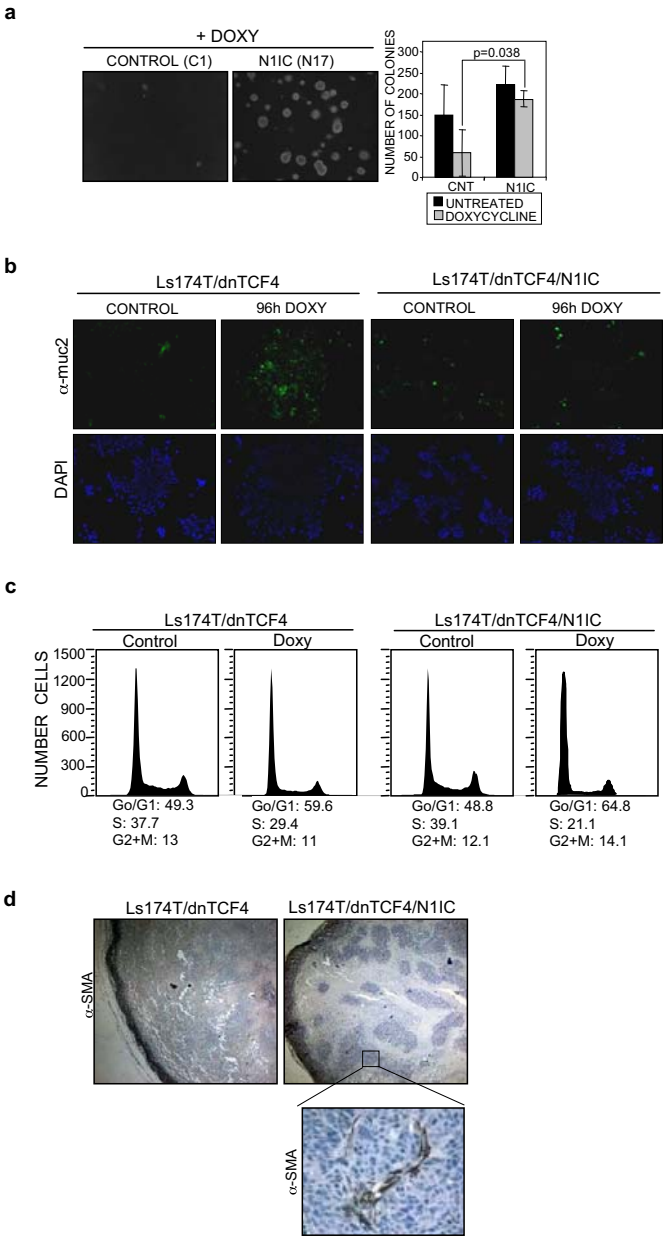

Fig. S2. (*a*) N1IC expression promotes colony formation in soft agar in the absence of Wnt signaling. Ls174T/dnTCF4 (CONTROL) and Ls174T/dnTCF4/N1IC (N1IC) were seeded in soft agar in the absence or presence of doxycycline. Colonies were counted after 7 days and representative images were obtained in an Olympus IX-10 at 40×. Average number of colonies of 2 independent experiments is represented. Error bars represent s.e.m. and P value is based on 2-sided Student's *t* test. (*b*) Immunostaining with α-muc2 antibody of the indicated cell lines untreated or treated with doxycycline. Representative images were obtained in an Olympus IX-10 at 200×. (*c*) Cell cycle profiles of untreated or doxycycline-treated (24h) Ls174T/dnTCF4 and Ls174T/dnTCF4/N1IC clones. Results from 1 representative of 3 different analyzed clones is shown. (*d*) α-SMA staining including a detail of vascularized tumor area (in the box) of representative tumors at 100x

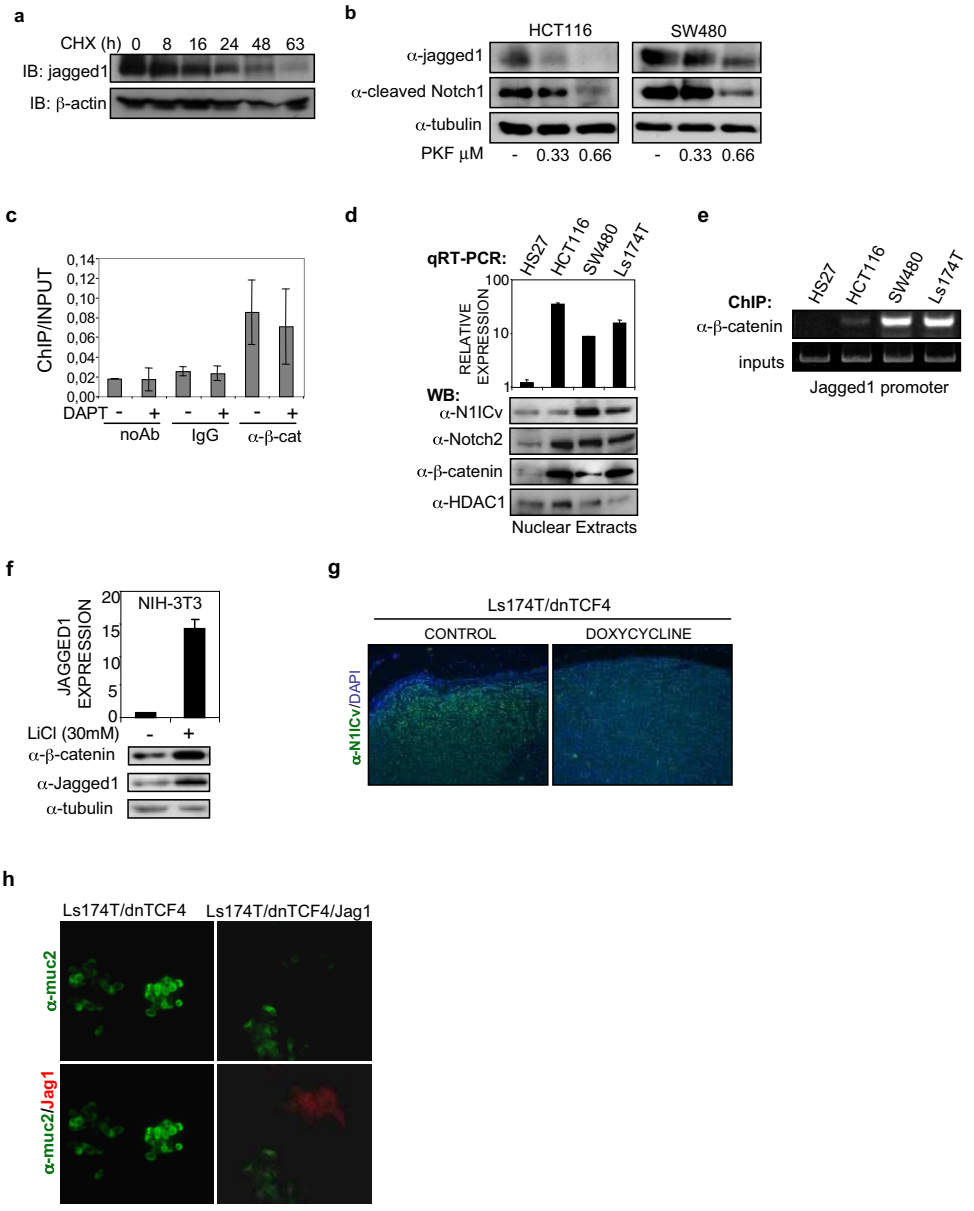

Fig. S3. (*a*) Half-life of the Jagged1 protein was determined by Western blot after incubation of Ls174T Cells with cycloheximide (CHX). (*b*) Pharmacological inhibition of β-catenin activity by PKF115–584 results in a dose dependent reduction of Jagged1 levels and inhibition of Notch activation as shown by Western blot analysis. (*c*) Recruitment of β-catenin to the Jagged1 promoter. qPCR to quantify the recruitment of β-catenin to the Jagged1 promoter in the absence or presence of the Notch inhibitor DAPT. (*d*) qRT-PCR was used to determine the expression of Jagged1 in CRC cell lines compared with nontransformed HS27 cells (*Upper*). Western blot analysis of CRC nuclear extracts with α-N1ICv, α-Notch2 and α-β-catenin antibodies (*Lower*). (*e*) Chromatin immunoprecipitation with α-β-catenin antibody from different cell lines compared with nontransformed HS27 cells. The presence of Jagged1 promoter in the precipitates was determined by semiquantitative PCR. (*f*) qRT-PCR and Western blot analysis to compare the mRNA and protein levels of Jagged1 in NIH 3T3 cells treated or untreated with the GSK3β-inhibitor LiCl. β-catenin and tubulin are shown as controls. (*g*) α-cleaved Notch staining of representative tumors at 100×. (*h*) Immunostaining with α-muc2 and α-Jagged1 antibodies of Ls174T/dnTCF4 cells transfected with mock or with Jagged1 plasmids, treated with doxycycline for 48 h. Representative images were obtained in an Olympus IX-10 at 400X.

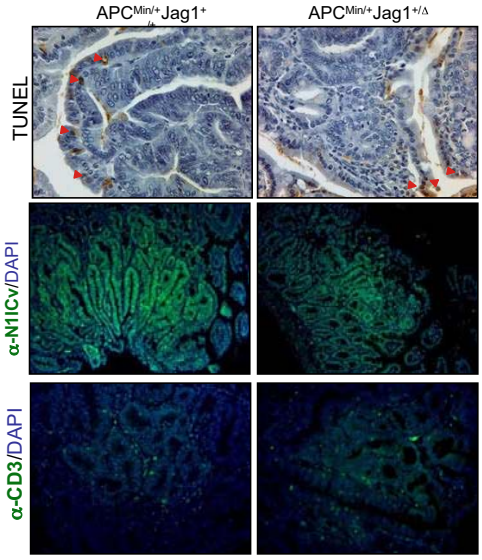

Fig. S4. TUNEL assay of representative tumors from different genotypes. Red arrows indicate apoptotic cells. Immunostaining with α-cleaved Notch1 (*Upper*) and α-CD3 (*Lower*) antibodies of representative tumors from $APC^{Min/+}$ or $APC^{Min/+}Jag1^{+/\Delta}$ mice. Representative images were obtained in an Olympus IX-10 at 200X.

a

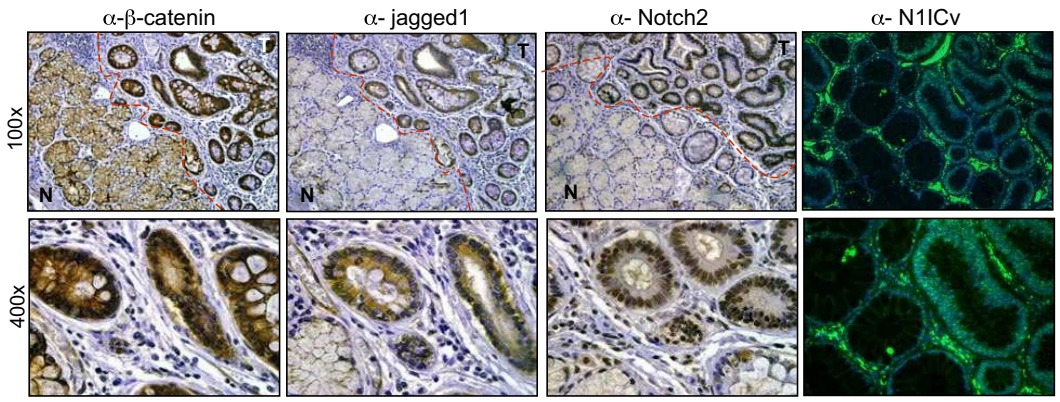

b

FAP PATIENTS	SAMPLE NUMBERS	GERM LINE MUTATION
FAP1	5, 11, 15	c.1958 G>A; exon 14 skipping
FAP3	9, 17	c.1958+3A>G +c.1959G>A; exon 14 skipping
FAP4	8, 16, 20	c.4175C>A; p.Ser1392X
FAP6	7, 14, 19	c. 4612_4613delGA; p.Glu1538IlefsX5
FAP8	6, 10, 12	c.1262G>A; c.1263G>A; W421X

Fig. S5. Serial sections of an adenoma sample from a different FAP patient stained with the indicated antibodies. Images were obtained with an Olympus BX-61 at 2 different magnifications (100× and 400×). (*b*) List of germ line mutations in the APC gene in patients included in the qRT-PCR analysis.

Other Supporting Information Files

Table S1
Table S2
Table S3
Table S4

ANNEXES

Annex A1. Table of Wnt mutant mice

Gene	Phenotype of knock-out or others functions	References
Wnt1	Loss midbrain, loss cerebellum and decrease in the number of thymocytes (with Wnt-4 deletion). Reduction in dorso-lateral neural precursors in the neural tube (with Wnt3A deletion). Deficiency in neural crest derivatives.	McMahon 1990, Thomas KR 1990, McMahon 1992, Ikeya M, Mulroy 2002
Wnt2	Placental defects, defective lung development (with Wnt2b deletion).	Monkley 1996, Goss 2009
Wnt2b/13	Retinal cell differentiation, defective lung development (with Wnt2b)	Goss 2009, Liu P 1999, M. Capecchi
Wnt3	Early gastrulation defects, axis formation, hair growth, defect in establishing the AER. Medial-lateral retinotectal topography, hippocampal neurogenesis.	Kubo 2003, Kubo 2005, Kishimoto 2000, Millar 1999. Barrow 2003, Schmitt 2005, Lie 2005
Wnt3a	Somites, tailbud defectsthrough loss expression Brachyury, this is mediated by Lef-1. Deficiency in neural crest derivatives, reduction in dorso-lateral neural precursors in the neural tube (with Wnt1). Loss hippocampus, Segmentation oscillation clock, Left right asymmetry, HSC self-renewal defect.	Takada 1994, Greco 1996, Yoshikawa Y 1997, Yamaguchi 1999, Galceran 2001. Lee 2000, Ikeya M, Aulehla 2003, Nakaya 2005, Luis 2008
Wnt4	Kidney defects, renal vesicle induction, Side-branching in mammary gland. Sex determination defects in female development. absence Mullerian Duct. Ectopic Testosterone synthesis in females. Decrease in the number of thymocytes (with Wnt1 deletion). Repression of the migration of steroidogenic adrenal precursors into the gonad. Anterior-posterior guidance of commissural axons (not tested in Wnt4 mutant).	Park 2007, Stark K 1994, Kim 2006 , Vainio S 1999, Brisken 2000, Lyuksyutova 2003, Mulroy 2002, Jeays-Ward 2003
Wnt5a	Truncated limbs, truncated AP axis, reduced number proliferating cells, Distal lung morphogenesis. Chondrocyte differentiation, longitudinal skeletal outgrowth, Inhibits B cell proliferation and functions as a tumor suppressor. Defects in posterior growth of the female reproductuve tract, Shortened and widened cochlea (planar polarity). Mammary gland phenotype, Prostate gland development, Intestinal elongation, Endothelial differentiation of ES cells.	Yamaguchi 1999, Roarty 2007, Cervantes 2009, Li 2002, Mericskay 2004, Yang 2009, Yang 2003, Qian 2007, Liang 2003, Huang 2009
Wnt7a	Limb polarity. Female infertility. Maintenance appropriate uterine patterning during the development of the mouse female reproductive tract. Delayed maturation synapses in Cerebellum. High levels cell death in response to DES in the Female Reproductive Tract. May promote neuronal differentiation. CNS vasculature (with Wnt7b).	Parr 1995, Parr 1998, Miller 1998, Hall 2000, Carta L, Sassoon D 2004, Hirabayashi 2004, Stenman 2008
Wnt7b	Placental developmental defects. Respiratory failure. defects in early mesenchymal proliferation leading to lung hypoplasia. Macrophage-induced programmed cell death also in LRP5 and LEF1 mutants). Lung development. CNS vasculature (with Wnt7a). Cortico-medullary axis in the kidney.	Parr 2001, Shu 2002, Lobov 2005, Rajagopal 2008, Stenman 2008, Liebner 2008. Yu 2009
Wnt8b	Â Loss of function mutant: no effect on neural development, but changes in gene expression.	Fotaki 2009
Wnt9a/14	Loss of function mutant: Joint integrity.	Spater 2006
Wnt9b/15	Regulation of mesenchymal to epithelial transitions. Renal vesicle induction. Planar cell polarity of the kidney epithelium.	Carroll 2005, Park 2007, Karner 2009

Wnt10b	Taste Papilla Development. Loss of function mutant: decreased trabecular bone. Loss gene promotes co-expression of Myogenic and Adipogenic program. Overexpression inhibits adipogenesis.	Iwatsuki 2007, Bennett 2005, Vertino 2005, Ross 2000
Wnt11	Ureteric branching defects. Cardiogenesis.	Majumdar 2003, Kispert A 1996. Pandur 2002
Wnt16	Activated by E2A-Pbx1 fusion protein in Pre-B ALL	McWhirter 1999

Annex A2. Table of microarray data (FIGURE R2)

List of genes selected from the microarray screening that showed a minimum of 1.3 fold downregulation in both conditions: doxycycline and DAPT treatment.

NAME	GENE SYMBOL	DOXY I	DOXY II	DAPT I	DAPT II	MEAN DOXY	MEAN DAPT
NM_005318	H1F0	**-2,12**	**-2,15**	**-3,94**	**-2,80**	-2,13	-3,37
NM_005524	HES1	**-1,36**	-1,25	**-2,90**	**-3,79**	-1,31	-3,34
NM_017534	MYH2	**-2,06**	**-2,73**	**-2,35**	**-3,86**	-2,40	-3,11
BC006322	ATF3	**-1,36**	**-1,90**	**-2,09**	**-3,91**	-1,63	-3,00
NM_005801	SUI1	**-2,75**	**-1,41**	**-3,70**	**-2,25**	-2,08	-2,97
NM_006979	SLC39A7	**-1,84**	**-2,10**	**-2,85**	**-2,79**	-1,97	-2,82
NM_016639	TNFRSF12A	**-1,58**	**-1,55**	**-2,90**	**-2,59**	-1,57	-2,75
NM_033260	FOXQ1	**-1,50**	**-1,65**	**-2,08**	**-3,12**	-1,58	-2,60
NM_006472	TXNIP	**-1,61**	**-2,15**	**-1,94**	**-3,25**	-1,88	-2,60
NM_024016	HOXB8	**-2,10**	**-2,80**	**-1,99**	**-3,09**	-2,45	-2,54
NM_003531	HIST1H3C	**-1,58**	**-1,91**	**-2,15**	**-2,87**	-1,75	-2,51
NM_021005	NR2F2	**-1,91**	**-2,10**	**-2,04**	**-2,91**	-2,01	-2,48
NM_005324	H3F3B	**-1,62**	**-2,39**	**-1,97**	**-2,98**	-2,00	-2,47
NM_005410	SEPP1	**-2,01**	-1,10	**-2,98**	**-1,90**	-1,56	-2,44
NM_014330	PPP1R15A	**-1,75**	**-1,44**	**-2,71**	**-2,11**	-1,59	-2,41
NM_001511	CXCL1	**-2,97**	**-3,17**	**-2,01**	**-2,79**	-3,07	-2,40
NM_003537	HIST1H3B	**-1,53**	**-1,84**	**-1,98**	**-2,72**	-1,68	-2,35
NM_016947	C6orf48	**-1,72**	**-1,48**	**-2,47**	**-2,20**	-1,60	-2,33
NM_005384	NFIL3	-1,12	**-1,48**	**-1,56**	**-3,06**	-1,30	-2,31
NM_052966	C1orf24	**-1,45**	**-1,81**	**-2,04**	**-2,58**	-1,63	-2,31
AB037851	KIAA1430	**-3,59**	**-1,47**	**-3,30**	**-1,32**	-2,53	-2,31
NM_021158	TRIB3	**-1,73**	-1,01	**-2,35**	**-2,27**	-1,37	-2,31
NM_005194	CEBPB	**-1,74**	**-1,44**	**-2,38**	**-2,22**	-1,59	-2,30
NM_003533	HIST1H3I	**-1,49**	**-1,69**	**-2,15**	**-2,44**	-1,59	-2,30
NM_021059	H3/o	**-1,37**	**-1,80**	**-1,88**	**-2,69**	-1,59	-2,28
NM_002089	CXCL2	**-1,64**	**-2,15**	**-1,75**	**-2,78**	-1,89	-2,26
NM_003729	RTCD1	**-1,53**	**-1,99**	**-1,71**	**-2,81**	-1,76	-2,26
NM_005564	LCN2	**-1,54**	**-1,59**	**-2,27**	**-2,24**	-1,57	-2,25
NM_003544	HIST1H4B	**-2,50**	**-2,76**	**-1,68**	**-2,78**	-2,63	-2,23
AK027341	KIAA1856	**-2,30**	**-1,78**	**-2,25**	**-2,20**	-2,04	-2,22
NM_053000	TIGA1	**-1,82**	**-1,99**	**-1,92**	**-2,51**	-1,91	-2,21
BC034962	15E1.2	**-2,89**	**-1,86**	**-2,57**	**-1,77**	-2,37	-2,17

NM_181803	UBE2C	**-1,59**	-1,01	**-2,32**	**-1,97**	-1,30	-2,15
BC017665	CXorf39	**-2,64**	**-1,75**	**-2,60**	**-1,69**	-2,19	-2,14
NM_003542	HIST1H4C	**-2,92**	**-2,79**	**-1,86**	**-2,41**	-2,86	-2,14
NM_003546	HIST1H4L	**-2,47**	**-2,95**	**-1,60**	**-2,64**	-2,71	-2,12
NM_003534	HIST1H3G	**-1,40**	**-1,66**	**-1,90**	**-2,32**	-1,53	-2,11
NM_006101	KNTC2	**-1,61**	**-2,00**	**-1,66**	**-2,50**	-1,81	-2,08
NM_000584	IL8	**-1,81**	**-1,97**	**-2,10**	**-2,04**	-1,89	-2,07
AL833872	DKFZp761P0423	**-1,55**	**-1,83**	**-1,63**	**-2,49**	-1,69	-2,06
NM_002520	NPM1	**-2,40**	**-1,32**	**-2,84**	-1,22	-1,86	-2,03
NM_003122	SPINK1	**-1,71**	**-1,64**	**-1,74**	**-2,32**	-1,67	-2,03
AB051487	DUSP16	**-1,54**	**-1,90**	**-1,53**	**-2,48**	-1,72	-2,01
NM_006948	STCH	-1,28	**-1,72**	**-1,41**	**-2,59**	-1,50	-2,00
NM_004902	RNPC2	**-1,52**	**-1,33**	**-1,71**	**-2,28**	-1,42	-1,99
NM_021144	PSIP1	**-2,38**	**-2,27**	**-2,09**	**-1,90**	-2,32	-1,99
NM_003539	HIST1H4D	**-2,32**	**-2,73**	**-1,51**	**-2,45**	-2,53	-1,98
NM_022893	BCL11A	**-2,53**	**-2,04**	**-2,08**	**-1,88**	-2,29	-1,98
L13689	PCGF4	**-1,69**	**-2,25**	**-1,58**	**-2,36**	-1,97	-1,97
NM_153631	HOXA3	**-1,79**	**-1,74**	**-1,89**	**-2,02**	-1,77	-1,95
THC1854890	LOC400782	**-1,33**	**-1,38**	**-1,65**	**-2,25**	-1,36	-1,95
NM_006756	TCEA1	**-1,45**	**-1,65**	**-1,61**	**-2,29**	-1,55	-1,95
NM_014685	HERPUD1	**-1,82**	**-1,47**	**-1,95**	**-1,94**	-1,64	-1,95
NM_000346	SOX9	**-2,23**	**-2,42**	**-1,91**	**-1,98**	-2,32	-1,94
NM_152626	ZNF92	-1,15	**-1,47**	**-1,32**	**-2,56**	-1,31	-1,94
NM_005719	ARPC3	**-1,52**	**-1,92**	**-1,49**	**-2,37**	-1,72	-1,93
NM_018420	SLC22A15	**-1,45**	**-1,73**	**-1,54**	**-2,28**	-1,59	-1,91
NM_003211	TDG	**-1,38**	**-1,34**	**-2,46**	**-1,36**	-1,36	-1,91
NM_016628	WAC	**-1,31**	**-1,46**	**-1,75**	**-2,04**	-1,39	-1,90
XM_066695	LOC139431	**-1,61**	**-1,62**	**-1,91**	**-1,88**	-1,61	-1,90
NM_001016	RPS12	**-2,42**	-1,23	**-2,48**	**-1,31**	-1,82	-1,89
NM_016201	AMOTL2	**-2,34**	**-3,05**	**-1,31**	**-2,47**	-2,70	-1,89
AY070137	SP3	**-1,56**	**-1,69**	**-1,65**	**-2,12**	-1,63	-1,89
AB028948	THRAP2	**-1,45**	**-1,31**	**-1,91**	**-1,85**	-1,38	-1,88
NM_006275	SFRS6	**-3,96**	**-2,66**	**-2,43**	**-1,33**	-3,31	-1,88
AL137671	SET	**-1,87**	**-1,85**	**-1,79**	**-1,96**	-1,86	-1,88
NM_016315	GULP1	**-1,66**	**-1,34**	**-2,03**	**-1,69**	-1,50	-1,86
NM_002928	RGS16	**-2,79**	**-2,99**	**-1,54**	**-2,12**	-2,89	-1,83
NM_001003	RPLP1	**-3,31**	-1,18	**-2,66**	-1,00	-2,25	-1,83
NM_018976	SLC38A2	**-1,89**	**-1,61**	**-1,95**	**-1,70**	-1,75	-1,82
NM_004152	OAZ1	**-1,95**	-1,03	**-2,37**	-1,23	-1,49	-1,80
NM_018237	CCAR1	-1,14	**-1,49**	**-1,32**	**-2,29**	-1,32	-1,80
NM_012248	SEPHS2	**-1,53**	**-1,50**	**-1,79**	**-1,81**	-1,51	-1,80
AL833530	NFE2L1	**-1,40**	**-1,36**	**-1,63**	**-1,96**	-1,38	-1,79
BC001373	MESDC1	**-1,52**	-1,08	**-2,03**	**-1,55**	-1,30	-1,79
NM_003368	USP1	**-1,36**	**-1,85**	**-1,31**	**-2,27**	-1,60	-1,79
NM_001023	RPS20	**-1,78**	-1,12	**-2,35**	-1,22	-1,45	-1,78
NM_006516	SLC2A1	-1,13	**-1,71**	-1,21	**-2,36**	-1,42	-1,78
NM_004064	CDKN1B	**-1,44**	**-1,96**	**-1,31**	**-2,23**	-1,70	-1,77
NM_016626	RKHD2	**-1,53**	**-1,53**	**-1,63**	**-1,90**	-1,53	-1,77
NM_001677	ATP1B1	**-3,35**	**-3,17**	**-2,42**	-1,10	-3,26	-1,76
NM_152437	ZFOC1	**-1,66**	**-2,10**	**-1,52**	**-2,00**	-1,88	-1,76
NM_014267	SMAP	**-1,46**	**-1,89**	**-1,50**	**-2,02**	-1,68	-1,76

NM_005842	SPRY2	**-1,64**	**-1,92**	**-1,56**	**-1,95**	-1,78	-1,76
NM_080820	HARS2	**-1,76**	**-2,00**	**-1,56**	**-1,94**	-1,88	-1,75
AK024274	SCYL2	-1,21	**-1,59**	**-1,30**	**-2,20**	-1,40	-1,75
NM_001031	RPS28	**-2,42**	-1,18	**-2,42**	-1,07	-1,80	-1,75
NM_016106	SCFD1	**-1,32**	**-1,84**	-1,23	**-2,25**	-1,58	-1,74
AK027632	DKFZp564K142	**-1,34**	**-1,59**	**-1,47**	**-2,00**	-1,46	-1,74
NM_001730	KLF5	**-1,52**	**-1,76**	**-1,56**	**-1,90**	-1,64	-1,73
NM_024921	POF1B	**-1,57**	**-1,46**	**-1,72**	**-1,74**	-1,51	-1,73
NM_002140	HNRPK	**-2,01**	**-2,25**	**-1,62**	**-1,84**	-2,13	-1,73
NM_003257	TJP1	**-1,30**	**-1,58**	**-1,42**	**-2,04**	-1,44	-1,73
NM_203472	SELS	**-1,33**	**-1,32**	**-1,80**	**-1,64**	-1,32	-1,72
NM_022074	FLJ22794	**-1,48**	**-1,98**	-1,29	**-2,15**	-1,73	-1,72
NM_006305	ANP32A	**-2,00**	**-1,59**	**-2,11**	**-1,32**	-1,80	-1,72
NM_018715	TD-60	**-1,56**	**-1,50**	**-1,81**	**-1,63**	-1,53	-1,72
NM_024640	YRDC	**-1,37**	**-1,53**	**-1,56**	**-1,87**	-1,45	-1,72
BC044649	ATP11A	**-1,79**	**-1,83**	**-1,43**	**-2,00**	-1,81	-1,72
AK026132	PHF17	**-1,73**	**-1,92**	**-1,38**	**-2,05**	-1,83	-1,72
NM_014028	OSTM1	**-1,43**	-1,28	**-1,72**	**-1,70**	-1,36	-1,71
NM_170715	RASSF1	**-1,50**	**-1,71**	**-1,57**	**-1,85**	-1,61	-1,71
AK056046	C18orf43	**-1,51**	**-1,76**	**-1,34**	**-2,08**	-1,64	-1,71
BC028704	ARRDC4	-1,26	**-1,49**	**-1,44**	**-1,96**	-1,37	-1,70
BC014089	LOC114984	**-1,77**	**-1,76**	**-1,61**	**-1,78**	-1,76	-1,69
NM_001386	DPYSL2	**-1,58**	**-1,50**	**-1,57**	**-1,81**	-1,54	-1,69
NM_002954	RPS27A	**-1,72**	-1,13	**-2,20**	-1,18	-1,43	-1,69
NM_004330	BNIP2	-1,14	**-1,52**	**-1,31**	**-2,07**	-1,33	-1,69
NM_170711	DAZAP1	**-2,06**	**-1,47**	**-1,85**	**-1,53**	-1,77	-1,69
NM_005520	HNRPH1	**-2,27**	**-1,98**	**-1,89**	**-1,47**	-2,13	-1,68
NM_002835	PTPN12	-1,22	**-1,47**	**-1,35**	**-2,01**	-1,35	-1,68
NM_080422	PTPN2	**-1,53**	**-2,09**	-1,22	**-2,13**	-1,81	-1,68
NM_139168	SFRS12	**-1,47**	**-1,47**	**-1,72**	**-1,62**	-1,47	-1,67
NM_001412	EIF1AX	**-1,90**	**-1,53**	**-1,82**	**-1,51**	-1,72	-1,67
NM_016038	SBDS	**-1,46**	**-1,54**	**-1,65**	**-1,68**	-1,50	-1,67
NM_001731	BTG1	**-1,35**	**-1,50**	**-1,59**	**-1,73**	-1,42	-1,66
NM_019022	TXNDC10	**-1,51**	**-1,84**	**-1,53**	**-1,78**	-1,68	-1,66
NM_152429	C10orf13	**-1,79**	**-1,82**	**-1,59**	**-1,71**	-1,81	-1,65
NM_000981	RPL19	**-1,63**	-1,06	**-2,15**	-1,15	-1,34	-1,65
NM_003212	TDGF1	**-4,03**	**-5,07**	-1,29	**-2,01**	-4,55	-1,65
AF107457	HLXB9	**-1,34**	**-1,44**	**-1,42**	**-1,85**	-1,39	-1,64
NM_030674	SLC38A1	-1,27	**-1,47**	**-1,40**	**-1,87**	-1,37	-1,63
NM_152829	TES	**-1,38**	**-2,00**	**-1,34**	**-1,92**	-1,69	-1,63
BC021662	FLJ22028	-1,20	**-1,49**	**-1,36**	**-1,90**	-1,35	-1,63
NM_012412	H2AFV	**-1,35**	**-1,54**	**-1,32**	**-1,94**	-1,44	-1,63
NM_004881	TP53I3	**-1,81**	**-1,98**	**-1,47**	**-1,79**	-1,90	-1,63
NM_003472	DEK	**-1,70**	**-1,65**	**-1,52**	**-1,73**	-1,67	-1,63
NM_003530	HIST1H3D	-1,21	**-1,56**	**-1,35**	**-1,90**	-1,38	-1,63
NM_015235	CSTF2T	**-2,01**	**-2,33**	**-1,67**	**-1,58**	-2,17	-1,62
NM_016080	C17orf25	**-2,14**	-1,24	**-1,99**	-1,26	-1,69	-1,62
NM_002356	MARCKS	**-1,73**	**-2,06**	-1,27	**-1,97**	-1,90	-1,62
AK056096	C9orf10OS	**-1,59**	**-2,01**	-1,28	**-1,96**	-1,80	-1,62
AK055693	FLJ35036	**-1,45**	**-2,30**	-1,03	**-2,21**	-1,87	-1,62
U92014	SEC31L1	-1,26	**-1,42**	**-1,38**	**-1,85**	-1,34	-1,61

NM_007212	RNF2	**-1,94**	**-1,48**	**-1,87**	**-1,36**	-1,71	-1,61
NM_022802	CTBP2	-1,28	**-1,95**	-1,15	**-2,07**	-1,62	-1,61
AY052478	RAB39B	**-1,55**	**-1,93**	**-1,32**	**-1,91**	-1,74	-1,61
NM_080632	UPF3B	**-1,62**	**-1,67**	**-1,65**	**-1,57**	-1,64	-1,61
NM_014153	ZC3HDC7	-1,25	**-1,49**	**-1,40**	**-1,81**	-1,37	-1,60
AB029039	RBM16	**-1,81**	**-1,62**	**-1,60**	**-1,60**	-1,71	-1,60
NM_022731	NUCKS	**-1,41**	**-1,36**	**-1,54**	**-1,66**	-1,38	-1,60
NM_002862	PYGB	**-1,63**	**-1,34**	**-1,99**	-1,20	-1,49	-1,60
NM_002032	FTH1	**-1,75**	-1,11	**-2,02**	-1,18	-1,43	-1,60
NM_012404	ANP32D	**-1,68**	**-1,35**	**-1,93**	-1,25	-1,52	-1,59
NM_002894	RBBP8	**-1,72**	**-2,21**	-1,29	**-1,89**	-1,97	-1,59
NM_002090	CXCL3	**-1,61**	**-1,60**	**-1,52**	**-1,66**	-1,60	-1,59
NM_007214	SEC63	**-1,36**	**-1,55**	**-1,45**	**-1,73**	-1,46	-1,59
NM_012158	FBXL3	-1,28	**-1,58**	-1,24	**-1,94**	-1,43	-1,59
NM_015630	EPC2	**-1,74**	**-1,90**	**-1,33**	**-1,83**	-1,82	-1,58
NM_018359	FLJ11200	**-1,30**	**-1,42**	**-1,51**	**-1,65**	-1,36	-1,58
NM_006451	PAIP1	**-2,23**	-1,21	**-1,40**	**-1,75**	-1,72	-1,57
NM_013438	UBQLN1	-1,29	**-1,62**	-1,20	**-1,94**	-1,46	-1,57
NM_005953	MT2A	**-2,83**	**-3,30**	**-1,33**	**-1,81**	-3,06	-1,57
NM_032705	MGC14801	**-1,44**	**-1,49**	**-1,45**	**-1,67**	-1,46	-1,56
NM_005794	DHRS2	**-1,89**	**-1,79**	**-1,67**	**-1,44**	-1,84	-1,56
NM_018147	FAIM	**-1,98**	**-2,16**	-1,21	**-1,90**	-2,07	-1,55
NM_002156	HSPD1	**-1,86**	**-1,35**	**-2,08**	-1,02	-1,60	-1,55
NM_024511	C4orf15	-1,23	**-1,38**	**-1,35**	**-1,75**	-1,31	-1,55
NM_000971	RPL7	**-1,51**	-1,13	**-2,01**	-1,09	-1,32	-1,55
NM_005500	SAE1	**-1,45**	**-1,67**	**-1,35**	**-1,74**	-1,56	-1,54
NM_173609	C15orf21	**-2,49**	**-2,07**	**-1,92**	-1,15	-2,28	-1,54
NM_014670	BZW1	**-1,62**	**-1,50**	**-1,59**	**-1,47**	-1,56	-1,53
NM_022154	SLC39A8	**-1,81**	**-2,17**	-1,26	**-1,80**	-1,99	-1,53
NM_018453	C14orf11	**-2,10**	-1,05	**-1,98**	-1,08	-1,58	-1,53
NM_016480	PAIP2	-1,30	**-1,86**	-1,23	**-1,82**	-1,58	-1,53
NM_139169	TRUB1	**-1,54**	**-1,78**	-1,26	**-1,79**	-1,66	-1,52
NM_020935	USP37	**-1,65**	**-1,37**	**-1,67**	**-1,37**	-1,51	-1,52
AJ131186	PRP19	**-1,62**	**-1,37**	**-1,97**	-1,06	-1,49	-1,52
NM_015934	NOP5/NOP58	**-2,09**	**-2,51**	-1,25	**-1,78**	-2,30	-1,51
NM_004865	TBPL1	-1,28	**-1,64**	-1,22	**-1,80**	-1,46	-1,51
NM_020371	AVEN	**-1,53**	**-1,79**	-1,21	**-1,82**	-1,66	-1,51
NM_145061	C13orf3	**-2,01**	**-1,99**	-1,29	**-1,73**	-2,00	-1,51
NM_001239	CCNH	-1,27	**-1,57**	-1,15	**-1,87**	-1,42	-1,51
NM_032876	JUB	**-1,86**	**-2,36**	-1,23	**-1,78**	-2,11	-1,51
NM_130469	JDP2	**-1,33**	**-2,00**	-1,10	**-1,90**	-1,67	-1,50
NM_003758	EIF3S1	**-1,78**	**-1,67**	**-1,46**	**-1,54**	-1,72	-1,50
NM_022336	EDAR	**-1,72**	**-1,70**	**-1,48**	**-1,51**	-1,71	-1,50
NM_005968	HNRPM	**-4,31**	**-3,80**	**-1,81**	-1,19	-4,06	-1,50
ENST00000332280	LOC391126	**-1,94**	-1,07	**-1,97**	-1,01	-1,51	-1,49
NM_033280	SEC11L3	**-1,66**	**-2,20**	-1,18	**-1,80**	-1,93	-1,49
NM_004134	HSPA9B	**-1,38**	**-1,64**	**-1,36**	**-1,62**	-1,51	-1,49
BC000024	C12orf14	**-1,42**	**-1,35**	**-1,42**	**-1,55**	-1,39	-1,49
NM_031157	LOC144983	**-1,64**	**-1,45**	**-1,89**	-1,08	-1,54	-1,49
NM_018339	RFK	**-1,35**	**-1,81**	-1,20	**-1,78**	-1,58	-1,49

NM_000311	PRNP	-1,21	**-1,48**	-1,24	**-1,74**	-1,34	-1,49
NM_001746	CANX	**-1,36**	**-1,53**	**-1,41**	**-1,56**	-1,45	-1,48
NM_016618	LOC51315	**-1,35**	**-1,52**	**-1,34**	**-1,63**	-1,44	-1,48
NM_003714	STC2	**-1,46**	**-1,42**	**-1,65**	**-1,32**	-1,44	-1,48
BC039468	NUP50	**-1,56**	**-1,92**	-1,26	**-1,70**	-1,74	-1,48
NM_015933	HSPC016	**-1,55**	**-1,32**	**-1,53**	**-1,42**	-1,44	-1,48
NM_018466	GLT28D1	**-1,36**	**-1,53**	-1,24	**-1,72**	-1,45	-1,48
NM_002105	H2AFX	**-1,72**	**-1,45**	**-1,58**	**-1,37**	-1,58	-1,48
NM_005392	PHF2	-1,25	**-1,46**	-1,28	**-1,67**	-1,35	-1,48
NM_153231	ZNF550	**-1,38**	**-1,50**	-1,27	**-1,68**	-1,44	-1,47
NM_001545	ICT1	**-1,44**	**-1,55**	**-1,44**	**-1,50**	-1,49	-1,47
NM_156036	HOXB6	-1,23	**-1,60**	-1,12	**-1,82**	-1,42	-1,47
NM_015327	EST1B	**-1,49**	**-1,41**	**-1,60**	**-1,33**	-1,45	-1,47
NM_006861	RAB35	**-1,33**	**-1,50**	**-1,40**	**-1,53**	-1,41	-1,47
NM_006807	CBX1	**-1,33**	**-1,92**	-1,05	**-1,88**	-1,63	-1,47
AK023624	HIS1	**-1,69**	**-1,62**	**-1,43**	**-1,51**	-1,66	-1,47
NM_004096	EIF4EBP2	**-1,65**	**-1,42**	**-1,49**	**-1,44**	-1,54	-1,47
NM_001969	EIF5	**-1,48**	**-1,37**	**-1,44**	**-1,49**	-1,42	-1,47
NM_001904	CTNNB1	**-1,87**	**-1,57**	**-1,72**	-1,21	-1,72	-1,46
AK056822	LOC400960	**-1,57**	**-1,57**	**-1,35**	**-1,57**	-1,57	-1,46
NM_022747	C14orf65	**-1,71**	-1,18	**-1,56**	**-1,36**	-1,44	-1,46
BC038454	ZNF326	**-2,06**	**-2,47**	-1,25	**-1,66**	-2,27	-1,46
NM_007187	WBP4	**-1,34**	**-1,44**	-1,27	**-1,64**	-1,39	-1,46
BC035153	FLJ22313	**-1,63**	**-2,15**	-1,17	**-1,74**	-1,89	-1,46
NM_138375	CABLES1	**-1,98**	**-2,14**	**-1,25**	**-1,66**	-2,06	-1,45
NM_000978	RPL23	**-1,44**	**-1,43**	**-1,64**	-1,26	-1,43	-1,45
NM_004071	CLK1	**-1,38**	**-1,44**	**-1,47**	**-1,43**	-1,41	-1,45
NM_173576	C10orf48	**-1,67**	**-1,93**	-1,23	**-1,67**	-1,80	-1,45
NM_004688	NMI	**-1,55**	**-1,85**	-1,15	**-1,75**	-1,70	-1,45
AK000814	PLA2G4B	**-1,55**	**-1,92**	-1,23	**-1,66**	-1,74	-1,45
NM_014432	IL20RA	**-1,82**	**-1,95**	-1,27	**-1,62**	-1,88	-1,45
AL137667	MAPK8	-1,30	**-1,53**	-1,20	**-1,69**	-1,42	-1,45
U39064	MAP2K6	**-1,46**	**-1,57**	**-1,34**	**-1,55**	-1,52	-1,44
D86962	GRB10	**-1,43**	**-1,92**	-1,08	**-1,80**	-1,68	-1,44
AL133014	C7orf20	-1,24	**-1,64**	-1,16	**-1,73**	-1,44	-1,44
NM_000321	RB1	**-1,99**	**-1,88**	**-1,45**	**-1,44**	-1,94	-1,44
AK096179	LOC285958	**-1,80**	**-2,34**	-1,17	**-1,71**	-2,07	-1,44
NM_001356	DDX3X	-1,21	**-1,53**	**-1,31**	**-1,57**	-1,37	-1,44
NM_007269	STXBP3	**-1,36**	**-1,76**	-1,10	**-1,78**	-1,56	-1,44
NM_004125	GNG10	**-1,55**	**-1,58**	**-1,33**	**-1,56**	-1,56	-1,44
NM_003404	YWHAB	**-2,05**	**-2,79**	-1,18	**-1,70**	-2,42	-1,44
NM_000224	KRT18	**-1,40**	**-1,32**	**-1,88**	-1,00	-1,36	-1,44
NM_002669	PLRG1	**-1,51**	**-1,54**	**-1,47**	**-1,41**	-1,52	-1,44
NM_001719	BMP7	**-1,56**	**-1,83**	**-1,29**	**-1,58**	-1,70	-1,44
NM_012110	CHIC2	**-1,33**	**-1,46**	**-1,38**	**-1,50**	-1,39	-1,44
NM_001530	HIF1A	-1,28	**-1,50**	-1,23	**-1,64**	-1,39	-1,44
NM_007104	RPL10A	**-1,52**	**-1,34**	**-1,74**	-1,13	-1,43	-1,44
NM_152680	FLJ32028	**-1,46**	**-1,57**	-1,24	**-1,63**	-1,52	-1,44
NM_016444	ZNF226	-1,27	**-1,57**	-1,11	**-1,75**	-1,42	-1,43
NM_152858	WTAP	**-1,99**	**-2,19**	-1,27	**-1,59**	-2,09	-1,43

M27396	ASNS	**-1,37**	-1,29	**-1,81**	-1,05	-1,33	-1,43
D87077	KIAA0240	**-1,46**	**-1,57**	**-1,39**	**-1,46**	-1,51	-1,43
NM_018981	DNAJC10	**-1,74**	**-2,07**	-1,18	**-1,67**	-1,90	-1,43
NM_018475	TPARL	**-1,36**	**-1,70**	-1,29	**-1,56**	-1,53	-1,42
NM_006013	RPL10	**-1,51**	-1,12	**-1,77**	-1,08	-1,32	-1,42
M96956	TDGF3	**-2,23**	**-2,26**	**-1,42**	**-1,42**	-2,24	-1,42
AB051540	ZC3HDC5	**-1,38**	**-1,46**	-1,26	**-1,59**	-1,42	-1,42
NM_000344	SMN1	**-1,31**	**-1,51**	-1,22	**-1,62**	-1,41	-1,42
AK056774	H19	**-1,61**	**-1,55**	**-1,75**	-1,09	-1,58	-1,42
NM_174908	C3orf6	**-1,30**	**-1,31**	**-1,31**	**-1,53**	-1,31	-1,42
NM_016304	C15orf15	-1,28	**-1,63**	-1,22	**-1,61**	-1,45	-1,42
AB051506	GRIP2	**-1,44**	-1,20	**-1,71**	-1,13	-1,32	-1,42
NM_006082	K-ALPHA-1	**-1,49**	**-1,35**	**-1,65**	-1,18	-1,42	-1,41
NM_018347	C20orf29	**-1,30**	**-1,74**	-1,10	**-1,72**	-1,52	-1,41
NM_015423	AASDHPPT	**-1,96**	**-2,09**	-1,23	**-1,59**	-2,02	-1,41
NM_153451	ORAOV1	**-1,32**	**-1,63**	-1,22	**-1,60**	-1,47	-1,41
NM_016205	PDGFC	**-1,38**	**-1,80**	-1,13	**-1,70**	-1,59	-1,41
NM_001029	RPS26	**-1,60**	-1,14	**-1,80**	-1,02	-1,37	-1,41
NM_153207	AEBP2	**-1,49**	**-1,80**	-1,18	**-1,64**	-1,64	-1,41
NM_016492	RANGNRF	**-1,45**	**-1,84**	-1,14	**-1,68**	-1,64	-1,41
NM_003653	COPS3	**-1,47**	**-1,81**	-1,18	**-1,63**	-1,64	-1,41
NM_002874	RAD23B	-1,27	**-1,41**	**-1,31**	**-1,50**	-1,34	-1,41
AY007811	KIAA1199	**-2,55**	**-3,42**	-1,26	**-1,55**	-2,98	-1,41
NM_002408	MGAT2	**-1,35**	**-1,73**	-1,10	**-1,71**	-1,54	-1,41
NM_001014	RPS10	**-1,80**	-1,09	**-1,78**	-1,03	-1,45	-1,40
BC065759	IRF2BP2	**-1,51**	**-1,44**	-1,26	**-1,55**	-1,47	-1,40
NM_016079	VPS24	-1,23	**-1,53**	-1,16	**-1,64**	-1,38	-1,40
NM_013943	CLIC4	**-1,41**	**-1,68**	-1,20	**-1,60**	-1,54	-1,40
THC1880732	HSPC129	-1,23	**-1,42**	-1,15	**-1,65**	-1,32	-1,40
NM_014223	NFYC	**-1,60**	**-1,68**	-1,30	**-1,50**	-1,64	-1,40
NM_002009	FGF7	**-1,37**	**-1,51**	-1,23	**-1,57**	-1,44	-1,40
AK096099	LOC90288	-1,26	**-1,71**	-1,14	**-1,65**	-1,48	-1,40
NM_022756	FLJ11730	**-1,70**	-1,18	**-1,66**	-1,13	-1,44	-1,40
BC021694	ADD3	**-1,50**	**-1,66**	**-1,31**	**-1,48**	-1,58	-1,39
NM_018105	THAP1	-1,24	**-1,37**	-1,21	**-1,57**	-1,30	-1,39
AF151813	PAI-RBP1	**-1,65**	**-1,71**	**-1,35**	**-1,44**	-1,68	-1,39
BC043386	LOC374920	**-1,37**	-1,24	**-1,43**	**-1,36**	-1,31	-1,39
NM_007052	NOX1	**-1,33**	**-1,30**	**-1,37**	**-1,42**	-1,31	-1,39
AK025166	C10orf12	**-1,50**	**-1,48**	-1,28	**-1,50**	-1,49	-1,39
NM_003541	HIST1H4K	-1,23	**-1,47**	-1,14	**-1,63**	-1,35	-1,39
NM_024017	HOXB9	**-1,50**	**-1,51**	**-1,42**	**-1,35**	-1,51	-1,39
NM_020792	KIAA1363	**-1,57**	**-1,33**	**-1,41**	**-1,36**	-1,45	-1,39
BC012895	SLC7A1	-1,24	**-1,40**	**-1,33**	**-1,44**	-1,32	-1,39
NM_013386	SLC25A24	**-1,43**	**-1,74**	-1,12	**-1,66**	-1,58	-1,39
NM_138425	GRCC10	-1,22	**-1,42**	-1,11	**-1,66**	-1,32	-1,38
NM_025138	C13orf23	**-1,41**	**-1,99**	-1,05	**-1,72**	-1,70	-1,38
NM_001968	EIF4E	**-1,55**	-1,09	**-1,65**	-1,12	-1,32	-1,38
NM_013390	TMEM2	**-1,54**	**-1,74**	**-1,32**	**-1,44**	-1,64	-1,38
NM_152283	ZFP62	**-2,25**	**-2,87**	-1,23	**-1,53**	-2,56	-1,38
NM_032476	MRPS6	**-1,33**	**-1,64**	-1,16	**-1,59**	-1,49	-1,38

NM_022770	FLJ13912	**-1,72**	**-2,04**	-1,22	**-1,54**	-1,88	-1,38
NM_002539	ODC1	**-1,87**	**-2,07**	**-1,43**	**-1,33**	-1,97	-1,38
NM_004642	CDK2AP1	**-1,37**	**-1,61**	**-1,27**	**-1,48**	-1,49	-1,38
BC029911	C9orf119	-1,29	**-1,41**	-1,29	**-1,46**	-1,35	-1,38
NM_014169	C14orf123	-1,27	**-1,54**	**-1,31**	**-1,44**	-1,41	-1,38
AK056882	RASEF	**-1,45**	**-1,53**	**-1,36**	**-1,38**	-1,49	-1,37
NM_005843	STAM2	-1,30	**-1,36**	**-1,35**	**-1,40**	-1,33	-1,37
AL833957	SETDB2	**-1,32**	**-1,31**	-1,28	**-1,46**	-1,32	-1,37
NM_033342	TRIM7	**-1,68**	**-2,10**	-1,14	**-1,60**	-1,89	-1,37
NM_019071	ING3	-1,20	**-1,66**	-1,10	**-1,63**	-1,43	-1,37
NM_014517	UBP1	**-1,93**	**-1,77**	**-1,42**	**-1,31**	-1,85	-1,37
NM_145306	C10orf35	-1,30	-1,30	**-1,40**	**-1,33**	-1,30	-1,37
NM_181523	PIK3R1	**-1,65**	**-1,36**	**-1,59**	-1,14	-1,51	-1,37
AF292100	RP42	**-1,67**	-1,23	**-1,63**	-1,10	-1,45	-1,36
NM_006938	SNRPD1	**-1,71**	-1,27	**-1,64**	-1,08	-1,49	-1,36
NM_007129	ZIC2	**-1,42**	-1,27	**-1,39**	**-1,34**	-1,35	-1,36
NM_152716	FLJ36874	**-1,51**	**-1,42**	-1,27	**-1,45**	-1,46	-1,36
D79986	BCLAF1	**-2,26**	**-3,16**	-1,04	**-1,68**	-2,71	-1,36
NM_020128	MDM1	**-1,62**	**-1,57**	**-1,34**	**-1,38**	-1,60	-1,36
NM_002909	REG1A	**-2,42**	**-2,37**	-1,15	**-1,57**	-2,40	-1,36
NM_173200	NR4A3	**-1,41**	**-1,49**	-1,29	**-1,42**	-1,45	-1,36
AL512717	DKFZp547E052	**-1,31**	**-1,66**	-1,16	**-1,55**	-1,48	-1,36
AK027900	FLJ10853	**-1,50**	**-1,82**	-1,23	**-1,48**	-1,66	-1,35
NM_001046	SLC12A2	**-3,05**	**-4,10**	-1,06	**-1,64**	-3,57	-1,35
AB007896	KIAA0436	**-2,18**	**-2,29**	-1,19	**-1,52**	-2,23	-1,35
BX640898	THUMPD1	**-1,46**	-1,29	**-1,47**	-1,23	-1,38	-1,35
NM_000969	RPL5	**-1,46**	-1,18	**-1,69**	-1,01	-1,32	-1,35
NM_015230	CENTD1	**-1,33**	**-1,36**	**-1,36**	**-1,34**	-1,34	-1,35
NM_014766	SCRN1	**-1,33**	**-1,45**	-1,19	**-1,51**	-1,39	-1,35
NM_032593	HINT2	**-1,40**	**-1,62**	-1,28	**-1,42**	-1,51	-1,35
X78926	ZNF268	**-1,67**	**-1,78**	-1,12	**-1,57**	-1,72	-1,35
THC1869938	CARD9	**-1,47**	**-1,31**	**-1,35**	**-1,34**	-1,39	-1,35
BC038180	OGT	**-2,10**	**-1,91**	**-1,46**	-1,23	-2,00	-1,34
NM_052965	C1orf19	**-1,57**	**-2,30**	-1,00	**-1,69**	-1,93	-1,34
NM_016404	HSPC152	**-1,50**	**-1,66**	-1,23	**-1,46**	-1,58	-1,34
NM_181838	UBE2D2	-1,28	**-1,60**	-1,22	**-1,47**	-1,44	-1,34
NM_004557	NOTCH4	**-1,44**	**-1,38**	-1,30	**-1,39**	-1,41	-1,34
NM_005949	MT1F	**-1,44**	**-1,60**	-1,15	**-1,53**	-1,52	-1,34
NM_170784	MKKS	-1,20	**-1,41**	-1,15	**-1,52**	-1,31	-1,34
NM_003589	CUL4A	**-1,79**	**-1,75**	**-1,30**	**-1,37**	-1,77	-1,34
BC020784	MGC14289	**-1,82**	**-2,23**	-1,09	**-1,58**	-2,03	-1,34
BC007436	FAM44B	-1,25	**-1,53**	-1,11	**-1,56**	-1,39	-1,33
NM_007280	OIP5	**-1,33**	**-1,53**	-1,08	**-1,58**	-1,43	-1,33
NM_003177	SYK	**-2,86**	**-2,98**	**-1,34**	**-1,33**	-2,92	-1,33
NM_005857	ZMPSTE24	**-1,82**	**-1,79**	**-1,31**	**-1,35**	-1,81	-1,33
NM_024516	MGC4606	**-1,39**	**-1,94**	-1,10	**-1,56**	-1,66	-1,33
NM_005805	PSMD14	-1,22	**-1,53**	-1,15	**-1,51**	-1,37	-1,33
AL050260	DKFZP547E1010	**-1,38**	**-1,43**	-1,26	**-1,40**	-1,40	-1,33
BC039145	LOC283464	-1,28	**-1,51**	-1,12	**-1,53**	-1,39	-1,33
BC002526	HSPA4	**-1,38**	-1,27	**-1,38**	-1,27	-1,33	-1,33

NM_006808	SEC61B	-1,24	**-1,41**	-1,14	**-1,52**	-1,33	-1,33
NM_001949	E2F3	-1,24	**-1,64**	-1,12	**-1,53**	-1,44	-1,33
BC008024	SLB	-1,25	**-1,64**	-1,03	**-1,63**	-1,45	-1,33
AF165518	FLJ10292	**-1,34**	**-1,69**	-1,00	**-1,64**	-1,51	-1,32
NM_002370	MAGOH	**-1,32**	**-1,53**	-1,18	**-1,46**	-1,42	-1,32
NM_002128	HMGB1	**-1,95**	**-2,01**	**-1,34**	-1,30	-1,98	-1,32
BC028932	RRM2	-1,22	**-1,63**	-1,22	**-1,41**	-1,43	-1,32
NM_006331	C2F	**-1,62**	**-1,85**	-1,27	**-1,36**	-1,73	-1,32
AB082526	NEK9	-1,20	**-1,53**	-1,08	**-1,55**	-1,37	-1,32
NM_001959	EEF1B2	**-1,61**	**-1,45**	**-1,61**	-1,02	-1,53	-1,32
THC1807966	SMAD1	**-1,55**	**-1,44**	**-1,22**	**-1,41**	-1,50	-1,32
NM_001274	CHEK1	-1,26	**-1,43**	-1,23	**-1,40**	-1,35	-1,31
NM_170695	TGIF	**-1,43**	**-1,36**	**-1,36**	-1,27	-1,40	-1,31
NM_176870	MT1K	**-2,89**	**-3,08**	-1,24	**-1,38**	-2,98	-1,31
NM_003655	CBX4	**-1,37**	-1,27	**-1,46**	-1,17	-1,32	-1,31
AB011134	KIAA0562	**-1,45**	**-1,71**	-1,16	**-1,46**	-1,58	-1,31
NM_052831	C6orf192	**-1,80**	**-1,80**	**-1,31**	**-1,32**	-1,80	-1,31
NM_003517	HIST2H2AC	-1,25	**-1,40**	-1,22	**-1,40**	-1,33	-1,31
NM_024945	C9orf76	**-1,35**	**-1,63**	-1,16	**-1,46**	-1,49	-1,31
NM_014577	BRD1	**-1,42**	**-1,38**	-1,30	**-1,33**	-1,40	-1,31
NM_173809	BLOC1S2	**-1,37**	**-1,49**	-1,23	**-1,39**	-1,43	-1,31
NM_013282	UHRF1	**-2,28**	**-2,13**	**-1,37**	-1,25	-2,20	-1,31
NM_003685	KHSRP	**-1,70**	**-1,39**	**-1,33**	-1,28	-1,55	-1,31
AF161386	HSPC268	**-1,55**	**-1,65**	-1,21	**-1,41**	-1,60	-1,31
NM_004438	EPHA4	**-1,45**	**-1,38**	**-1,14**	**-1,47**	-1,42	-1,30
NM_021968	HIST1H4J	**-1,39**	-1,25	-1,14	**-1,47**	-1,32	-1,30
NM_005782	THOC4	**-2,31**	**-1,63**	**-1,58**	-1,03	-1,97	-1,30
NM_032997	ZWINT	**-1,91**	**-2,16**	-1,18	**-1,42**	-2,03	-1,30
NM_006303	JTV1	**-1,36**	**-1,55**	-1,17	**-1,43**	-1,46	-1,30
AK026606	MESDC2	**-1,39**	**-1,38**	-1,27	**-1,33**	-1,39	-1,30
NM_144591	C10orf32	**-2,04**	**-2,07**	-1,24	**-1,36**	-2,06	-1,30
AK023950	C11orf23	**-1,34**	**-1,33**	**-1,35**	-1,24	-1,34	-1,30

Annex A3. Table of microarray data (FIGURE R4)

List of genes that are up-regulated ≥1.3 fold in Ls174T/dnTCF4/N1ICD expressing clones and were downregulated by both treatments.

NAME	GENE SYMBOL	MEAN DOXY	MEAN DAPT	NIC-14 I	NIC-14 II	NIC-15 I	NIC-15 II	MEAN NIC
BC006322	ATF3	-1,63	-3,00	2,21	3,00	12,93	8,17	**6,58**
NM_005194	CEBPB	-1,59	-2,30	2,08	3,57	5,98	5,55	**4,30**
NM_002928	RGS16	-2,89	-1,83	2,00	3,24	6,17	5,39	**4,20**
NM_006472	TXNIP	-1,88	-2,60	3,28	5,38	4,42	3,31	**4,10**
NM_021158	TRIB3	-1,37	-2,31	2,02	4,62	3,32	4,05	**3,50**
NM_052966	C1orf24	-1,63	-2,31	2,18	4,30	3,38	3,25	**3,28**
AK056774	H19	-1,58	-1,42	1,88	2,68	4,52	3,58	**3,16**
NM_053000	TIGA1	-1,91	-2,21	2,32	3,61	3,60	3,07	**3,15**

NM_005384	NFIL3	-1,30	-2,31	2,34	2,88	4,48	2,63	**3,08**
NM_005318	H1F0	-2,13	-3,37	2,51	4,20	2,70	2,83	**3,06**
NM_016947	C6orf48	-1,60	-2,33	2,64	4,16	2,50	2,16	**2,87**
NM_005564	LCN2	-1,57	-2,25	2,18	3,25	3,08	2,39	**2,73**
M27396	ASNS	-1,33	-1,43	1,99	3,11	2,91	2,84	**2,71**
NM_014685	HERPUD1	-1,64	-1,95	1,93	3,26	2,44	2,71	**2,59**
NM_016201	AMOTL2	-2,70	-1,89	1,92	2,29	3,66	2,29	**2,54**
NM_005524	HES1	-1,31	-3,34	1,67	1,58	4,23	2,57	**2,51**
NM_006516	SLC2A1	-1,42	-1,78	2,32	2,95	2,67	1,91	**2,46**
NM_016618	LOC51315	-1,44	-1,48	2,02	2,88	2,56	2,28	**2,43**
AL833872	DKFZp761P0423	-1,69	-2,06	1,81	2,73	2,23	2,76	**2,38**
NM_013943	CLIC4	-1,54	-1,40	1,77	2,12	3,21	2,42	**2,38**
AY052478	RAB39B	-1,74	-1,61	1,69	2,39	2,93	2,49	**2,37**
AY007811	KIAA1199	-2,98	-1,41	2,14	3,24	2,05	1,96	**2,35**
BC038180	OGT	-2,00	-1,34	1,87	2,67	2,36	2,18	**2,27**
BC021662	FLJ22028	-1,35	-1,63	1,87	2,75	2,03	2,00	**2,16**
NM_014330	PPP1R15A	-1,59	-2,41	1,51	2,40	2,54	2,19	**2,16**
NM_006948	STCH	-1,50	-2,00	2,04	2,41	2,50	1,65	**2,15**
NM_004438	EPHA4	-1,42	-1,30	1,61	2,02	2,63	2,19	**2,11**
NM_033260	FOXQ1	-1,58	-2,60	1,47	1,75	2,89	2,34	**2,11**
NM_018976	SLC38A2	-1,75	-1,82	1,49	2,18	2,17	2,44	**2,07**
NM_003714	STC2	-1,44	-1,48	1,47	1,98	2,40	2,38	**2,06**
NM_156036	HOXB6	-1,42	-1,47	2,22	2,86	1,82	1,31	**2,05**
NM_016639	TNFRSF12A	-1,57	-2,75	1,16	1,86	2,31	2,87	**2,05**
NM_003257	TJP1	-1,44	-1,73	1,54	2,01	2,52	2,05	**2,03**
NM_001731	BTG1	-1,42	-1,66	1,90	2,72	1,85	1,56	**2,00**
NM_018420	SLC22A15	-1,59	-1,91	1,85	2,61	1,83	1,61	**1,98**
NM_005801	SUI1	-2,08	-2,97	1,37	2,72	1,48	2,26	**1,96**
BC028704	ARRDC4	-1,37	-1,70	1,91	2,37	2,01	1,53	**1,96**
NM_152829	TES	-1,69	-1,63	1,50	1,91	2,22	2,15	**1,95**
NM_130469	JDP2	-1,67	-1,50	1,82	1,88	2,40	1,64	**1,93**
NM_007052	NOX1	-1,31	-1,39	1,47	1,72	2,64	1,84	**1,92**
D86962	GRB10	-1,68	-1,44	1,77	2,08	2,12	1,69	**1,92**
AL833530	NFE2L1	-1,38	-1,79	1,65	2,13	2,13	1,74	**1,91**
NM_003729	RTCD1	-1,76	-2,26	1,93	2,17	2,04	1,42	**1,89**
AB051487	DUSP16	-1,72	-2,01	1,59	1,71	2,29	1,92	**1,88**
NM_203472	SELS	-1,32	-1,72	1,66	2,46	1,69	1,64	**1,87**
NM_032705	MGC14801	-1,46	-1,56	1,63	2,29	1,74	1,70	**1,84**
THC1854890	LOC400782	-1,36	-1,95	1,73	2,20	1,82	1,57	**1,83**
NM_152680	FLJ32028	-1,52	-1,44	1,43	1,75	2,21	1,86	**1,81**
NM_024921	POF1B	-1,51	-1,73	1,43	1,81	2,02	1,99	**1,81**
NM_003212	TDGF1	-4,55	-1,65	1,81	2,49	1,43	1,30	**1,76**
NM_030674	SLC38A1	-1,37	-1,63	1,59	1,98	1,88	1,57	**1,76**
AK096099	LOC90288	-1,48	-1,40	1,91	2,33	1,44	1,34	**1,76**
NM_007214	SEC63	-1,46	-1,59	1,87	2,16	1,66	1,31	**1,75**
AB028948	THRAP2	-1,38	-1,88	1,57	2,40	1,48	1,54	**1,75**
BC012895	SLC7A1	-1,32	-1,39	1,46	1,71	1,80	1,68	**1,66**
AB082526	NEK9	-1,37	-1,32	1,70	1,86	1,74	1,29	**1,65**
NM_173576	C10orf48	-1,80	-1,45	1,54	2,01	1,65	1,39	**1,64**
NM_152429	C10orf13	-1,81	-1,65	1,47	1,97	1,63	1,49	**1,64**
AL833957	SETDB2	-1,32	-1,37	1,39	1,72	1,75	1,66	**1,63**
NM_032593	HINT2	-1,51	-1,35	1,46	1,95	1,40	1,43	**1,56**

NM_004071	CLK1	-1,41	-1,45	1,37	1,76	1,55	1,53	**1,56**
AK024274	SCYL2	-1,40	-1,75	1,45	1,50	1,90	1,37	**1,55**
U92014	SEC31L1	-1,34	-1,61	1,35	1,53	1,73	1,60	**1,55**
NM_004064	CDKN1B	-1,70	-1,77	1,52	1,49	1,85	1,31	**1,54**
NM_019022	TXNDC10	-1,68	-1,66	1,52	1,96	1,39	1,26	**1,53**
AK056882	RASEF	-1,49	-1,37	1,44	1,65	1,60	1,42	**1,53**
NM_152283	ZFP62	-2,56	-1,38	1,35	1,41	1,80	1,49	**1,52**
NM_015630	EPC2	-1,82	-1,58	1,31	1,30	1,94	1,50	**1,51**
NM_016106	SCFD1	-1,58	-1,74	1,60	1,52	1,78	1,14	**1,51**
NM_052965	C1orf19	-1,93	-1,34	1,42	1,40	1,87	1,33	**1,51**
NM_016628	WAC	-1,39	-1,90	1,26	1,44	1,65	1,64	**1,50**
BC000024	C12orf14	-1,39	-1,49	1,50	1,78	1,38	1,29	**1,49**
NM_002835	PTPN12	-1,35	-1,68	1,45	1,57	1,59	1,31	**1,48**
NM_002009	FGF7	-1,44	-1,40	1,43	1,68	1,46	1,33	**1,48**
NM_006756	TCEA1	-1,55	-1,95	1,62	1,77	1,40	1,09	**1,47**
X78926	ZNF268	-1,72	-1,35	1,27	1,37	1,82	1,42	**1,47**
NM_001239	CCNH	-1,42	-1,51	1,37	1,35	1,76	1,38	**1,46**
U39064	MAP2K6	-1,52	-1,44	1,38	1,66	1,39	1,40	**1,46**
NM_018359	FLJ11200	-1,36	-1,58	1,46	1,79	1,27	1,30	**1,45**
NM_003655	CBX4	-1,32	-1,31	1,23	1,67	1,40	1,51	**1,45**
AK056096	C9orf10OS	-1,80	-1,62	1,29	1,45	1,62	1,45	**1,45**
NM_013438	UBQLN1	-1,46	-1,57	1,32	1,25	1,82	1,41	**1,45**
NM_080632	UPF3B	-1,64	-1,61	1,25	1,37	1,64	1,52	**1,44**
NM_174908	C3orf6	-1,31	-1,42	1,29	1,32	1,72	1,41	**1,44**
NM_005324	H3F3B	-2,00	-2,47	1,25	1,70	1,28	1,52	**1,44**
AB051540	ZC3HDC5	-1,42	-1,42	1,20	1,62	1,35	1,56	**1,43**
NM_005843	STAM2	-1,33	-1,37	1,32	1,45	1,54	1,40	**1,43**
AK027341	KIAA1856	-2,04	-2,22	1,34	1,62	1,41	1,34	**1,43**
NM_002669	PLRG1	-1,52	-1,44	1,41	1,80	1,23	1,24	**1,42**
D87077	KIAA0240	-1,51	-1,43	1,45	1,59	1,42	1,20	**1,42**
NM_003122	SPINK1	-1,67	-2,03	1,29	1,59	1,37	1,40	**1,41**
NM_016304	C15orf15	-1,45	-1,42	1,52	1,60	1,42	1,10	**1,41**
NM_080820	HARS2	-1,88	-1,75	1,44	1,71	1,32	1,17	**1,41**
NM_139169	TRUB1	-1,66	-1,52	1,31	1,35	1,57	1,36	**1,40**
NM_003533	HIST1H3I	-1,59	-2,30	1,25	1,68	1,24	1,40	**1,39**
AL512717	DKFZp547E052	-1,48	-1,36	1,36	1,38	1,52	1,28	**1,38**
NM_021059	H3/o	-1,59	-2,28	1,25	1,67	1,16	1,43	**1,38**
NM_003537	HIST1H3B	-1,68	-2,35	1,28	1,50	1,31	1,38	**1,37**
NM_000346	SOX9	-2,32	-1,94	1,36	1,50	1,44	1,16	**1,37**
NM_144591	C10orf32	-2,06	-1,30	1,17	1,32	1,57	1,40	**1,37**
NM_014169	C14orf123	-1,41	-1,38	1,30	1,52	1,33	1,31	**1,36**
NM_022893	BCL11A	-2,29	-1,98	1,36	1,54	1,38	1,16	**1,36**
NM_003758	EIF3S1	-1,72	-1,50	1,34	1,60	1,29	1,20	**1,36**
NM_003534	HIST1H3G	-1,53	-2,11	1,25	1,55	1,28	1,35	**1,35**
NM_001904	CTNNB1	-1,72	-1,46	1,27	1,39	1,48	1,25	**1,35**
NM_016444	ZNF226	-1,42	-1,43	1,19	1,23	1,64	1,32	**1,34**
NM_001730	KLF5	-1,64	-1,73	1,33	1,37	1,50	1,17	**1,34**
NM_001386	DPYSL2	-1,54	-1,69	1,25	1,31	1,56	1,25	**1,34**
NM_014432	IL20RA	-1,88	-1,45	1,37	1,58	1,22	1,11	**1,32**
AB011134	KIAA0562	-1,58	-1,31	1,32	1,53	1,28	1,11	**1,31**
BC017665	CXorf39	-2,19	-2,14	1,22	1,23	1,51	1,26	**1,31**
AF107457	HLXB9	-1,39	-1,64	1,21	1,38	1,34	1,28	**1,30**

NM_004557	NOTCH4	-1,41	-1,34	1,16	1,22	1,47	1,35	**1,30**
NM_014153	ZC3HDC7	-1,37	-1,60	1,35	1,44	1,28	1,14	**1,30**